J. M. Hoover D. T. Moeller J. M. Pitt S. G. Smith N. W. Wainaina

Performance of Randomly Oriented, Fiber-Reinforced Roadway Soils

A Laboratory and Field Investigation

December 1982

Iowa DOT Project HR-211
ERI Project 1427
ISU-ERI-Ames-83192

Sponsored by the Iowa Department of Transportation, Highway Division

report

College of Engineering
Iowa State University

The opinions, findings, and conclusions expressed in this publication are those of the authors and not necessarily those of the Highway Division of the Iowa Department of Transportation.

J. M. Hoover
Principal Investigator

D. T. Moeller
J. M. Pitt
S. G. Smith
N. W. Wainaina
Contributors

Final Report

Performance of Randomly Oriented, Fiber-Reinforced Roadway Soils

A Laboratory and Field Investigation

December 1982

Submitted to the Highway Division,
Iowa Department of Transportation

Iowa DOT Project HR-211
ERI Project 1427
ISU-ERI-Ames-83192

Department of Civil Engineering
Engineering Research Institute
Iowa State University, Ames

TABLE OF CONTENTS

PURPOSE AND OBJECTIVES

Several primary techniques have been developed through which soil-aggregate road material properties may be improved. Such techniques basically involve a mechanism of creating a continuous matrix system of soil and/or aggregate particles, interlocked through the use of some additive such as portland cement, lime, or bituminous products. Details by which soils are stabilized vary greatly, but they are dependent on the type of stabilizing agent and nature of the soil, though the overall approach to stabilization has the common feature that improvement is achieved by some mechanism(s) forcing individual particles to adhere to one another. This process creates a more rigid material, most often capable of resisting the influx of water during freezing, loss of strength due to high moisture content and particle dispersion during thawing, and loss of strength due to migration of fines and/or water by capillarity and pumping.

The study reported herein, took a new and relatively different approach to strengthening of soils, i.e., improvement of roadway soils and/or soil-aggregate materials by structural reinforcement with randomly oriented fibers.

The purpose of the study was to conduct a laboratory and field investigation into the potential of improving (a) soil-aggregate surfaced and subgrade materials, including those that are frost-prone and/or highly moisture susceptible, and (b) localized base course materials, by uniting such materials through fibrous reinforcement. The envisioned objective of the project was the development of a simple construction technique(s)

that could be (a) applied on a selective basis to specific areas having a history of poor performance, or (b) used for improvement of potential base materials prior to surfacing.

Little background information on such purpose and objective was available. Though the envisioned process had similarities to fibrous reinforced concrete, and to fibrous reinforced resin composites, the process was devoid of a cementitious binder matrix and thus highly dependent on the cohesive and frictional interlocking processes of a soil and/or aggregate with the fibrous reinforcement; a condition not unlike the introduction of reinforcing bars into a concrete sand/aggregate mixture without benefit of portland cement. Thus the study was also directed to answering some fundamental questions: (1) would the technique work; (2) what type or types of fibers are effective; (3) are workable fibers commercially available; and (4) can such fibers be effectively incorporated with conventional construction equipment, and employed in practical field applications? The approach to obtaining answers to these questions, was guided by the philosophy that an understanding of basic fundamentals was essential to developing a body of engineering knowledge, that would serve as the basis for eventual development of design procedures with fibrous products for the applications previously noted.

REVIEW OF LITERATURE

Fiber reinforcement of construction materials dates to prehistoric times, when civilizations in Mesopotamia added straws to mud bricks (19). The aim was to provide integrity to a weak matrix by arresting the growth

of cracks; i.e., more or less the same objective for many modern applications. At a much later date, Europeans utilized horse hair for reinforcing plastics, and civilizations in Australia and New Zealand utilized vegetable fibers for reinforcing plaster-boards (19). Such applications were confined to small scale operations. Composite material technology remained relatively undeveloped till the early part of this century, when it took a quantum leap with the development of reinforced concrete, and asbestos cement (19).

Early developments in soil fiber composites were in the area of reinforced earth. Vidal (26) conducted studies in the late 1960s on utilization of galvanized steel for reinforcing retaining wall backfill. This study demonstrated that retaining walls could be constructed at less cost than more conventional techniques.

In the mid 1970s, Fang and Mehta (9) performed studies on the possibility of utilizing sulfur treated bamboo for reinforcing slopes, earth dams and backfill materials for retaining walls. This study showed that bamboo reinforcement enhanced the shear strength of soil and could be economically used to reinforce such engineered structures. For existing dams and embankments, it was proposed that the bamboo be installed vertically, with its length exceeding the depth of a theoretical failure plane. For new embankments or dams, it was proposed that the bamboo should be placed horizontally, either in strips or the form of a mat. Bamboo reinforced earth also showed better resistance to seismic excitations than non-reinforced earth.

It was not until the mid 1970s when studies on utilization of fabrics in roadway soils were first reported (27). Handfelt (12) showed that non-woven fabrics could reduce frost boiling and increase stability of soil

aggregate roads.

Gray and Ohashi (10) conducted studies on utilization of both natural and synthetic fibers for reinforcing sandy soils at predetermined fiber orientations. This study showed that shear strength was dependent on fiber type, fiber length, fiber orientation and fiber volume fraction.

Fiber Composites

Constituents of a fiber composite are fibers coupled with a matrix material. The mechanical behavior of fiber composites is thus influenced by the type of interactions occurring between the individual constituents.

In an introduction to fiber composites, Krenchel (17) classified matrix materials into organic and inorganic. Organic matrixes are comprised of polymeric materials such as epoxy, polyester, plastics, etc. Most available literature on fiber composites is on the interaction of fibers and such matrixes. Procedures for interfacing organic matrixes and fibers range from mixing to liquid infiltration. In general, the interfacial bond developed between fibers and organic matrixes produces composite materials of high strength and stiffness, low weight and high resistance to corrosion. Composite failure is usually characterized by breakage of the high content of fibers.

Inorganic matrixes are composed of granular particulate materials such as aggregates, concrete, cement, soil, etc. (17). Fabrication of these composites presents some technical problems, and no universal technique has yet been adopted. One of the methods that have been used in fiber concrete involves adding fibers and aggregate into a concrete mixer, then mixing thoroughly prior to adding water and cement. Another technique

involves fiber pretreatment, in order to separate individual fibers, so that the matrix material can penetrate into the fibers. The developed interfacial bond is mainly frictional, and these composites usually experience a progressive type of failure, characterized by cracking of the matrix material, followed by fiber debonding and pullout. Fiber debonding and pullout signifies a weak interfacial bond between fibers and matrix. Therefore, the composite fails before the tensile strength of the fibers is fully mobilized. The quantity of fibers required for such composites is usually low; between 1% and 20% by volume (17). Such composites are less expensive than those containing an organic matrix, since the cost of matrix materials such as cement and soil is lower than that of an organic matrix, and the required quantity of fibers is smaller.

Fibers are added into inorganic matrixes to improve their ductility, tensile strength, flexural strength and impact resistance (16). Fibers improve such properties since extra energy is required to debond and stretch the fibers, thus absorbing more energy prior to experiencing failure.

Fibers

Characteristics of fibers that play a dominant role in determining the integrity of fiber composites are type, geometry, amount, and orientation in the matrix (24). Generally, fibers are broadly classified into synthetic and natural.

Synthetic fibers are produced by various chemical processes, and are classified into high modulus, high strength fibers, and low modulus, high elongation fibers. The former includes fibers such as steel, fiberglass, carbon, etc., while the latter includes fibers such as polypropylene and

and polyethelene (20). Low modulus fibers are generally more expensive, and have not been used extensively in the construction industry (15).

Synthetic fibers have two advantages over natural fibers. First, these fibers can be produced according to desired specifications; for example, geometry of fibers can be controlled, shape of fibers and surface conditions can be altered in order to enhance the frictional properties of the fibers (17). Second, most synthetic fibers do not biodegrade when subjected to variable environments of moisture, heat, cold or sunlight (17).

Natural fibers can be classified into cellulose fibers and asbestos. Cellulose fibers are the reinforcing fibers found in vegetation, and in their crystalline form, form the backbone of various wood and natural textile fibers (23). They are usually classified according to that part of the plant from which they are derived (23). Cellulose fibers usually have lower values of Young's modulus and tensile strength than most synthetic fibers, but are available in large quantities and are replenishable (17). High quantities of these fibers can be used without incurring excessive costs. A disadvantage of natural fibers is that they may be affected by varying environments (23). In addition, fiber geometry is not a constant parameter, thus complicating any design procedure. Such fibers may also be susceptible to microbiological attack and rotting, and biodegrade in alkaline environments (23, 17).

Asbestos fibers have high chemical resistance and good mechanical properties, such as high tensile strength and Young's modulus (17). They can also withstand severe pretreatment conditions during mixing and are available at low cost in large quantities. These fibers have been used

extensively for reinforcing cement mortars, but in recent years their usage has declined due to the discovery that asbestos may be responsible for some forms of human cancer (17). Properties of fibers frequently used in civil engineering are summarized in Table 1.

Fiber content is usually expressed in terms of volume fraction or weight fraction, either term representing the amount of fiber in a composite as a percentage of total volume and total weight of the composite respectively, (1).

Fiber geometry

Length is a major criteria used to classify fibers. Composites produced with fibers shorter than 3 inches are usually classified as short fiber composites. Composites made up of longer fibers are referred to as continuous fiber composites since in most cases the fibers extend throughout the mass of the matrix (1). The mechanics of stress transfer differ in both classifications. For short fiber composites, applied stresses are first transferred to the matrix material, then to the fibers through the fiber ends, and the surfaces of fibers near the fiber ends. For continuous fiber composites, applied stresses are transferred to the fibers and matrix at the same time (1).

For short fiber composites, load transfer length (L_t) and critical length (L_{cr}) may be defined (1). Load transfer length denotes the minimum fiber length in which maximum fiber stress can be achieved. The maximum fiber stress is dependent on the stress applied to the composite. The limiting value of this stress is the stress that would be accepted by a fiber of continuous or infinite length, for a given stress applied to the

Table 1. Properties of fibers commonly used in civil engineering materials (15)

Fiber Type	Diameter μm	Length mm	Density $Kg/m^3 \times 10^3$	Young's Modulus MN/M^2	Poisson's Ratio	Tensile Strength MN/M^2	Elongation at Break %	Typical Volume in Composite %
Asbestos								
Chysotile	0.02-30	40	2.55	164	0.3	200-1800	2-3	10
Crocidolite	0.1 -20	-	3.37	196	-	3500	2-3	-
Cellulose Fibers			1.2	10		300-500		10-20
E-Fiberglass	8-10		2.54	72	0.25	3500	4.8	
Polypropylene								
Monofilament	100-200	5-50	0.9	5	0.29-0.46	400	18	0.1-6
Fibrillated	500-4000	20-75	0.9	8	0.29-0.46	400	8	0.1-6

composite (1). Critical fiber length is the minimum fiber length in which the fiber ultimate strength is achieved. The ultimate fiber strength is independent of the stress applied to the composite, and therefore the critical fiber length is also independent of applied stress, representing the maximum value of load transfer length (1).

A parameter closely associated with fiber length is the aspect ratio, obtained by dividing length by diameter (L/d). The aspect ratio plays a role in determining the magnitude of interfacial shear developed during loading. The larger the aspect ratio, the smaller the amount of interfacial shear developed and hence the stronger must be the fiber matrix interfacial bond (1).

Fiber orientation

In the fabrication of fiber composites, fibers may be arranged in one, two, or three dimensional orientations. One dimensional orientation involves aligning the fibers parallel to one another and in the direction of any applied stresses (2). The principle of reinforced earth approximates the concept of unidirectional long-fiber reinforcement (26). For two and three dimensional arrangements, the fibers may be randomly oriented, or ordered in some way during fabrication. In recent years the introduction of soil-fabric composites has developed a form of soil reinforcement bearing a resemblance to fiber composite technology (12, 27). The difference between two dimensional and three dimensional orientation is that in the former, fibers lie approximately in a plane, while in the latter, fibers extend in space in all directions (2). The principles of reinforcement are the same in all three cases, except that for the two and three

dimensional cases some strength reduction factors occur. In fiber composites, only the fibers aligned normal to the applied stress, carry any stress. Therefore, for two and three dimensional orientations, some fibers do not carry any stress at all and this is accounted for by strength reduction factors, more commonly termed efficiency factors. Figure 1 summarizes the classification of fiber composites based on fiber length and orientation.

Unidirectional filament composites

In fiber composite technology, the simplest and oldest form of reinforcement is the employment of long filaments in strategic alignment with the direction of anticipated principal stresses. Aspect ratios of these filaments are taken to be infinity. This assumption greatly simplifies analysis of the system by eliminating the concentration of stresses occurring at the ends of more discreet fibers. The basic assumption which allows for modeling of other fiber reinforced systems, is that the bond established between the fiber and matrix is perfect. This allows for complete transfer of load from the matrix to the fibers. The basic expression for the reinforcing mechanism is

$$R_c = R_m + R_f \tag{1}$$

Where R denotes the load, and c, m, f denote the composite, matrix and fiber respectively. This equation is the simplest form of the Law of Mixes, the principal theorem of composite technology (7). As is typical of nearly all theorems, the basic simplicity of the general equation belies considerable complexity when employed in actual practice. Equation 1 is

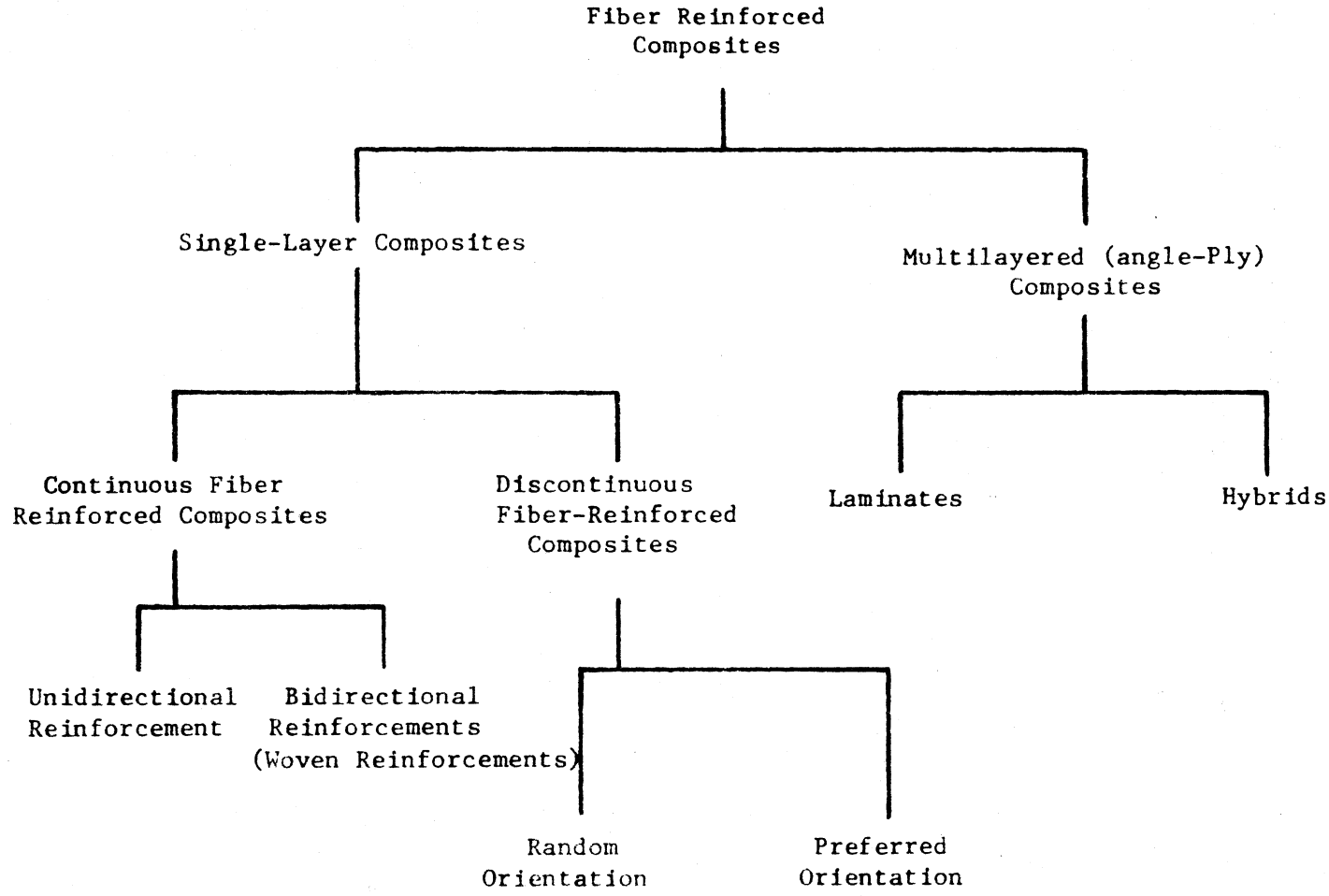

Figure 1. Classification of fiber composite materials (1)

more commonly adapted to the terms of stress (σ) and area (A) by assuming that the cross sectional area of the matrix and fiber combination remains constant. Equation 2 is the product of this substitution.

$$\sigma_c A_c = \sigma_m A_m + \sigma_f A_f \tag{2}$$

Similarly, the constant cross section assumption allows for the substitution of a volume term (V) into the Law of Mixes thereby producing an expression for stress in the composite in terms of easily controlled quantities.

$$\sigma_c V_c = \sigma_m V_m + \sigma_f V_f \tag{3}$$

In practical situations, where disparity between the unit densities of the matrix and fibers is great, the substitution of weight fraction for volume fraction is made. The level of stress in the composite is therefore controlled by the relation of the fiber properties, in comparison with properties of the matrix. Manipulation of these properties allows for control of the mode of failure that the composite will demonstrate.

The assumption of perfect bonding further allows for the determination of a value of Young's Modulus (E) for the composite. Given this bonding condition and linearly elastic components, Hooke's Law applies.

$$\sigma_f = E_f \varepsilon_f \text{ and } \sigma_m = E_m \varepsilon_m \tag{4}$$

Application of these elastic relations to the Law of Mixes results in

$$E_c \varepsilon_c V_c = E_m \varepsilon_m V_m + E_f \varepsilon_f V_f \tag{5}$$

The assumption of a perfect bond further allows for division of the strain term throughout the equation. This is based upon the perfect transfer of

load from the matrix to the fibers resulting in the more common form of this expression.

$$E_c V_c = E_m V_m + E_f V_f \quad (6)$$

The secondary effects of elasticity due to varying Poisson's ratio are most frequently neglected in composite design, since the error induced by this assumption is quite small (23)

It is of benefit at this point to qualitatively examine the effects of unidirectional reinforcement and to establish some frame of reference for the trends related to it. The enhancement of coaxial tensile strength properties and moduli is the primary benefit gained from unidirectional reinforcement. Improvement of these properties appears to be independent of the matrix properties,yet highly dependent upon the quality of the bond developed between the fiber and the matrix. Volume fraction also bears significantly into the overall strength of unidirectional filament composites (23).

Figure 2 illustrates the relation between composite tensile strength versus volume fraction of reinforcing agent. Parratt (23) has shown that, particularly in ductile matrixes, there exists a critical volume fraction of fibers below which the effects of fiber reinforcement are nil and very often detrimental due to the reduction of matrix brought about by the addition of fiber. Quantitative generalities in regard to these values cannot be achieved without the evaluation of specific systems, although this trend appears to be widespread among similar composites.

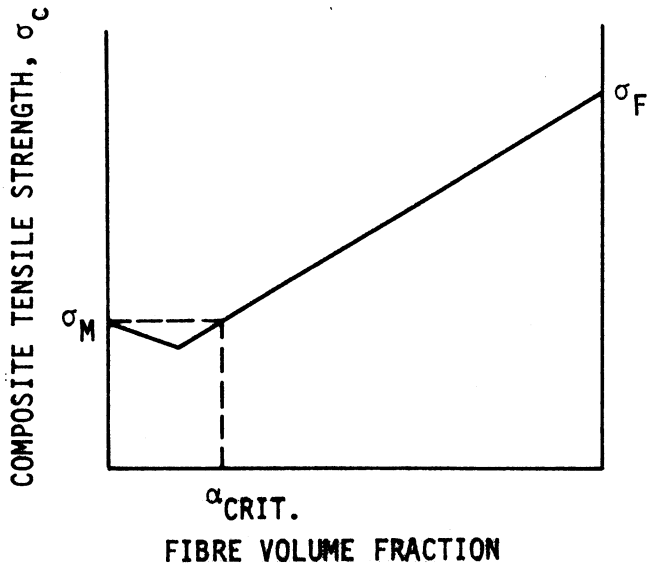

Figure 2. Typical relation of composite tensile strength versus fiber volume fraction in fiber reinforced plastic (23).

Mechanical properties at angles other than those corresponding to the direction of the principally applied load are characteristically low, Figure 3. Experimental determination of the composite stresses σ_L, σ_T, and σ_{LT} (lateral, transverse and interlaminate respectively) allows for determination of the composite strength parameters at an angle θ from the axial direction. This is done by taking into account the cross sectional areas and resolution of forces.

Details of the derivation of the above relationship are not relevant; however, descriptive results of the work of Cooper and Kelly (8) in this regard are pertinent. Quality of the bond, classically assumed to be perfect for the sake of determinancy of the original composite model, is the critical factor in determination of strength in any direction.

Thus, it can be illustrated from the literature that the parameters of greatest importance in the formation of a unidirectional fiber reinforced composite are the volume fractions of reinforcing agent and the quality of bond developed between the fiber and matrix. Geometry of the fiber cross section does not appear to greatly influence the analysis, nor does the ductility of the matrix (1). The effects brought about by the introduction of discrete fiber length necessitate considerably more analysis.

Short fiber composites

Long fiber reinforced composites perform well when the application of loading direction and magnitude is known. When the load and its direction is not known, or can change, long fiber composites do not perform as well. In such cases, short, randomly oriented fiber reinforced composites may be preferred (1). Short discreet fibers, however, mean that the fiber's geometry will influence composite performance much more than in long fiber

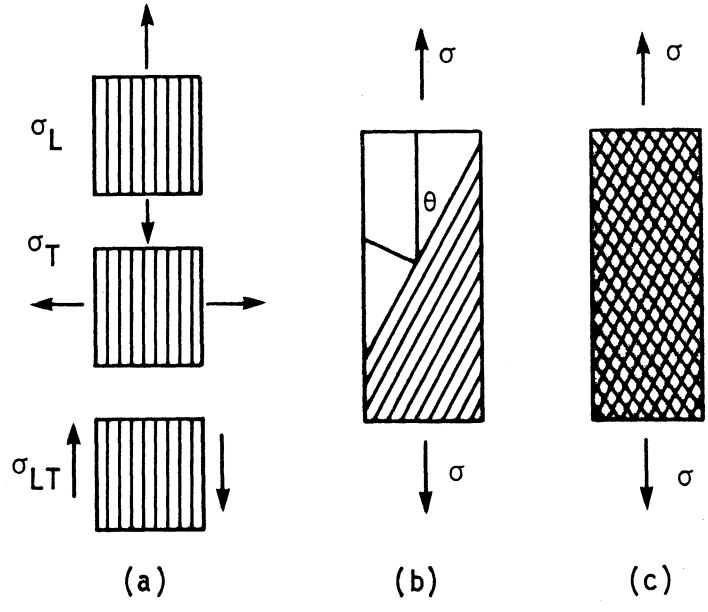

Figure 3. Strength and fiber orientation relations, (a) Strength in principal directions, (b) off-axis loading, (c) less critical dependence upon loading (23).

composites. The load transfer length of short fibers is a critical determination, and is related to the matrix shear strength, fiber diameter, and fiber stress by the following expression (1):

$$\ell_t = \frac{(\sigma_f)_{max} d}{2\tau} \tag{7}$$

where

ℓ_t = load transfer length; the minimum length to mobilize maximum fiber stress,

d = fiber diameter (d = a/b for fiber taper where a and b are the long and short sides of a rectangular cross section respectively),

$(\sigma_f)_{max}$ = maximum measured stress of the fiber,

τ = interfacial shear strength.

Through a rigorous derivation based upon equation 7, Agarwal and Broutman related ultimate fiber strength $(\sigma_f)_{ult}$ to critical fiber length (ℓ_c) independent of experimentally determined values (1).

$$\ell_c = \frac{(\sigma_f)_{ult} d}{2\tau} \tag{8}$$

This approach is generally used in composite analysis due to the difficulty in measuring actual fiber stress (1). As ℓ_c is based on ultimate fiber stress, so long as the bond with the matrix is perfect, the composite will fail by fiber rupture rather than fiber pullout if fiber length is greater than, or equal to, ℓ_c.

Use of short fibers means that fiber end stress conditions can not be neglected, and stress distributions along the fiber will vary. Assuming that the matrix is ideally plastic, Figure 4 indicates fiber stress distributions for various lengths of fibers. These stress distributions are only approximate, as most matrices actually exhibit elastic-plastic behavior (1).

It is often convenient, and without serious error, to consider the average stress ($\bar{\sigma}_f$) as expressed by the following equation (1).

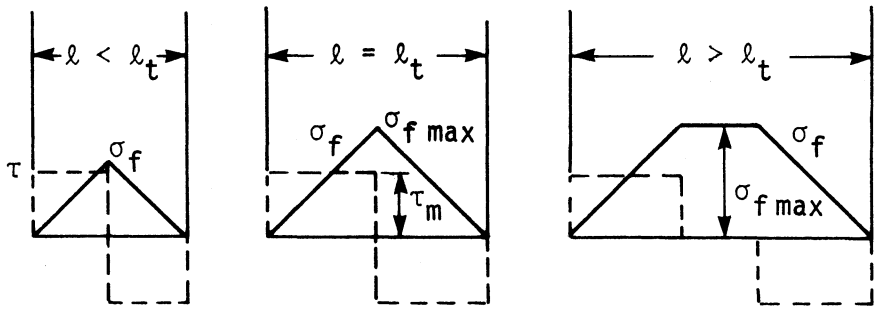

Figure 4. Varaiations of fiber stress and interface shear stress (τ) for different fiber lengths (1).

$$\bar{\sigma}_f = \frac{1}{\ell} \int_0^{\ell} \sigma_f \, d_z \tag{9}$$

where

ℓ = fiber length

σ_f = fiber stress, and

d_z = incremental fiber length.

Thus for the approximate stress distributions shown in Figure 4:

$$\bar{\sigma}_f = \frac{1}{2} (\sigma_f)_{max} = \frac{\tau_m \ell}{d} \qquad \text{where } \ell < \ell_t \tag{10}$$

$$\bar{\sigma}_f = (\sigma_f)_{max} \left(1 - \frac{\ell_t}{2\ell}\right) \qquad \text{where } \ell > \ell_t \tag{11}$$

It is important to remember that the above relationships were based on the assumption of linear elasticity, perfect fiber-matrix bonding, and ideally plastic behavior of the matrix. Numerical solutions and finite element analyses have been applied to specific complex problems but the approximate values are usually sufficient for design purposes (1).

A more generalized means of determining moduli for short fiber composites was developed by Halpin and Tsai (11). Expressions were derived for longitudinal and transverse moduli (E) of unidirectionally oriented fibers. Based on laboratory results, the moduli expressions were acceptable when the fiber volume fraction was less than unity. Unfortunately, this method of moduli calculation is not applicable to randomly oriented fiber composites, as irrational values are generated. Halpin and Tsai then developed an empirical relation for Young's Modulus of random fiber composites.

$$E_R = 3/8\ E_L + 5/8\ E_T \tag{12}$$

Where E is Young's Modulus, R, L, and T represent the randomly oriented fiber composite, longitudinal direction and transverse direction, respectively (11).

Short fiber composite theory thus illustrates several important assumptions, concepts and trends. Foremost is the basic assumption of perfect fiber-matrix bonding, which is approached in some plastic and resin matrix composites but not in fiber reinforced concrete. The concept of critical fiber length and the increasing role of fiber geometry becomes important in composites with randomly oriented, discreet fiber reinforcement. Trends involved with the fiber volume fraction present in the composite influences the composite performance.

Fatigue properties

In general, the resistance of fiber composites to fatigue damage depends on the type of fibers, type of matrix, fiber volume fraction, fiber orientation, interfacial bond strength, type of loading system,

frequency of loading, fiber length and environment (1). Fiber length is an important parameter due to its effect on the mechanism of fiber strengthening. In continuous fiber composites, the fibers carry a larger proportion of the fatigue load; in short fiber composites the fatigue load is shared between the matrix and the fibers (1). Short fiber composites made up of inorganic matrixes are generally less resistant to fatigue damage because the weak matrix sustains a larger portion of any cyclic load. Failure occurs by initiation of localized failures in the matrix, which eventually spread through the whole matrix (1).

In randomly oriented short fiber composites, fatigue damage is initiated by debonding of the fibers that lie perpendicular to the direction of loading, but propagation of fatigue cracks is controlled by the toughness of the matrix material (1). In brittle matrixes, cracks propagate easily and fast. For ductile matrixes, very few cracks are usually observed and failure is caused by massive debonding of the fibers and matrix. In most cases, fatigue cracks increase the degree of water permeability, which can lead to accelerated material deterioration (1).

In contrast to continuous fiber composites, very few fatigue studies have been done on discontinuous fiber composites, though it appears that fatigue damage is a function of the fiber volume fraction (1). Usually, the higher the fiber volume fraction, the more resistant the composite is to fatigue damage.

Compressive characteristics

Dow (28) suggested that the failure of a fiber composite under compressive load was due to the elastic buckling of the fibers. In his study,

he used an E glass fiber-epoxy resin system which was cured at a temperature of 250° F, and then allowed to cool to room temperature. Cooling of the system produced a shrinkage of the matrix which led to the development of compressive strain on the fiber. Photoelasticity studies were conducted on the system, and it was found that the stress pattern along the length of the fiber was repetitious, an indication that the fibers had buckled. It was also found that the wave length and amplitude of the buckling varied with fiber diameter (28). This phenomenon was found to be analogous to the buckling of a column on an elastic foundation.

In the above case, only one fiber was considered whereas an actual unidirectional fiber composite contains a series of parallel fibers. Therefore, an analytical model was developed (29). The model was considered to be two dimensional, having a series of parallel, equi-spaced, continuous fibers, and the load was assumed to be applied to the fibers only. For this model, two buckling modes were possible. Either all the fibers buckle at the same wavelength with the adjacent fibers out of phase, or all fibers buckle at the same wavelength and in phase with one another. The first was referred to as the extension mode, because the predominant form of deformation was extension. The latter was referred to as the shear buckling mode since the predominant form of deformation was shear (29).

In evaluating buckling stresses, an energy method was adopted wherein

$$\Delta u_f + \Delta u_m = \Delta T \tag{13}$$

where

Δu_f = change in strain energy of fiber

Δu_m = change in strain energy of matrix

ΔT = work done by fiber loads.

It can be recalled that loads were applied to the fibers only. Therefore, the work done by the fiber loads was the energy required to buckle the fibers and strain the matrix as the composite changed from the compressed but unbuckled state, to the buckled state.

From the basic energy relationship given above, the compression strength and critical vertical strain could be obtained for either the extension or shear mode from mathematical relationships given by Dow (28). Actual derivations of these relationships is beyond the scope of the study herein, therefore only the final equations are presented.

Within the extension mode

$$\sigma_c = 2V_f \left\{\frac{V_f E_m E_f}{3(1 - V_f)}\right\}^{1/2} \tag{14}$$

$$\varepsilon_{cr} = 2\left\{\frac{V_f}{2(1 - V_f)}\right\}^{1/2} \left(\frac{E_m}{E_f}\right)^{1/2} \tag{15}$$

whereas within the shear mode

$$\sigma_c = \frac{G_m}{(1 - V_f)} \tag{16}$$

$$\varepsilon_{cr} = \left\{\frac{1}{V_f (1 - V_f)}\right\} \left(\frac{G_m}{E_f}\right) \tag{17}$$

where

σ_c = compressive stress in the composite at time of failure

G_m = shear modulus of the matrix

ε_{cr} = critical strain or strain at which failure occurs.

From equations 14 and 15 it is apparent for the extension mode, that compressive stress and critical strain are a function of the fiber volume

fraction, and Young's modulus of both fiber and matrix. Equations 16 and 17 show that for the shear mode, the compressive stress varies with the fiber volume fraction and the shear modulus of the matrix material, and critical strain is a function of the fiber volume fraction, matrix shear modulus, and Young's modulus of the fibers.

Figure 5 (1) illustrates the variation of compressive strength with fiber volume fraction, for a composite made up of glass fibers incorporated into an epoxy matrix. Compressive strength increased with increasing fiber volume fraction to an optimum of 50%. Beyond this point, a decrease in compressive strength was observed. At low fiber weight fractions, the extension mode of buckling was critical, while at high fiber volume fractions the shear mode governed failure of the composites (1).

Fiber Reinforced Concrete

Serious evaluation of random fiber reinforced concrete has accelerated since the forming of the American Concrete Institute Committee 544 in 1966 (3). Determination of strength and various design moduli have evolved around fiber concentrations, orientation, and geometry, as well as the usual water-cement ratio, air content, density and other related factors. Development of a bond between the matrix and fiber is of critical importance (16). Experimental verification of fiber reinforced concrete has led to the application of classical composite theory.

Fiber reinforced concrete exhibits a failure pattern of a brittle matrix with tensile reinforcement (18). The stress-strain failure curve is linear up to a proportional limit, then non-linear to the ultimate strength value. There have been two traditional approaches employed in evaluating fiber reinforced concrete. The first relates the proportional

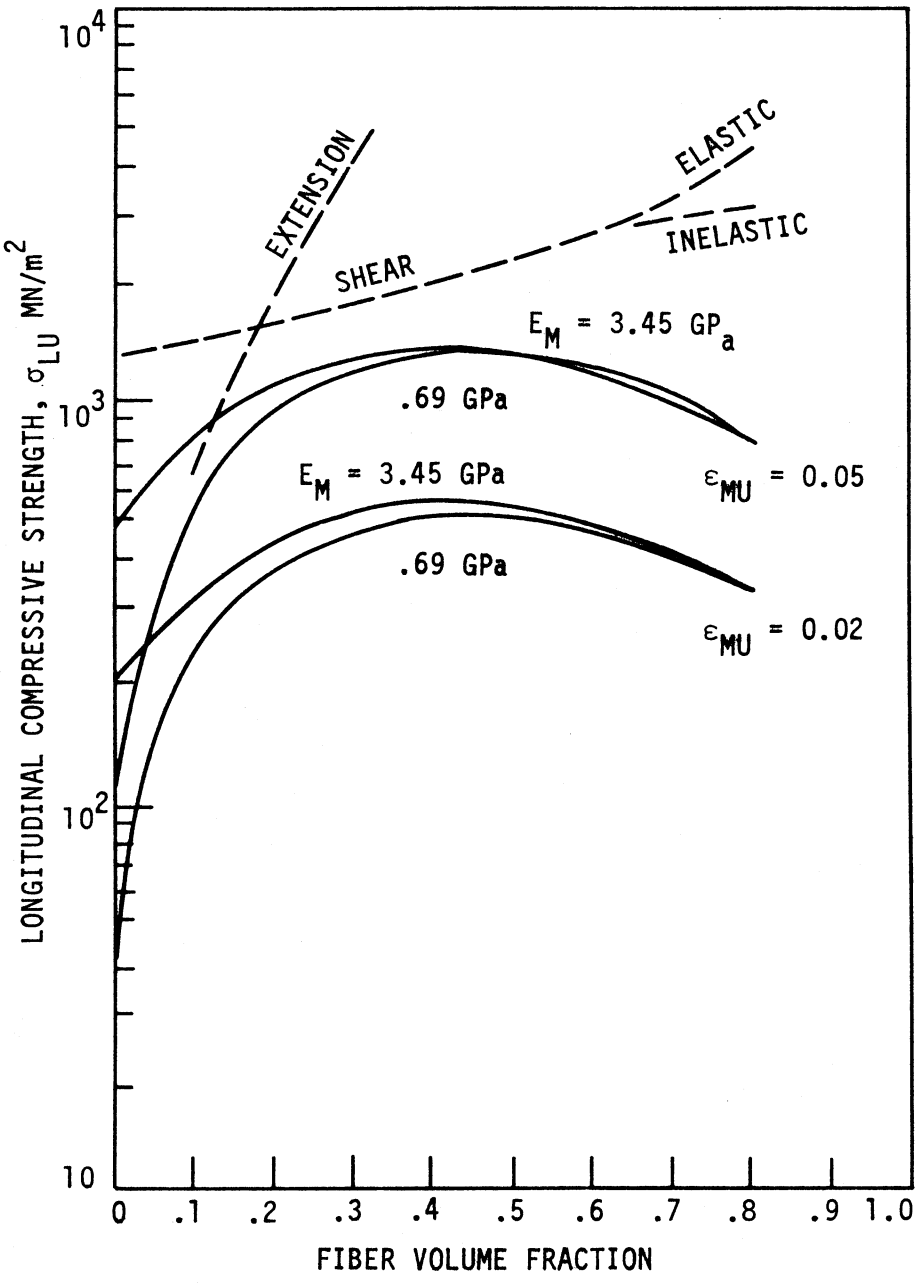

Figure 5. Variation of longitudinal compressive strength with fiber volume fraction (1).

limit to fiber spacing, while the second employs the Law of Mixes. A recent report by the American Concrete Institute (ACI) concluded that the ultimate strength of fiber reinforced concrete is relatively insensitive to fiber spacing but depends upon fiber volume, geometry and bonding characteristics (3).

Application of fiber composite theory follows that of short fiber composites. The basic assumption of perfect bonding, linear elasticity, and negligible effects of Poisson's Ratio are applied. However, the introduction of randomly oriented fibers coupled with the reality of non-perfect bonding and differing Poisson's Ratios of fiber and matrix, results in the addition of an efficiency factor, λ, into the Law of Mixes equation:

$$E_c = \lambda E_f V_f + E_m V_m \tag{18}$$

λ varies from $\lambda = 1$ for fibers oriented parallel to the force, to $\lambda = 0$ for fibers oriented perpendicular to the applied force (16). For randomly oriented fibers uniformly distributed over all directions, Krenchel, cited in Hoff (16), concluded that $\lambda = 1/5$. Stress distribution on fiber ends was considered by Pakotiprapha, cited in Hoff (16), which reduced λ by 0.52 to 0.64 times that of Krenchel (16). The range of values of λ appears related to the volume and type of fibers found in the composite. Application of classical composite theory to fiber reinforced concrete post cracking failure, follows a similar derivation to that of critical length, and determination of various moduli. However, in the ACI report, a third set of efficiency factors were introduced that accounted for the type of fiber used, and the matrix properties of various concretes. This led to a range of 0.17 to 0.80 for the overall efficiency factor (3).

Critical fiber length is also determined for fiber reinforced concrete.

The same approach is taken as with classical short fiber composite analysis. Equation 7 is applied with one important difference. If bond failure occurs, τ_m then represents the frictional bonding force between matrix and fiber, rather than the matrix shear strength, as the bonding is not perfect (24).

Investigations of fiber reinforced concrete indicate general trends that are of interest in evaluating fiber reinforced soil. Addition of fibers increased the tensile strength of concrete, up to a peak fiber volume fraction, beyond which no increase in tensile strength was observed (16). Bonding between the matrix and fibers, varied with fiber types and geometries. Round polypropylene fibers developed weak bonds, while employment of fibrillated polypropylene tape allowed the cement paste to work into the twists, developing a better bond. Increasing the length of polypropylene fibers also improved bond strength. Fiberglass fibers developed an even better bond with the matrix as indicated by significant increases in flexural strengths (up to 4.9 times greater than unreinforced concrete), as well as increased tensile strengths. The wide range of previously mentioned efficiency factors reflects the difficulty of attaining suitable bond strength between fiber and concrete. To improve this bond, it was found that increasing the fiber length generally attained a better bond and hence better reinforcing. One draw back to this trend is that increased length of fiber adversely affects the workability of the mix (16).

Soil-Fiber Composites

As previously mentioned, early work in earth reinforcement consisted of utilizing high modulus steel strips for reinforcing retaining walls (10). Other forms of reinforcement such as woven and nonwoven fabrics have more recently attracted attention and are finding wider applications in practice. Unlike metal strips, reinforcing fabrics have a much lower modulus (10). McGown, et al. (21) recognized these differences and classified earth reinforcement into two major categories, ideally inextensible and extensible inclusions. The former include the high modulus metal strips and bars; the soil reinforced with these materials being known as reinforced earth. The latter includes relatively low modulus natural and synthetic fibers, plant roots, and polymeric fabrics. Soil reinforced with these materials has been termed "Plysoil" (10). Properties of these two types of reinforced soil are summarized in Table 2.

Gray and Ohashi (10) conducted a study to ascertain the contribution of fiber reinforcement to the shear strength of sand, and how fibers modify the stress-strain response of sand. A related objective was to determine the consequence of fiber reinforcement on the stability of sandy slopes. A mathematical model based on limiting equilibrium of forces was developed, which identified important test parameters and fiber/sand variables. Direct shear tests were then run on dry fiber reinforced sand to confirm validity of the model.

The fiber reinforcement mathematical model was based on assumption that the fibers to be used were long, elastic, and extending an equal length on either side of a potential shear plane in the sand (10). Fibers were oriented either perpendicular to the shear plane, or at some arbitrary

Table 2. Comparative behavior of earth reinforcement (21)

Type of Reinforced Soil	Type of Reinforcement	Stress Deformation Behavior of Reinforcement	Role and Function of Reinforcement
Reinforced Earth (Vidal, 1978)	Ideally <u>inextensible</u> inclusions (Metal strips, bars, etc.) $E_R/E_S > 3000$[a]	Inclusions may have rupture strains which are less than the maximum tensile strains in the soil without inclusions, under the same operating stress conditions, i.e., $(E_R)_{Rup} < (E_S)_{max}$ Depending on the ultimate strength of the inclusion, in relation to the imposed loads these inclusions may or may not rupture.	Strengthens soil (increases apparent shear resistance) and inhibits both internal and boundary deformations. Catastrophic failure and collapse of soil can occur if reinforcement breaks.
"PLY-SOIL" (McGown, et al, 1978)	Ideally <u>extensible</u> Inclusions (natural and synthetic fibers, roots, fabrics, geotextiles) $E_R/E_S < 3000$	Inclusions may have rupture strains larger than the maximum tensile strains in the soil without inclusions, i.e., $(E_R)_{Rup} > (E_S)_{max}$ These inclusions can not rupture no matter their ultimate strength or the imposed load.	Some strengthening, but more importantly provides greater extensibility (ductility) and smaller loss of post peak strength compared to soil alone or to reinforced earth.

[a] E_R/E_S is the ratio of reinforcement modulus (longitudinal stiffness) to average sand modulus. The limits shown are tentative; reinforcement/sand modulus ratios for all materials tested ranged from 71-2940.

angle, i. Shearing distorted the fiber orientation, thereby mobilizing tensile resistance in the fiber. The tensile force in the fiber was divided into components normal and tangential to the shear plane. The normal component increased the confining stress on the failure plane, while the tangential component directly resisted shear. The fiber was assumed to be thin enough that it offered little if any resistance to shear displacement from bending stiffness.

The model showed that development of a fiber's tensile stress depended on a number of parameters and test variables; i.e., the fibers must be long enough and adequately frictional to avoid pullout, or conversely, the confining stress must be high enough so that pullout forces did not exceed skin friction along the fiber (10). This study also showed that distribution of tensile stress along the length of the fiber could be either linear or parabolic, with tensile stress being a maximum at the shear plane and decreasing to zero at the fiber ends.

Several equations were obtained from the model for computing shear strength of fiber reinforced sand at different fiber orientations (10). All equations used the mobilized tensile strength, instead of the actual tensile strength of the fibers. In practice, actual fiber tensile strength is seldom realized, because composites fail before the fibers break. But if a limiting upper boundary estimate for shear strength is desired, the actual tensile strength of fibers can be substituted for mobilized tensile strength. Also, using the actual tensile strength of fibers, the minimum fiber length necessary to prevent fiber pullout could be defined as follows:

$$L_{min} \geq \frac{T_R \cdot D_R}{2\tau_R} \tag{19}$$

where

L_{min} = minimum length required for full mobilization of fiber tensile strength

T_R = actual tensile strength of fiber

D_R = diameter of fiber

τ_R = skin friction stress along fiber.

The type of soil used for the laboratory investigation was a clear quartz beach sand, which had a mean grain diameter of 0.23 mm and a coefficient of uniformity of 1.5. Minimum and maximum void ratios were 0.50 and 0.73, the corresponding friction angles measured in direct shear were 39° and 31°, respectively (10). The types of fibers used were both natural and synthetic and were selected in such a way as to give a range of elastic moduli (longitudinal stiffness). Fiber diameters ranged from 1-2 mm, lengths from 2 to 25 cm, and their several properties are summarized in Table 3.

Table 3. Properties of fibers used to reinforce sand (10)

Type of Reinforcement	Diameter D_R (mm)	Skin Friction Angle, δ (degrees)	Tensile Strength, T_R (psi)[a]	Young's Modulus, E_R (psi) x 10^6
# 2 Reed[b]	1.8	30	4860	0.22
Plastic (PVC)	2.2	23	4500	0.30
Polmyra[c]	1.2	30	25800	2.4
Copper Wire	1.0	21	29000	8.5

[a] 1 psi = 6.89 kN/m^2.

[b] Common basket reed (phragmites communis).

[c] A tough fiber obtained from the African polmyra palm (Borassus flabelliformis) often used as a heavy duty broom fiber.

Laboratory testing was conducted using a standard laboratory direct

shear apparatus. The sand was tested dry, with and without reinforcement, in both the loose and dense states. Fibers were placed in a regular pattern at approximately equal spacings from each other, and from the sides of the shear box, and in either a perpendicular orientation to the shear plane or at some other predetermined orientation (10). The shear tests were strain controlled, both shear stress and vertical deformation being recorded as a function of shear or horizontal displacement up to a total displacement of 0.2 in (0.5 cm). Tests were run at a number of vertical confining stresses up to 144 kN/m^2 in order to completely define the shear strength envelope.

The theoretical model showed that six test parameters considerably influenced the behavior of fiber reinforced materials (10). These parameters were, (1) fiber length, (2) fiber diameter, (3) modulus of longitudinal stiffness of fibers, (4) angle of initial fiber orientation, (5) fiber concentration, and (6) vertical confining stress or shear strength of the matrix. During the laboratory investigation, as many of these parameters as possible were varied in a systematic fashion to ascertain their influence and determine the validity of the theoretical models.

The laboratory shear test investigation showed that fiber reinforcement of sand increased the ultimate shear strength of the composite and limited the reduction in post peak shearing resistance (10). Presence of fibers across the shear plane limited the amount of vertical deformation or dilatation of a dense sand. There was a minimum amount of fibers that were necessary for any increase in shear strength to be realized. Beyond this fiber content, the shear strength increased linearly with increasing fiber weight fraction up to a maximum fiber content where a levelling occurred, and further increase in fiber content did not enhance the shearing strength.

Maximum shear strength increase was obtained when the fibers were oriented at an angle of 60 degrees from the horizontal plane of failure in the direction of shear. This behavior was attributed to the tensile axis in a direct shear apparatus being at an angle of 60°, so full mobilization of a fiber's tensile strength occurred when the fibers were oriented at 60°. At an angle of 120°, a reduction in shear strength was observed. Fibers oriented at an angle of 90° portrayed the same characteristics as randomly oriented fibers. These findings suggested that a simpler perpendicular fiber reinforcement model could be used as a satisfactory mean approximation for predicting shear strength increases across a shear surface crossed by randomly oriented fibers (10). None of the tested fibers broke in tension. Fibers either pulled out, or stretched, depending upon confining stress, length and type of fiber. This behavior was consistent to what would be expected of plysoils (21), since the fibers have a higher modulus than the soil, and experience a considerable amount of elongation. Therefore, before the fibers break, the composite must experience a considerable amount of deformation which may not be possible since the soil matrix can not sustain large strains. In most fiber reinforced sand composites, it was found that less than 25% of the actual tensile strength of the fiber was usually mobilized.

MATERIALS

Soil Selection

The principle guideline for selection of soil matrices revolved around the employment of fiber reinforcement in potential field test sections. The overall project schedule for the investigation of soil fiber composites called for the construction of the first group of test sections

Table 4. Engineering properties of soils

Location	AASHTO Classification	Particle Size Distribution (%)				Liquid Limit, %	Plasticity Index, %	AASHTO T-99	
		Gravel (> 2.00 mm)	Sand (2.0-0.075 mm)	Silt (0.075-0.005mm)	Clay (<0.005 mm)			Maximum Dry Density, pcf	Optimum Moisture Content, %
Linn County;									
Troy Mills Section 1	A-6(2)	20	35	24	21	30.0	13.2	115.0	13.2
Troy Mills Section 2	A-2-4(0)	24	47	14	14	20.5	4.7	122.5	11.0
Prairieburg	A-4(0)	4	49	27	20	23.2	4.4	114.0	12.0
Story County;									
Mortenson Road	A-6(3)	18	38	24	20	34.0	13.7	114.5	14.5
Sioux City;									
West 3rd St.	A-4(2)	2	6	65	27	30.8	1.5	109.4	17.4
38th Street	A-4(0)	14	27	39	20	25.5	2.1	115.5	13.4
Borrow Pit	A-4(8)	0	1	82	17	33.0	6.4	103.5	17.9

in 1980. Coordination with the county engineers in Linn and Story Counties, plus the Director of Public Works in Sioux City, resulted in the selection of several secondary roads and streets as potential field test sites. Table 4 provides a synopsis of the soil/aggregate materials encountered in these sites. It should be noted that the sites were selected so as to represent a relatively wide range of soil properties.

Fiber Selection

As originally envisioned and proposed, the project reported herein included selection and testing of both natural and synthetic fibers. Natural fibers included wood chips, corn stalks and ground corn cobs, oat and flax straws, and manilla fibers. Initial laboratory results of natural fiber reinforcement were negative. In addition, such products were considered potentially degradable in an Iowa roadway environment, and as such were removed from further study by mutual consent of the Iowa Highway Research Board and ISU. Thus the project was concentrated on the availability and use of synthetic or man-made fibers.

Synthetic fiber selection involved a degree of familiarity with terminology utilized within the fiber industry. A brief summary of the most pertinent terms follows:

1. Fiber - As utilized in this project, a general term encompassing all filaments, yarns, bristles, staples and non-woven entities.

2. Filament - An untwisted, individual fiber. Filaments have a characteristically high length/diameter ratio and may be either crimped or uncrimped. Crimping is used to prevent filament separation when bundles are formed.

3. Yarn - Refers to a bundle or series of filaments twisted to

produce a single fiber in which the individual filaments cannot be separated.

4. Tow - A long continuous roll of a single filament, groups of filaments, or yarns.

5. Staple - A cut length of fiber, measured and expressed in inches; i.e., a one-inch staple refers to a cut length of one inch.

6. Denier - The weight in grams of 9000 meters of a fiber. Denier is an indirect measure for fiber diameter. For example, if 9000 meters of nylon filament weigh 100 grams, it is classed as a 100 denier filament. All subsequent fiber properties such as tenacity, elongation at break, elastic properties etc., are based upon the denier of the fiber. It is possible to convert denier to more conventional diametric measure by relating denier (grams/meter) to specific gravity, through the volumetric relation for a circular cylinder. As an example, a 75 denier filament would have a diameter corresponding to a fine textured human hair, while a 2500/250 denier yarn would correspond in size to packing twine. Finally, in regard to denier measure, a 2500/250 yarn of fiber denotes a fiber with a 2500 total denier measure but composed of 250 individual filaments each of which is 10 denier.

7. Aspect Ratio - In order to present fiber dimensions in a more conventional manner, an aspect ratio consisting of length divided by diameter is used herein. This is not terminology from the fiber industry, but appeared applicable to the purposes of this research project.

8. Tenacity - A measure of tensile strength expressed in terms of grams/denier. A 100 denier filament that breaks under a 250 gram load is rated at 2.5 grams/denier.

9. Elongation at break - Refers to the strain characteristic of the fiber; i.e., a measure of the amount of longitudinal deformation that

occurs prior to rupture, and expressed as a percentage.

10. Regain - Tendency of the material to absorb moisture.

An extensive literature search (including Corps of Engineers Waterways Experiment Station, Fort Belvoir Engineer School Library, etc.) yielded no information on fiber-reinforced soil, other than that presented in the Review of Literature. Because of the absence of information on this type of research, fiber selection for use in the project was quite arbitrary. Based on discussions with fiber industry representatives, it was realized that potential economic success of fiber-reinforced soil might possibly depend on employment of random length waste products, and a range of cut lengths were thus selected such that the impact of this variable could be evaluated. Also, different materials (i.e. nylon, polypropylene, etc.) possessing a variety of physical and chemical properties were evaluated. Some typical physical properties are given in Table 5, and a listing of fibers that were evaluated is presented in Table 6. In general, the nylon represented high strength and rigidity, while less of either property was displayed by the polyesters. The polypropylene, currently used in many geofabrics, is comparable to the lower range of the polyester strength/rigidity scale. It was hoped that by evaluating these varied fiber properties, some general criteria regarding strength and stiffness could be established.

Other factors which appeared significant in terms of successful soil reinforcement were: (1) fiber surface properties; (2) whether or not the fibers were crimped; and (3) rate of biochemical degradation. Based on available manufacturers literature and discussion with industry representatives, the best estimate of influence of these factors was that crimped

Table 5. Typical Fiber Material Properties[a]

Fiber Type	Specific Gravity	Tensile Str., psi, x 10^3	Tensile Modulus, psi	Elongation At Break, %	Elastic Recovery	Survivability	Approximate Cost, $/lb.
Nylon[b]	1.14	131.3	6 x 10^5	10 - 15	High	Mod.	2 - 4
Polypropylene	.91	64.1	1.1 x 10^6	70	High	High	.75 - 1.5
Polyester[c]	1.39	103.2	-[d]	30	Low	Mod.	2 - 7
	1.39	92.5	-	45	Low	Mod.	2 - 7
	1.39	71.2	-	60	Low	Mod.	2 - 7
	1.39	58.7	-	43	Low	Mod.	2 - 7
Type E Fiberglass	2.54	300	10 x 10^6	2 - 3.5	Low	High	<1.0

[a]Values obtained from manufacturers for fiber samples provided.

[b]Values for monofilament (whiskers) .9 mil diameter.

[c]Susceptible to alkaline decomposition.

[d]Average polyester tensile modulus 1.6 x 10^6 psi. Exact tensile moduli not provided by manufacturer.

Table 6. Synthetic fibers evaluated.

Manufacturer	Type	Denier	Staple, Inches	Remarks
Allied Chemical Company	Nylon	6	Tow	1260/204 Uncrimped Fiber
		7	Tow	2600/384 Uncrimped Fiber
Celanese	Polypropylene	1.5	.75	Crimped
		1.5	1.5	Crimped
		3	3	Crimped
		6	4	Crimped
Chevron Chemical Co., Vectra Corp.	Polypropylene	6	1.25	Crimped
			2.5	Crimped
			3.5	Crimped
			6	Crimped
		15	1.5	Crimped
			3.5	Crimped
			6	Crimped
			7	Crimped
E.I. DuPont de Nemours & Co.	Dacron 54	3	Tow	
		6	Tow	
	Nylon 54	6	Tow	
	Kevlar	-	.5	
			.75	
	Lycra	3-6	Tow	Yarn
	Tynex	3(mills)	Tow	
Hoechst Fiber	Polyester T121	1.5	1.5	High Intensity
	T221	1.5	1.5	High Modulus
		3	2	Normal Tenacity, normal modulus
		15	6	Pentalobal Cross section
Phillips Petroleum Co.	Polypropylene	3	.25	Uncrimped
			.5	Uncrimped
			.75	Uncrimped
			1.00	Uncrimped
Mini Fibers, Inc.	Polypropylene	15	.25	
			.75	
			1.5	
		360	.25	Fibrillated Tape
			.50	
			1.0	
			1.5	
Owens Corning Fiberglass	Type E	.008	.25	Tape
		.009	.50	
		.008	1.25	

fibers might be less effective than uncrimped versions, since (a) crimped fibers could potentially ball-up during mixing, and (b) an unknown portion of the crimping could be lost in a reinforced soil during compaction and before the fiber reinforcing contribution could be realized. Also, it was known that at least some of the synthetic fibers being evaluated were coated with various lubricants, used as an aid to fabric manufacturing processes. These lubricants ranged from water soluble, naturally derived coatings, to petroleum based products, and their influence was checked by testing washed fiber. Due to proprietary reasons, manufacturers did not divulge the coatings constituents, but provided instructions for their removal. In the initial selection of fiber types, the chemical and biological degradation characteristics were not considered. It was soon noted however, that most synthetic fibers are quite resistant to bio-chemical degradation.

As a consequence of the above evaluations, a series of arbitrary guidelines was initiated to select a group of fibers suitable to long term employment in a roadway soil system. Of considerable concern was the survivability of the material within the soil. The varying nature of the soil-water system in regards to alkalinity, chemical composition, temperature and environmental variations were taken into consideration.

Second, was the importance of procurement cost for the fibers. It was determined that high cost materials such as polyesters, Kevlar, and nylon, Table 5, should be eliminated as potential reinforcing agents based upon low cost effectiveness.

Third, was the ready availability of these materials in fiber cuts

that would allow for the range of length evaluation desired. All fibers listed in Table 6 represented those cuts available from manufacturers on an "off the shelf" basis. The fibers of Table 6 also represented a range of denier and maximum range of acceptable geometries. It should be noted that variations in these lengths and denier could be made commercially available. However, manufacturers required a minimal order of 1500-2000 lbs of fiber in order to justify resetting of their cutters to supply specially requested lengths.

A fourth consideration in the fiber material selection process was the range of mechanical properties of the materials. While this consideration might normally be of paramount importance, it was not felt to be a critical determinant for use in a soil-fiber composite. This was due to the suspected lack of strong interfacial bonding between the fiber and soil. As presented earlier, the quality of bond of a fiber to the matrix renders the matching of fiber properties to those of the matrix more critical. It was qualitatively determined that the degree of excellence of the soil-fiber interfacial bond would be considerably below that found in reinforced plastics, or fiber reinforced concrete. This assumption reduced the criticality of matching fiber properties to those of the soil as a means of controlling the mode of failure that might occur. All materials ultimately considered, possessed tensile strengths and moduli far in excess of any comparable properties encountered in soil systems, Table 5.

A fifth guideline in the final fiber selection involved the potential inability to properly incorporate fibers into the soil to a random state of orientation. Such inability would prohibit evaluation of the performance of fibers as a soil reinforcement. Therefore, it was decided

that mix-ability to produce a random orientation and uniform distribution would be a major guide in fiber selection. Fibers listed in Table 6 were combined with the Linn and Story County soils so as to determine incorporation feasibility. Mixing was accomplished in the laboratory by a hand folding mixing process to simulate blade grader incorporation, and by mixing with a laboratory pugmill mixer to simulate higher speed incorporation anticipated in the field if conventional travelplant processing were used.

In this series of testing, two pound batches of soil were separated, and varying weight fractions of fiber combined into the soil specimens. In cases involving the incorporation of fibers of less than 15 denier diameter, excessive fiber matting occurred regardless of fiber length or cross sectional configuration. The .009 inch diameter nylon whiskers, 15 dpf x 1.5 in. polypropylene monofilaments, 360 dpf x 1.0 in. fibrillated polypropylene tape, and .009 inch diameter Type E fiberglass fibers demonstrated acceptable mixing potential. Incorporation of these fibers at lengths varying from .25 inch to 1.5 inches resulted in uniformly random fiber distribution, in general without regard to type of mixing procedure used. Pug mill mixing did not effectively blend longer length fibers, mainly because the tines gathered and balled the fibers. Distribution of long relatively stiff fibers was as good as that achieved for shorter fibers, but appeared to influence compaction.

Based upon the results of the mixing study and upon the qualitative parameters expressed earlier, polypropylene and Type E fiberglass fibers were selected for extensive evaluation. These materials are currently

marketed in mat or fabric form for employment in geotechnical engineering problems, and have demonstrated a satisfactory resistance to biochemical degradation based upon field tests (11). In addition, fiber cuts of varying sizes and lengths, including fibrillated fibers of polypropylene, appear readily obtainable. Table 7 lists those fibers thus selected for detailed evaluation.

Fly ash can be melted at high temperatures and a fiberglass-like fiber can be produced. Fly ash is pozzolanic to cementitious, though it was unknown if fibers produced from fly ash would retain such qualities. Attempts were made to produce fly ash fibers in cooperation with the Materials Science and Engineering Department at ISU. Using ash obtained from the Neal IV power plant near Sioux City, results of fiber production were relatively poor since the process used was unable to control either size or quality of the resulting fiber. A small sample of fibers was received from a commercial firm that was also investigating fly ash fiber production. The fibers were of better quality, but length and diameter still varied considerably. Such fibers were used however in limited portions of the laboratory study.

LABORATORY INVESTIGATION

Selection of testing procedures was based on their relevance to the research proposal of effects of fiber reinforcement on roadway soils, and the need for a relatively rapid evaluation of data for (1) selection of fibers showing potential for field trials, and/or (2) more detailed laboratory investigations.

Table 7. Fibers selected for primary evaluation.

Fiber Type		Fiber Diameter, in	Fiber Length, in	Cost per Pound, $[a]	Manufacturer	Remarks
Type E Fiberglass	885BB 1/4 in.	.008	.25	0.69	Owens Corning Fiberglass	Fibers come as chopped strand tape and break into individual fibers upon mixing.
	832BB 1/2 in.	.008	1.25	0.69		
	453BB 1/2 in.	.009	.50	0.69		
Polypropylene	15 dpf x 1/4 in.	.002	.25	.92	Mini Fibers, Inc.	Round cross-section, monofilaments
	15 dpf x 1/2 in.	.002	.50	.92		
	15 dpf x 1.5 in.	.002	1.50	.92		
Polypropylene	15 dpf x 1.5 in.	.002	1.50	-	Chevron Chemical Co., Vectra Corp.	Crimped, monofilament
Polypropylene Fibrillated Tape	360 dpf x 1/4 in.	.009	.25	.65	Mini Fibers, Inc.	Multifilamentary tapes twisted in manufacture to maintain cross section upon mixing. Employed in fiber reinforced concrete evaluations.
	360 dpf x 1.0 in.	.009	1.0	.65		
	360 dpf x 1.5 in.	.009	1.5	.65		
Fly Ash Fiber	-	-	-	-	Not commercially available	Fiber diameter and length varied

[a]Per pound costs noted herein are 1980-81 quotations and are presented as a means of relative cost comparison only. 1982 costs appear to be higher, but only fragmentary information is available.

Due to the variable length of fibers employed in this study, most of the test procedures utilized Proctor size specimens (4.56 inches deep by 4 inches in diameter) to insure random dispersion of fibers within each compacted specimen. Mixing of fibers was generally accomplished by a combination of hand and scraper folded machine mixing. All Proctor size specimens were molded with an automatic compactor in accordance with ASTM D698, wrapped and sealed, and placed in a controlled environment at about 72° F and near 100% relative humidity for a minimum of 24 hours prior to testing, the length of cure depending on the type of test being conducted.

Calculations of much of the data were performed on a Sol remote computer, with ICOM magnetic disc reader. Raw test data were entered into the system, checked for accuracy of entry, and subjected to required calculations discussed within the test descriptions. Where needed, P-plot capabilities of the SOL computer were also utilized.

Iowa K-Test

The Iowa K-Test employed Proctor size specimens placed into a split restraining, constant elasticity mold, and vertically loaded (30). The test is essentially a rapid stress-path triaxial test in that the constantly changing lateral deflection of the split mold is monitored as well as the applied vertical load and deformation. Through knowledge of the elastic stress-strain calibration of the mold coupled with the measurement of vertical and horizontal strains for specific loadings, values of engineering properties can be continuously calculated. The ratio of

horizontal to vertical stress yields K, the nominal uncorrected lateral pressure ratio. The vertical deformation modulus, E, and Poisson's Ratio, μ, as defined in soil mechanics, are obtained from manipulation of the vertical deformation of the specimen and the tangential expansion of the mold. The shear parameters of cohesion, c, and friction angle, ϕ, are calculated through a linear regression of the p-q diagram, the latter representing the plots of peaks of Mohr's Circles constructed for each loading condition. Shear parameters c and ϕ were also utilized for computation of ultimate bearing capacity (Q_o), rendering each test result more readily comprehensible in terms of composite strength, and more able to be correlated to the unconfined compressive strength values obtained for like specimens. To this purpose, Terzaghi's classic equation for the calculation of bearing capacity of soil under a circular footing was applied. A 12 inch diameter bearing area was selected as representative of the bearing area of a set of dual tires thereby reducing the classical equation from

$$Q_o = cN_c + \gamma D_f N_q + \frac{1}{2}\gamma B N_\gamma \tag{20}$$

to

$$Q_o = 1.2\ cN_c + \gamma D_f N_q + 3.6\ \gamma N_\gamma \tag{21}$$

which included the shape factors for a circular footing and where

c = cohesion

D_f = depth of footing; 0 inches in this case

γ = soil unit weight

N_c, N_q, and N_γ are empirical bearing capacity factors dependent on ϕ.

In more conventional composite materials, the number of variables introduced into the system is of a relatively low level due to the ability to predict and control properties of the matrix. Given the variable nature of soil, coupled with random orientation of the reinforcing fibers, plus the variations by addition of different fiber types and sizes, moisture contents, etc., the difficulty of data analysis for a soil-fiber composite became evident. To this latter effect, the Statistical Analysis System (SAS) available at the Iowa State University Computer Center was employed. That program of greatest value to this initial phase of soil-fiber composite analysis was the SAS procedure determining the best least squares regression based upon correlation coefficients and levels of confidence. In addition, the SAS capability to perform multivariable as well as single variable regression analysis was employed in an attempt to develop some form of predictive relationships. Analysis was performed on the data gleaned from combinations of the several soils, 10 fibers, and varying moisture contents. For each specimen produced, the variables of dry density, moisture content, fiber content, and fiber geometry were evaluated.

To illustrate the SAS technique employed, the following example is provided. The input of raw data was made and graphically represented as in Figure 6. The response in this case was bearing capacity, Q_o, compared to the single variable of moisture content. SAS analysis indicated that the best correlation between the response, Q_o, and moisture content of the specimens was the quadratic equation $Q_o = 1920 - 17.8\ w^2$, where w = specimen moisture content. The correlation coefficient, R, equaled 0.85, signifying

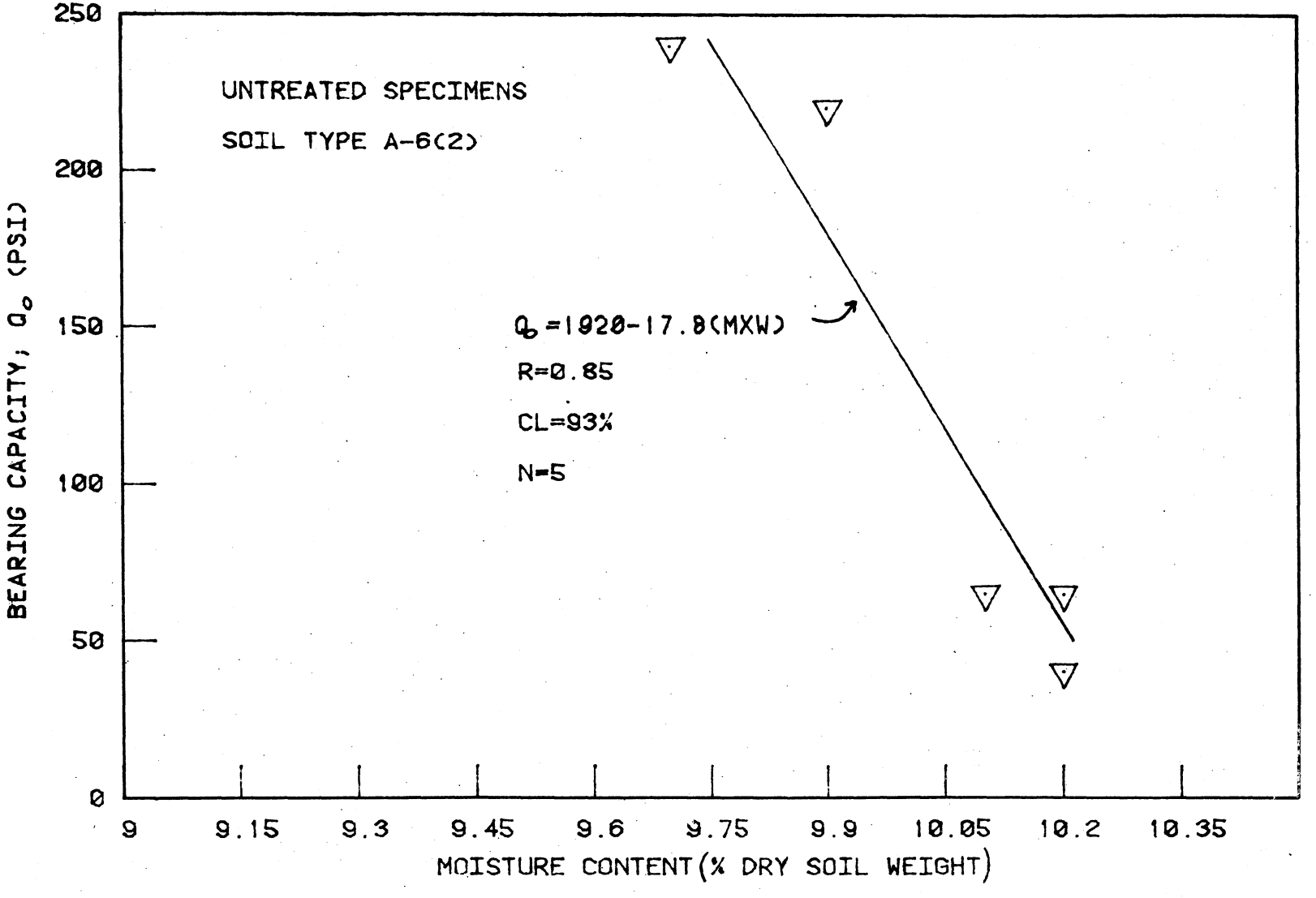

Figure 6. Sample relation for bearing capacity and moisture content.

that 85% of the variation observed in this data was attributed to the functional relationship, and the remaining 15% was due to experimental error, variability in test procedures and/or materials. The greater the value of the correlation coefficient, the more representative the relationship of the raw data. Similarly, the confidence level, CL, was 93%. In short, the confidence level provides an indication of the worth of overall analysis.

The addition of fibers to the matrix however, introduced a multivariable system requiring a three dimensional solution. The raw data display for a system where the response, R_e, is a function of two variables, x and y, is represented as a plane surface as hypothetically illustrated in Figure 7. In the example case, the response was Q_o and the variables x and y were moisture and fiber contents. The SAS multivariable regression provided a relationship for the response produced from the desired variables, for whatever level of confidence or correlation coefficient was deemed acceptable. A general form of this relation would appear as

$$R_e = \beta_o + \beta_1 C_f + \beta_2 w + \beta_3 C_f^2 + \beta_4 w^2 + \beta_5 C_f w + \beta_6 C_f^2 w \text{ etc.} \qquad (22)$$

where

R_e = response (bearing capacity, cohesion, friction angle, etc.)

β = constants determined from the SAS analysis

C_f = fiber weight fraction by dry unit weight, %

w = moisture content, %.

Figure 8 represents a raw data plot for a single soil with varying moisture contents and fiber weight fractions. The presentation in two

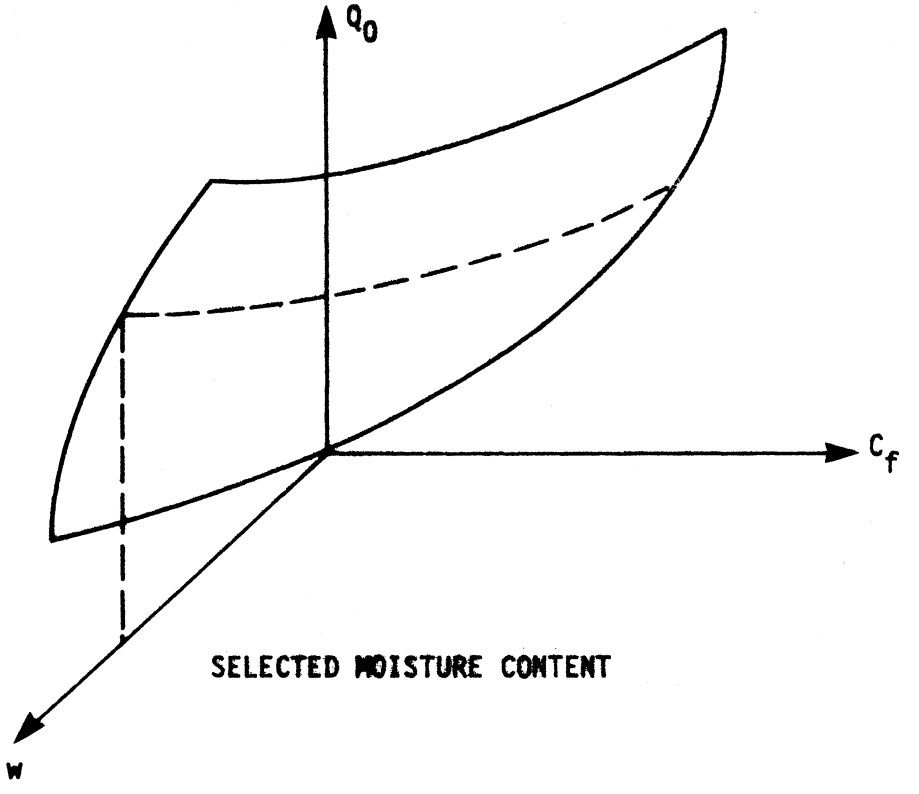

Figure 7. Three dimensional representation of response versus treatment.

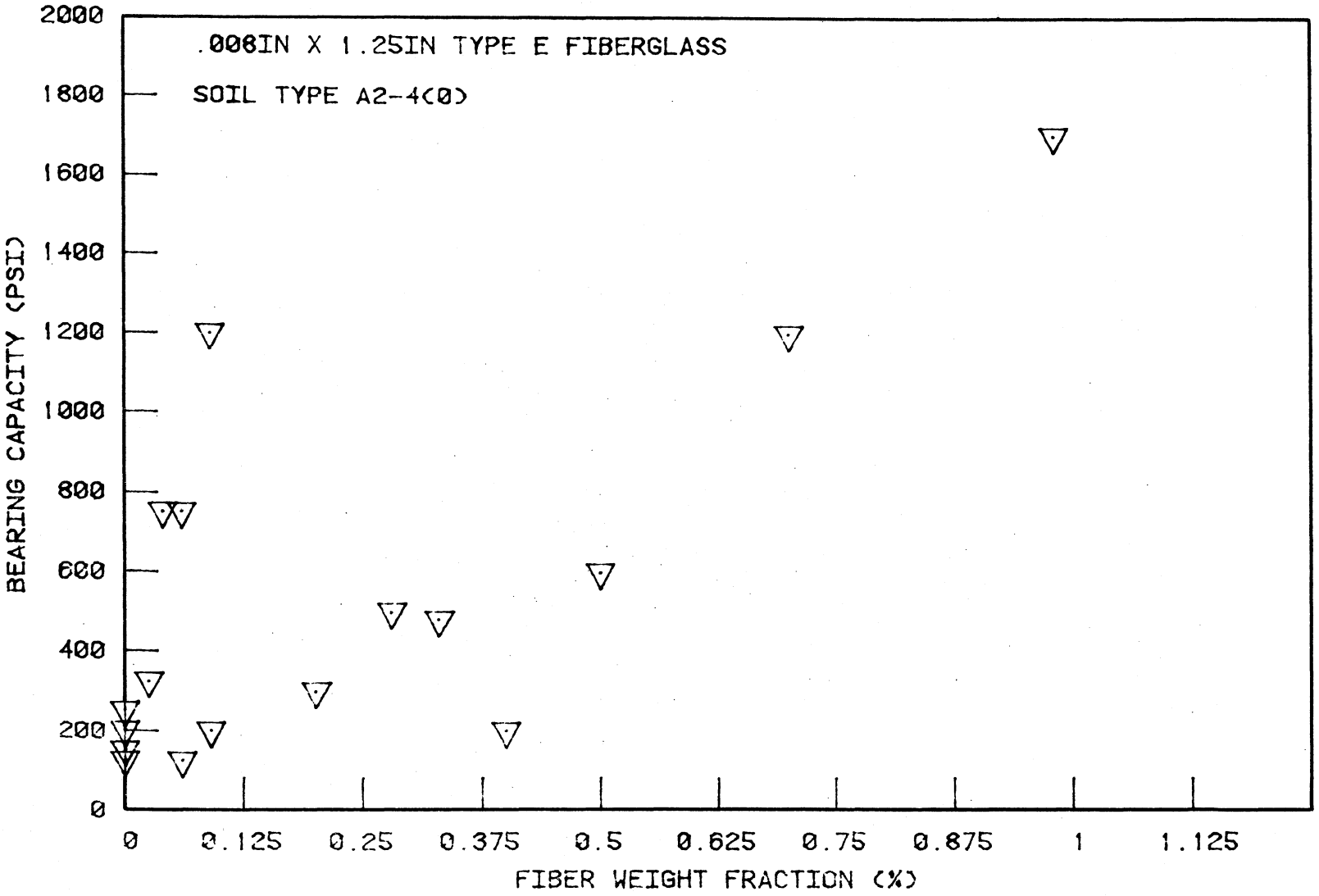

Figure 8. Sample data for bearing capacity versus fiber content.

dimensions, of the three dimensional system, presents a picture of considerable scatter, as Figure 8 represents in two dimensions the theoretical surface described in Figure 7. The SAS response having the highest correlation coefficient, R, for this data was $Q_o = 32726.0 + 747C_f - 6174w + 291w^2$, where R = .90 and CL = 99.99 for a sample size of 17 observations. With this relationship known, the data were then presented in a more understandable manner by setting either the fiber content or moisture content equal to a constant value. Doing this for moisture content produced a plot in the form of Figure 9. The presence of only three variables in the response, C_f, w, w^2, indicated that other terms did not appreciably effect the accuracy of the model.

Additional variables, if desired, could be added into the SAS model thereby raising the dimensionality of the equation with each additional term.

For purposes of this study, the minimum criteria for acceptance of any model were that the model possess a correlation coefficient, R, of not less than .75, since it was felt that in order to justifiably support conclusions drawn from the examination of test results, the model must describe at least 3/4 of the data presented.

Results from 276 Iowa K-Tests performed on the Linn County A-2-4(0) soil, were analyzed utilizing the methodology and qualifications noted in the previous paragraphs. Of these tests, 186 were performed after a minimum cure time of 24 hours while the remaining 90 tests were performed after termination of a 10 day freeze-thaw subjection. The analysis of K-Tests and KF-Tests (K-Tests conducted after subjection to freeze-thaw)

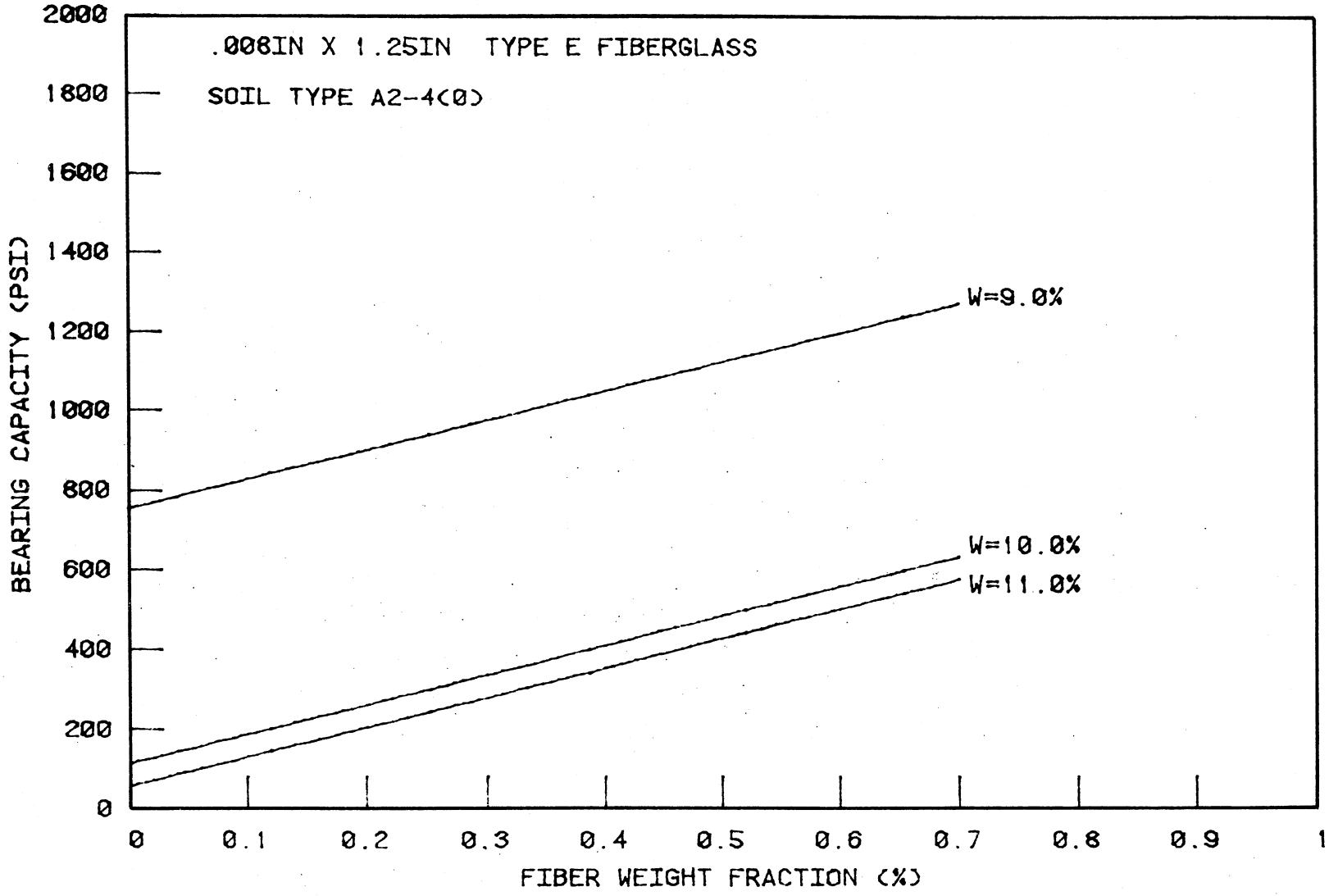

Figure 9. A typical two variable model at normalized moisture contents.

was performed separately. Modeling was attempted for the four test parameters of E, ϕ, c, and K, and for the calculated bearing capacity, Q_o. Moisture content utilized in the evaluation was of the sample at the time of test. Results of the SAS analysis for each parameter are listed in Table 8 by fiber type and size. Values of R included in the table represent the highest correlation coefficients attained from the statistical analysis regression. No K-Tested soil-fiber composite series produced any appreciable correlation for the model employed, thereby indicating a randomness in the data that would preclude the establishment of any predictable trends, utilizing the chosen model.

In spite of considerable care taken to insure uniformity of specimen preparation and test performance, it was decided that a highly controlled series of K-Tests were to be conducted in order to eliminate experimental error as a possible source of lack of data correlation. To this effect, a series of 23 specially prepared specimens was molded. Moisture content was kept as close to standard optimum as possible, and 360 dpf x 1.0 in. fibrillated polypropylene fibers were incorporated into the soil at varying percentages. Results were then subjected to the same SAS modeling as were the original K-Tests. Table 9 illustrates the fruits of this evaluation.

A similar special series of specimens were constructed, subjected to freeze-thaw action, K-Tested, and analyzed. Tables 10 and 11 illustrate the statistical modeling results obtained from these, as well as from the original KF-Test data. Tables 10 and 11 indicate that various test responses for the K and KF Tests approached or exceeded the minimum correlation coefficient required for further analysis.

Table 8. SAS results of K-Test specimen modeling, soil type A2-4(0) Linn County, Iowa

Fiber Type	Response	R	CL	Sample Size N
Polypropylene	Q_o	.48536	.9201	64
15 dpf x .75 in.	ϕ^o	.39266	.6171	
	c	.41924	.7310	
	K	.43931	.8039	
	E	.54931	.9854	
15 dpf x 1.5 in.	Q_o	.47382	.8615	60
	ϕ^o	.43311	.7303	
	c	.47357	.8609	
	K	.45752	.8152	
	E	.56651	.9857	
360 dpf x 1.0 in.	Q_o	.56165	.9967	72
	ϕ^o	.36339	.5743	
	c	.46777	.9364	
	K	.39446	.7289	
	E	.54513	.9938	
360 dpf x 1.5 in.	Q_o	.69483	.9995	63
	ϕ^o	.54779	.9366	
	c	.55637	.9479	
	K	.59972	.9832	
	E	.55784	.9496	
Type E Fiberglass	Q_o	.43989	.8870	73
.008 in. x .25 in.	ϕ^o	.35840	.5745	
	c	.49915	.7900	
	K	.36004	.5827	
	E	.58848	.9991	
.009 in. x .50 in.	Q_o	.50198	.9590	
	ϕ^o	.48385	.9355	
	c	.59451	.9981	
	K	.43153	.8111	
	E	.63787	.9997	
.008 in. x 1.25 in.	Q_o	.65143	.9999	
	ϕ^o	.44440	.8681	69
	c	.53759	.9869	
	K	.42073	.7958	
	E	.52706	.9839	

Table 9. SAS evaluation results of special series Iowa K-Tests for 360 dpf x 1.0 in. fibrillated polypropylene fibers, and soil type A2-4(0), Linn County, Iowa

Response	R	CL	N
Q_o	.69096	68.53	23
ϕ	.63683	50.56	23
c	.63542	50.10	23
K	.61182	42.31	23
E	.70699	73.48	23

Table 10. SAS evaluation results of KF-Test conducted after freeze-thaw subjection, soil type A2-4(0), Linn County, Iowa

Fiber	Response	R	CL	N
Polypropylene				
15 dpf x 1.5 in.	Q_o	.721936	99.98	34
	ϕ_o	.72420	98.67	34
	c	.72423	98.67	34
	K	.78432	99.76	34
	E	.68530	96.90	34
Fibrillated tape				
360 dpf x 1.0 in.	Q_o	.74460	99.86	50
	ϕ_o	.88560	99.99	50
	c	.56110	88.50	50
	K	Not evaluated		
	E	.74220	99.78	50
Fiberglass Type E				
.008 in. x 1.25 in.	Q_o	Not evaluated		34
	ϕ_o	.90010	99.99	34
	c	.39260	33.90	34
	K	Not evaluated		34
	E	.75640	99.43	34

Table 11. SAS evaluation results of special series Iowa KF-Tests conducted after freeze-thaw evaluation, soil type A2-4(0) Linn County, Iowa

Response	R	CL	N
360 dpf x 1.0 in. fibrillated polypropylene fibers			
Q_o	.53124	14.05	22
ϕ	.78859	86.31	22
c	.49007	8.20	22
K	.70804	63.66	22
E	.56818	32.34	22

A series of sixty-one specimens were prepared using the Sioux City West 3rd St. soil and fiber weight fractions from 0 to 0.5 percent of 360 dpf fibrillated polypropylene fibers, one inch length, over a range of moisture contents. Results of the SAS model are summarized in Table 12 and presented graphically in Figures 10 through 13.

The generated models, as well as the raw data points, appeared to indicate that addition of this fiber was detrimental to the performance of the soil-fiber composite. Values of c, ϕ, and E decreased from the untreated soil specimens for fiber weight fractions up to about 0.2 percent. A slight increase was then observed up to the maximum 0.5 percent. Values of stress ratio, k, slightly increased with increasing fiber weight fraction. The SAS model for Q_o did not meet the correlation coefficient criteria.

K-Test results of the Sioux City soil were checked by utilizing the unconfined compression test with the same fiber and soil at the same moisture contents. Unconfined strengths were improved at fiber weight

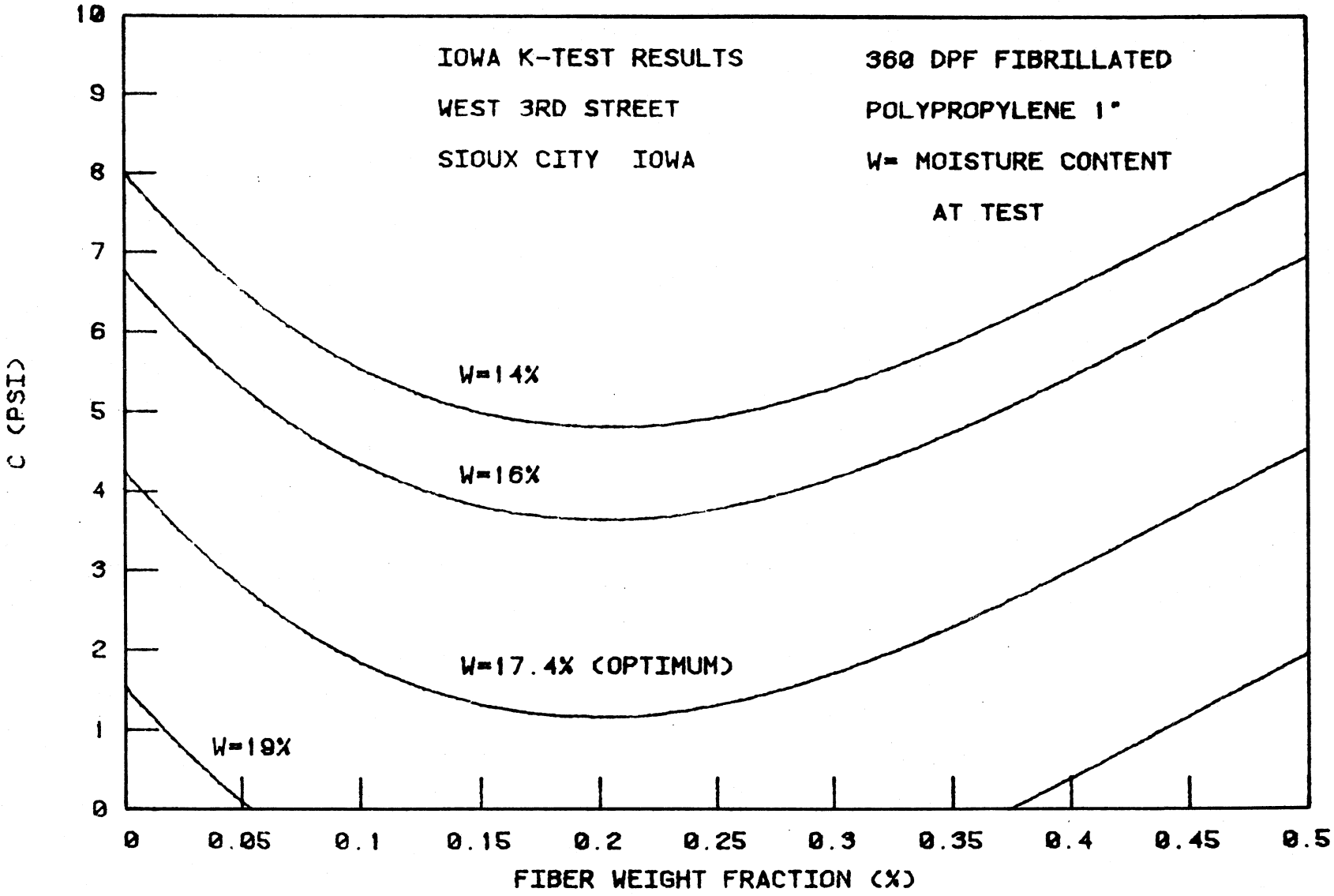

Figure 10. Cohesion versus fiber weight fraction.

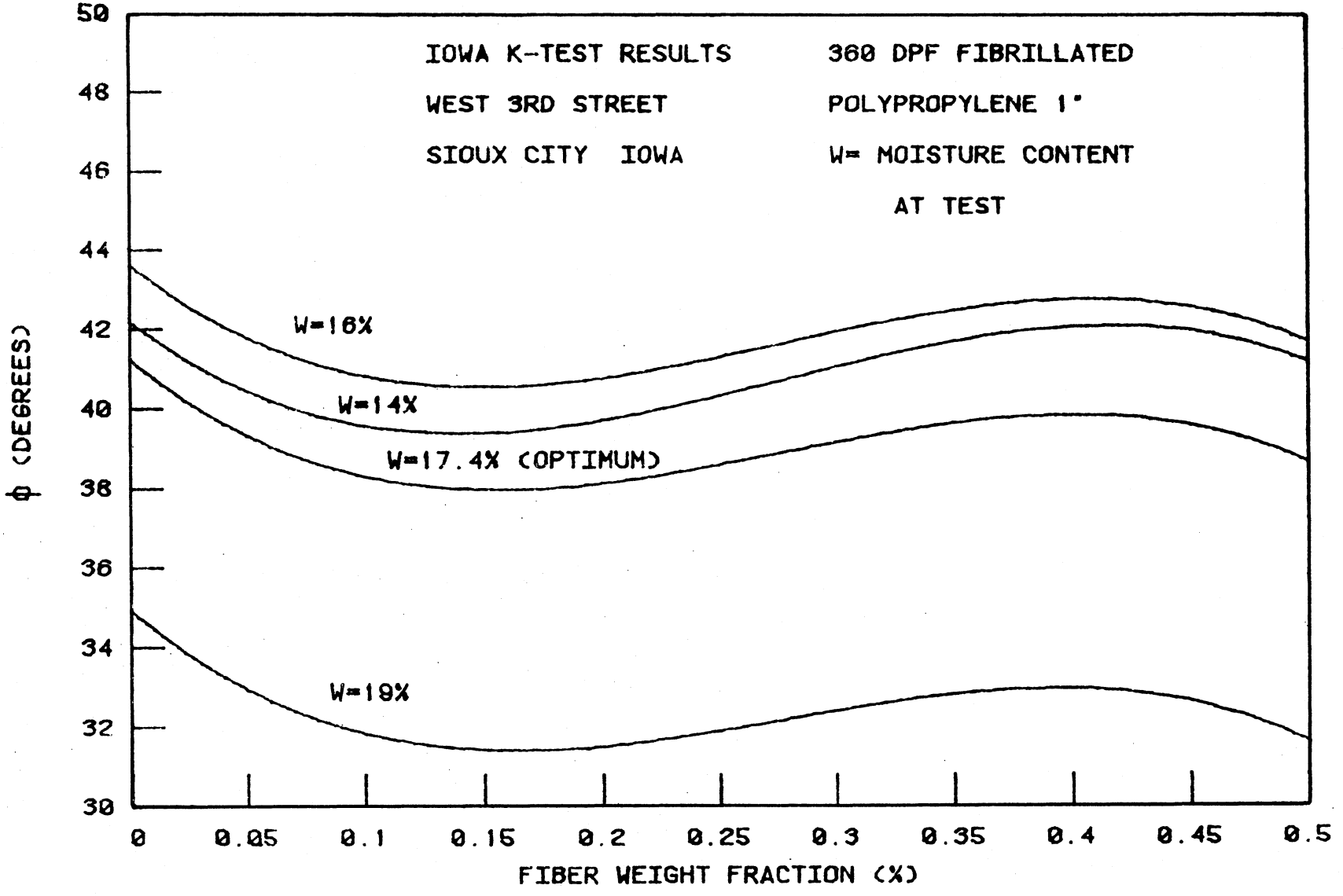

Figure 11. ϕ versus weight fraction.

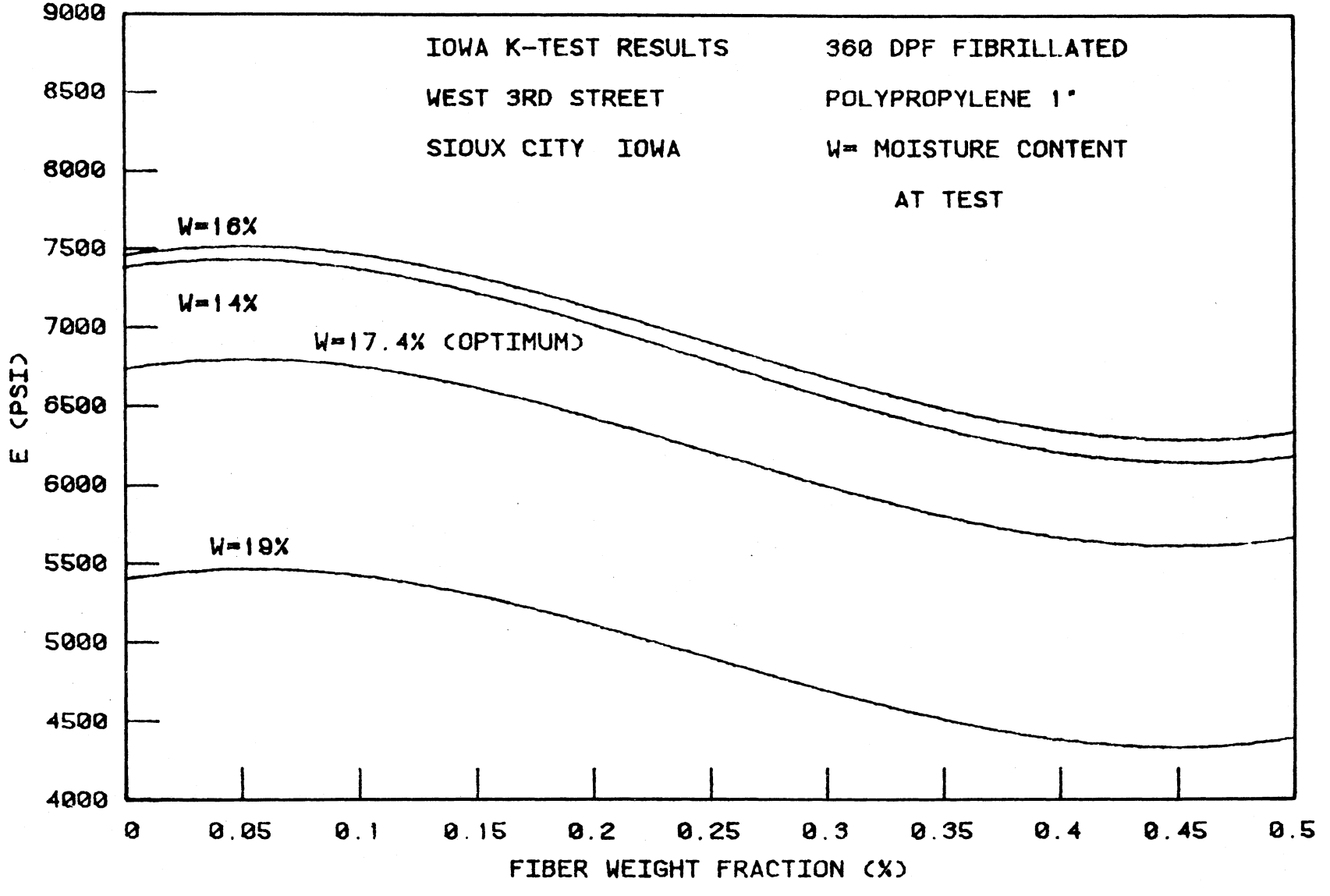

Figure 12. E versus fiber weight fraction.

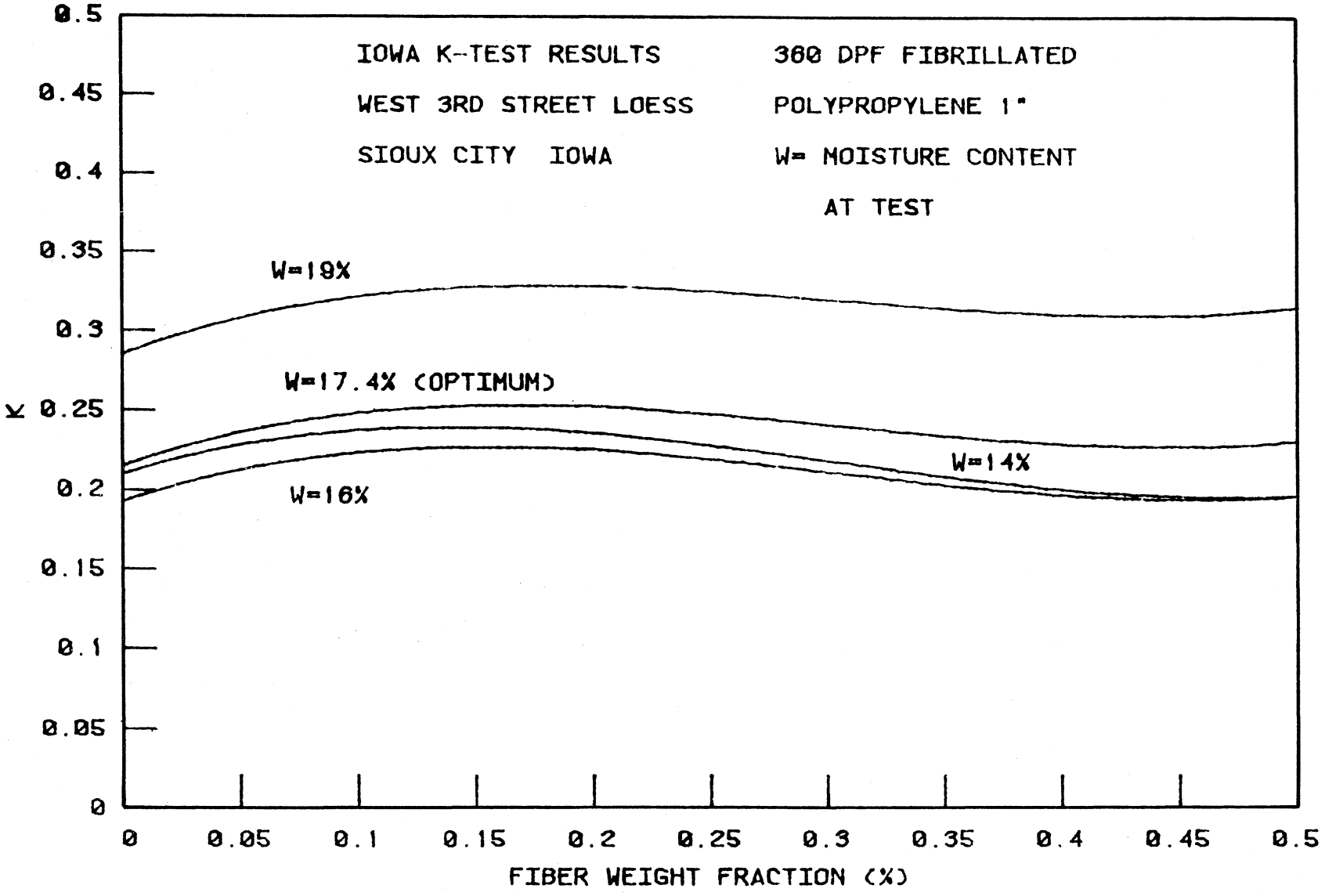

Figure 13. Stress ration versus fiber weight fraction.

Table 12. SAS regression models[a] of Iowa K-Test results of 1 inch, 360 dpf fibrillated polypropylene fiber composites, West 3rd Street soil, Sioux City, Iowa

R_e	B_o	B_1	B_2	B_3	B_4	B_5	B_6	B_7	r	Moisture Measure[b]
Q_o	-	-	-	-	-	-	-	-	0.7209	M
Q_o	-	-	-	-	-	-	-	-	0.7041	A
ϕ	-134.4	-65.1	23.9	235.7	-0.9	-238.0	0.005	0.3	0.9037	M
ϕ	-105.6	-31.9	17.9	216.0	-0.4	-260.1	-0.006	-0.9	0.9106	A
c	-234.1	-54.4	43.9	140.1	-2.6	-93.8	0.05	0.5	0.8355	M
c	-365.6	-36.8	68.0	110.8	-4.0	-82.4	0.08	0.15	0.8411	A
E	17,070.5	-6365.4	-2557.1	-15,272.1	-218.2	29,437.4	-6.0	275.4	0.8260	M
E	-73,330.6	1133.0	13289.5	-27,756.5	-694.5	36,973.8	11.2	79.1	0.8510	A
k	2.11	0.63	-0.25	-2.34	0.01	2.05	-	-	0.9108	M
k	0.36	0.24	0.08	-2.27	-0.01	2.51	-	0.02	0.9123	A

[a]Confidence limit = 99.9 for all models.

[b]M = moisture measured at molding; A = moisture measured after testing; moisture contents range 12.5 to 21.1 percent.

fractions above 0.1 percent.

Further expenditure of resources on the evaluation and subsequent testing required to define modeling problems encountered with the K-Test did not appear warranted. However, the general lack of correlation among the K-Test results, and to a lesser extent those results from the KF-Test series, necessitated some form of cause-effect analysis at a macroscopic level.

The lack of predictability in the test results was thus felt to have occurred due to one or a combination of four factors:

1. A randomization induced in the soil matrix due to incorporation of fibers.

2. A randomization induced through experimental error and lack of conformity in the test procedure.

3. The inability of the test to measure phenomena occurring within the stressed specimen.

4. A randomization induced due to variability between specimens regarding fiber distribution and specimen preparation.

While each of these hypotheses undoubtedly contributed in part to the lack of correlation in the data, the inability of the stiff constant elasticity K-Test mold, to accurately measure tensile reinforcement of the soil-fiber composite was most probably the weighted factor. The strict control in specimen preparation, fiber mixing and testing exercised during the special series of K and KF tests did not significantly improve the quality of data as reflected by the SAS modeling. Random orientation of fibers in a specimen would induce a certain randomness to the data, provided

this composite system followed the trends established by more conventional fiber reinforced materials; however, subsequent SAS analysis of unconfined compression test data tended to discredit this assumption. The answer appeared to lie in the confining nature of the semirigid constant elasticity mold, which did not allow sufficient radial strains to develop within each specimen. Were the interfacial bonding between fiber and soil perfect, a limitation of radial strain would not affect the ability of the matrix to transfer induced stresses to the fibers, thereby utilizing their greater tensile strength properties. However, the bond between the fibers and soil was far from perfect if analyzed in the composite technology sense. This relatively poor bonding coupled with the confined nature of the test, combined to render this form of K-Test inapplicable to the evaluation of fiber reinforced soil specimens.

To place the above hypothesis in a somewhat different perspective, any reinforcing mechanism of fiber seemed to require large strains in order to become apparent. The stiff constant elasticity laboratory K-Test mold prohibited the amount of radial strain necessary to mobilize fiber reinforcement. Addition of fibers reduced maximum dry density of the composite when compared to untreated soil. The stiff mold then caused the K-Test to act more like a consolidation test, with the soil matrix failing in shear prior to mobilizing fiber reinforcement.

Unconfined Compression Testing

In view of the Iowa K-Test results, the unconfined compression test was selected as an evaluative procedure for screening of fiber reinforcement of the several soils. Standard Proctor specimens were tested in accordance with ASTM D2166 on a Soil Test AP-170 unconfined compression testing unit at a deformation rate of 0.1 inch per minute. Failure was defined as the maximum load achieved during the test. Sufficient readings of vertical deformation versus load were taken to obtain data for complete stress-strain analysis. Values of the unconfined compressive strength, q_u, Young's Modulus, $E = \sigma/\varepsilon$, and strain at failure, ε, were obtained from the stress-strain plots. Application of the SAS procedures and models, resulted in a number of satisfactory correlations for models involving each of the preceeding responses.

Several specimens were prepared for each selected fiber weight fraction over a spread of moisture contents, generally ranging from below to above standard optimum moisture. In this manner, any trends in fiber reinforcement could be observed when compared to the results of similarly prepared untreated soil specimens.

Linn County soil

Utilizing the Linn County A-2-4(0) soil, 134 unconfined compression tests were performed with seven different fibers. Two of these fibers, .008 in. x .25 in. and .009 in. x .50 in., Type E fiberglass were not subjected to the statistical analysis as they failed to demonstrate any improvement in unconfined compressive strength regardless of fiber weight fraction.

Figure 14 is a plot of the raw data values for unconfined compressive strength versus fiber weight fraction for the 0.25 inch Type E fiberglass fibers. Taking the average value of compressive strength for untreated specimens within the same moisture range as the treated specimens, and superimposing this value onto the raw data plots, illustrated the deleterious effects of adding these short fibers to the soil. Figure 15 however, illustrates the raw data plot of unconfined compressive strength versus fiber weight fraction for polypropylene 15 dpf x .75 in. monofilaments in the same soil. This lack of improvement in q_u with the shorter fibers would tend to indicate that .75 inches might be a minimum length of fiber required to achieve some form of strength enhancement for this particular sandy soil.

Of the seven fibers evaluated with the Linn County A-2-4(0) soil, only those listed in Table 13 produced improvement in test results that could be modeled within the established SAS minimum guidelines.

Table 13. Fibers demonstrating satisfactory SAS modeling for unconfined compression test results, Soil A2-4(0), Linn County, Iowa.

Fiber Type	Manufacturer Designation	Diameter (Inches)	Length (Inches)
Polypropylene Monofilament	15 dpf x .75 in.	.002	0.75
	15 dpf x 1.5 in.	.002	1.50
Polypropylene Fibrillated Tape	360 dpf x 1.0 in.	.009	1.00
	360 dpf x 1.5 in.	.009	1.50
Fiberglass Type E Monofilament	832 BB 1 1/4 in.	.008	1.25

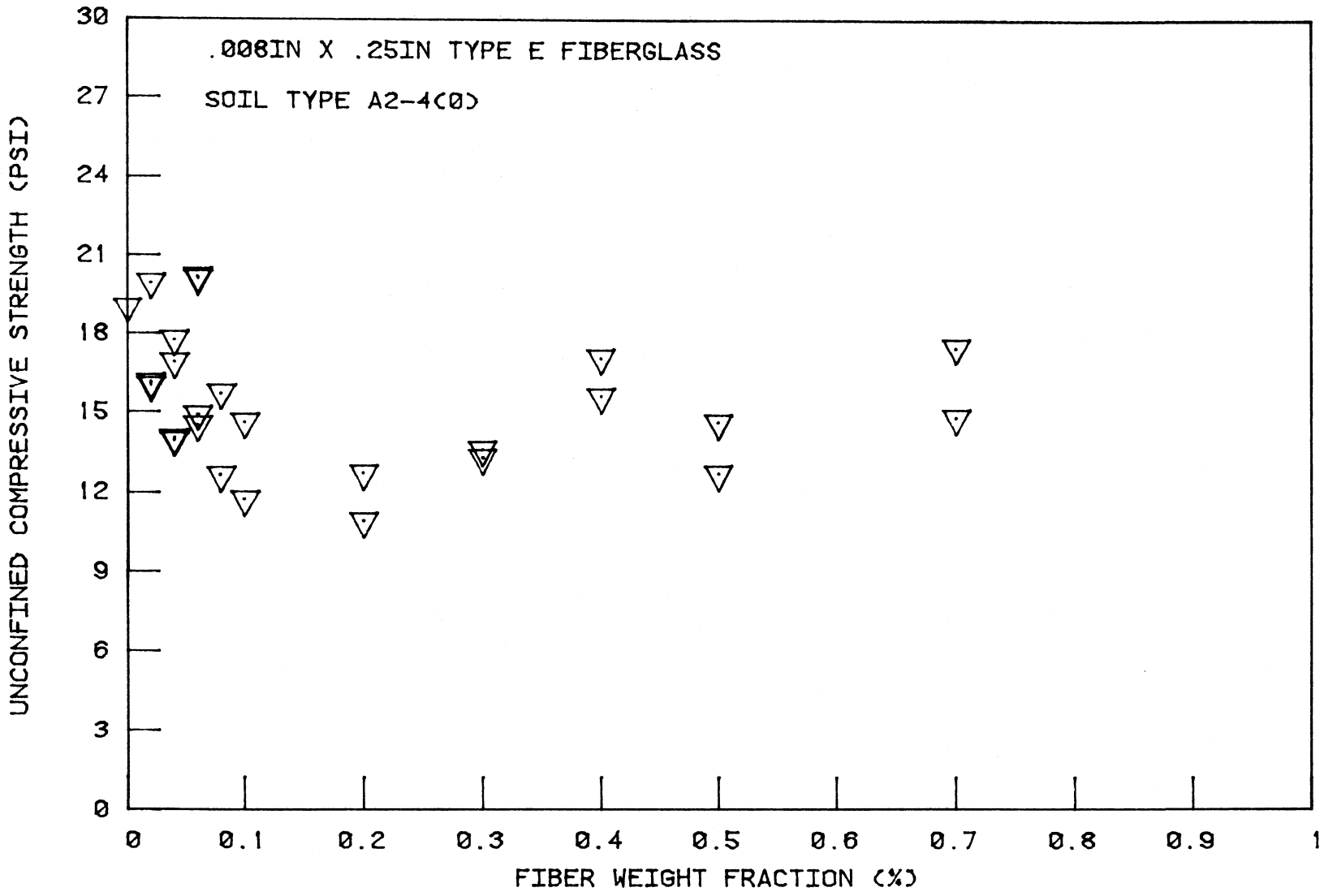

Figure 14. Unconfined compressive strength versus fiber weight fraction

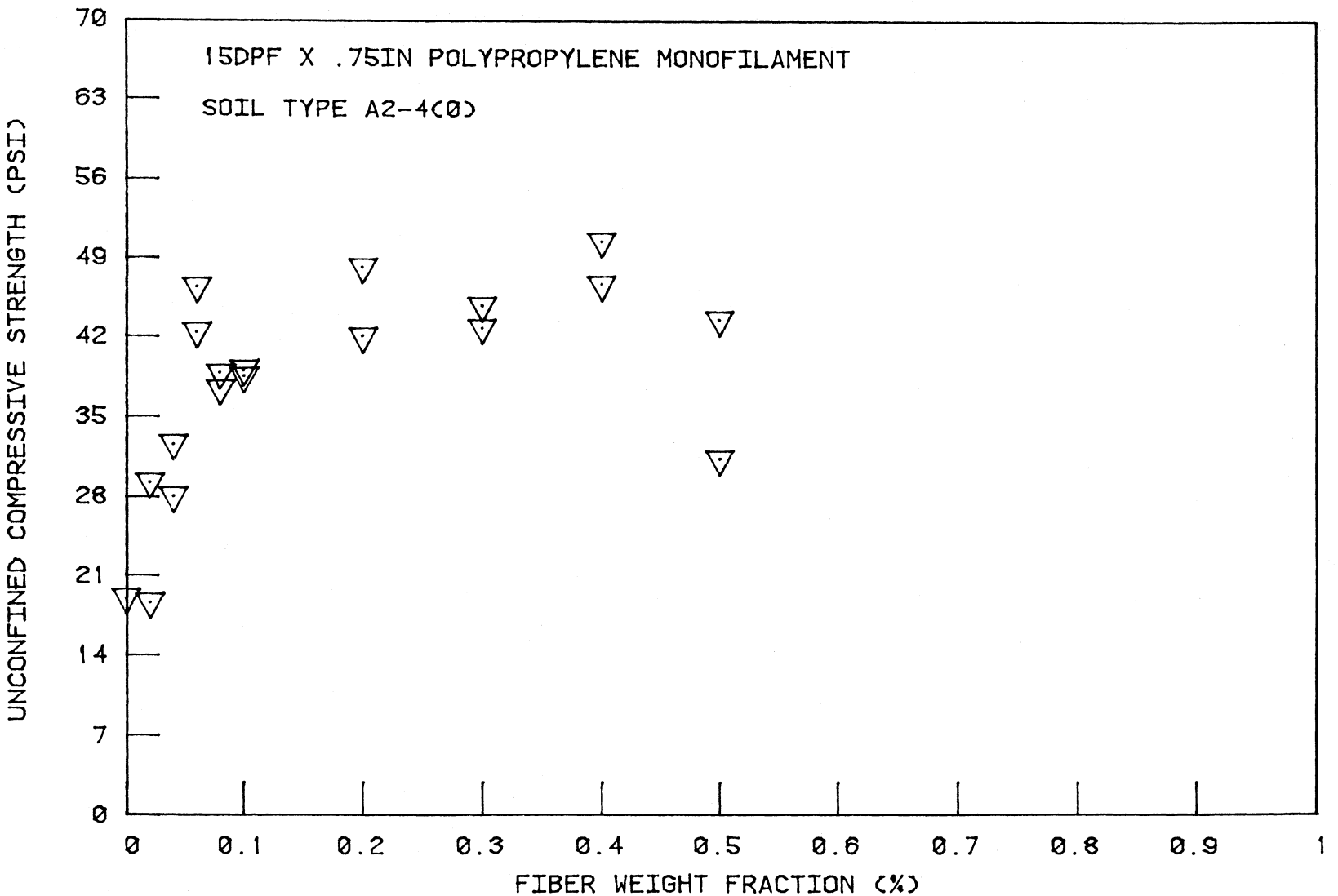

Figure 15. Unconfined compressive strength versus fiber weight fraction

Table 14 lists the above fibers and corresponding results of regression modeling. Figures 16 through 19 illustrate plots of raw data for two of the above fibers followed by plots of the SAS model normalized for the moisture content range applicable to each test series. It must be noted at this point, that the reliability of the SAS model lies solely within the range of moisture contents and fiber weight fractions of the raw data. This stage of analysis did not eliminate those statistical outliers of moisture content that adversely influenced accuracy of the model. Moisture contents utilized in the normalization of the three dimensional models were those representative of the majority of specimens. Normalization employing values outside the range of moisture contents most representative of the data resulted in nonsensical plots.

Evaluation of the numerous modeling plots substantiated the Statistical Analysis System as a viable means of interpreting data gathered from the UCS testing. Plots of unconfined compressive strength versus fiber weight fraction each indicated increased strength with the addition of various fibers. The increase in strength began to level off for the 15 dpf x .75 in. polypropylene monofilament and the 360 dpf x 1.5 in. polypropylene fibrillated fibers, Figure 17, at fiber weight fractions of .1%. Indicators were that those plots illustrating a leveling trend were the more representative of occurring reinforcing phenomena. Plots for the 15 dpf x 1.5 in. polypropylene monofilament and 360 dpf x 1.0 in. polypropylene fibrillated fiber indicated an unattainable maximum fiber weight fraction, beyond which reinforcement was not realized; i.e., unconfined strength continued to increase with increasing fiber content.

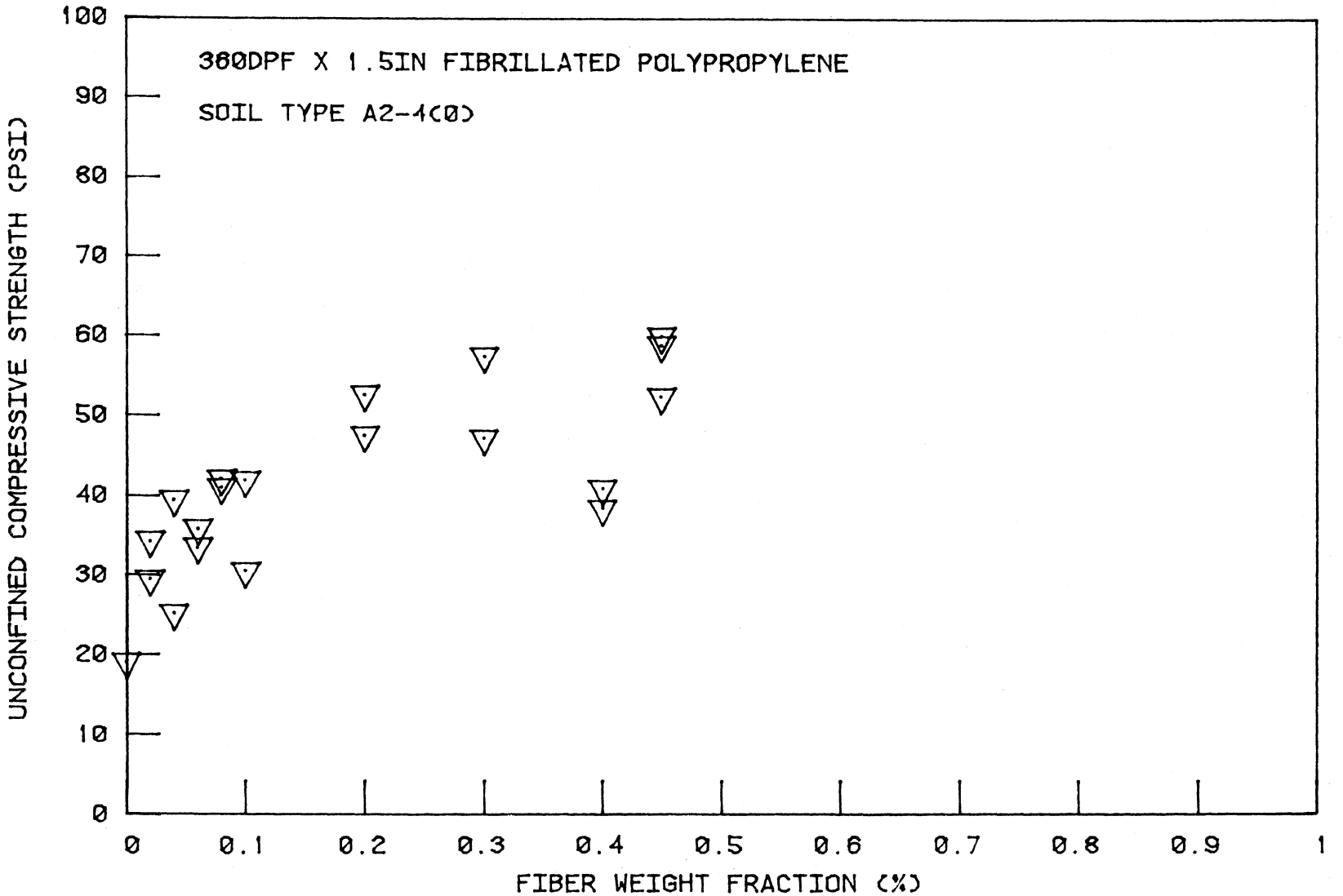

Figure 16. Unconfined compressive strength versus fiber weight fraction

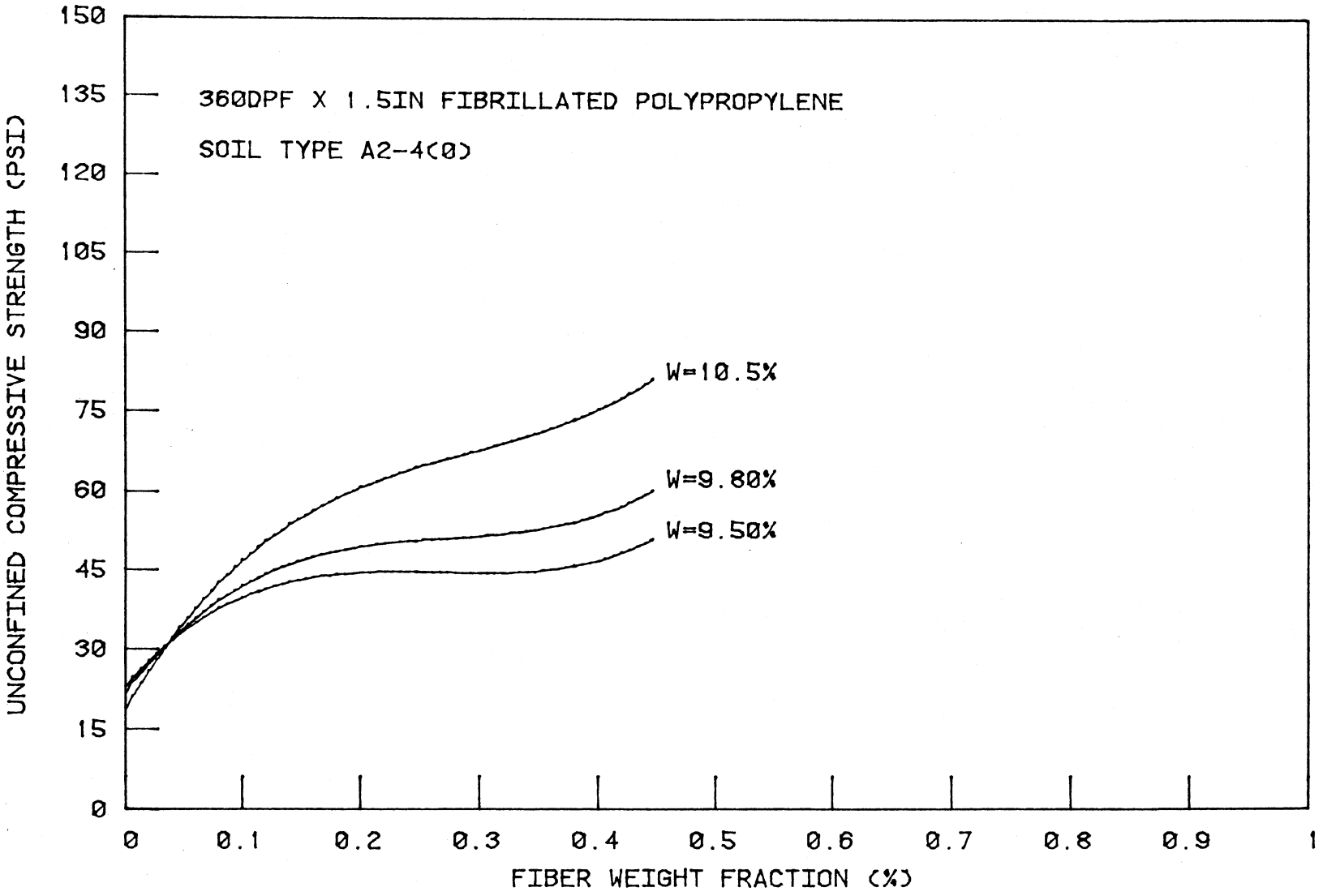

Figure 17. Unconfined compressive strength versus fiber weight fraction

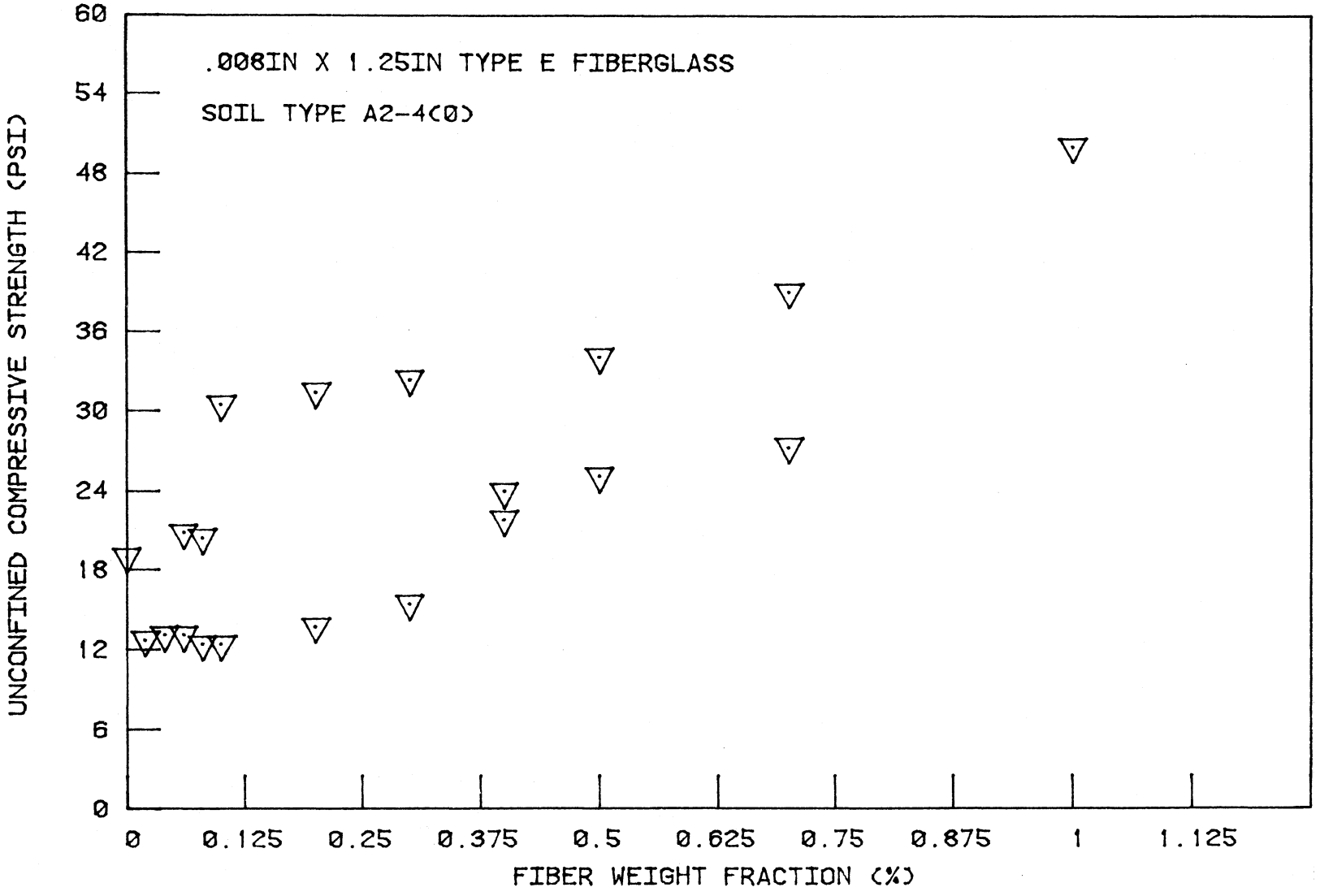

Figure 18. Unconfined compressive strength versus fiber weight fraction

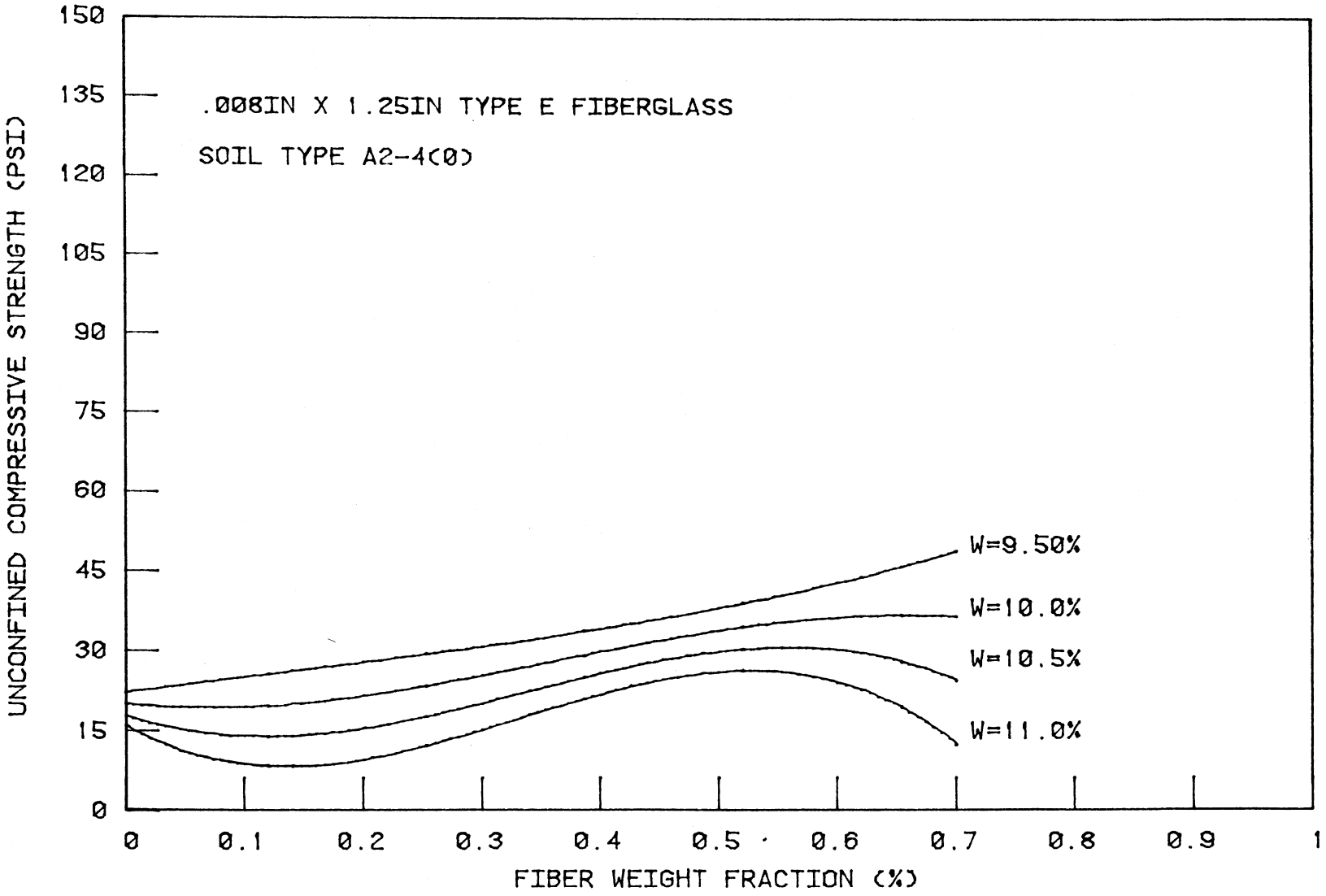

Figure 19. Unconfined compressive strength versus fiber weight fraction

Table 14. Summary of SAS modeling for unconfined compression testing, soil A2-4(0), Linn County, Iowa

Line No.	Response	R	CL	N
Polypropylene Monofilament				
15 dpf x .75 in.	$q_u = 31.276-1041.9325(C_f^2)+1004.9116(C_f^3)-0.0018(w^3) + 30.376\ (C_f \times w)$	.86862	99.99	41
	$\varepsilon_m = 0.02046-5.242(C_f^2)+13.405(C_f^3)+0.00002(w^3)+ .52998(C_f^2 xw)-1.291(C_f^3 xw)$	.86083	99.99	41
15 dpf x 1.50 in.	$q_u = 54.71448+29.765(C_f)-3.3983(w)+83.7894(C_f^2)$	.94890	99.99	26
	$\varepsilon_m = 0.0450 + 0.2161(C_f)$	.96250	99.99	26
Polypropylene Fibrillated Tape				
360 dpf x 1.0 in.	$q_u = 34.1243-0.012836(w^3)+7763.5492(C_f^3)-727.31588 (C_f^3 \times w)$	.95781	99.99	28
	$\varepsilon_m = 0.0451176-37.80665(C_f^2)+7.48638(C_f^3)+3.80185 (C_f^2 \times w)$	.96081	99.99	28
360 dpf x 1.5 in.	$q_u = 35.4824-914.921(C_f)+1222.686(C_f^3)-0.01444 (w^3)+122.917(C_f \times w)-102.315(C_f^2 \times w)$	.90810	99.99	42
Type E, Fiberglass				
-008 in. x 1.25 in.	$q_u = 16.2+1012.7(C_f)+20.85(w)-3857.99(C_f^2)-2.813 (w^2)+4076.4(C_f^3)+.103(w^3)-103.5(C_f xw)+404.5 (C_f^2 xw)-424.98(C_f^3 xw)$	.75390	99.99	42
	$m = 1.167+.9359(C_f)+.3669(w)-4.147(C_f^2)-.0372(w_2^2)+ 3.356(C_f^3)+.0013(w^3)-.0907(C_f xw)+ .4131 (C_f^2 xw)-.3347(C_f^3 xw)$	.75430	99.95	42

Notes: q_u = Unconfined compressive strength, psi; ε_m = Maximum unconfined compressive axial strain at failure, in/in; C_f = Percent fiber by dry unit weight of soil, % ; w = Percent moisture content of specimen at testing, %.

In general, increases in unconfined compressive strength on the order of 2.0 to 2.5 times that of the untreated soil could be realized. This increase occurred at percentages of approximately .1% fiber weight fraction. Subsequent addition of shorter monofilaments did not increase measured strength; however, results for the 1.5 inch fibrillated polypropylene fiber indicated that the leveling off of unconfined compressive strength may not be so drastic, given a fiber of greater length and larger cross section. These conclusions appeared to be verified by the results of the California Bearing Ratio Tests presented later in this report.

Results gained from the incorporation of Type E fiberglass fibers of 1.25 inch in length, Figures 18 and 19, did not appear to follow either trend established by the polypropylene fibers. The increase in unconfined compressive strength appeared nearly linear with the addition of greater amounts of fiber, although magnitude of the strength increase was considerably lower at corresponding percentages of fibers than those for the polypropylene. Comparable strength increases were not gained for the fiberglass-soil composite until fiber weight fractions of .7% were realized. This high fiber weight fraction was difficult to handle in the laboratory preparation of specimens. Indications of preliminary field incorporation were that this high percentage was equally unworkable in the field.

A trend of interest with the A2-4(0) soil is as illustrated in Figure 17, and regards the effects of small increases in moisture content upon the SAS modeled plots. As fiber weight fractions increased, the difference between the plots normalized at different moisture contents also tended to increase. Indications were that at higher fiber percentages (.4% and

higher) the unconfined compressive strength increased with increasing moisture content of the composite specimens. The inflection point where this phenomenon occurred lay between .05% and .10% fiber content. This trend was not demonstrated however, by the Type E fiberglass fibers, Figure 19. In fact, the fiberglass fibers reflected the more intuitive conception of what ought to occur with increasing moisture content. The investigation of this phenomenon will be of interest in the pursuit of developing soil-fiber reinforcing technology; however, such analysis and testing was beyond the scope of the project.

Analysis of modeling for strain at failure versus fiber weight fraction indicated that the addition of fibers to the A-2-4(0) soil increased maximum axial strain at which q_u, the unconfined compressive strength, was measured. Plots of strain versus fiber weight fraction for the 1.0 inch and .75 inch polypropylene fibers both presented a similar concave upwards trend as illustrated in Figure 20. The initial increase in strain at failure for both fibers was small until a fiber weight fraction of about .3% was attained, after which a radical increase in strain at failure was produced. The concave nature of this trend tended to decrease with increasing moisture content as shown in Figure 20 for the 15 dpf x .75 in. polypropylene monofilament. At fiber lengths of 1.50 and 1.25 inches, the strain versus fiber weight fraction plots were very nearly linear with little variation in slope for both the 15 denier polypropylene monofilament and the Type E fiberglass.

For the 1.0 inch fibrillated polypropylene fibers, maximum unconfined compressive strength occurred at .274 in./in. strain, or 27% deformation

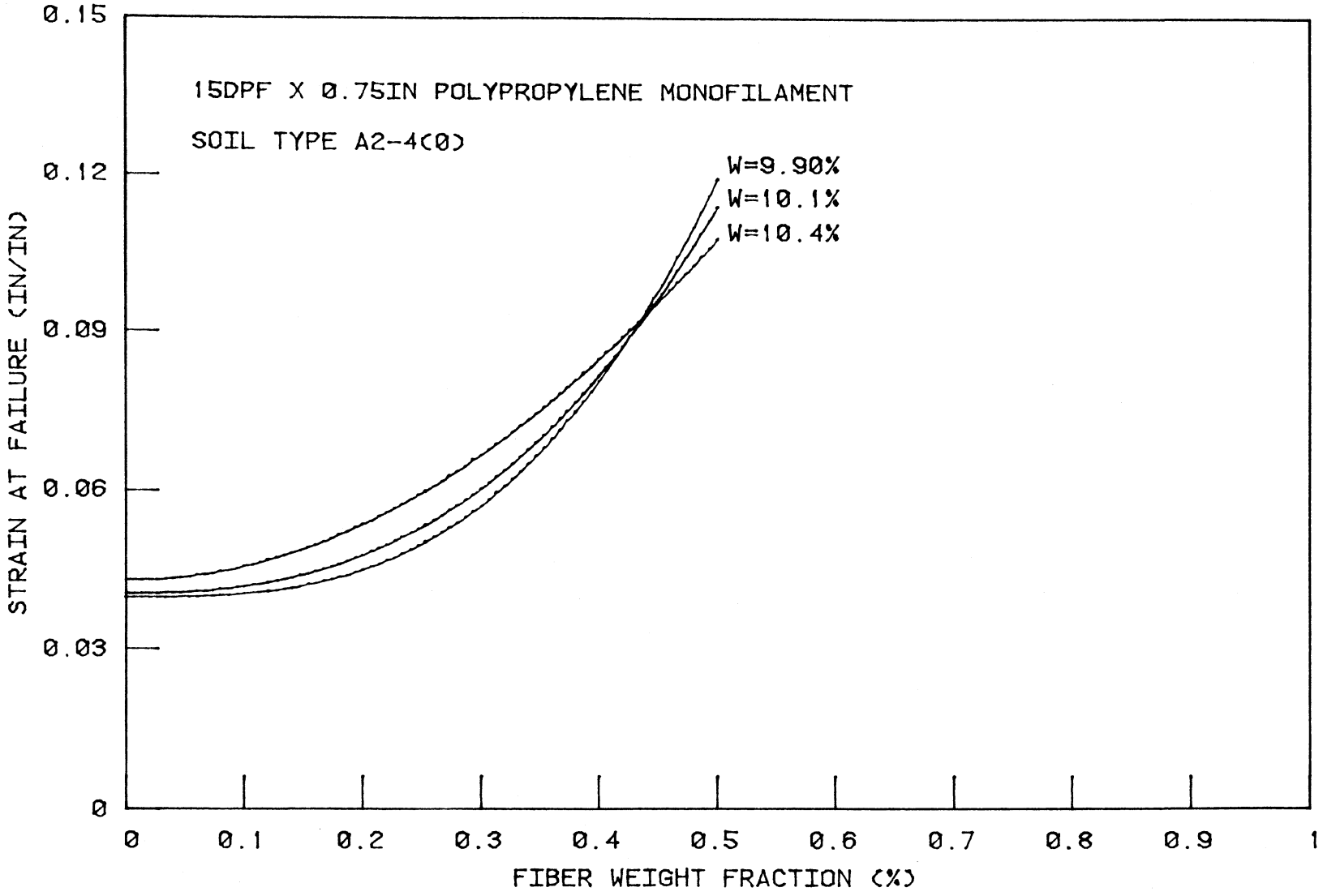

Figure 20. Strain at failure versus fiber weight fraction

of the original 4.56 inch tall specimens. However, for the 1.5 inch fibrillated fiber, maximum strain at failure never occurred. Specimens containing this fiber at moisture contents of 9.1%, 9.9%, and 10.2%, and fiber weight fractions of .45% did not fail based upon the defined failure criteria. Peak q_u values of 59.9, 58.8, and 52.3 psi were respectively attained and continued to hold while undergoing increasing strain. These tests were ultimately terminated at strains in the 30-35% range to avoid damage to the test apparatus. Strain phenomena thus observed, might be explained by recalling that fibers used in fiber reinforced concrete enhance the ductility thereof (16). This increase in ductility has been attributed to the energy that is spent stretching the fibers, and breaking the matrix-fiber interfacial bond. In addition, in fiber concrete, crack propagation is slowed, since the crack path is increased, allowing the composite to absorb more energy than the matrix material only, and thus experiencing larger deformations without attaining failure. Therefore, the 1.5 inch, 360 dpf fibrillated polypropylene fiber specimens appear to have sustained larger unit strains than their 1.0 inch counterparts due to their length being able to continue stress transfer from the matrix material.

Figure 21 is a raw plot of strains at failure versus fiber weight fraction for unconfined compression tests involving 1.5 inch, 360 dpf fibrillated polypropylene fibers. All test moisture contents, with the exception of the .083 in./in. strain at .3% fiber weight fraction, fell within the 9.7 - 10.7 percent range. The graph was essentially linear up to .4% fiber content then underwent a rapid increase in strain between .4%

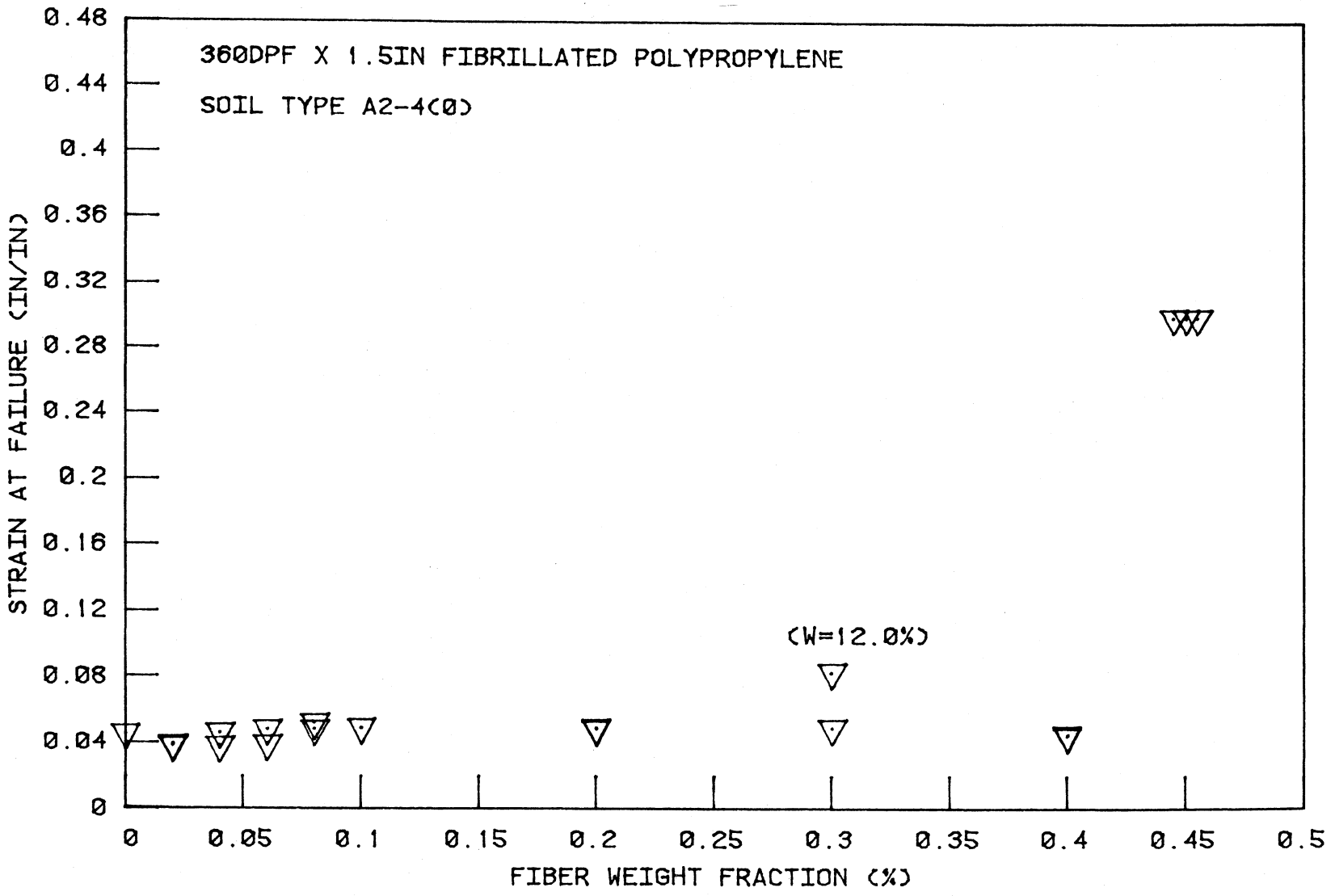

Figure 21. Strain at failure versus fiber weight fraction

and .45% fiber weight fraction. The trend for horizontal linearity in the 0%-.4% fiber content range and the lack of defined failure occurring in the specimens at .45% fiber weight fraction discredited a hypothesis that any of these points were statistical freaks. Furthermore, the concavity expressed in the 15 dpf x .75 in. and 360 dpf x 1.0 in. fiber reinforced specimens, coupled with the data reflected for the 360 dpf x 1.5 in. fibrillated fiber reinforced specimens, showed increasing strains at the .3%-.4% fiber content range. Such trends appear too predictable to be coincidental, and may again relate to the soil-fiber interfacial bonding, an area in need of further research.

Qualitative observations were made from the stress-strain curves of the Linn County soil regarding Young's Modulus, $E = \sigma/\varepsilon$, and the strain level at which specimens appeared to leave the linear and enter into the plastic range of deformation. Statistical modeling for E did not result in a model that approached the standard for correlation set in the research. However, in many of the treated specimens, an inflection point was detectable at an initial strain of about 0.08 in./in., at which the linear slope of the stress-strain curve changed, thereby producing two possible values for E. Table 15 presents the average experimental moduli values for those specimens showing inflections in the stress-strain plots. As may be noted, some significant improvements occurred in E, apparently due to incorporation of the fibers. However, due to the number of specimens exhibiting this phenomenon, no statistical evaluation could be made as to whether or not the phenomenon occurred as a direct result of the test, was due to initial compression densification of the specimens, or

was a definitive outgrowth of the fiber reinforcing mechanism. If the result of compression densification, then stiffness of the composite would probably be defined by the stress-strain slope E after inflection.

Table 15. Average of Young's Modulus from specimens exhibiting inflection point and dual linear paths, soil type A2-4(0), Linn County, Iowa.

Fiber	Young's Moduli		
	Untreated	Before Inflection	After Inflection
15 dpf x .75 in.	524.5	752.8	1060
15 dpf x 1.50 in.	524.5	564.0	859.0
360 dpf x 1.0 in.	524.5	818.0	1632.
360 dpf x 1.5 in.	524.5	698.0	1062.

At this stage of developmental research however, the only major conclusion was, and would appear to be substantiated from the lack of correlation achieved utilizing the Iowa K-Test, that a certain amount of vertical strain must develop prior to the fibers beginning to appreciably pick up any applied load. Further investigation into this area is needed.

Sioux City Soil

Table 16 lists the fibers selected for use in unconfined compression testing with Sioux City soils. Selection of these fibers was partially based on results and observations obtained from similar lab tests with the Linn County soil. All Proctor size test specimens were prepared as previously noted over a range of moisture contents from below to above untreated standard optimum. Values of unconfined compressive strength, q_u, strain at failure, ε, and Young's modulus, E, of the fiber reinforced

Table 16. Soil-fiber combinations, Sioux City soils

Fiber	Source	Fiber Weight Fraction %
15 dpf polypropylene monofilament, 1 1/2 inches	Borrow Pit	0.1, 0.17, 0.2, 0.3
15 dpf crimped polypropylene monofilament, 1 1/2 inches	Borrow Pit	0.05, 0.1, 0.2
832 bb Type E Fiberglass 1 1/4 inches	West 3rd Street	0.02, 0.08, 0.15, 0.3, 0.5
	Borrow Pit	0.1, 0.17, 0.2, 0.3
360 dpf fibrillated polypropylene, 1 inch	West 3rd Street	0.02, 0.04, 0.06, 0.08, 0.15 0.3, 0.5
	Borrow Pit	0.1, 0.17, 0.2, 0.3
360 dpf fibrillated polypropylene, 1 1/2 inches	Borrow Pit	0.1, 0.2, 0.3
Fly Ash Fiber	West 3rd Street	0.1
	Borrow Pit	0.17

specimens were compared to those of the untreated soil. Values of E were determined by linear regression of data comprising the initial straight line portion of the stress-strain curve. Criteria for acceptance of any value of E was that the regression coefficient was 0.98 or greater.

In general, examination of the data and graphical outputs indicated several trends for fiber reinforcement of the loessial soils. Most fibers exhibited a critical fiber weight fraction, below which q_u of the composite was not particularly improved. The composites generally attained a slightly higher strain at failure than the untreated specimens, indicating that the composite could undergo larger deformations without fracture or crumbling which could be beneficial in some roadway performance. Consistent with those fiber weight fractions producing higher values of q_u, they also produced higher values of E than the untreated soil. Regardless of fiber content, dry densities of treated specimens were lower than those of the untreated soil. Figure 22 through 27 illustrate the general range of data obtained from unconfined compression testing of the Sioux City materials.

Unconfined compressive strength of the borrow pit loess was enhanced by the addition of 15 dpf polypropylene monofilament, 1 1/2 inch length. Increasing fiber weight fraction tended to increase q_u to a maximum observed value about 1.4 times greater than the untreated. The maximum fiber weight fraction tested was 0.3 percent, a quantity found difficult to mix in order to obtain a discreet, random distribution of fiber. Several specimens at the 0.3% fiber weight fraction did not attain a maximum q_u during testing, but continued to support increased load with increased strain. Addition of this fiber increased the composite strain

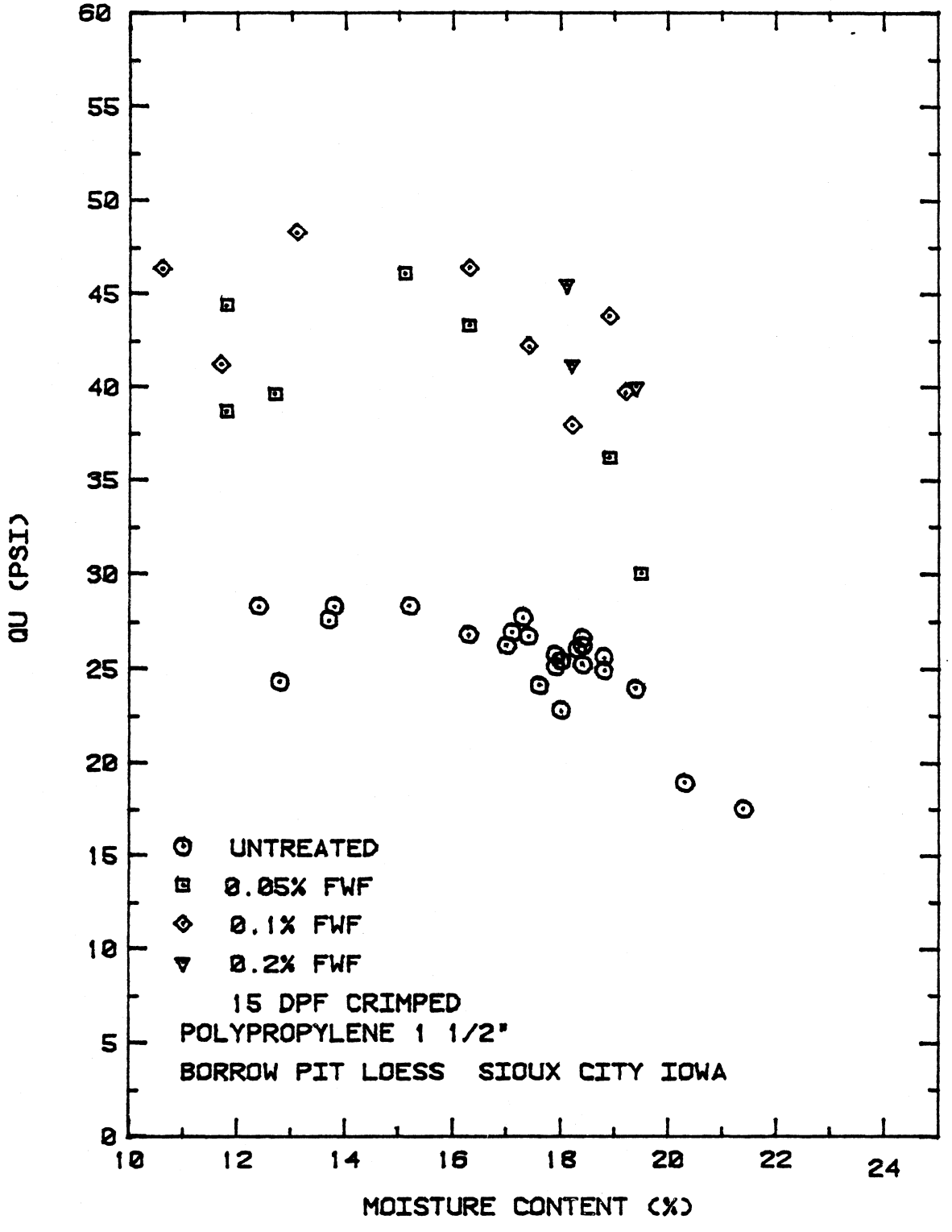

Figure 22. Unconfined compressive strength versus moisture content

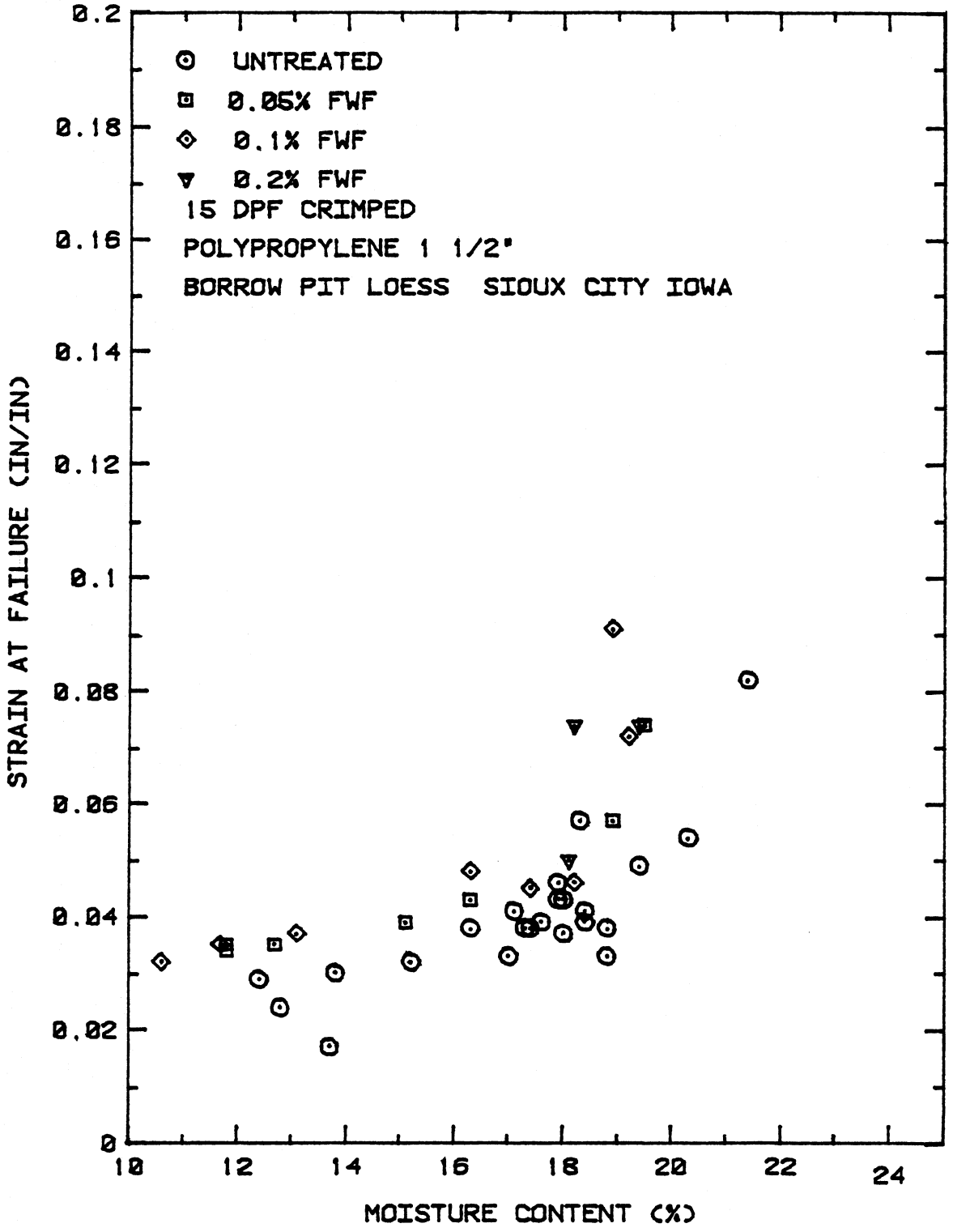

Figure 23. Strain at failure versus moisture content

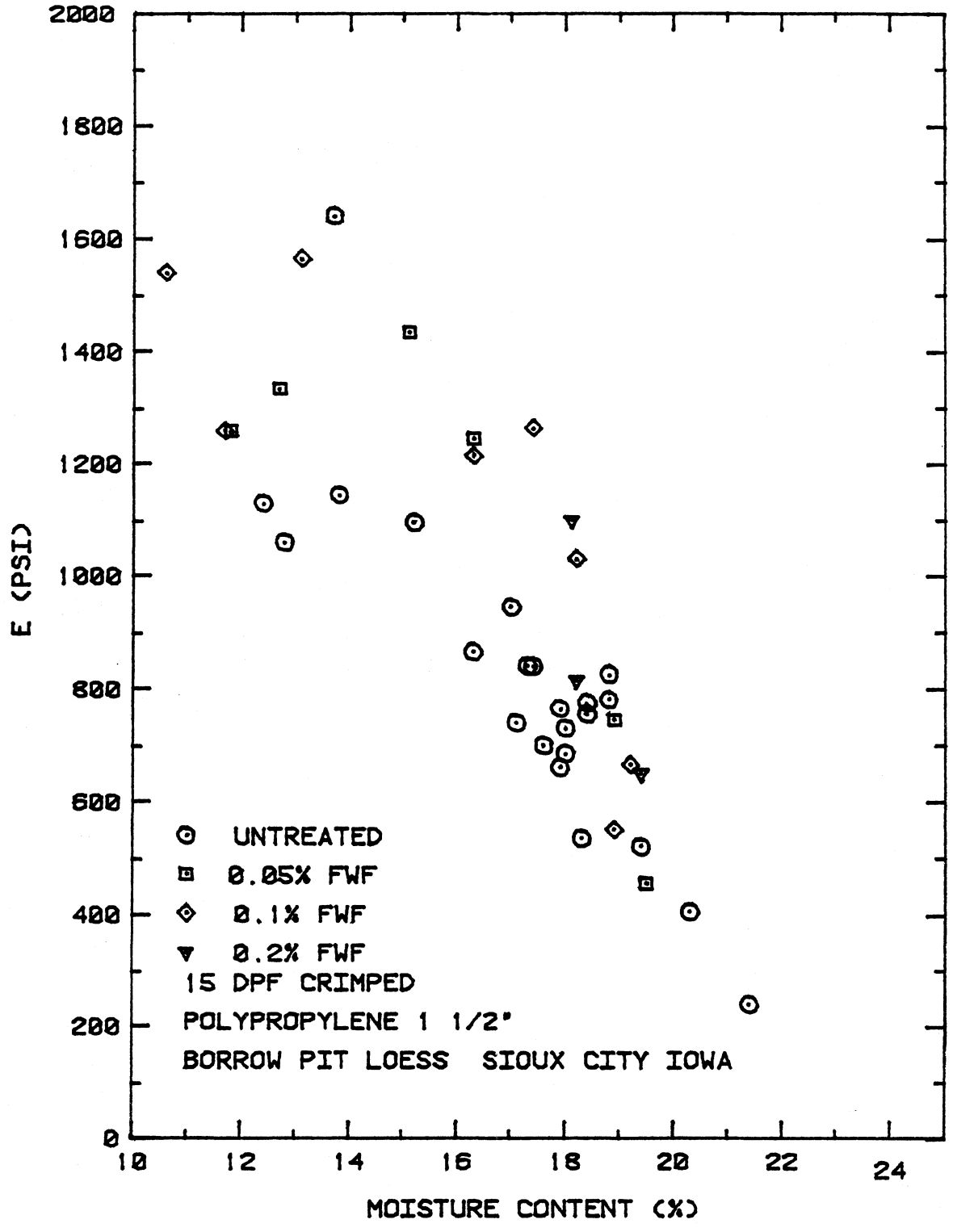

Figure 24. Modulus versus moisture content

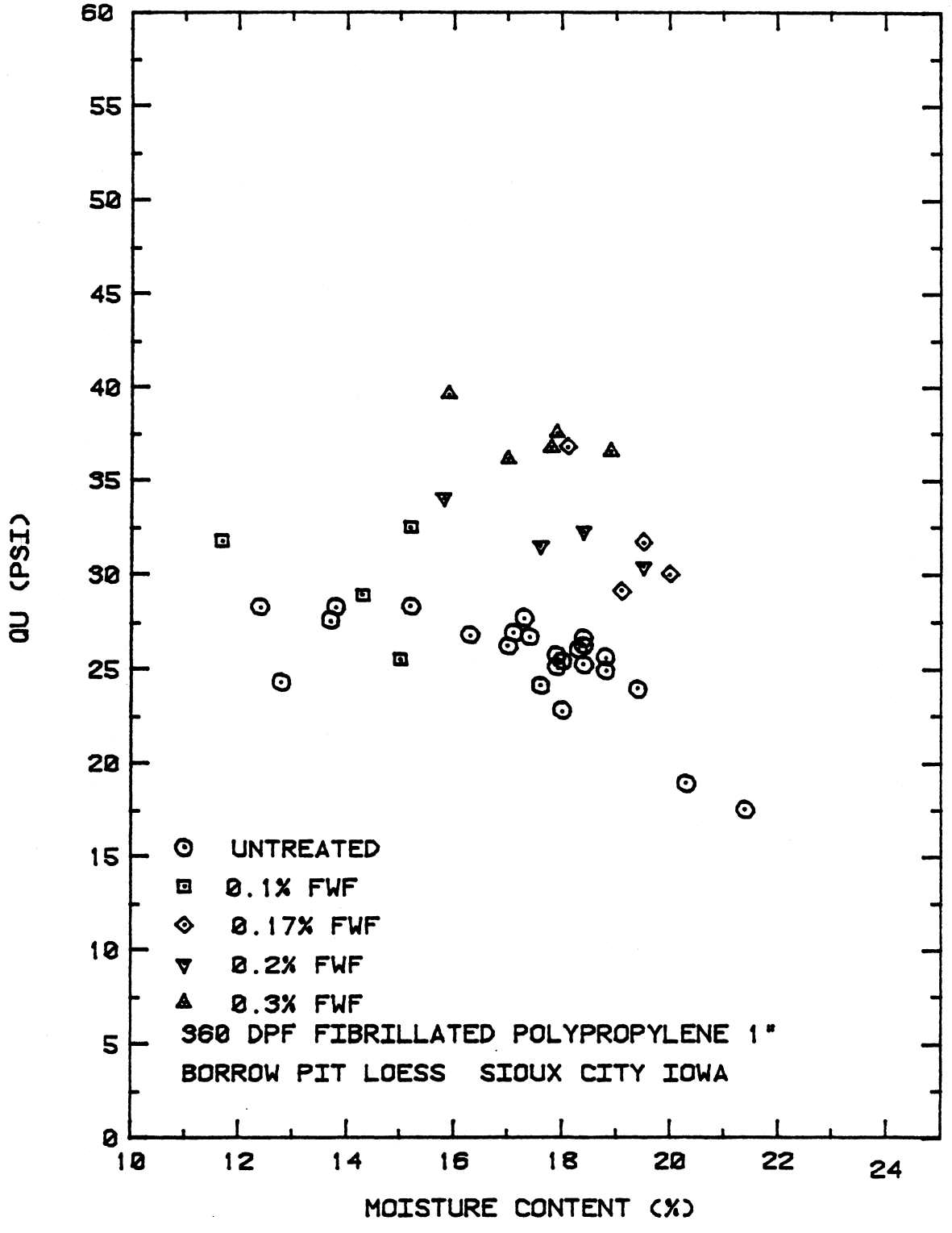

Figure 25. Unconfined compressive strength versus moisture content

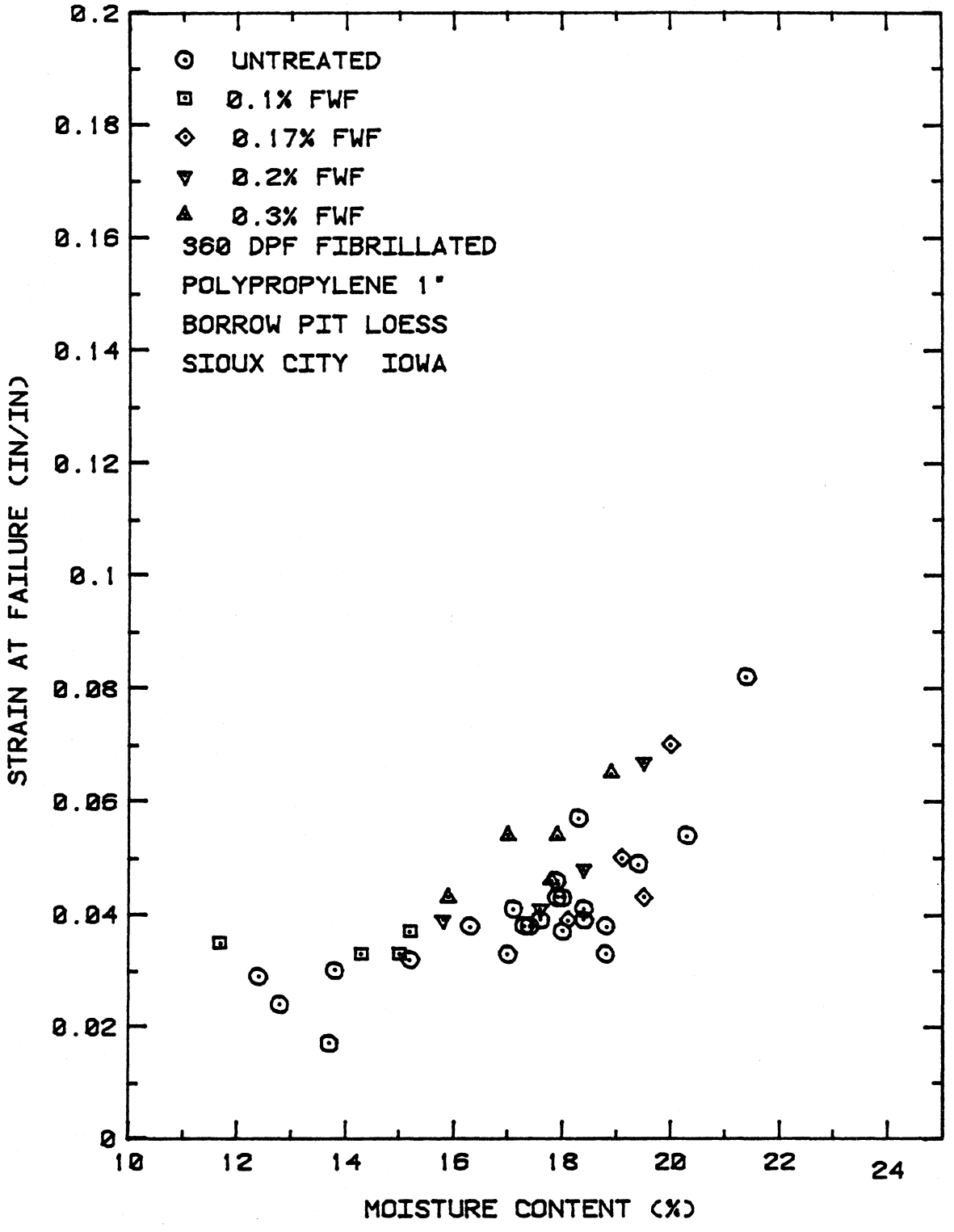

Figure 26. Strain at failure versus moisture content

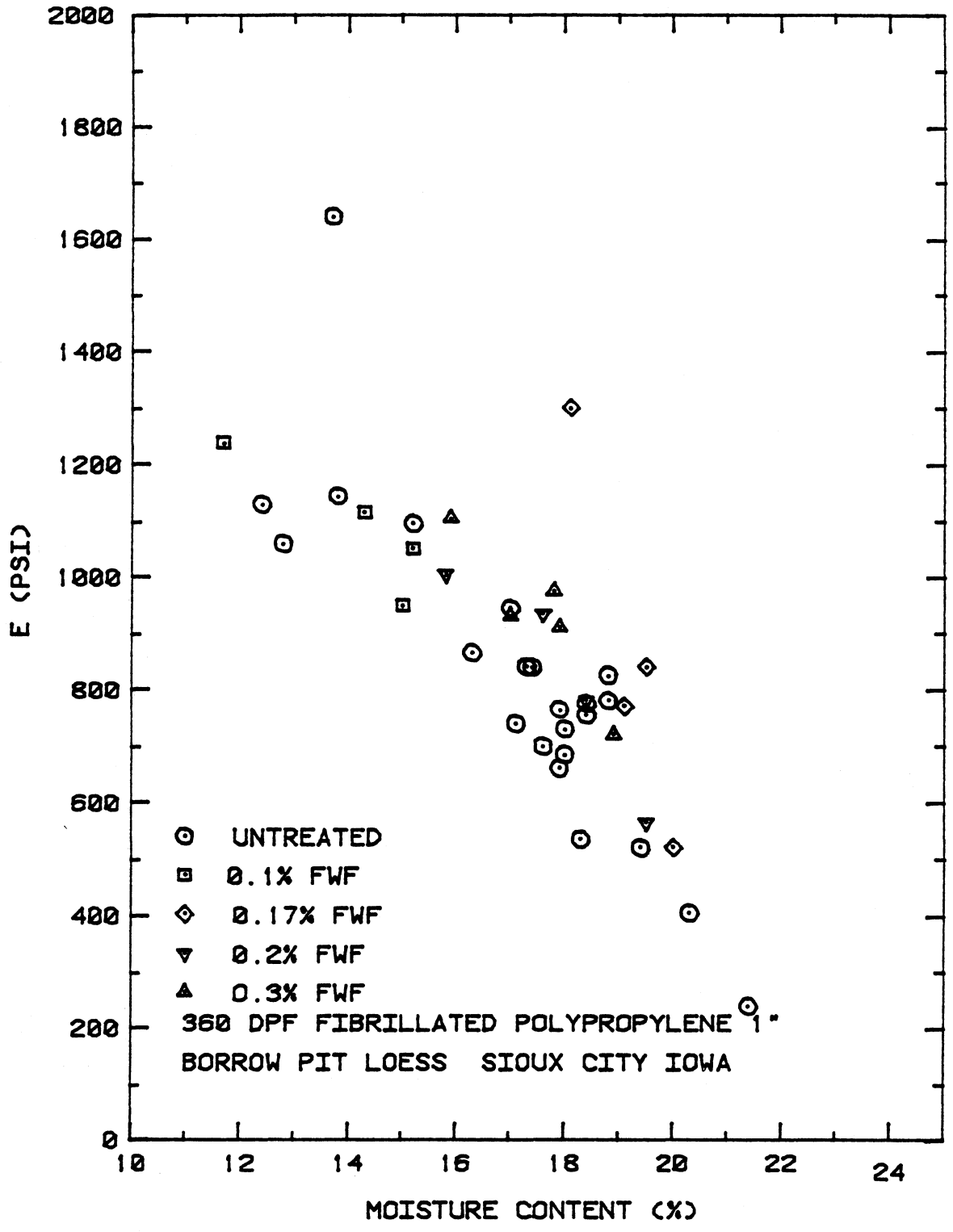

Figure 27. Modulus versus moisture content

at failure for all fiber weight fractions. Even though q_u values were higher at all fiber weight fractions, values of E were not consistent. All aspects considered, this fiber appeared to perform well with the loessial soil.

Addition of the 15 dpf crimped polypropylene monofilament, 1 1/2 inch length fiber produced the most dramatic increases in strength of any fiber tested with the Sioux City soils, even though much lower fiber weight fractions were used. Maximum increase in q_u was about 1.8 times that of untreated soil at 0.2 percent fiber weight fraction, Figure 22, including above optimum moisture content. Strains at failure and E values were generally higher than the untreated soil, Figures 23 and 24. However, the crimping of the fiber coupled with its fineness made mixing somewhat difficult. To achieve complete random distribution of these fibers, the specimens were mixed for several minutes with a Hobart Model S-601 mixer prior to compaction. The overall good performance of this crimped fiber warranted continued investigation. It was also observed that a larger diameter crimped polypropylene fiber of similar length should be evaluated, but such was not obtainable from the various manufacturers noted in Table 6.

Lower fiber weight fractions of 832 BB type E fiberglass, 1 1/4 inch length fiber did not improve the unconfined strength of either West 3rd Street or borrow pit soils. However, as the fiber weight fraction was increased, q_u values also increased. Maximum enhancement of strength was about 1.5 times the untreated q_u for the West 3rd Street soil at 0.5% fiber weight fraction, and about 1.3 times for the borrow pit soil at 0.3 percent fiber weight fraction. Regardless of fiber quantity, strains at failure were not markedly different from the untreated specimens. Young's

Modulus values were somewhat improved for West 3rd Street specimens, but improved only slightly for the borrow pit specimens. Since the specific gravity of fiberglass is almost three times that of polypropylene, many less fiberglass fibers comprise a given fiber weight fraction when compared to polypropylene fibers. As a result, maximum fiber content may not have been achieved with the fiberglass fibers, but any content above 0.5% was considered uneconomical.

The 360 dpf fibrillated polypropylene, 1 inch length, was used with the West 3rd Street and borrow pit soils. Above 0.1 percent fiber weight fraction, values of q_u increased as the amount of fiber increased in the composite. Maximum improvement was about 1.4 times the untreated value for borrow pit specimens at 0.3 percent fiber weight fraction, Figure 25, and about 1.7 times for West 3rd Street specimens at 0.5 percent fiber weight fraction. This fiber also produced good q_u improvement above optimum moisture content with the borrow pit soil. With increasing unconfined compressive strength, strains at failure, Figure 26, and values of Young's Modulus, Figure 27, were also slightly increased over untreated specimens.

The 360 dpf fibrillated polypropylene, 1 1/2 inch length fiber did not appear to improve the comparative parameters any more than the 1 inch length of the same fiber discussed above. However, it is important to remember that the longer fiber means that fewer fibers are present at equal fiber weight fractions when compared to the shorter length fiber.

Addition of fly ash fiber to specimens of both the West 3rd Street and borrow pit loess did not appreciably increase unconfined compressive

strength, strain at failure, or values of Young's Modulus, above those obtained with the untreated specimens. Due to a limited supply of fibers, only small fiber weight fractions were used, but considerable effort was required to adequately mix this fiber with the soil. In light of difficulties for controlled fiber production and no indication of composite strength enhancement, further study of this fiber as a singular type of reinforcement additive was suspended.

As with the Linn County soil, the soil-fiber bond appeared critical to enhancement of Sioux City soil-fiber composite strength. In an effort to improve this bonding, two series of specimens were prepared, one utilizing hydrated lime as an additional additive, the other, Type I Portland cement. Both of these additives are capable of stabilizing the Sioux City soils alone. Normally, in excess of 7% Portland cement for example, would be required for full stabilization of these soils. However, only small amounts of each, 1% and 3% by soil dry weight, were chosen for this series of tests. Specimens were prepared (1) untreated, (2) treated with lime or cement alone, and (3) with lime or cement plus various fibers. The Borrow pit loess was used exclusively as the soil matrix for specimen preparation. The fiber weight fraction was held constant at 0.17% for all fibers, since this content appeared to provide some strength enhancement regardless of fiber type with the borrow pit soil. In addition, this fiber content allowed for a maximum number of specimens to be prepared utilizing the small remaining supply of fly ash fibers, with lime treatment. All specimens were prepared near optimum moisture content and maximum standard density, wrapped and sealed, then subjected to a set curing

schedule in a controlled environment of about 72° F and near 100 percent relative humidity. As soil-lime reaction occurs over a long time period, all lime treated specimens were tested after 7 and 28 days moist curing. Since Portland cement hydration is much quicker, these specimens were tested after 24 hours and 7 days moist curing. Duplicate or more specimens were made for each treatment and curing time so that average values could be used for comparison.

Figures 28-30, illustrate comparative ratios of q_u, strain at failure, and E, of the 3% lime and various fiber treatments after 28 days curing. Ratios were calculated by dividing the average treated specimen response, by the response of the untreated soil. Ratios for composites of soil plus fiber only are also shown for comparison. Points of reference for actual values of q_u, ε and E can be made in Figures 22-27 at a moisture content of 17.9%.

As anticipated, addition of small percentages of lime to the soil appreciably increased the unconfined compressive strength. The slow reaction between lime and soil was apparent by the increase in strength between the 7 and 28 day tests. One percent lime treatment increased q_u by about 1.2 times, and 1.6 times that of the untreated soil after 7 and 28 days curing, respectively. Three percent lime treatment produced a more dramatic increase of q_u, about 4 times after 7 days, and about 7 times after 28 days, Figure 28A. Lime treated specimens behaved in a brittle manner, attaining significantly higher values of Young's Modulus than the untreated soil, Figure 30A.

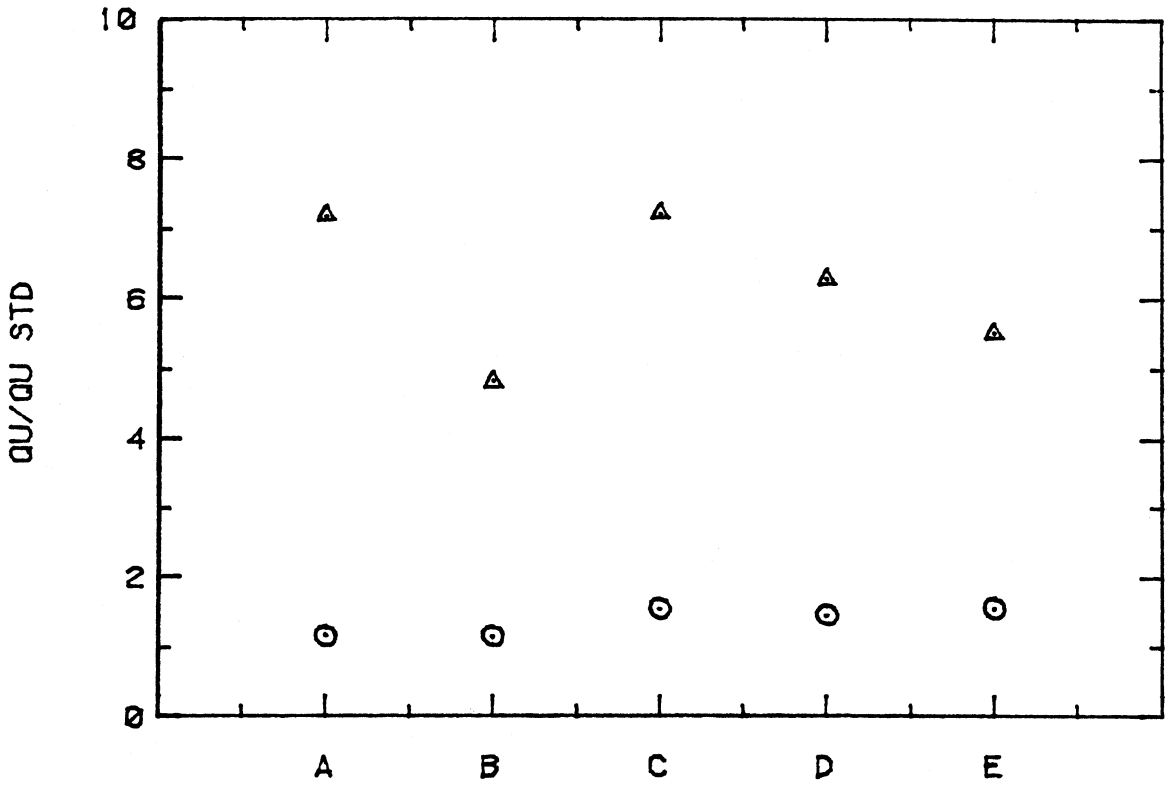

Figure 28. Unconfined compressive strength ratios, 3 percent lime treatment

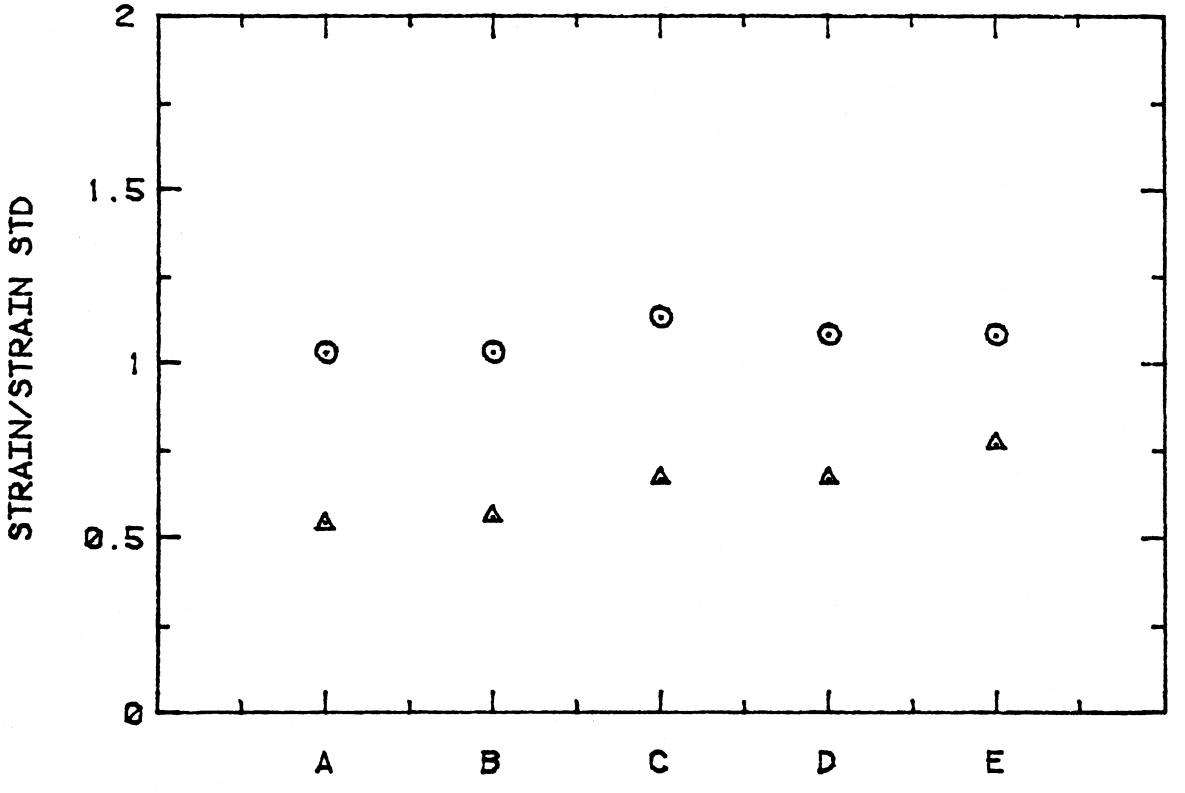

Figure 29. Strain at failure ratios, 3 percent lime treatment

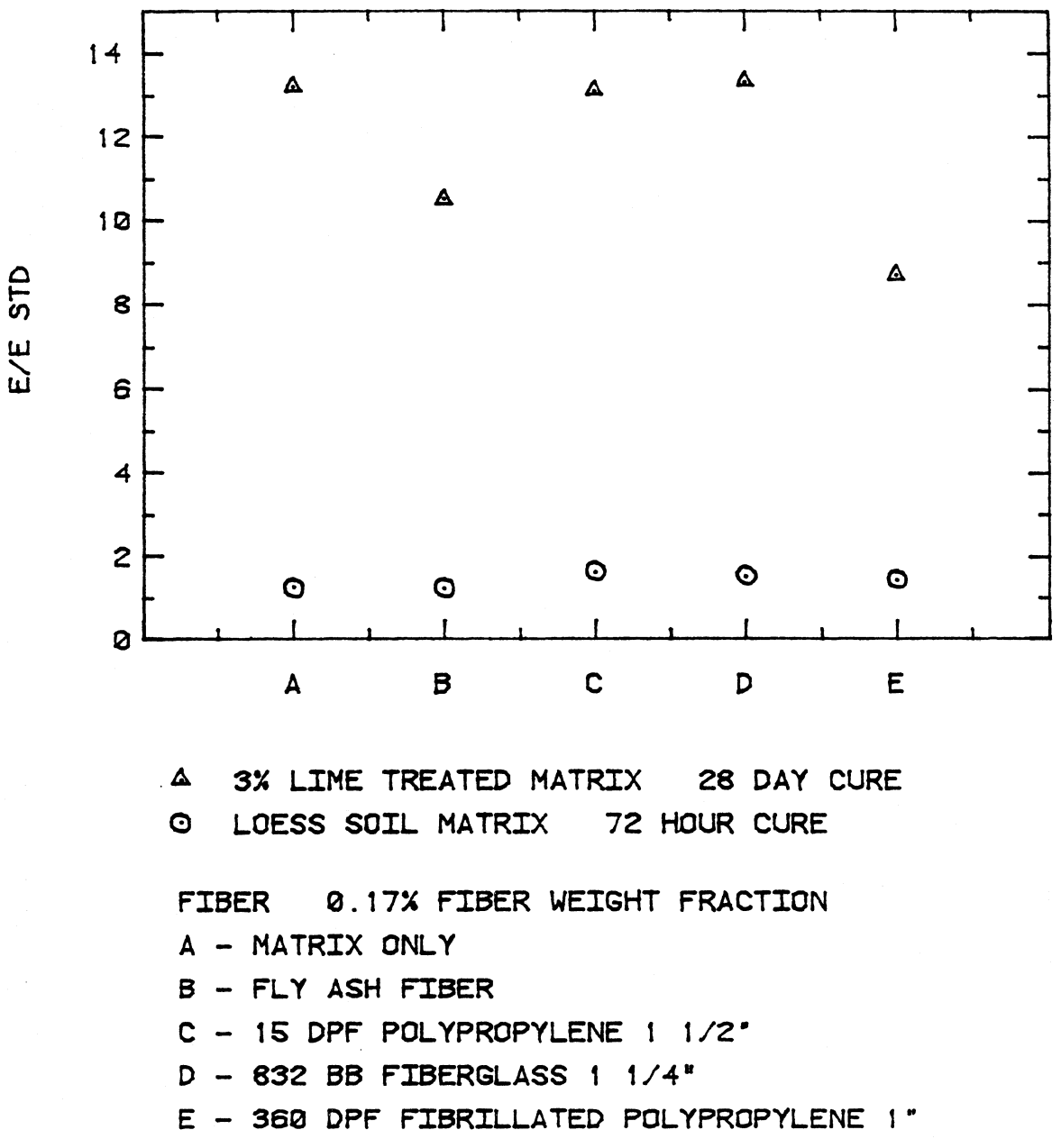

Figure 30. Modulus ratios, 3 percent lime treatment

Specimens produced using fly ash fibers and 1 percent lime showed no improvement in q_u, strain at failure, and E. Examination of these specimens after testing, revealed unchanged fibers, indicating that the fly ash fibers were not pozzolanic.

Fly ash, 15 dpf polypropylene, 832 bb fiberglass, and one inch 360 dpf fibrillated polypropylene fibers were employed with 3 percent lime treated soil specimens. After 7 days curing, strength of all fiber reinforced composites except the fibrillated polypropylene specimens was greater than lime treatment only. However, after 28 days curing, q_u values of fiber reinforced specimens were not appreciably improved over the 3 percent lime treatment only, Figure 28, indicating that the addition of lime to the composite did not further improve the soil-fiber bond. Addition of fiber produced a slightly less brittle behavior, with strains at failure increasing over lime treatment only, Figure 29. Values of E were in the same range for both lime treatment only and fibers plus lime, Figure 30. Addition of lime increased the unconfined strength and modulus much greater than fiber alone, but the strain at failure was decreased.

Both straight and crimped 15 dpf polypropylene, 832 bb fiberglass, and both 360 dpf fibrillated polypropylene fibers were utilized in the Portland cement treated series.

Specimens treated with 1 percent Type I Portland cement only, attained unconfined strengths slightly lower than the untreated soil after both 24 hour and 7 day curing periods. Addition of all fibers to those specimens nearly doubled unconfined strengths, but cement treatment made the soil behave in a brittle manner, with strain at failure for cement treatment

only, less than that of the untreated soil. Addition of all fibers increased the strain at failure to levels near that of the untreated soil, indicating a more ductile response to loading. However, the composite could undergo more deformation without cracking which may be more suitable for roadway use. Young's Modulus was improved by the addition of 1 percent cement, with addition of fiber further enhancing E.

After 24 hours, all fiber reinforced specimens performed somewhat better than those treated with 3 percent cement only. Values of q_u, strains at failure and E were each greater, Figures 31, 33, and 35. After 7 days curing, only those specimens reinforced with 15 dpf crimped polypropylene fiber attained a significant improvement over those with 3 percent cement treatment only, attaining higher values of q_u and E, Figures 32 and 36. Other fibers attained values of q_u and E near or lower than cement treatment only. However, all fibers imparted some measure of ductility to the composite as indicated by the greater strains at failure. Specimens treated with 3 percent cement only, displayed very brittle failure with development of large cracks and failure surfaces, while fiber reinforced specimens failed without development of visibly noticeable failure surfaces. This observation further demonstrated the increased ductility of fiber-soil-cement composites over cement modified soils only, and indicated a potential for control of reflective cracking in a base or subbase constructed of low cement contents. Further investigation of this increased ductility should be undertaken.

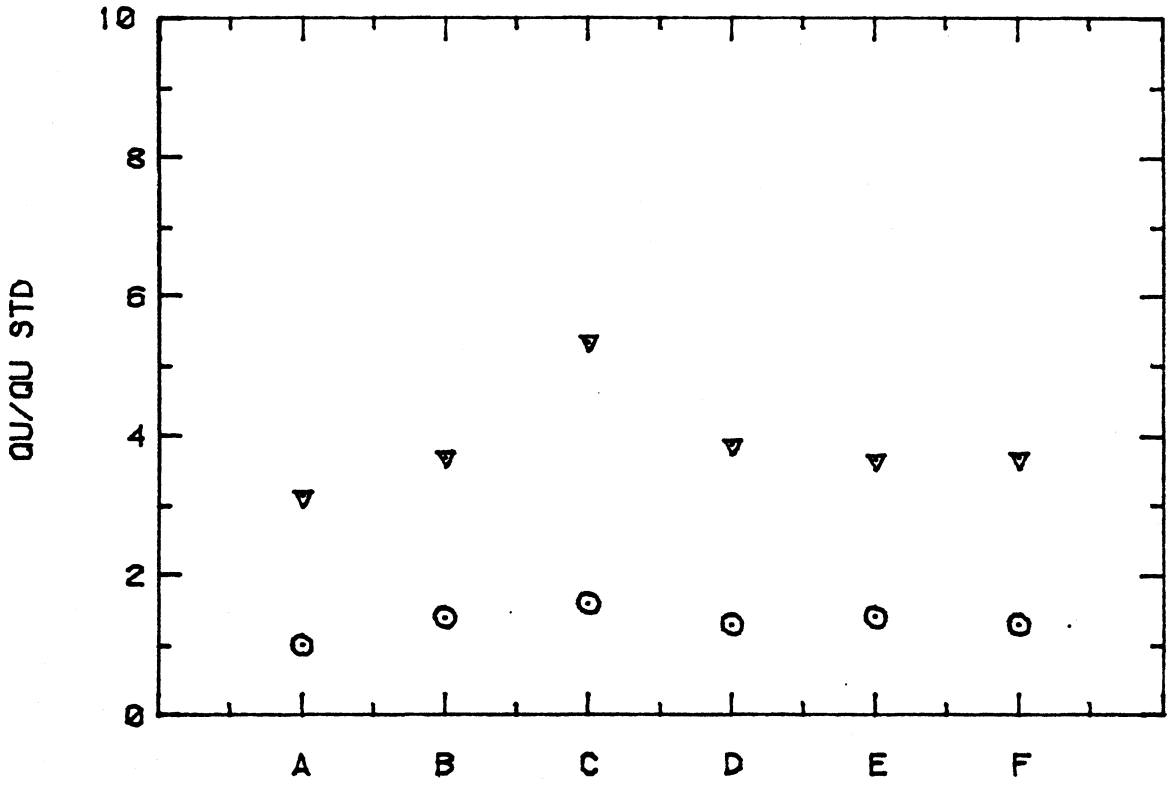

▽ 3% TYPE I PORTLAND CEMENT TREATED MATRIX
24 HOUR CURE
⊙ LOESS SOIL MATRIX 72 HOUR CURE

FIBER 0.17% FIBER WEIGHT FRACTION
A - MATRIX ONLY
B - 15 DPF POLYPROPYLENE 1 1/2"
C - 15 DPF CRIMPED POLYPROPYLENE 1 1/2"
D - 832 BB FIBERGLASS 1 1/4"
E - 360 DPF FIBRILLATED POLYPROPYLENE 1"
F - 360 DPF FIBRILLATED POLYPROPYLENE 1 1/2"

Figure 31. Unconfined compressive strength ratios, 3 percent cement treatment, 24 hour cure

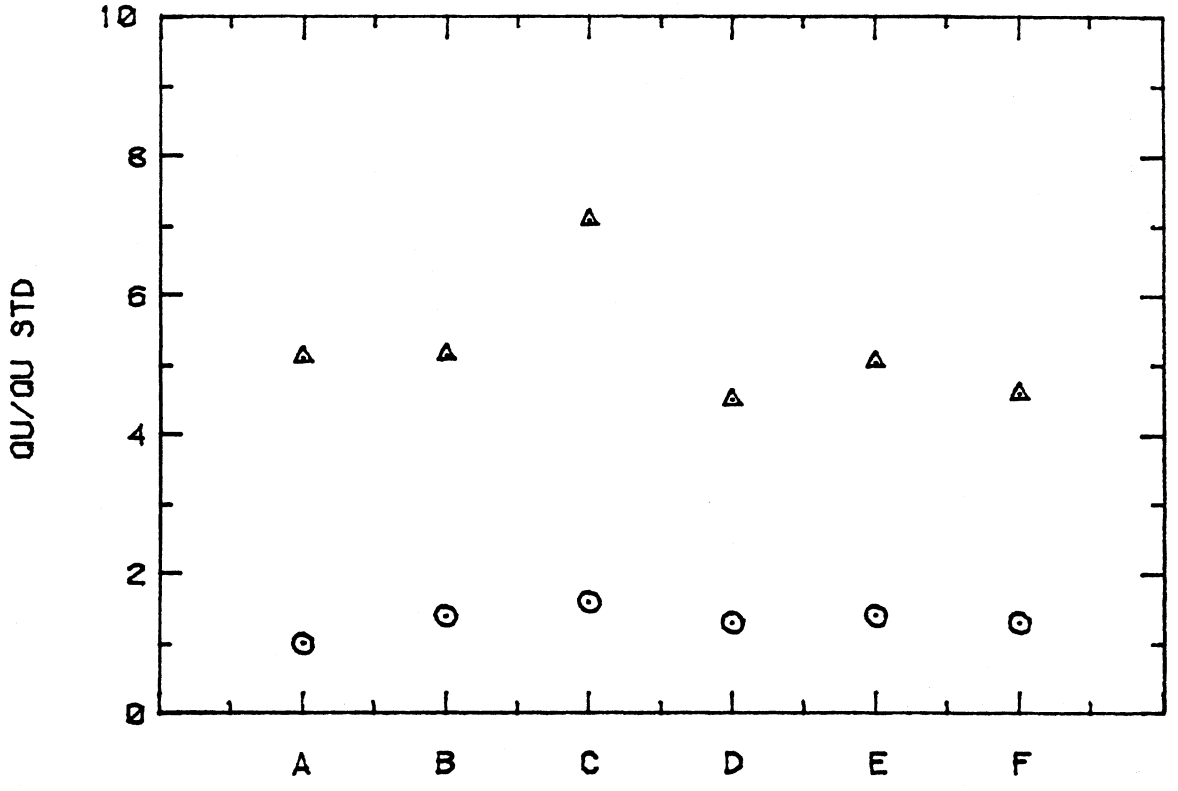

△ 3% TYPE I PORTLAND CEMENT TREATED MATRIX
7 DAY CURE

⊙ LOESS SOIL MATRIX 72 HOUR CURE

FIBER 0.17% FIBER WEIGHT FRACTION

A - MATRIX ONLY

B - 15 DPF POLYPROPYLENE 1 1/2"

C - 15 DPF CRIMPED POLYPROPYLENE 1 1/2"

D - 832 BB FIBERGLASS 1 1/4"

E - 360 DPF FIBRILLATED POLYPROPYLENE 1"

F - 360 DPF FIBRILLATED POLYPROPYLENE 1 1/2"

Figure 32. Unconfined compressive strength ratios, 3 percent cement treatment, 7 day cure

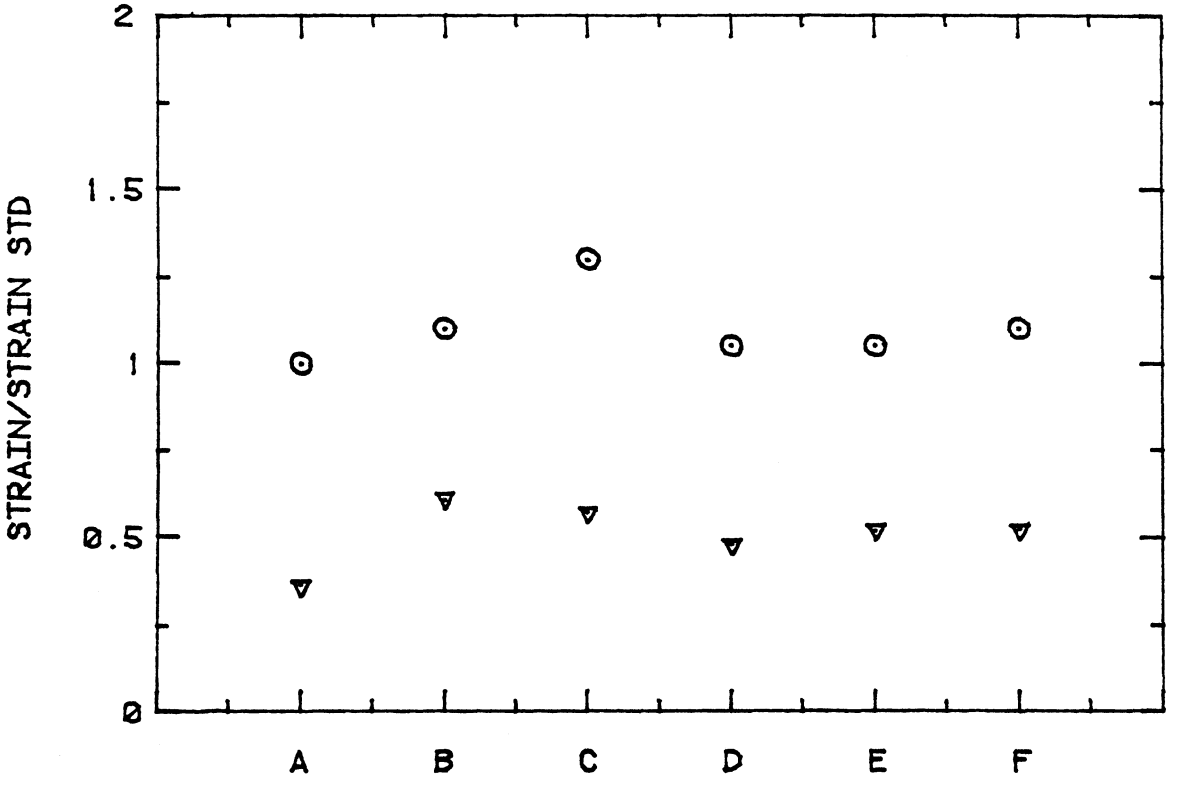

▽ 3% TYPE I PORTLAND CEMENT TREATED MATRIX
24 HOUR CURE
⊙ LOESS SOIL MATRIX 72 HOUR CURE

FIBER 0.17% FIBER WEIGHT FRACTION
A - MATRIX ONLY
B - 15 DPF POLYPROPYLENE 1 1/2"
C - 15 DPF CRIMPED POLYPROPYLENE 1 1/2"
D - 632 BB FIBERGLASS 1 1/4"
E - 360 DPF FIBRILLATED POLYPROPYLENE 1"
F - 360 DPF FIBRILLATED POLYPROPYLENE 1 1/2"

Figure 33. Strain at failure ratios, 3 percent cement treatment, 24 hour cure

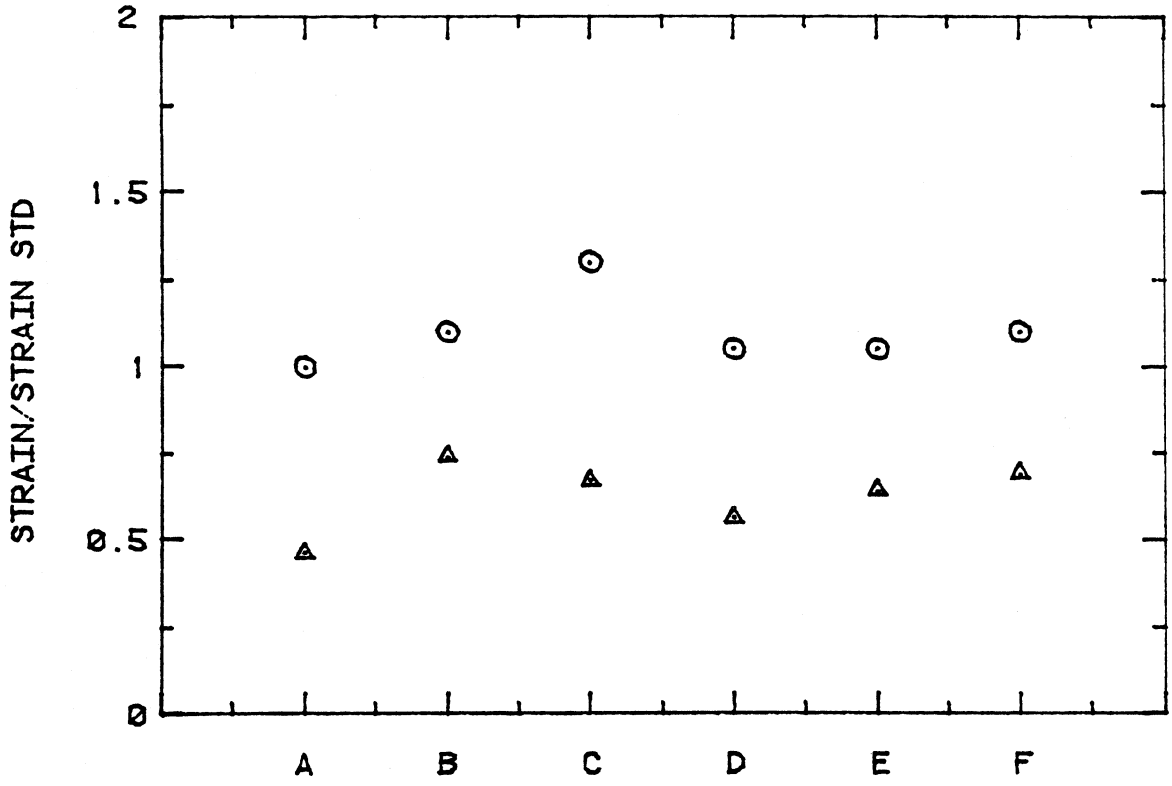

△ 3% TYPE I PORTLAND CEMENT TREATED MATRIX
7 DAY CURE

⊙ LOESS SOIL MATRIX 72 HOUR CURE

FIBER 0.17% FIBER WEIGHT FRACTION

A - MATRIX ONLY

B - 15 DPF POLYPROPYLENE 1 1/2"

C - 15 DPF CRIMPED POLYPROPYLENE 1 1/2"

D - 832 BB FIBERGLASS 1 1/4"

E - 360 DPF FIBRILLATED POLYPROPYLENE 1"

F - 360 DPF FIBRILLATED POLYPROPYLENE 1 1/2"

Figure 34. Strain at failure ratios, 3 percent cement treatment, 7 day cure

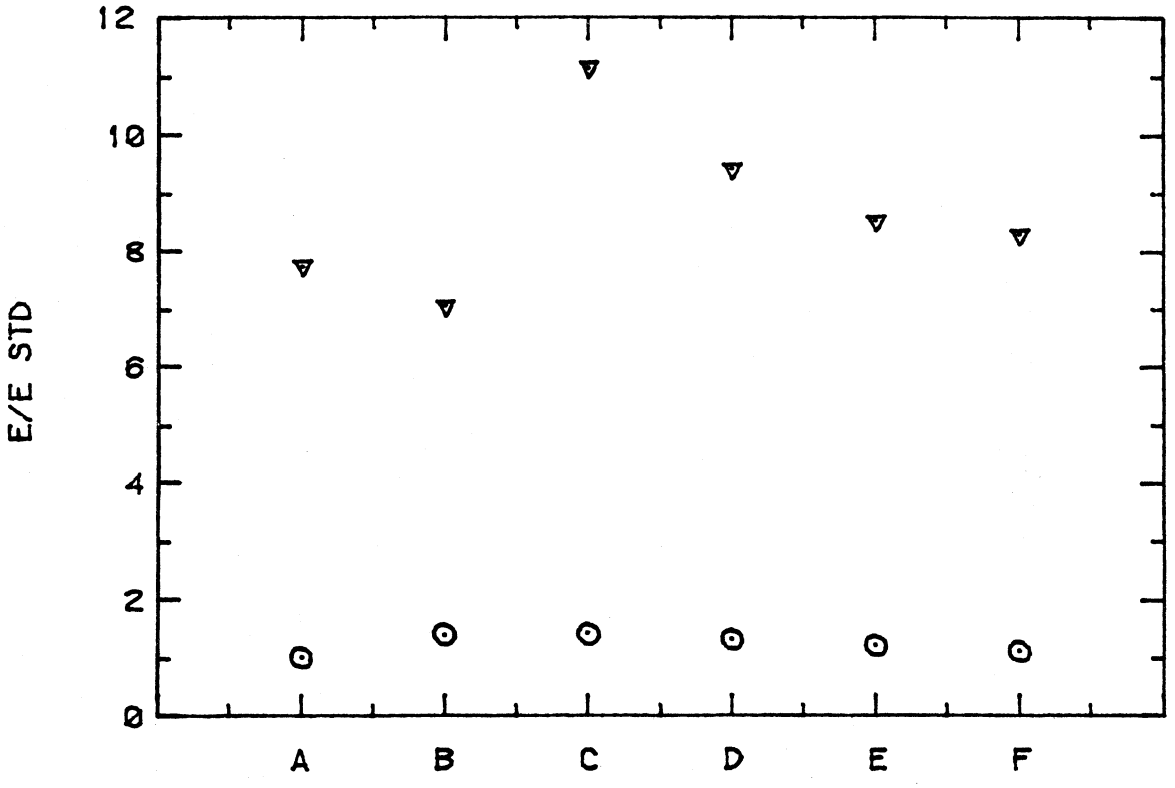

Figure 35. Modulus ratios, 3 percent cement treatment, 24 hour cure

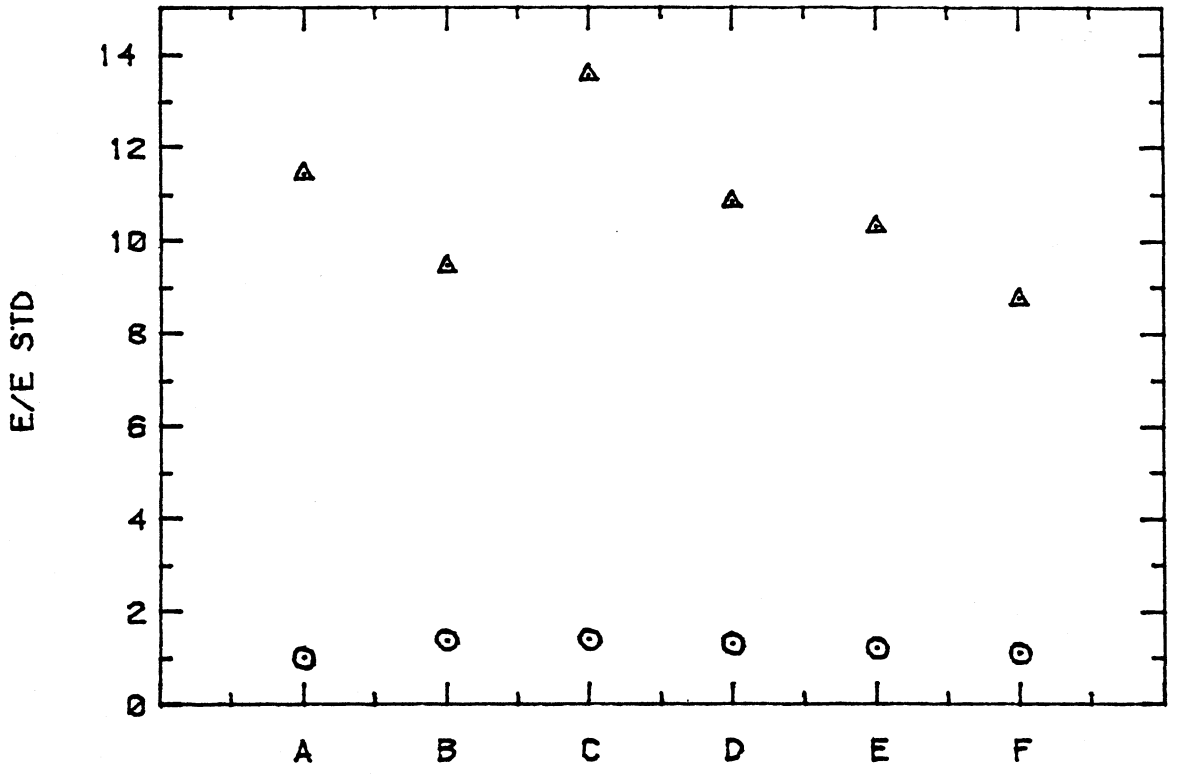

Figure 36. Modulus ratios, 3 percent cement treatment, 7 day cure

Story County, Mortenson Road Soil

Based on data and observations from the Linn County and Sioux City soils, the 360 dpf fibrillated polypropylene, 1.5 inch length fibers were used in conjunction with the more plastic A-6(3) Mortenson Road soil. All Proctor size unconfined compression test specimens were prepared and cured as previously discussed.

The first series of tests consisted of duplicate specimens molded to near untreated optimum moisture content with varying fiber weight fractions. Figure 37 presents the stress-strain relationships produced at the varying fiber weight fractions. Stiffness and q_u of the composites increased as fiber content increased up to a fiber weight fraction of 0.3%. At 0.5%, q_u and stiffness tended to decrease, thus indicating an optimum fiber weight fraction at 0.3-0.5 percent. As may be noted from Figure 37, the strain at maximum q_u increased with increasing fiber content, once again implying that fiber inclusion into a soil matrix produces greater ductility.

In a quantitative sense, toughness is defined as the area under a stress-strain curve for either compressive or tensile loading conditions (16). In some respects, toughness is related to the ductility of a material, because the more ductile a material, the larger is the area under the curve. Fiber inclusion in concrete makes it more ductile since fibers inhibit crack growth and extra energy is required to propagate cracks. In addition, energy is required to debond and stretch the fibers. Therefore, the strain energy required to fail a fiber concrete specimen is much greater than that required to fail a specimen made of plain concrete.

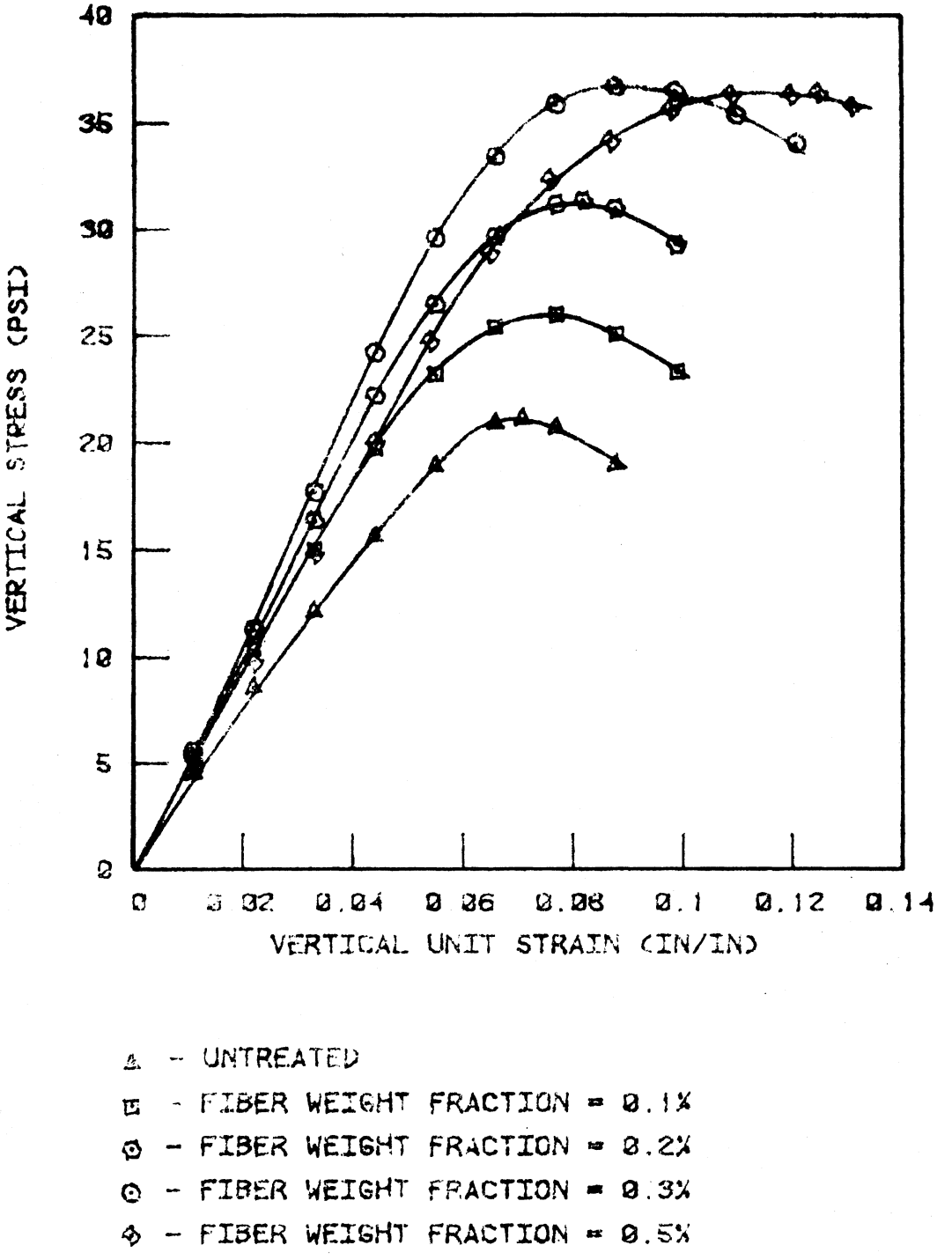

Figure 37. Average stress-strain relationship for specimens treated at varying fiber weight fractions of 360 dpf fibrillated polypropylene, 1.5 ".

Concrete toughness increases with increasing fiber weight fraction (16). Shah and Rangan (31) showed that up to an aspect ratio of 75, increasing the length of fiber resulted in an increase in toughness both in flexure and in direct tension. They also found that fiber alignment and orientation influences the toughness of concrete. Therefore, the same parameters that were found to be important in determining tensile and compressive strengths of fiber concrete, also greatly influences the toughness of fiber concrete.

Shah and Rangan (31) noted a relationship between ultimate flexural stress and toughness of the composite as a function of fiber weight fraction. Both parameters increased with increasing fiber weight fraction, though the increase in toughness was far more drastic than the increase in flexural strength. One case was quoted wherein a fiber volume fraction of 1.25% increased toughness twenty times that of the untreated. and the corresponding increase in flexural strength was less than two times. This phenomenon was attributed to the fact that fiber addition into a concrete matrix considerably enhances the ductility of the matrix, since fibers stretch or elongate when tensile stresses are imposed. Therefore, in fiber concrete, energy is spent on stretching the fibers as well as deforming the composite, increasing the amount of energy required to fail the composite.

The relationships just noted for toughness and flexure of fiber reinforced concrete are not unlike those which may occur in fiber reinforced soil. Using the definition of toughness as the area under the stress-strain curve to the point of maximum compressive stress, this parameter was determined for each curve presented in Figure 37. Results are noted in

Figure 38 and Table 17 for each fiber weight fraction with the Mortenson Road soil.

Stress-strain relationships noted in Figure 37 indicate a straight line portion followed by a curve. In elastic theory, the point at which curvature begins is the proportional limit. Stress at the proportional limit was determined for each of the fiber composite specimens and is also presented in Figure 38.

Figure 38 was plotted in terms of ratios of the fiber treated versus untreated, and illustrates the variation of each abovementioned parameter with fiber weight fraction. The maximum increase in q_u was about 60% at a fiber content of 0.3 - 0.5%. The strain modulus, E, also produced a maximum improvement of about 60%, but at a fiber weight fraction of 0.2%, beyond which E reduced.

The stress at proportional limit, Figure 38, increased with increasing fiber weight fractions, showing a maximum stress at about 0.3% content, then reducing at 0.5%. This appears contrary to what occurs in fiber concrete (16). Inclusion of fibers in a concrete matrix does not significantly increase the proportional limit stress, since the tensile strength of fibers in concrete is not mobilized until after first crack strength, which is beyond the proportional limit. The phenomenon is thus different in soil, and may be related to the fact that soil is less brittle than concrete. In soil, large vertical strains occur even at stresses below the proportional limit, indicating the possibility that tensile stresses of the fiber may be mobilizing prior to attaining the proportional limit stress.

The modulus of toughness produced the same trend as q_u but magnitudes

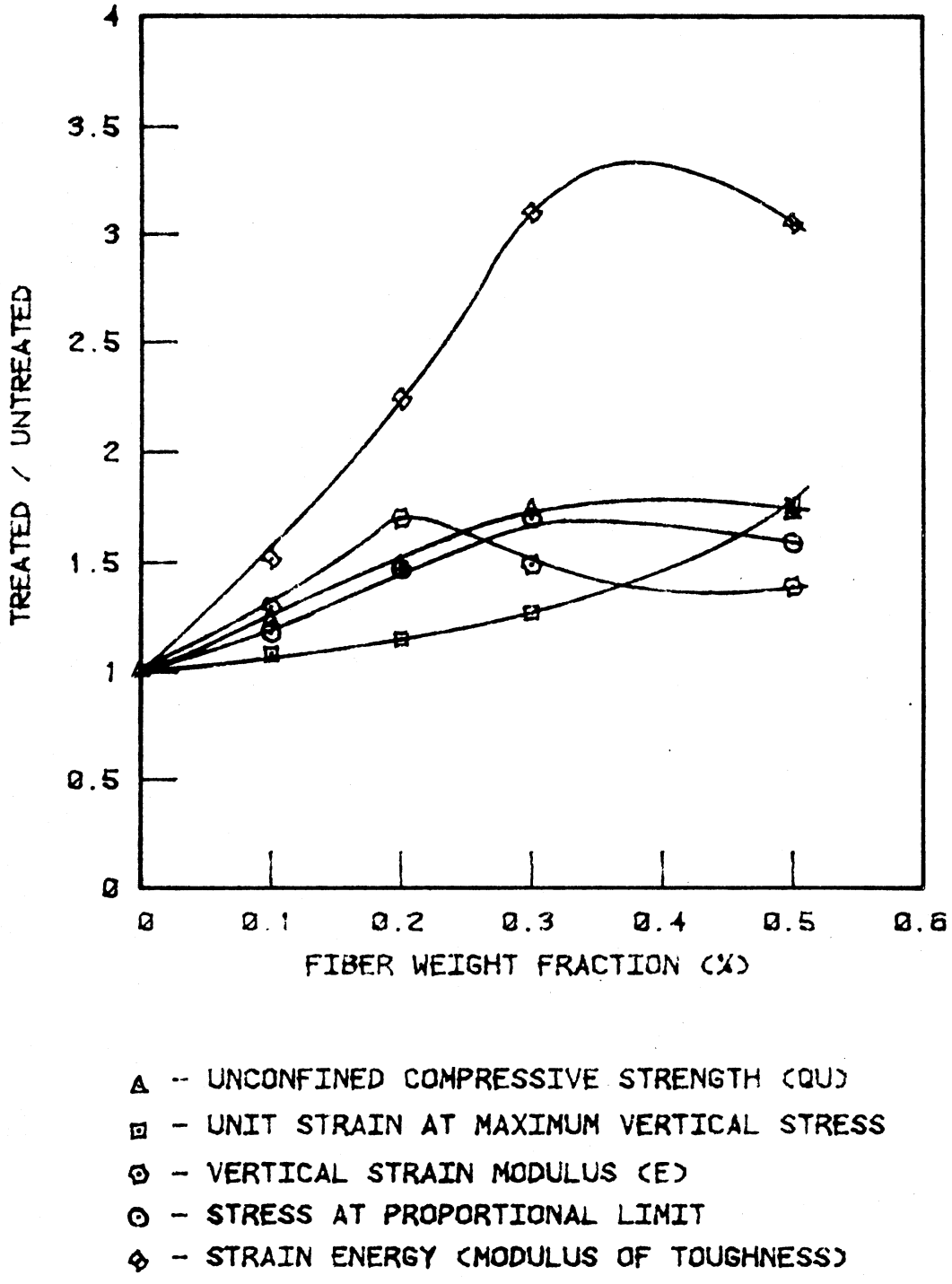

Figure 38. Effect of stress strain parameters with various fiber weight fractions of 360 dpf fibrillated polypropylene, 1.5".

Table 17. Average unconfined compression values for 360 dpf fibrillated polypropylene (1.5 in) specimens at varying fiber weight fractions, Mortenson Road soil

Fiber Weight Fraction, %	Moisture Content, %	Dry Density, pcf	Unconfined Compressive Strength, q_u, psi	Vertical Strain at Failure, ε, in/in	Strain Modulus, E, psi	Modulus of Toughness, lb-in/in^3
0	13.8	116.3	21.10	0.071	400	212.6
0.1	13.4	119.3	25.97	0.077	520	323.1
0.2	12.9	119.8	31.37	0.082	680	476.2
0.3	14.6	118.3	36.71	0.090	596	659.1
0.5	13.6	120.3	36.38	0.125	556	648.4

differed tremendously. At a fiber weight fraction of 0.3%, the modulus of toughness increased by a factor greater than 3, implying that the amount of work, or energy, required to fail the fiber treated soil specimens was 3 times greater than that required to fail untreated specimens. In fiber treated specimens, energy is spent on breaking interfacial bonding between the soil and fiber, stretching and pulling the fibers as the matrix material fails, and fiber pullout is taking place. This same phenomenon was previously noted as having been observed in fiber concrete (31).

The concept of strain energy, or toughness, of a material is related to its ductility. If highly ductile, the material will require increased energy or work to cause complete failure. The more ductile a material, the greater its capability to resist impact stresses, since it can absorb more energy before rupture than its less ductile counterpart.

A second series of Mortenson Road specimens was molded at a constant fiber weight fraction of 0.4% using the 1.5 inch 360 dpf fibrillated polypropylene, but with moisture content being varied between about 8 and 16 percent. The 0.4% content was an arbitrary compromise based on maximum beneficiations noted in the first test series. Table 18 summarizes the average values obtained from this series of specimens.

Figure 39 illustrates the variation of dry density with varying moisture content for both the untreated and fiber treated specimens. Maximum dry density and optimum moisture content for the untreated specimens were respectively about 125 pcf and 10.5% while for the treated specimens about 121 pcf and 12.5%. Differences in maximum dry density and optimum moisture content between untreated and fiber treated specimens occurs due to displacement of soil particles caused by the addition of fibers.

Table 18. Average unconfined compression test values for 360 dpf fibrillated polypropylene (1.5 in) specimens at varying moisture contents, Mortenson Road soil

Fiber Weight Fraction, %	Moisture Content, %	Dry Density, pcf	Unconfined Compressive Strength, q_u, psi	Vertical Strain at Failure, ε, in/in	Strain Modulus, E, psi	Modulus of Toughness, lb-in/in^3
0	8.0	120.4	23.4	0.038	770	268.4
0	9.6	123.4	20.9	0.044	440	197.4
0	11.0	124.7	15.0	0.060	300	109.6
0	13.0	119.4	7.1	0.100	82	24.3
0	14.9	114.9	2.5	0.165	17	2.8
0.4	8.9	115.5	44.8	0.098	643	988.7
0.4	10.5	118.3	52.5	0.132	674	1372.4
0.4	12.5	120.9	35.6	0.52	332	622.3
0.4	14.4	116.4	13.8	0.222	100	93.1
0.4	16.0	113.8	7.3	0.217	62	25.9

In addition, the specific gravity of soil is higher than that of the fibers, resulting in a fiber treated specimen weighing less than an untreated specimen of equal volume. Also, fiber inclusion in a soil matrix increases the amount of voids, thus increasing the amount of water required to reach standard AASHTO T-99 optimum.

At a moisture content of 9%, the increase in q_u due to fiber addition was 120%, while at 14% moisture the increase was 230%, Figure 40. At 8% moisture content, the untreated soil had a q_u of about 23 psi, while the fiber treated material produced the same q_u at better than 5% additional moisture. Both examples illustrate that at higher moisture contents, significant increases in unconfined compressive strength were obtained.

Figure 41 illustrates the variation of vertical strain modulus, E, versus moisture content for both untreated and fiber treated specimens of the Mortenson Road soil. For the untreated specimens, E decreased with increasing moisture content. For fiber treated specimens, a slight increase in strain modulus was observed when moisture content was increased from 9-11 percent, then decreased with increasing moisture content. Strain moduli for the fiber treated specimens was always higher than the untreated; at 14% moisture content the increase was 300%, demonstrating that fiber reinforcement was effective at moisture contents above optimum.

Figure 42 shows that unit strain at maximum stress increased with increasing moisture content, and that unit strain was generally higher for the fiber treated specimens. Unit strain appeared to level off however at 14-16% moisture.

Magnitude of increase in the modulus of toughness was significantly greater than the magnitude of strength gained due to inclusion of the

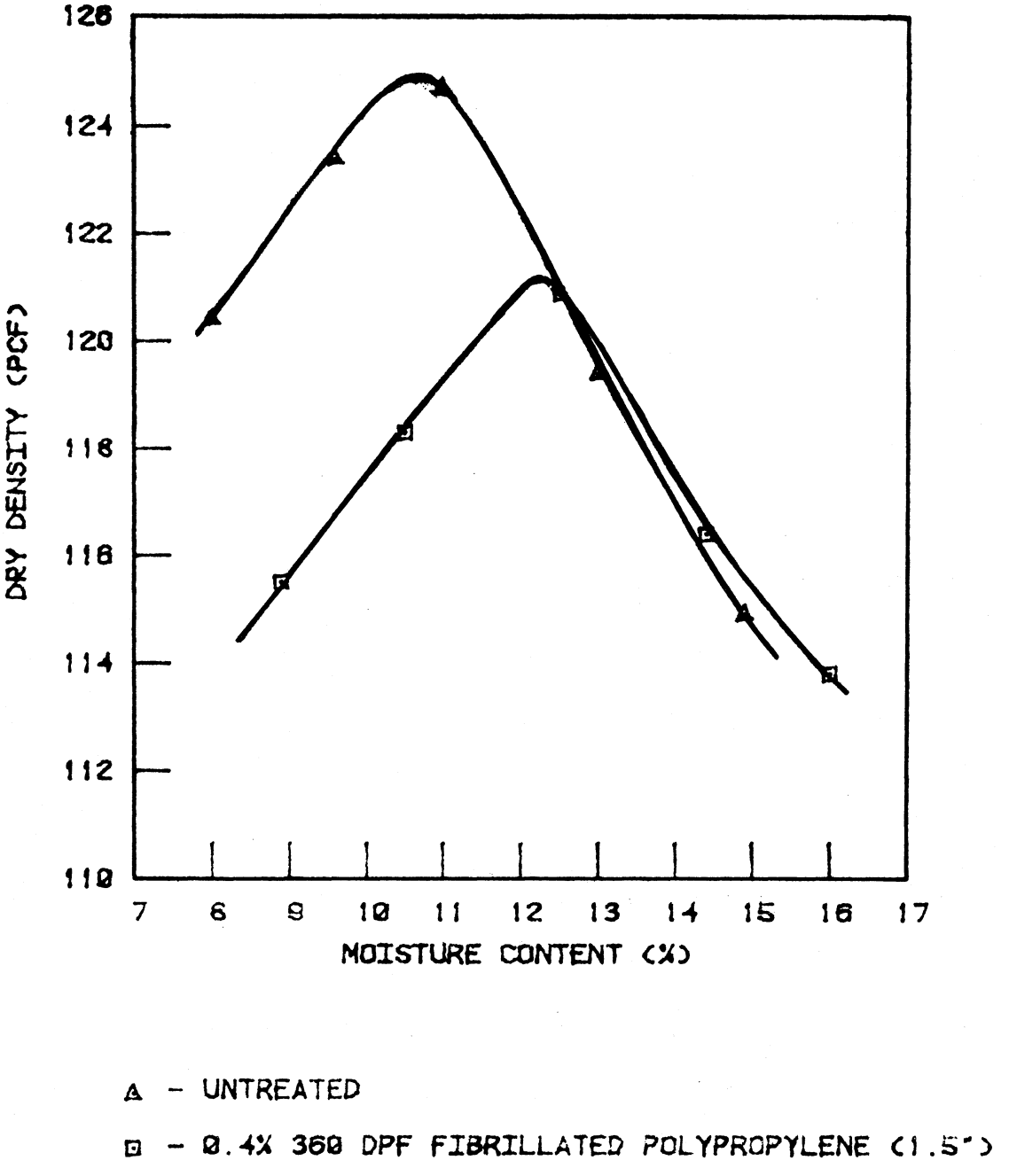

Figure 39. Variation in soil moisture-density under standard compaction due to inclusion of 360 dpf fibrillated polypropylene fibers, 1.5 inches.

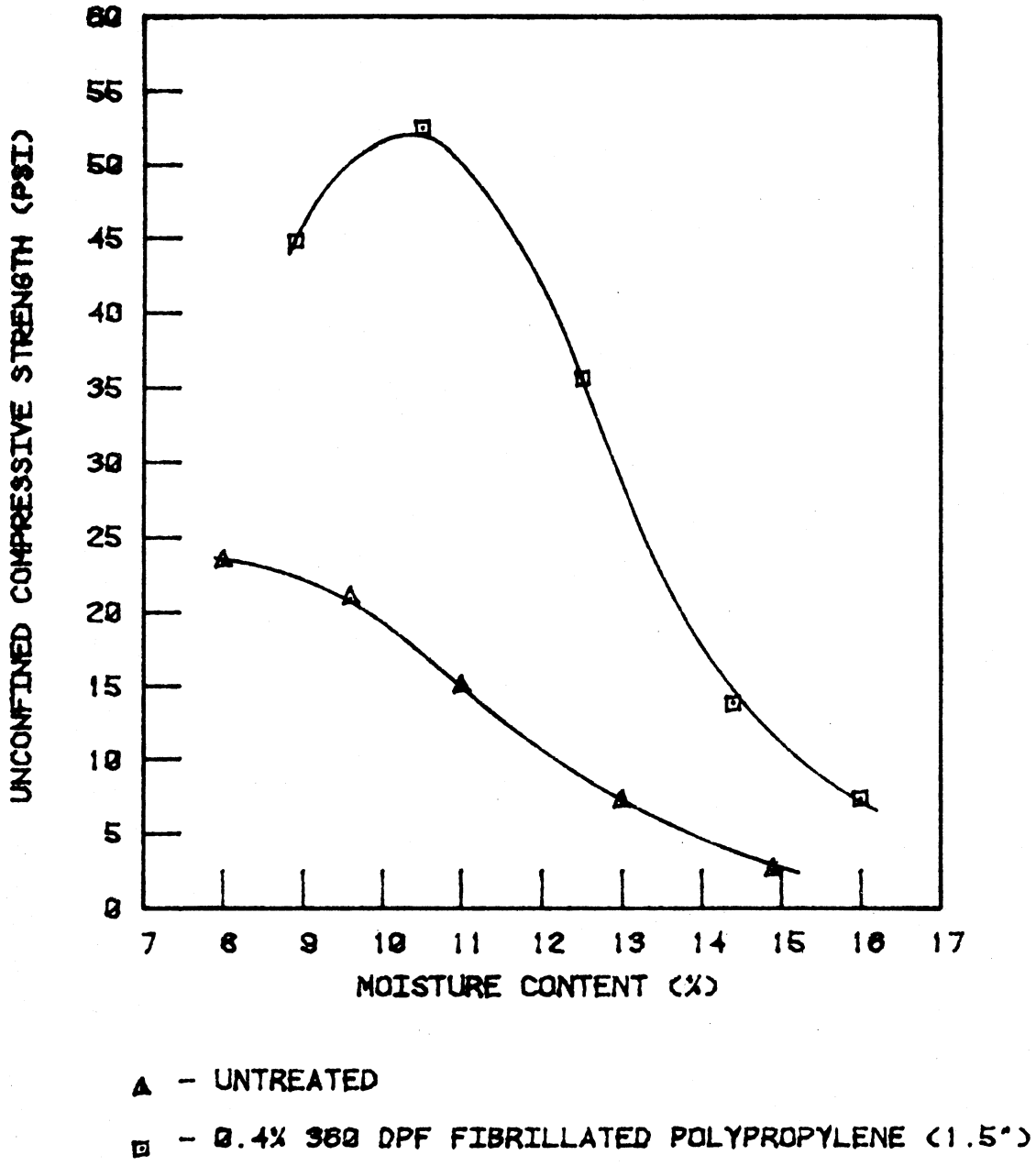

Figure 40. Variation of unconfined compressive strength versus moisture content due to inclusion of 360 dpf fibrillated polypropylene fiber, 1.5 inches.

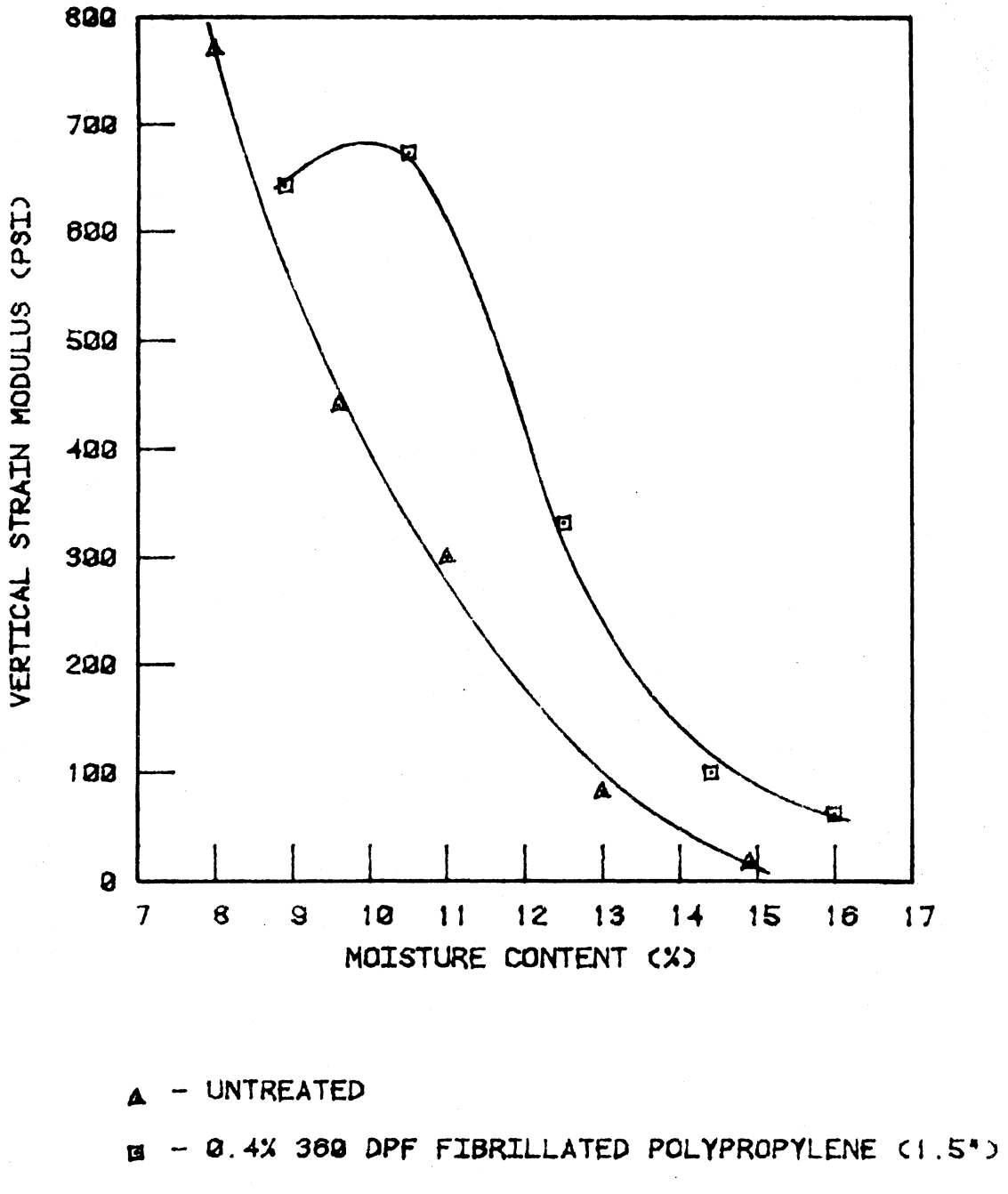

Figure 41. Variation of strain modulus (E) versus moisture content due to inclusion of 360 dpf fibrillated polypropylene fiber, 1.5 inches.

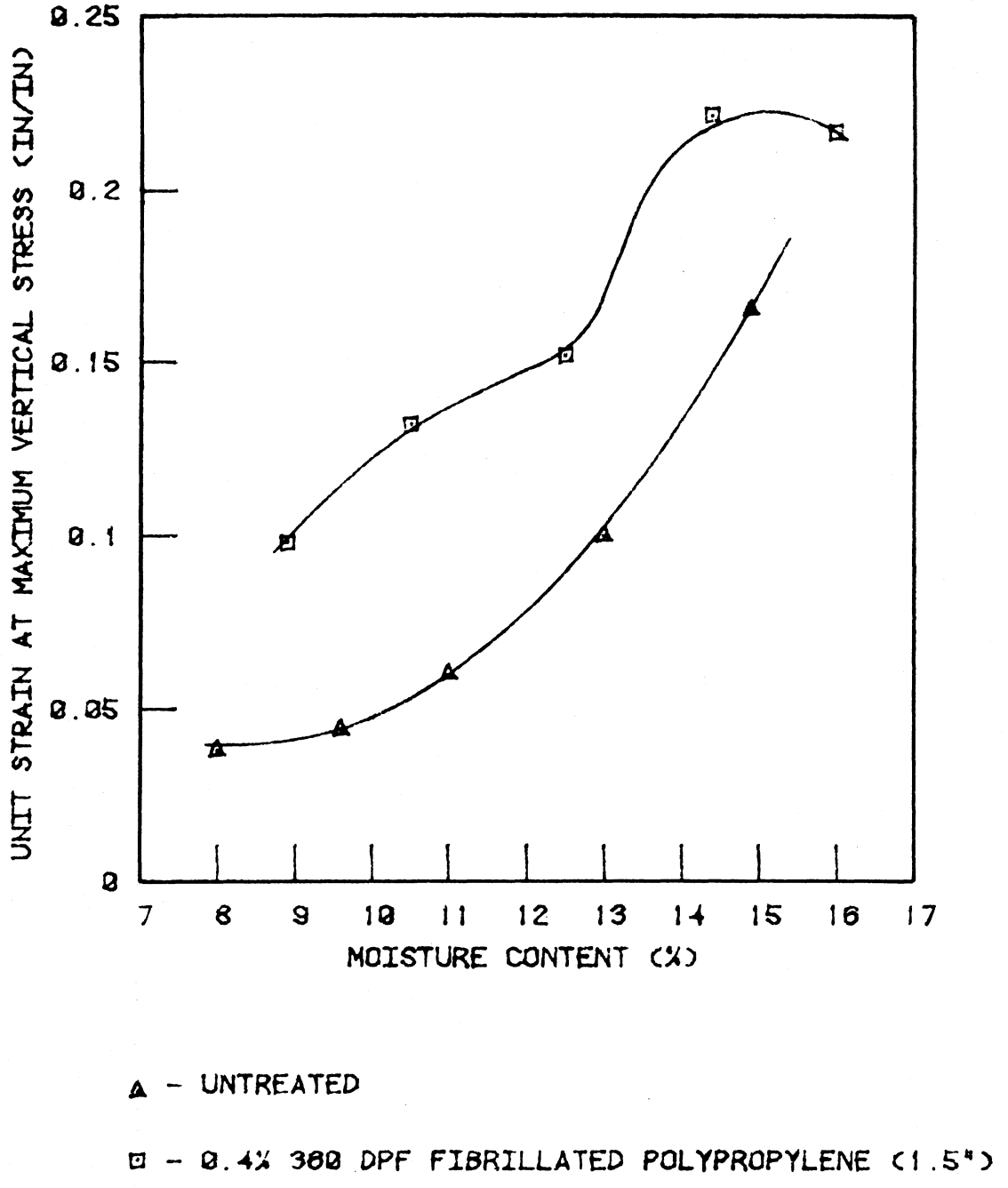

Figure 42. Variation of unit strain at maximum stress versus moisture content due to inclusion of 360 dpf fibrillated polypropylene fiber, 1.5 inches.

fibers, Figure 43. For example, at a moisture content of 9%, increase in modulus of toughness due to fiber inclusion was about 300% while at 14% moisture the increase was by more than 10 times. The increase in q_u obtained at the same moisture contents was 120% and 230%, respectively.

In order to observe the influence of a higher degree of compactive energy on the mechanical properties of soil fiber composites, a series of Mortenson Road soil specimens were molded at different fiber weight fractions, using 1.5 inch 360 dpf fibrillated polypropylene, 1.5 inch 15 dpf crimped polypropylene, and 1.5 inch 15 dpf polypropylene monofilament. Moisture contents were maintained at approximately modified compaction optimum, and compaction was accomplished using the AASHTO T-180 procedure. All specimens were wrapped and stored as previously noted. Unconfined compression test results are summarized in Table 19 and Figures 44-47; in the latter, all values are expressed as ratios of values obtained for untreated specimens molded under the standard T-99 compaction procedure.

In general, the unconfined compressive strength increased with increasing fiber weight fractions for each fiber, Figure 44. An exception occurred at 0.1% with the 15 dpf crimped polypropylene, where increased compaction did not improve q_u. The 15 dpf polypropylene monofilament produced the highest increase in q_u.

Similar trends were portrayed for modulus of toughness as shown in Figure 45, but magnitudes of change were significantly greater. For untreated specimens, the increase was of an order of magnitude of about 14, while at 0.2% 15 dpf polypropylene monifilament fiber treated specimens, the increase was about 30 times. Such increases in toughness further shows

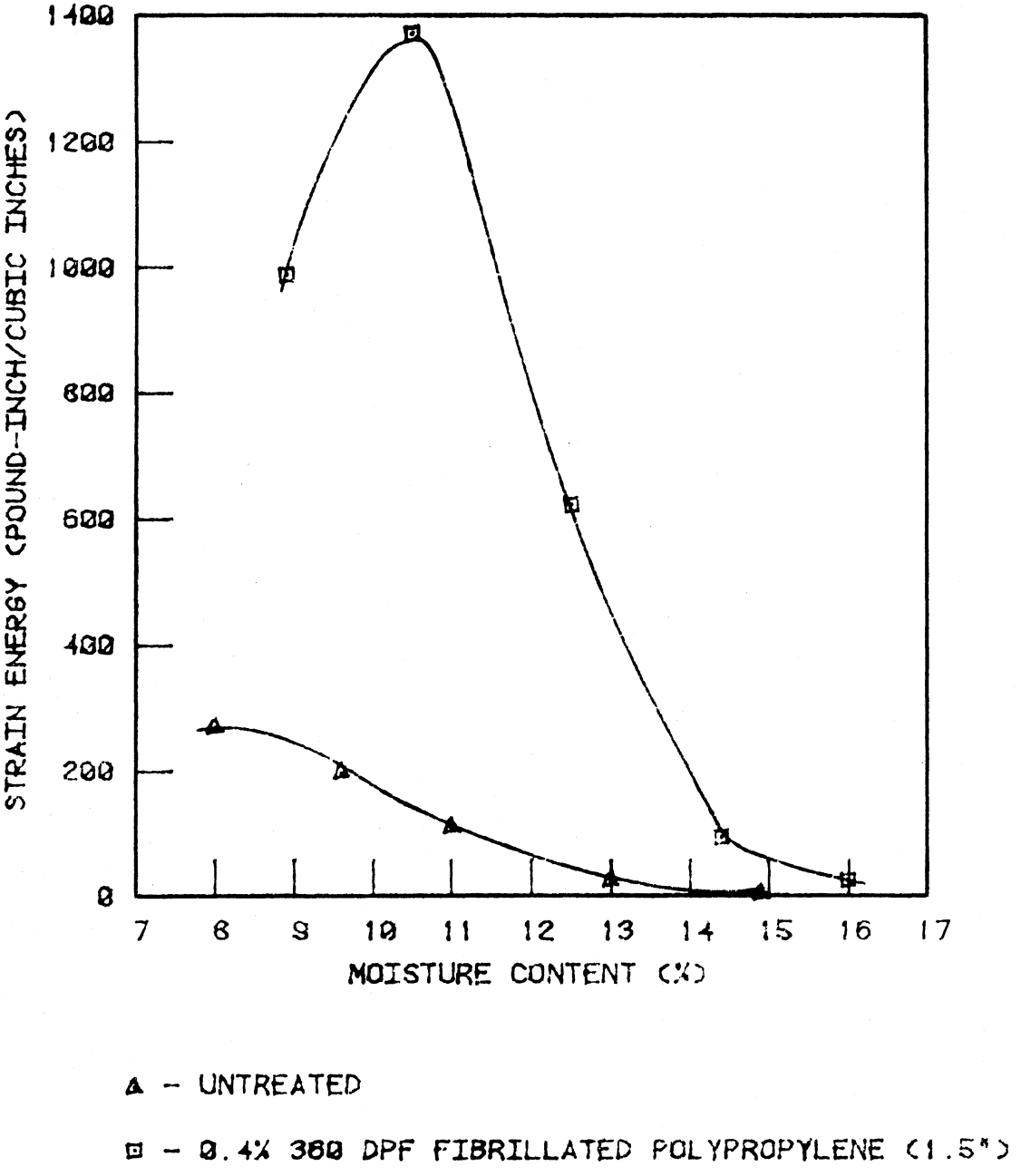

Figure 43. Variation strain energy (modulus of toughness) versus moisture content due to inclusion of 360 dpf fibrillated polypropylene fiber, 1.5 inches.

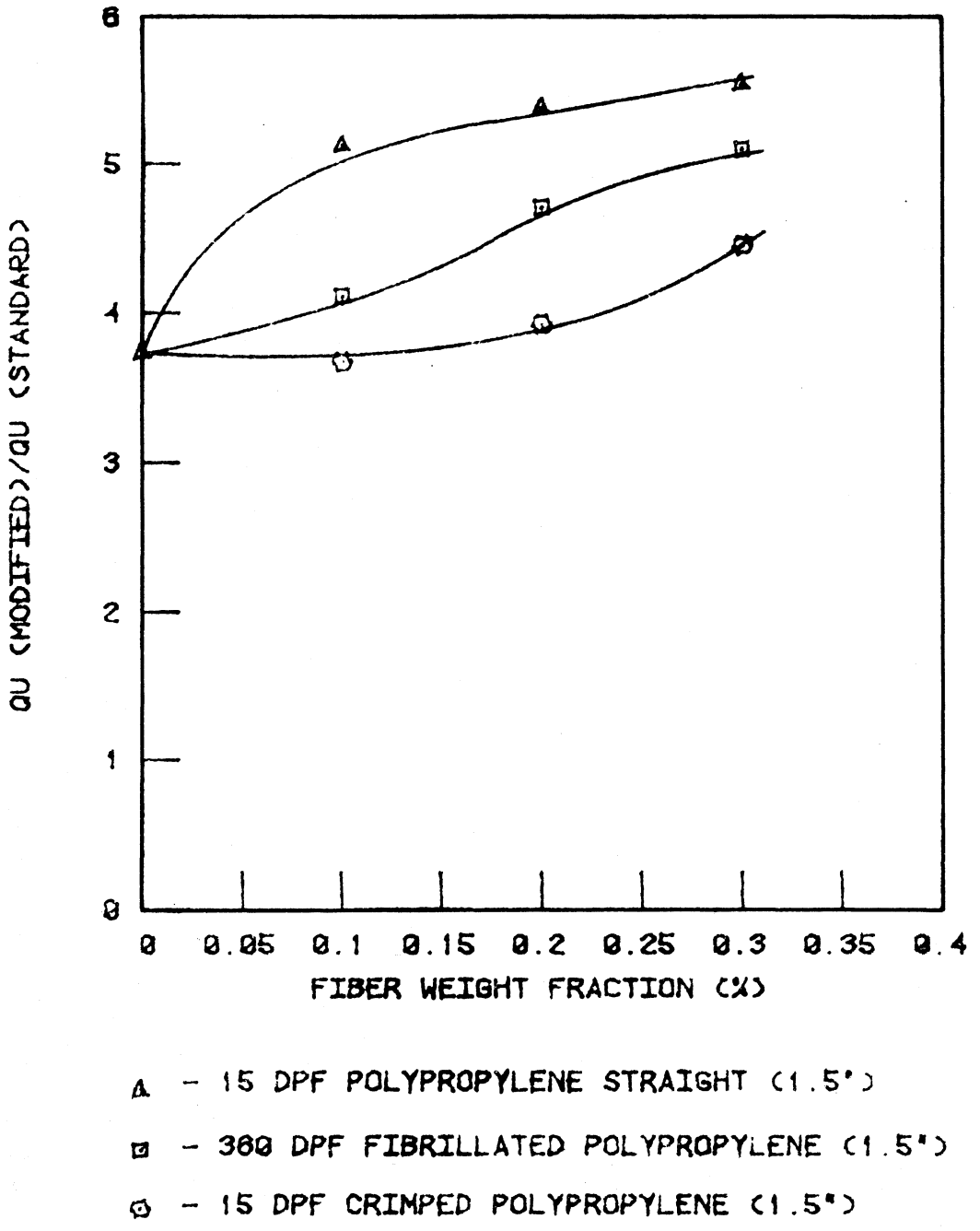

Figure 44. Ration of unconfined compressive strength under modified compaction to untreated q_u under standard compaction versus fiber weight fraction.

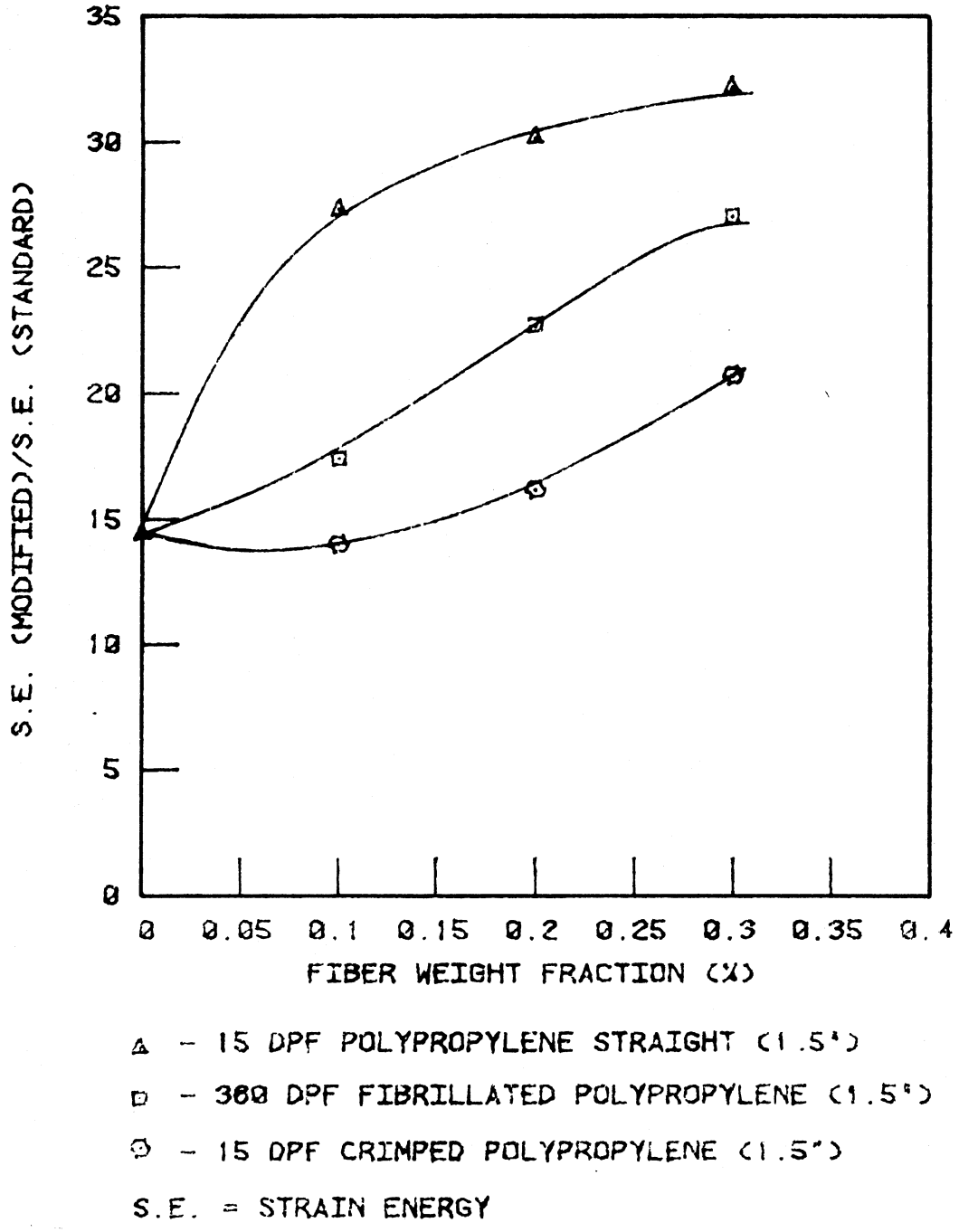

Figure 45. Ratio of strain energy under modified compaction to untreated strain energy under standard compaction versus fiber weight fraction.

Table 19. Unconfined compression test results for specimens molded under modified AASHTO T-180 compaction procedure at optimum moisture content (modified OMC = 10.4%, maximum dry density = 127 lb/ft^3

Fiber Weight Fraction, %	Moisture Content, %	Dry Density, pcf	Unconfined Compressive Strength, q_u, psi	Vertical Strain at Failure, ε in/in	Strain Modulus, E, psi	Modulus of Toughness lb-in/in^3
15 dpf polypropylene straight (1.5")						
0	9.9	128.2	78.7	0.046	2480	3061.2
0.1	10.0	126.2	108.0	0.064	2900	5818.6
0.2	10.1	125.2	113.5	0.074	2280	6433.7
0.3	9.9	124.6	116.8	0.073	2375	6868.6
360 dpf fibrillated polypropylene (1.5")						
0	9.9	128.2	78.7	0.046	2480	3061.2
0.1	9.8	127.9	86.8	0.056	2500	3712.3
0.2	10.4	127.1	99.1	0.069	2400	4828.5
0.3	10.4	126.4	107.6	0.087	2380	5760.1
15 dpf crimped polypropylene (1.5")						
0	9.9	128.2	78.7	0.046	2480	3061.2
0.1	10.9	122.4	77.5	0.060	1852	2990.0
0.2	10.4	124.6	82.7	0.071	1706	3453.0
0.3	10.6	124.2	93.8	0.085	1869	4417.0

the previously noted observation that inclusion of fibers in a soil matrix improves strain energy absorption.

In general, no major differences occurred in strain modulus, E, between untreated and fiber treated specimens due to the increased compactive effort, since increased compaction apparently caused a significant increase in brittleness of the composites, Figure 46. When vertical stresses are applied, only small vertical strains are mobilized prior to reaching the proportional limit stress, and as such, there may not be sufficient lateral movement to mobilize the tensile strength of the fiber.

The above hypothesis is further confirmed in Figure 47. Unit strain at maximum stress was reduced by nearly 40% for the untreated specimens, then slightly increased with increasing fiber weight fractions. At a fiber weight fraction of about 0.2%, the unit strain at peak stress for all fibers was basically equal to that of the specimens compacted at standard T-99 energy. All fibers appeared to increase the unit strain of the composites by about equal proportions.

Comparison of unconfined test data for the 1.5 inch 360 dpf fibrillated polypropylene fiber treated Mortenson Road soil under standard and modified compaction indicates significant improvements from increased compactive energy, Tables 17, 18, and 19. Increased compaction reduced the quantity of voids in the composites, bringing the soil particles and fibers closer together, increasing the number of contact points, and consequently increasing the frictional resistance provided by the composite. As noted from the literature review, the strength of interfacial bonding depends on strength of the matrix and fibers. Increasing the degree of compaction did

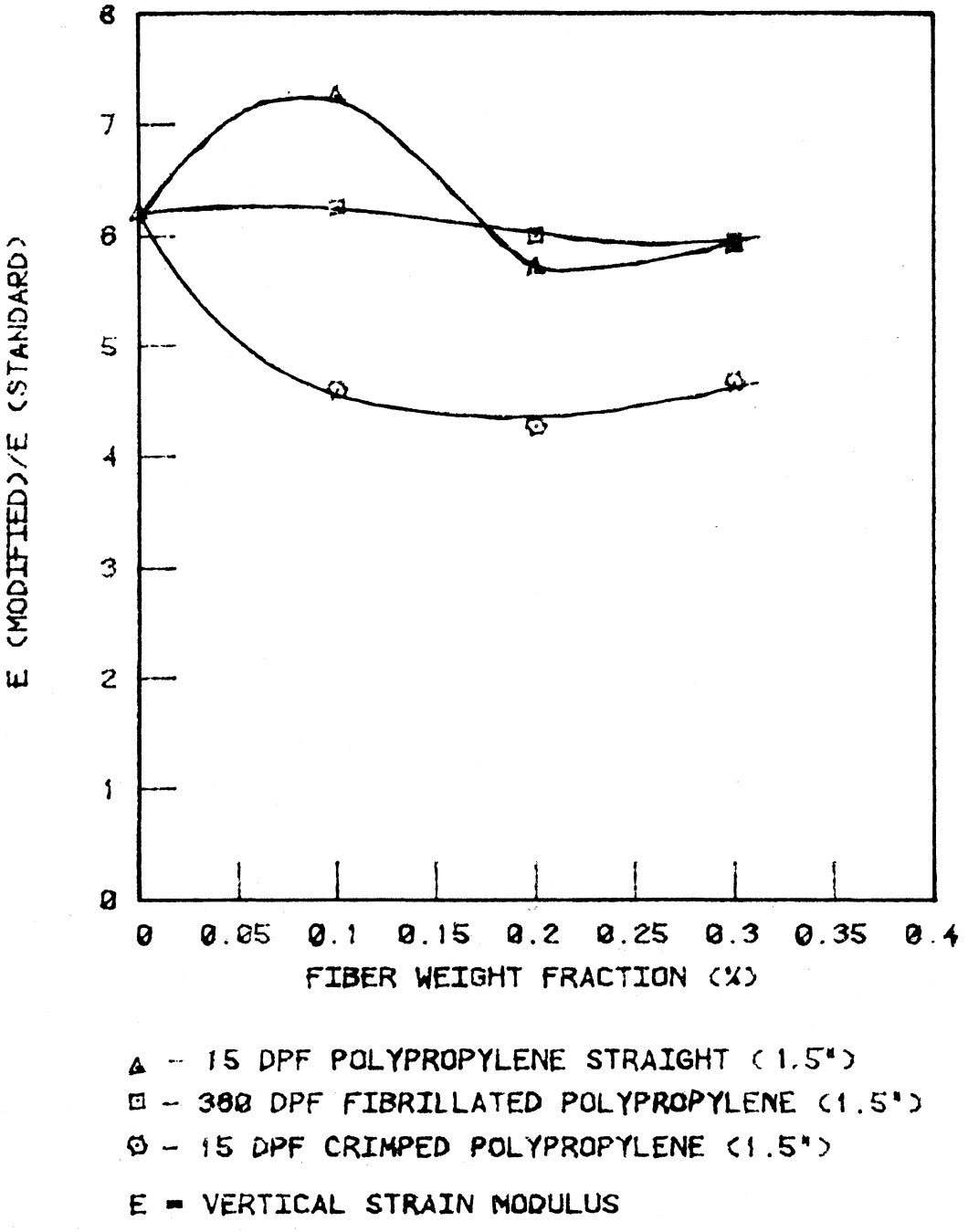

Figure 46. Ratio of strain modulus, E, under modified compaction to untreated E under compaction versus fiber weight fraction.

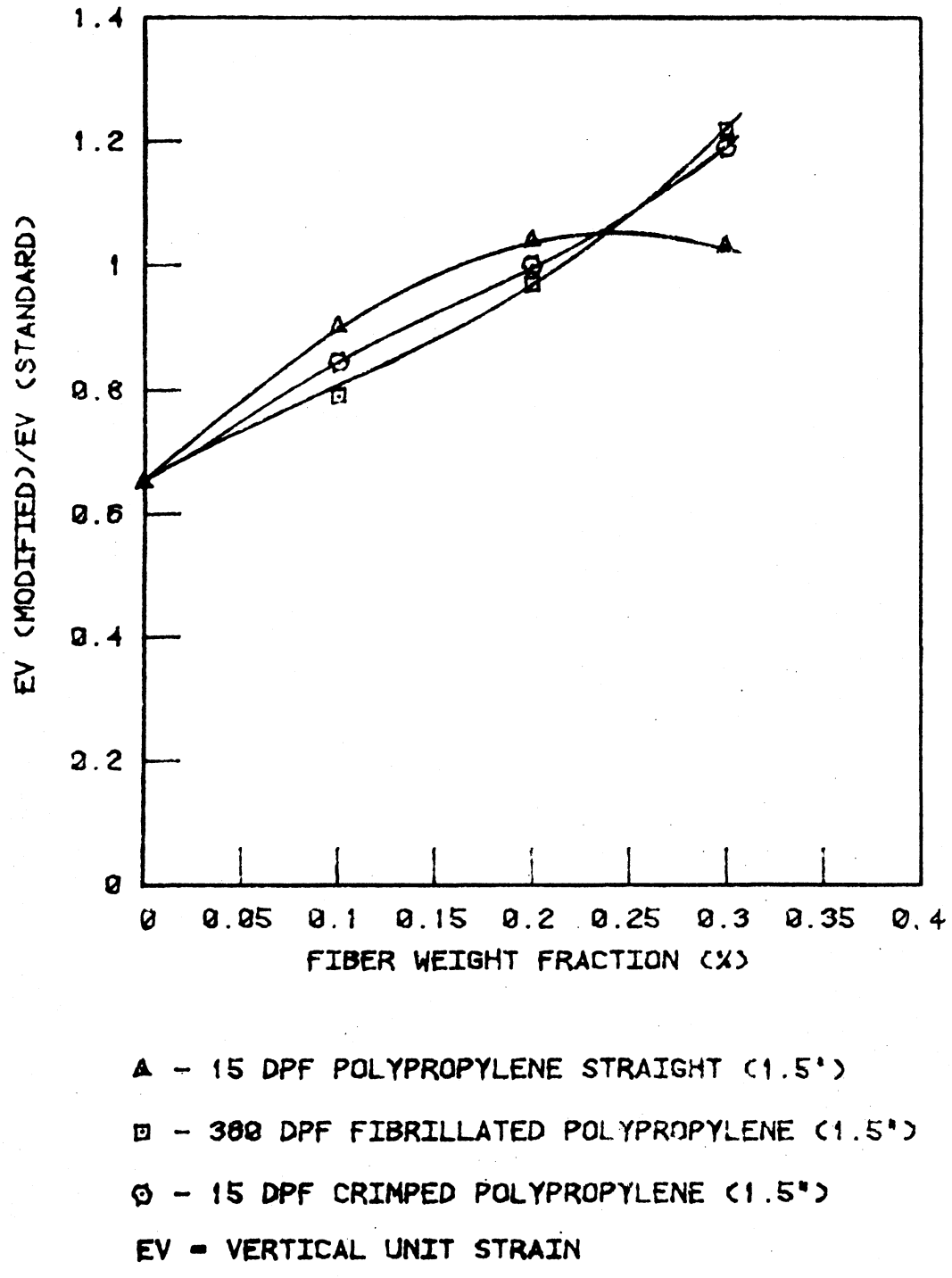

Figure 47. Ratio of unit strain under modified compaction to untreated unit strain under standard compaction versus fiber weight fraction.

not apparently alter strength of the fibers, but significantly increased the strength of the matrix, implying that a better interfacial fiber-matrix bond was obtained.

California Bearing Ratio Test

The California Bearing Ratio Test (CBR) is occasionally employed in the field of pavement design. While modifications to the test were necessary based upon available equipment, the procedures employed generally complied with specifications outlined in ASTM D1883 and AASHTO T193. The only variations in test technique employed from that prescribed was the increase of rate of loading from the required .05 inches per minute to .1 inches per minute and elimination of the soaked form of test. Due to the comparative nature of the analysis performed, the increased rate of strain was felt to have little effect upon the overall quality of results.

CBR tests were performed on both the Linn County A2-4(0) soil from Troy Mills, and the more plastic A-4(0) soil from Prairieburg, Table 4. Though nearly 100 CBR tests were performed on these two soils, the quantity of such tests were significantly less than the duplication of specimens performed in the K-Test and unconfined compression tests; therefore, a statistical analysis model of the data was not obtained.

Figures 48 through 53 illustrate average California Bearing Ratios versus fiber weight fractions obtained with various fibers for the two Linn County soils at near their respective standard optimum moisture contents. It should be noted that while moisture contents of these specimens were controlled, some variation was unavoidable. The CBR test demonstrated a

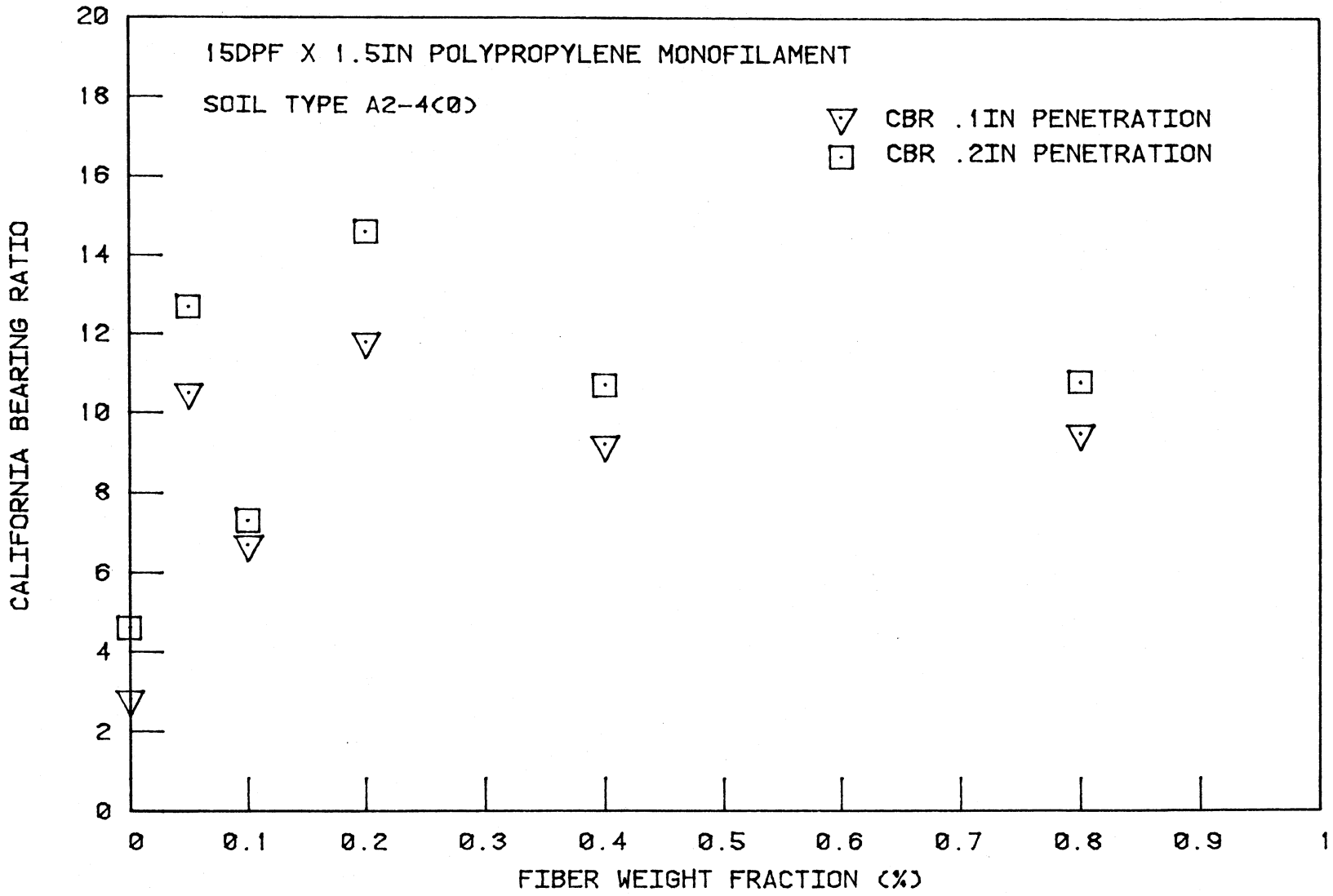

Figure 48. California Bearing Ratio versus fiber weight fraction

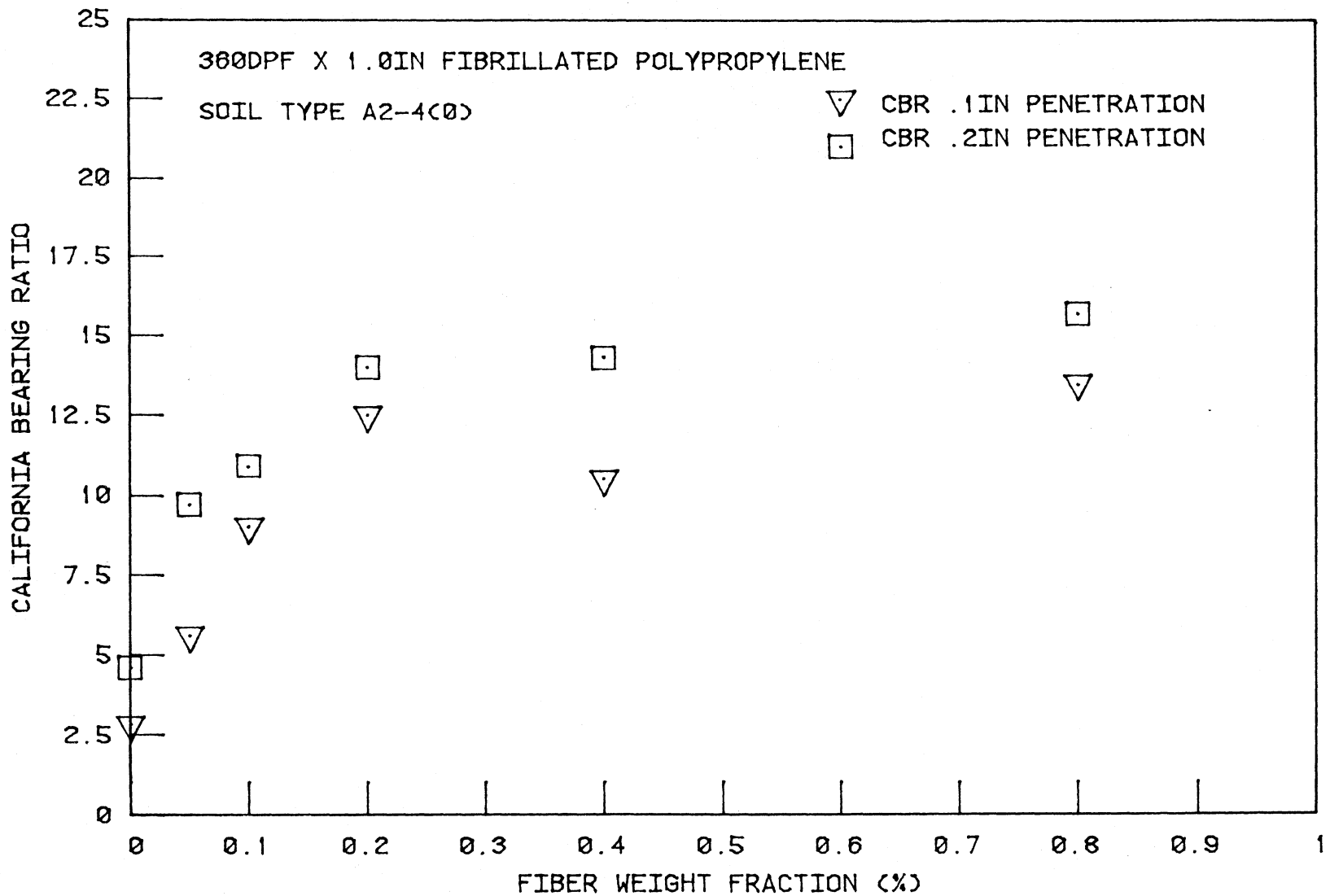

Figure 49. California Bearing Ratio versus fiber weight fraction

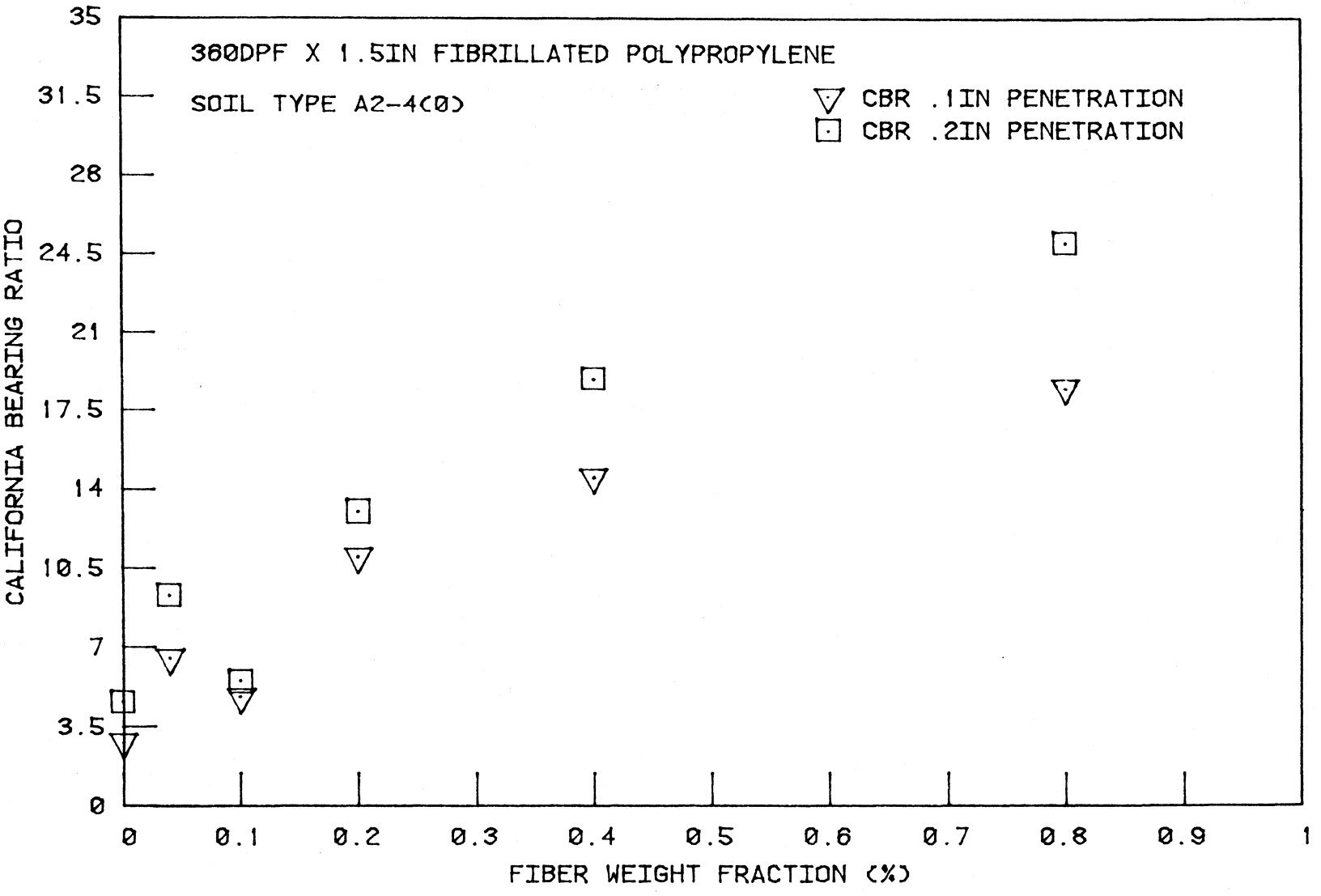

Figure 50. California Bearing Ratio versus fiber weight fraction

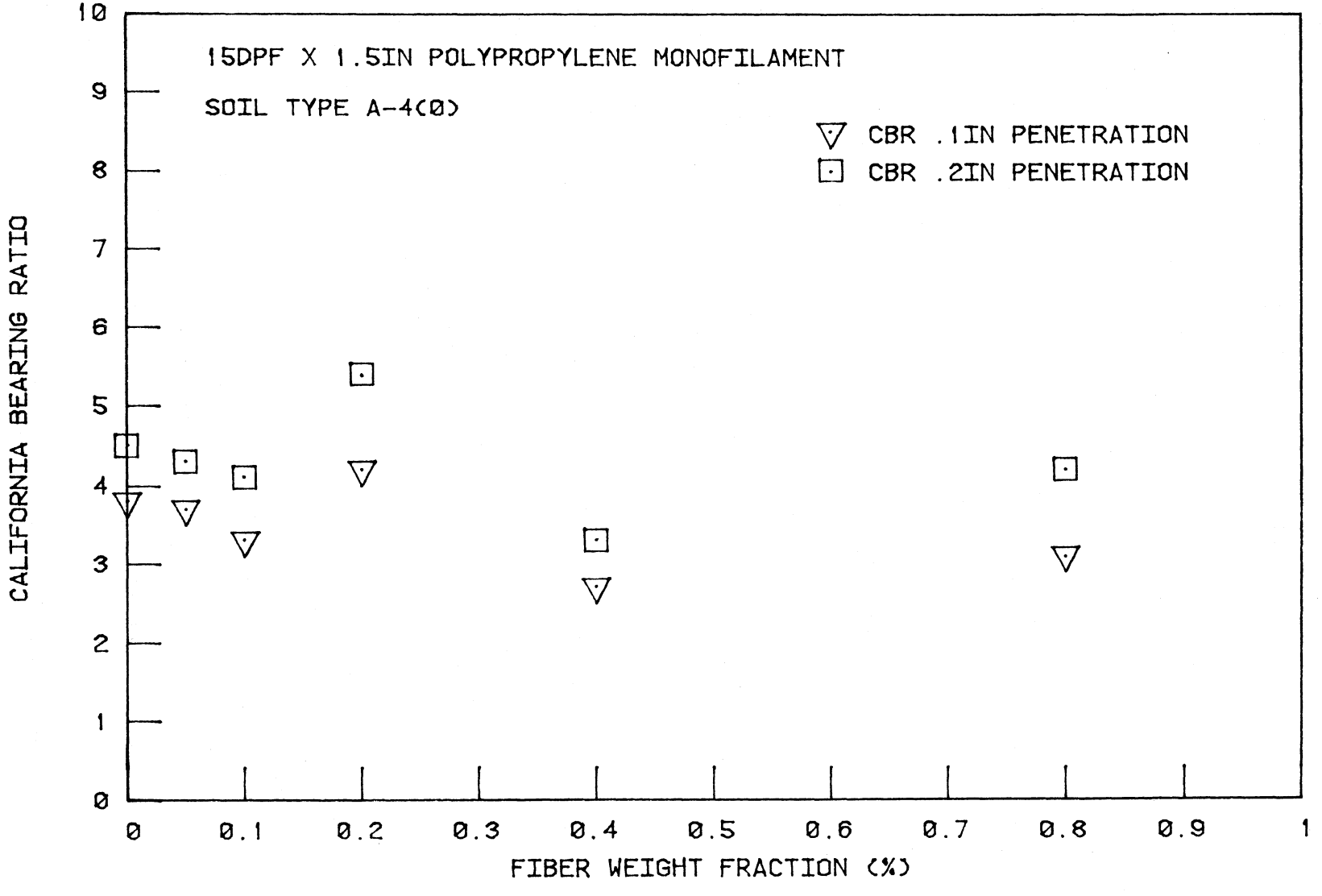

Figure 51. California Bearing Ratio versus fiber weight fraction

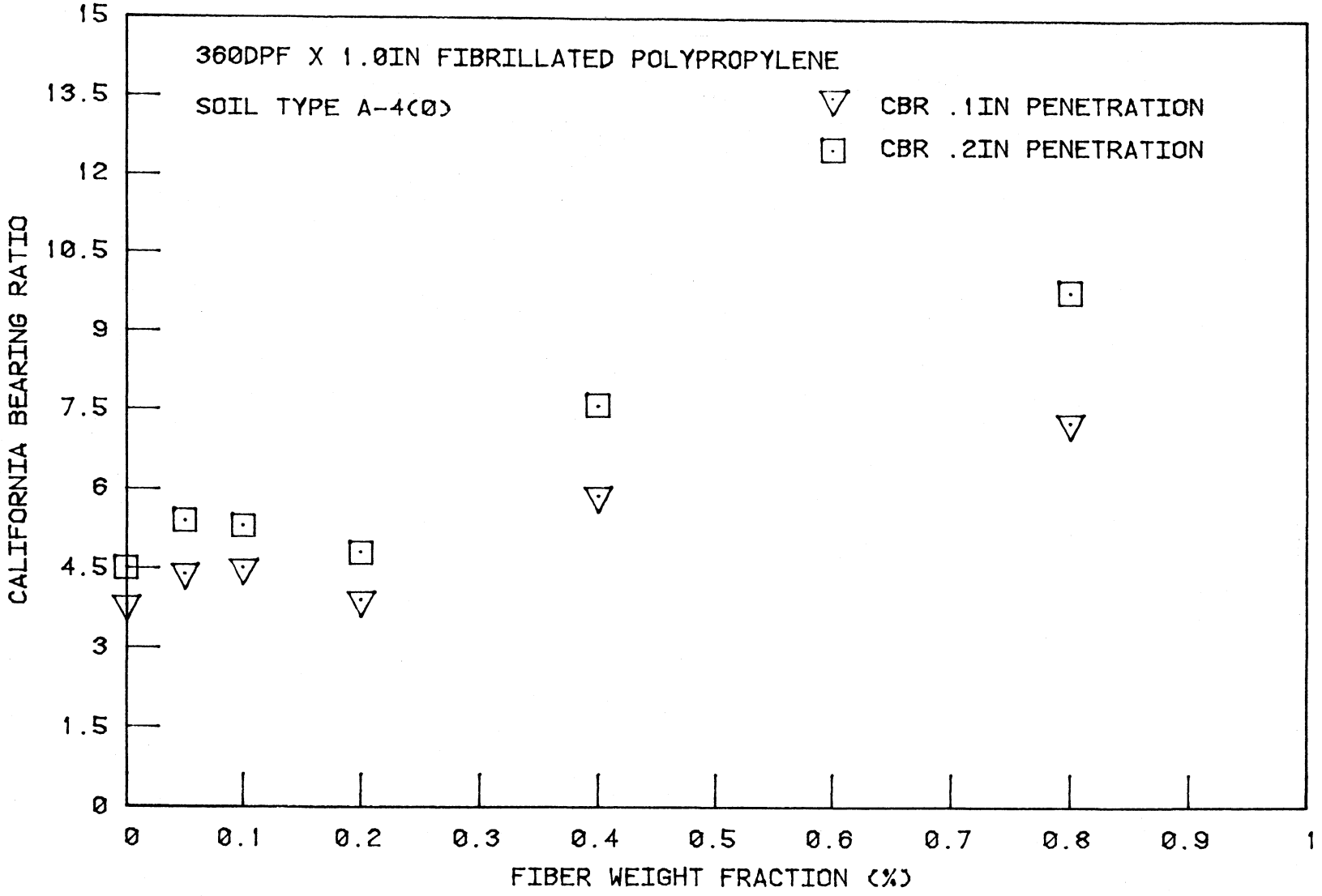

Figure 52. California Bearing Ratio versus fiber weight fraction

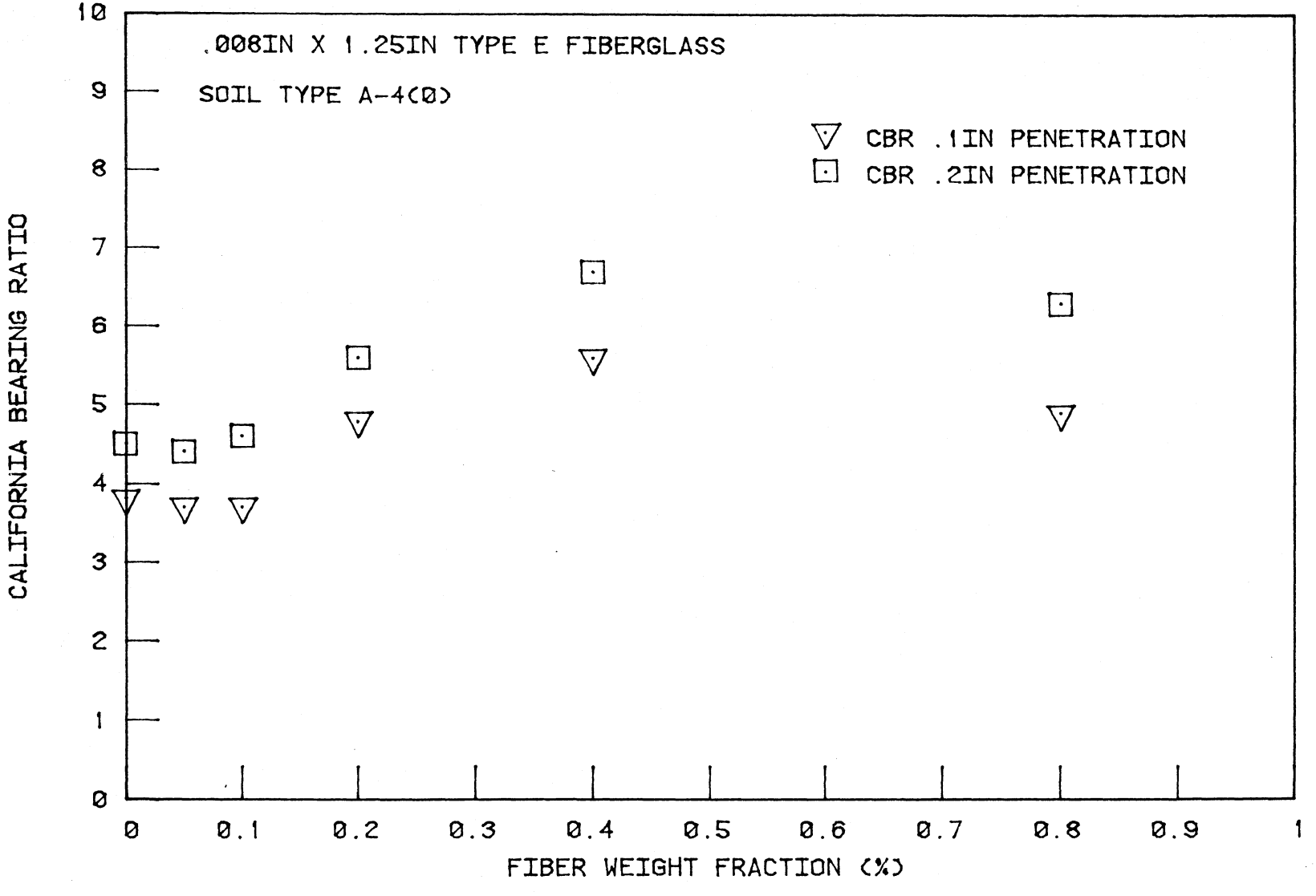

Figure 53. California Bearing Ratio versus fiber weight fraction

high sensitivity to very small moisture content fluctuations among untreated specimens of the same soil type, Figure 54. Consequently, this sensitivity was probably carried over into the treated specimens and compounded by the additional variability induced by randomization of fiber reinforcement.

In spite of the possible moisture sensitivity, Figures 48 through 53 reflect several definite trends. Fiber reinforcement in both soils illustrated some of the same general leveling of values as did results of the unconfined compression test results. CBR increases with the 15 dpf 1.5 inch polypropylene monofilament and the 360 dpf 1.0 inch fibrillated polypropylene in the A2-4(0) soil began to level off at the .1% fiber weight fraction, Figures 48 and 49, and were of the order of 2.5 - 3.0 times CBR of the untreated specimens. Bearing ratio improvements increased nearly linearly to a maximum of 6 times that of the untreated at .8% fiber weight fraction for the 1.5 inch long 360 dpf fibrillated polypropylene fibers, Figure 50, illustrating some of the previously noted effects of length on matrix-fiber interlock.

Figures 51 through 53 illustrate the results of CBR tests performed utilizing the same polypropylene fibers plus the .008 in. x 1.25 in. Type E fiberglass monofilaments, conducted with the more plastic A-4(0) soil. Test conditions and methods along with specimen preparation did not vary between this series of tests and the series run on the sandier less plastic A-2-4(0) soil; however, results of the testing varied greatly. Only two of the fibers, 1.5 inch fibrillated polypropylene and the 1.25 inch Type E fiberglass, reflected any improvement in CBR and then generally at higher

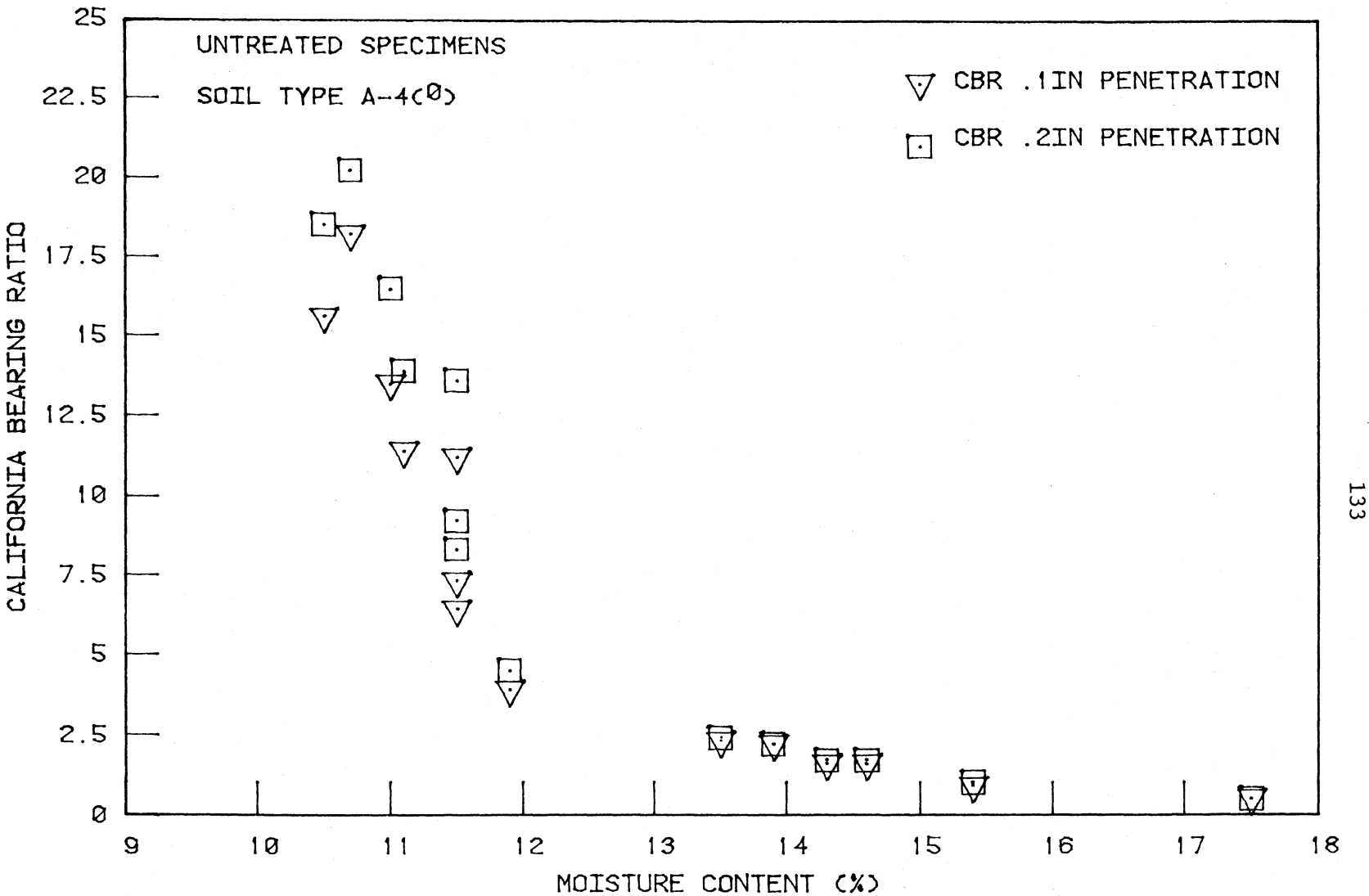

Figure 54. California Bearing Ratio versus moisture content

fiber weight fractions than in the A-2-4(0) soil; a maximum improvement of about 1.5 times that of the untreated for the .008 in. x 1.25 in. Type E fiberglass. Variability of CBR improvement with the same fiber under nearly identical test conditions within two soils indicates the variability of soil fiber bonding due to the change in soil matrix properties.

Figures 55 and 56 present CBR data from an evaluation of the effects of increasing moisture contents for the Linn County A-4(0) soil. At moisture contents of 18.5% and 15.5% (OMC = 11.0%), the effects of fiber addition were nil for the polypropylene monofilament and fibrillated fibers respectively, both of 1.5 inches length. Such loss of CBR versus moisture content indicates either or both of (1) a significant weakening of the soil-fiber bond, and (2) susceptibility of the CBR test to changes in moisture; the latter being shown in Figure 54.

Cyclic Load Test

Imposition of cyclic stresses may cause a material to experience fatigue failure after a period of time, even though applied stresses are below the material's ultimate static strength. This phenomena is important in the integrity of a roadway structure which depends on any materials capacity to resist cyclic, rather than static stresses. To more fully understand the behavior of randomly oriented fibers in roadway soils, a cyclic load test was devised to examine several properties of the soil fiber composites not normally ascertained through static tests such as the unconfined compression or CBR.

Using the concepts of constant cyclic stress (stress controlled), the

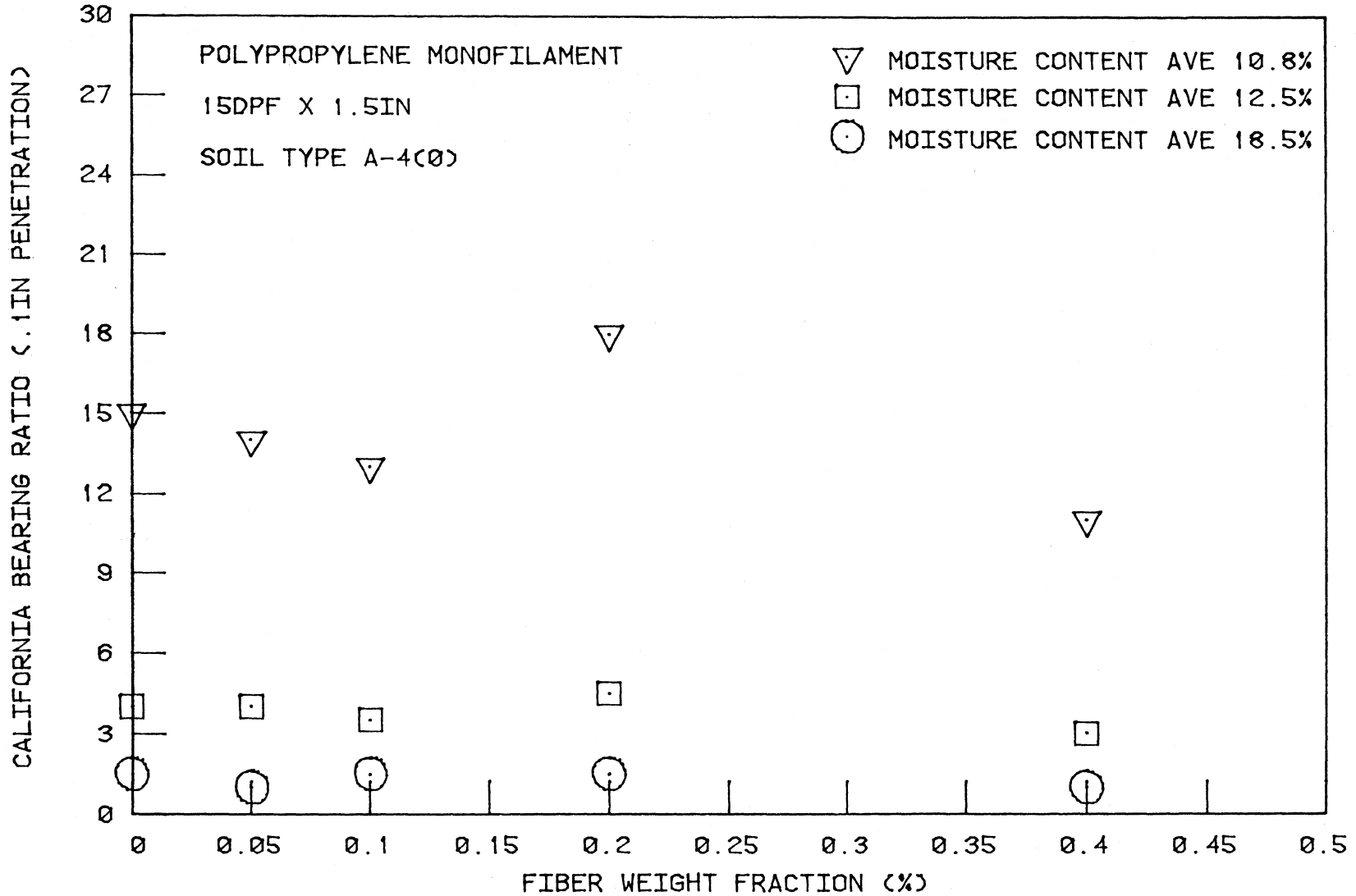

Figure 55. Comparison of California Bearing Ratio at 0.1 in. penetration versus fiber weight fraction at varying moisture contents.

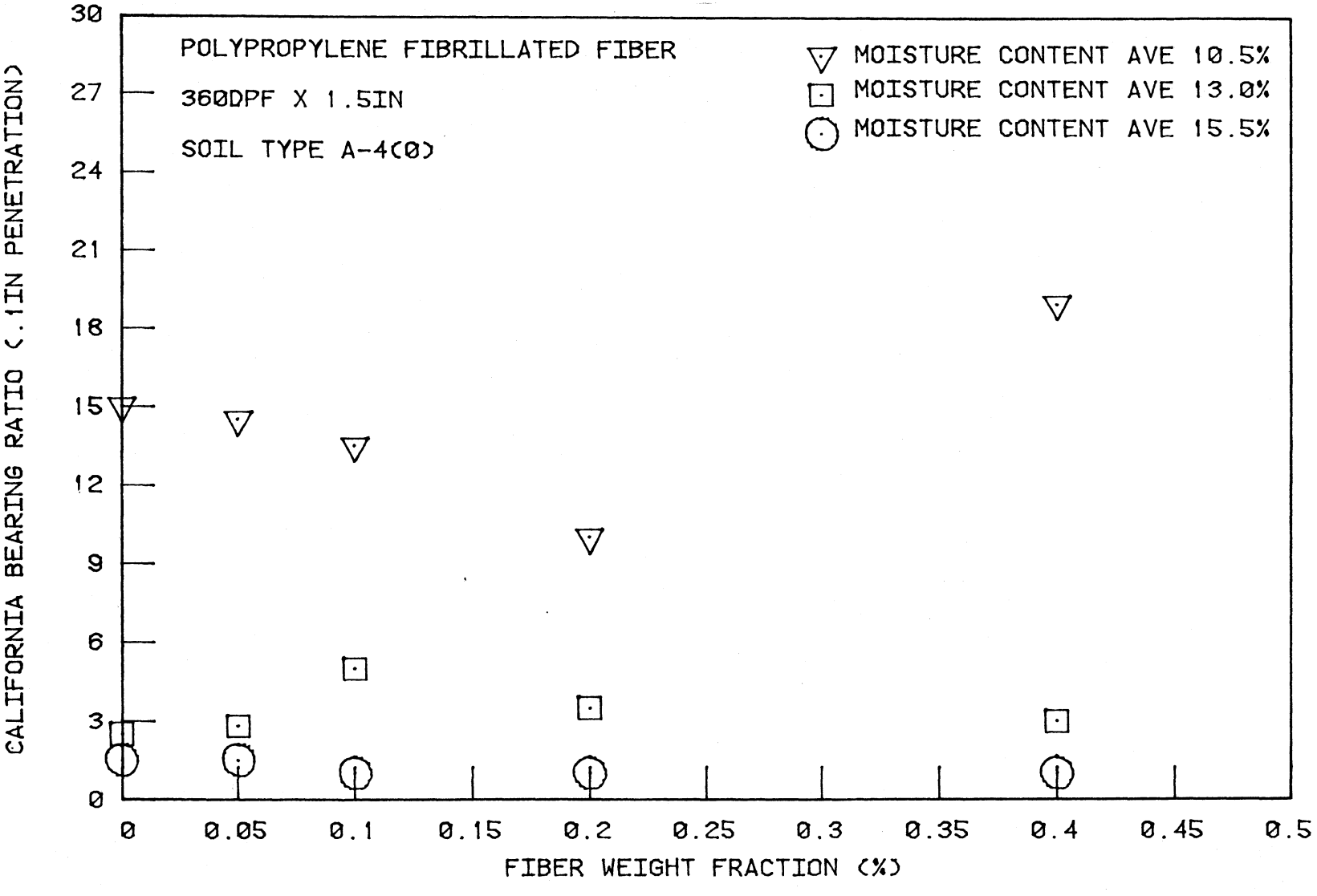

Figure 56. Comparison of California Bearing Ratio at 0.1 in. penetration versus fiber weight fraction at varying moisture contents.

cyclic load test procedure utilized standard Proctor specimens of untreated or fiber treated materials, at moisture contents equal to or exceeding optimum. Each specimen was wrapped with Parafilm paper in order to reduce soil/mold friction, placed in a variable expansion thin-walled Iowa K-Test unit, and subjected to cyclic loading. All loadings were cycled from zero to maximum vertical stress, the latter being held for 0.3 sec. dwell time. Vertical and circumferential deformations were measured with linear variable differential transducers (LVDT) while vertical stresses were monitored with a pressure transducer. All measurement outputs were tied to a SOL computer equipped with plotter and printer. A computer program automatically provided for processing and printout of data at specified numbers of load cycles during testing. All calculated data at maximum vertical stress was stored in a disc for later plotting of the various responses versus number of cycles. Since the test was stress controlled, the required vertical stress was established and maintained by the operator. All results were obtained as the average of tests performed on duplicate untreated and fiber treated specimens.

Characterization of the soil or soil-fiber composite material under constant vertical load was expressed in terms of vertical strain, horizontal strain, horizontal stress, stress ratio, vertical strain modulus, volumetric strain, and permanent set, and computed as follows:

$$\varepsilon_v = \frac{\Delta H}{H} \text{ , in/in}$$

$$\varepsilon_H = \frac{\Delta C}{C} \text{ , in/in}$$

$$\sigma_H = \varepsilon_H \text{ (MC), psi}$$

$$K = \frac{\sigma_H}{\sigma_v}$$

$$\frac{\Delta V}{V} = -\varepsilon_v + 2\varepsilon_H, \text{ in/in}$$

where

σ_v = maximum vertical stress, psi

σ_H = horizontal stress, psi

ε_v = vertical strain, in/in

ε_H = horizontal strain, in/in

ΔH = change in height, in

H = initial height of specimen

K = stress ratio

MC = mold constant (approximately equal to the strain modulus, E, obtained from the unconfined compression test of untreated soil)

ΔC = initial circumference of specimen, in

V = initial volume of specimen, cu. in.

ΔV = change in volume, cu. in.

Cyclic loading comprised both a loading and unloading phase. A vertical strain modulus, E, was obtained by regression of the loading phase stress-strain data at each recorded cycle and assumed as the slope of the regression. At each recorded cycle, utilization of a regression of the unloading phase stress-strain data and the intercept of the regression line with the vertical strain axis, provided an evaluation of permanent set. Permanent set may be defined as the non-recoverable, non-elastic strain, or cumulative permanent deformation of the soil or soil-fiber composite

following each recorded load repetition.

Story County, Mortenson Road Soil

Preliminary tests were conducted on the Mortenson Road material to develop a uniform testing procedure. Vertical stress levels of 75, 100 and 125 psi were selected. All specimens were molded at optimum moisture content, the treated specimens containing 0.2% 15 dpf polypropylene straight fibers, 1.5 in. length.

Figures 57 through 63 present the average measured responses obtained from each of the three stress levels noted above. Each response was expressed in terms of the ratio of treated versus untreated values. In interpreting these graphs it should be recognized that if the ratio is equal to one, fibers had no effect on the composite. If the ratio was less than or greater than one, the fibers had either adverse or beneficial effects, depending on the parameter. For example, a vertical strain modulus ratio greater than 1.0 indicated an increase in composite stiffness due to fiber inclusion. For all other parameters, a ratio greater than 1.0 indicated composite deterioration, while a ratio less than 1.0 implied that fiber inclusion enhanced the composites resistance to mobilization of vertical unit strain, horizontal strain, volumetric strain, horizontal stress, stress ratio, and permanent set. Occassional variations in the plotted responses occurred due to erroneous recording of data by the LVDT's.

Figure 57 illustrates that at 75 psi, the treated soil generally experienced higher vertical strains than the untreated soil. Both the untreated and treated specimens showed an increase in vertical strain for the first 200 cycles at 75 psi but thereafter the untreated specimens attained complete equilibrium while the treated specimens continued to

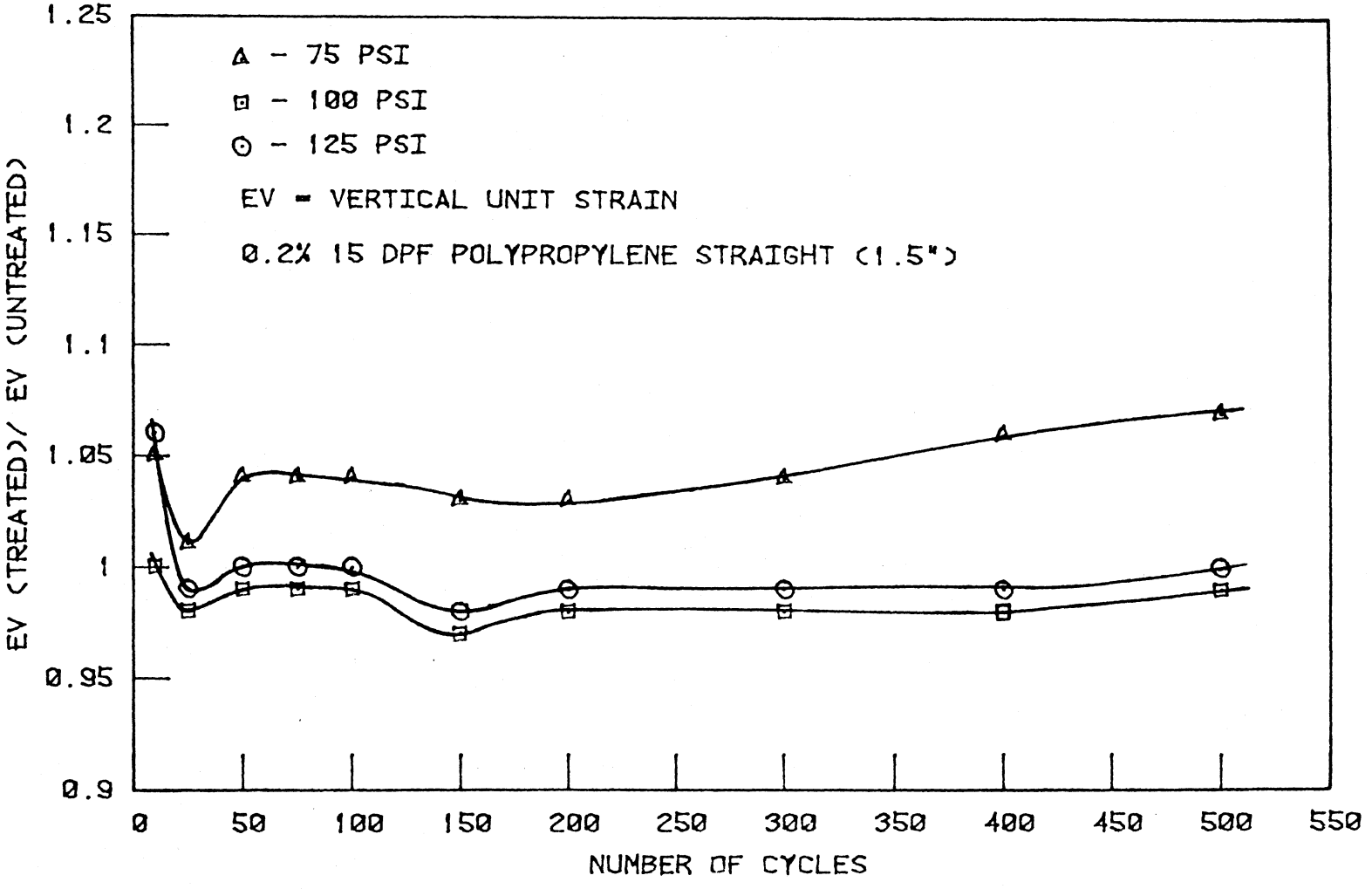

Figure 57. Vertical unit strain versus number of cycles at varying vertical stress levels

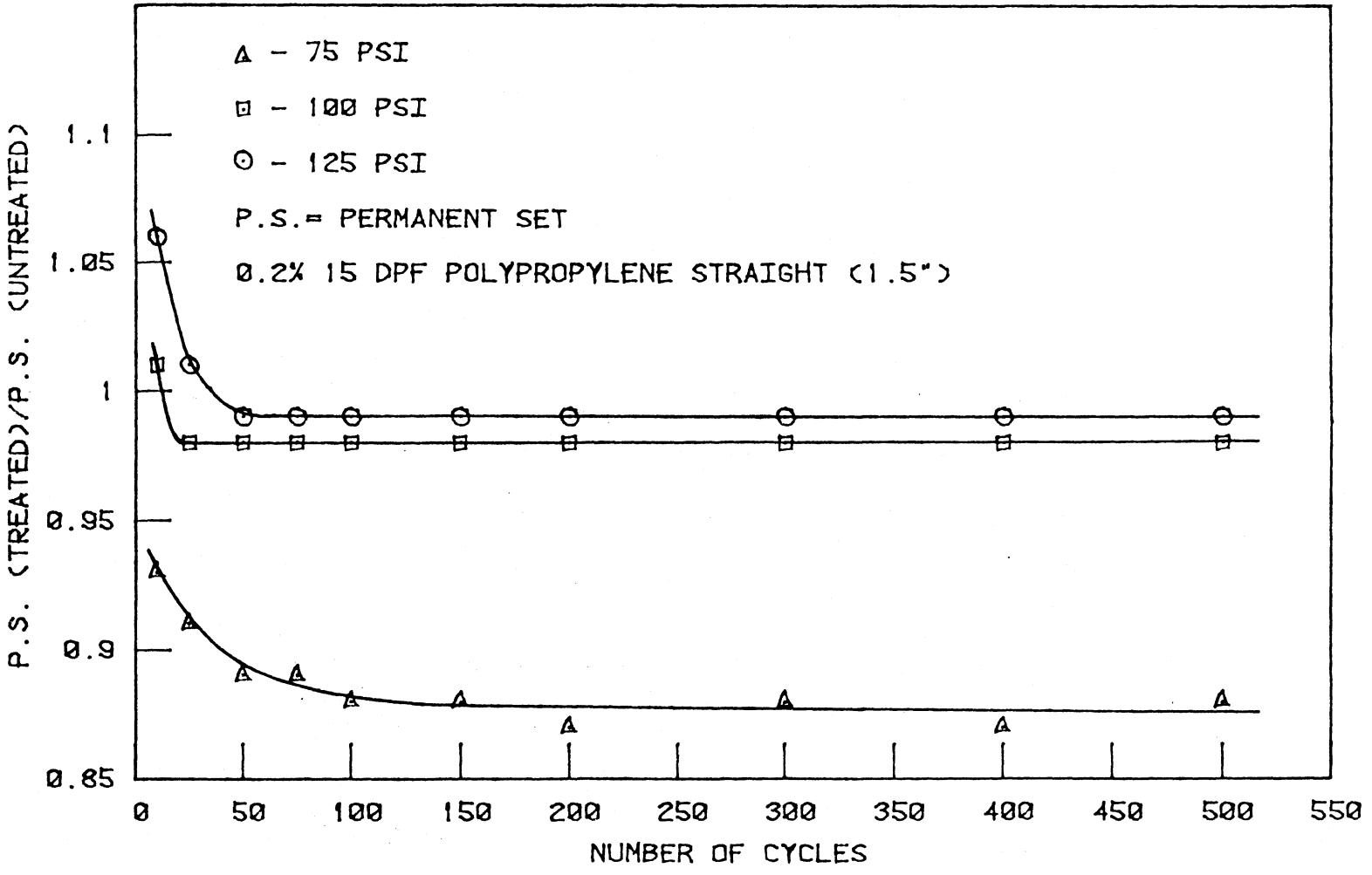

Figure 58. Permanent set versus number of cycles at varying vertical stress levels

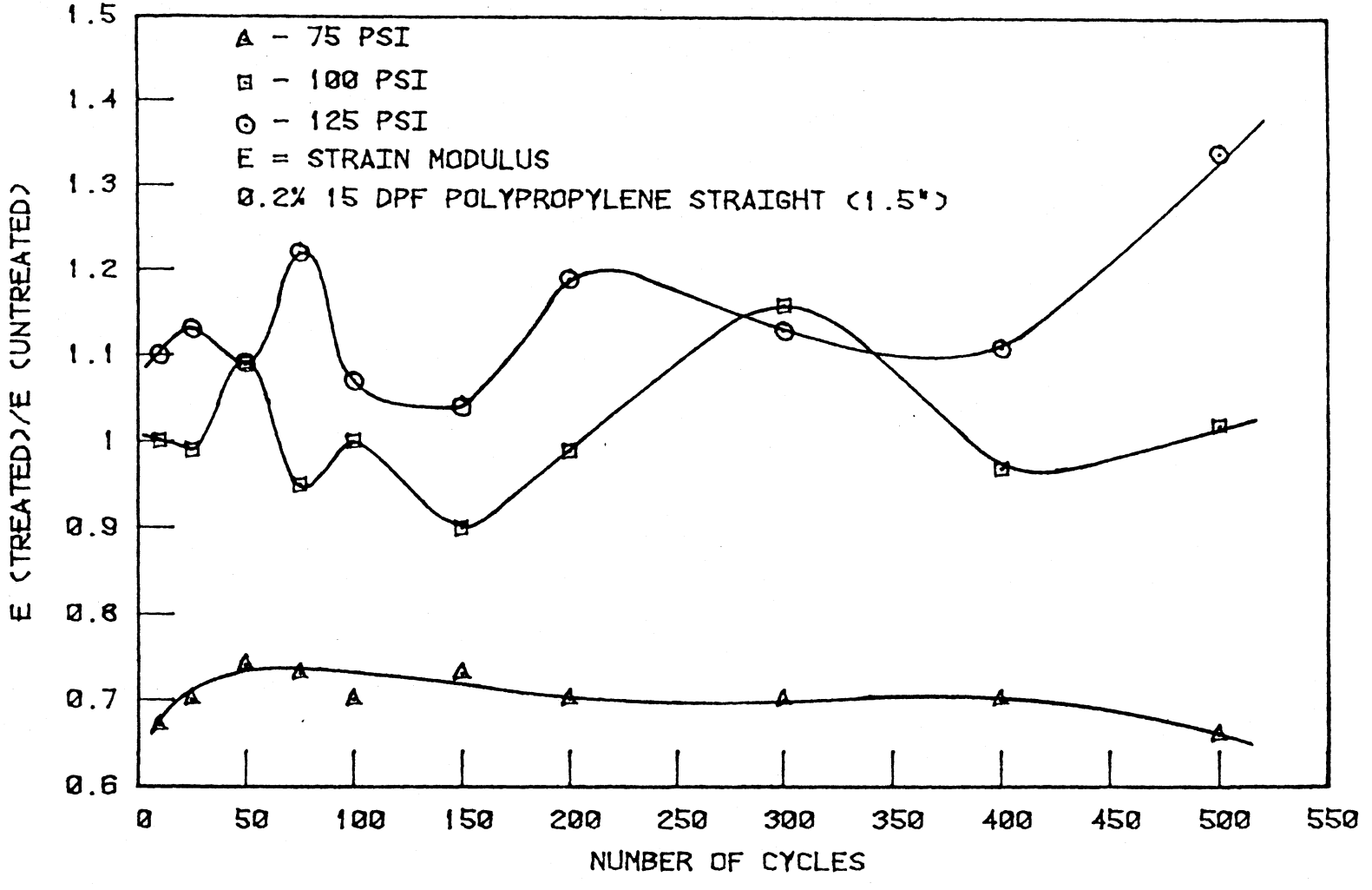

Figure 59. Vertical strain modulus versus number of cycles at varying vertical stress levels

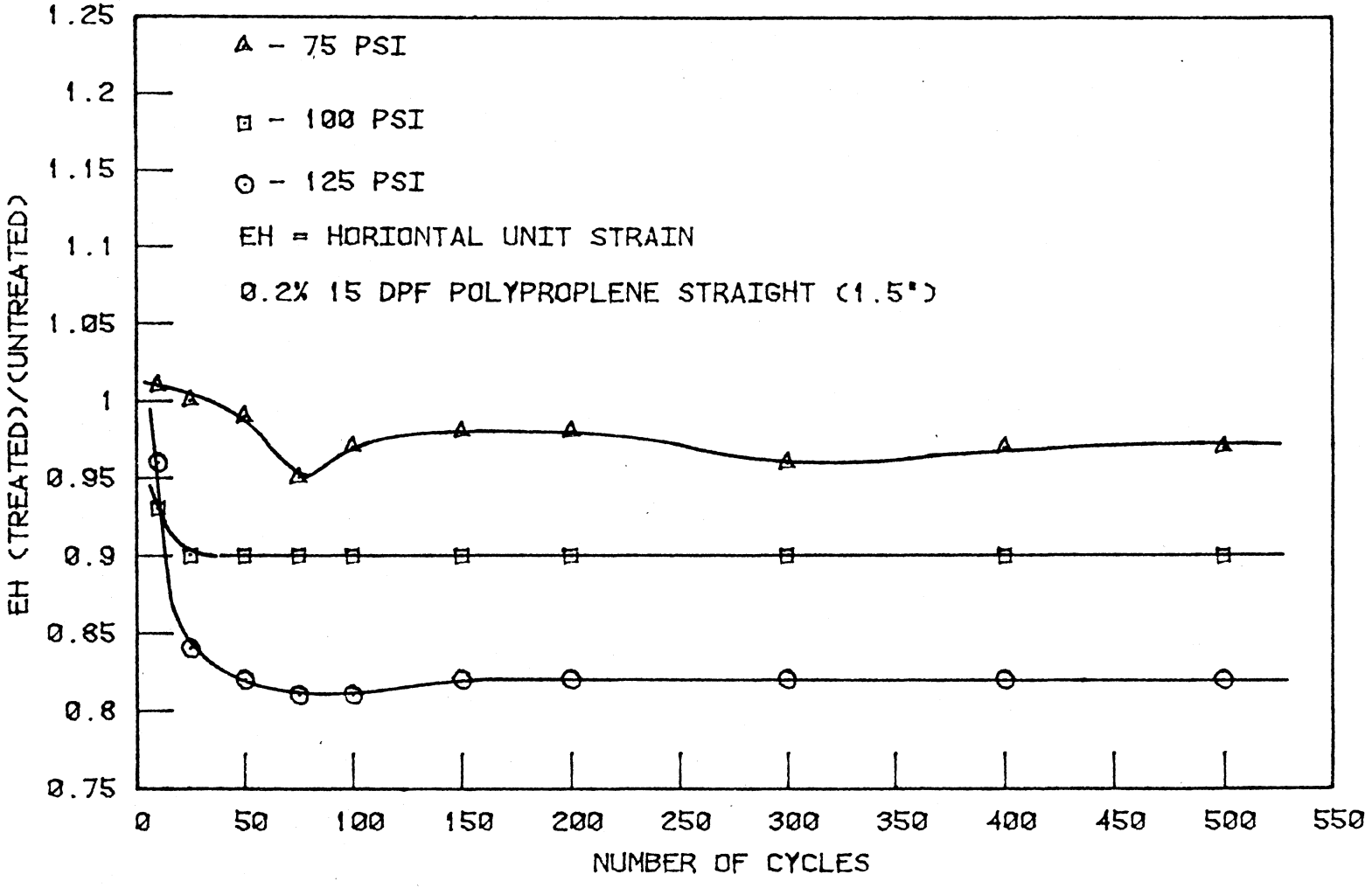

Figure 60. Horizontal unit strain versus number of cycles at varying vertical stress levels

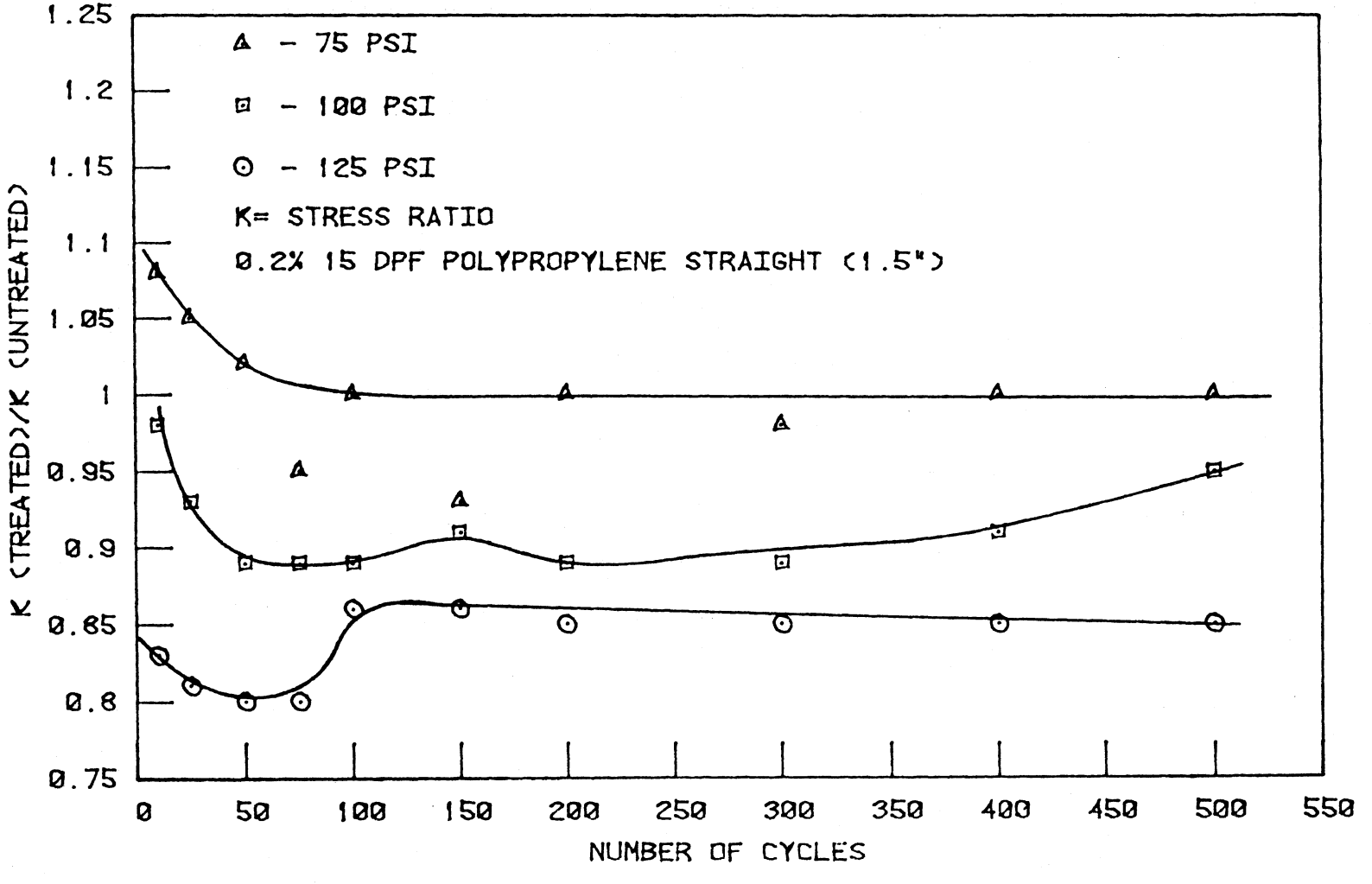

Figure 61. Stress ratio versus number of cycles at varying vertical stress levels

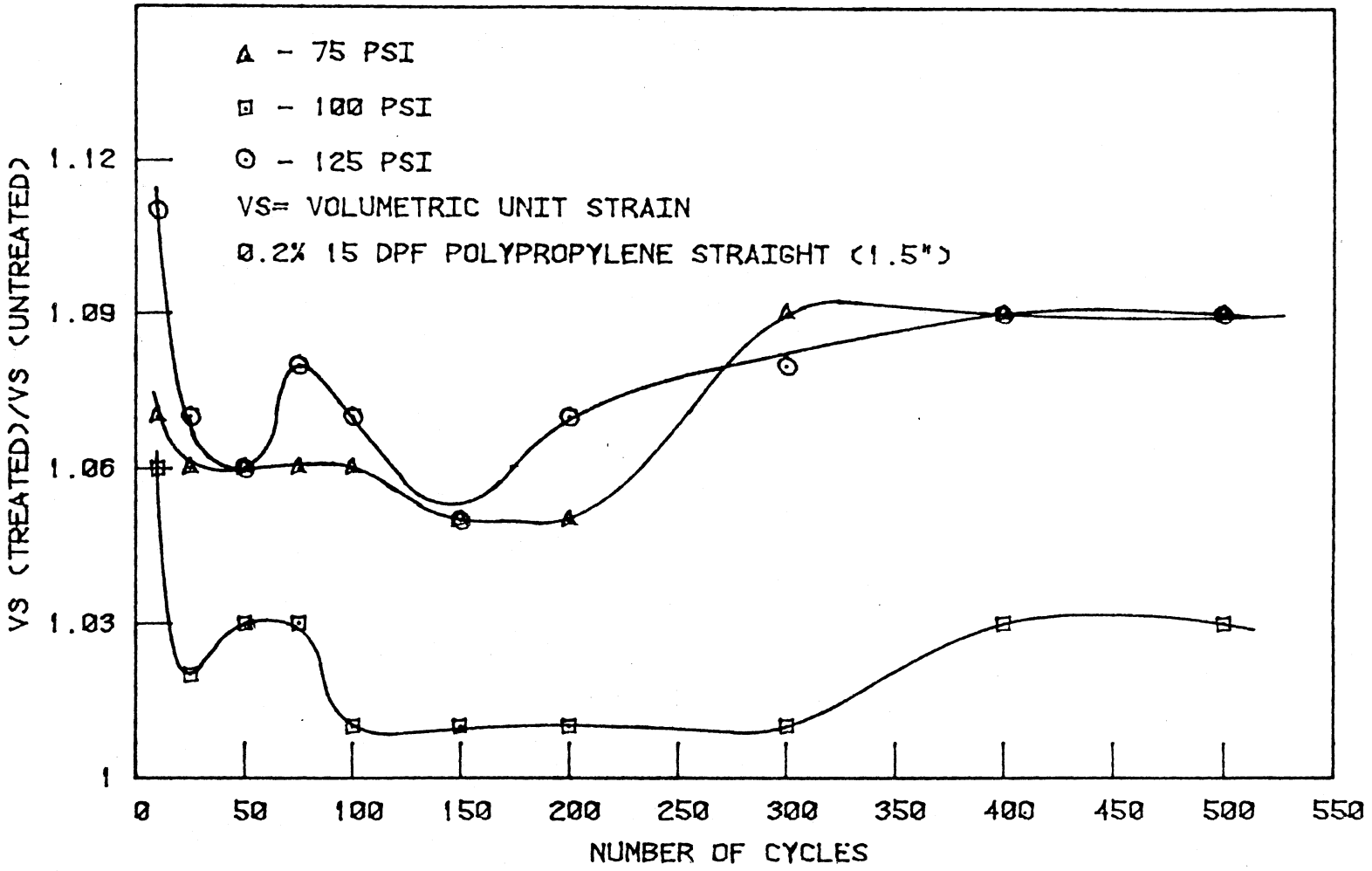

Figure 62. Volumetric strain versus number of cycles at varying vertical stress levels

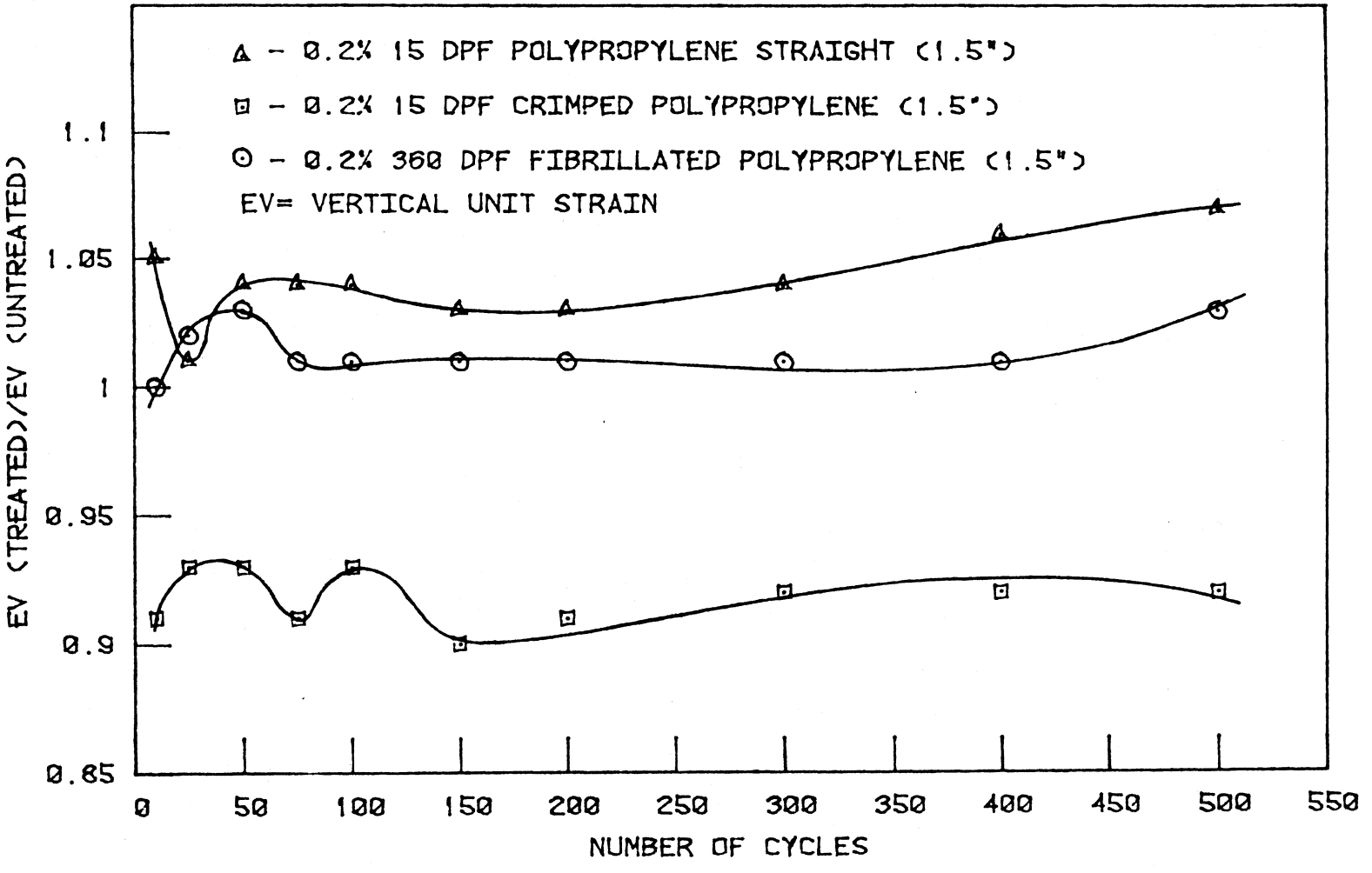

Figure 63. Vertical unit strain versus number of cycles for varying fiber types

experience minor increases in vertical unit strain. At 100 and 125 psi, the ratios were approximately equal to one.

Figure 58 illustrates that at 75 psi, permanent set of the treated specimens was about 88% that of the untreated soil after about 100 cycles. This reduction in set implied that the treated soil experienced a larger amount of elastic rebound than the untreated soil. At 100 and 125 psi, the permanent set ratio experienced in both the untreated and treated soil was basically unity beyond about 50 cycles, indicating a loss of elastic rebound and a probable loss of fiber-soil matrix bonding at such stress levels.

Figure 59 illustrates that at 75 psi the vertical strain modulus for the treated soil was about 30% smaller than that of the untreated soil, implying a decrease in material stiffness due to the addition of fibers. At 100 and 125 psi, erratic variations in ratios were observed, but generally, the vertical strain modulus for the treated soil was greater than that of the untreated. Observations made from Figure 59 indicate that fibers were capable of enhancing vertical strain modulus as higher vertical stress levels were applied.

Figure 60 illustrates the variation of horizontal unit strain with the number of cycles for different vertical stress levels. At 75 psi the treated specimens experienced an average reduction in horizontal strain of about 3%; the general trend being a slight decrease in ratios with increasing number of cycles. At 100 psi the reduction in horizontal strain was about 10%. At 125 psi horizontal strain was reduced by nearly 20%,

the trend being basically similar to that portrayed at 100 psi. The observations in Figure 60 imply that the effectiveness of fibers in reducing horizontal strain increases with increasing applied vertical stress. This could be attributed to the fact that at higher vertical stresses, larger vertical unit strains were mobilized (Figure 57), and it was observed that large vertical strains produced large horizontal strains. Therefore, fibers reduced lateral strain at higher stresses because sufficient lateral strains necessary to mobilize the fiber's tensile strength were obtained.

Horizontal stress is a function of lateral strain and the mold constant. Since the mold constant did not change, this means that the horizontal stress is a function of lateral strain only. As a consequence, horizontal stress exhibited trends similar to those of lateral strain.

Stress ratio, K, is a function of both horizontal and vertical stresses. Since the repetitive load Iowa K-Test is a stress controlled test, the stress ratio was a function of horizontal stress, and the trends obtained for stress ratio were similar to those obtained for both horizontal stress and horizontal strain, Figure 61.

Volumetric strain is a function of both vertical and horizontal strains. This parameter measured the total amount of deformation experienced by the material in three dimensions. As illustrated in Figure 62, the volumetric strain obtained in the treated specimens was slightly greater than that of the untreated specimens at all vertical stress levels. This phenomenon could be explained by observing that fiber inclusion into the soil matrix increases the amount of voids. Therefore, when stresses are applied, treated specimens experience larger vertical deformations than the

untreated. Volumetric strain was generally sensitive to the vertical strain in this study, primarily because the magnitude of vertical strain was always approximately ten times that of the horizontal strain. As a consequence, any difference in vertical strain would show up in volumetric strain.

The foregoing established basic response relationships between the various parameters and different levels of vertical stress. The next stage of cyclic load testing involved evaluating the effect of different types of fibers when the soil fiber composites were subjected to dynamic stresses. Types of fibers used, were 15 dpf crimped polypropylene (1.5"), 360 dpf fibrillated polypropylene (1.5"), and 15 dpf polypropylene straight (1.5"). A constant fiber weight fraction of 0.2% was used, and specimens were molded at standard optimum moisture content. Throughout the remainder of the cyclic load tests, all specimens were tested at a constant vertical stress of 75 psi coupled with 0.3 sec. dwell time.

Figure 63 illustrates the variation of vertical strain versus number of load repetitions for the three types of fibers. Composites molded with the 15 dpf crimped polypropylene showed the best response; vertical strains averaging about 93% of the untreated, or a 7% reduction. Although the 360 dpf fibers did not enhance the resistance of the soil fiber composite to vertical deformation, neither did they affect it in a detrimental way. The 15 dpf polypropylene straight did not enhance the resistance of the composites to vertical deformation, experiencing about 5% higher vertical strains than the nontreated specimens.

Figure 64 illustrates the variation of permanent set versus number of cycles for the three types of fibers. The 15 dpf polypropylene straight fibers provided about 13% reduction in set, while the 15 dpf crimped polypropylene produced about 6% reduction. A near 5% increase in permanent set was produced by the 360 dpf fibrillated polypropylene. Recalling that the 15 dpf crimped polypropylene fibers provided a 7% reduction in vertical strain, demonstrates that these fibers did not basically affect the degree of vertical elastic rebound of the soil. The percent reduction in vertical strain was about equal to that obtained for permanent set. Therefore, it is apparent that the crimped fibers reduced the amount of vertical deformation, but did not appear to affect the degree of elasticity or plasticity of the soil. In a like manner, the 15 dpf polypropylene straight fibers did not affect the degree of elasticity or plasticity, and indeed, further reduced the magnitude of permanent set of the composite.

Trends exhibited in vertical strain modulus (E) by the 15 dpf crimped polypropylene and the 360 dpf fibrillated polypropylene fibers were generally similar, Figure 65. The vertical strain modulus increased with increasing number of cycles and at 500 cycles, the increase was approximately 35% greater than the untreated. This trend implies that a cyclic dependent material hardening occurred; a phenomena having significant implications in roadway soils, in that these materials would greatly strengthen with time and increasing number of load applications. The 15 dpf polypropylene straight however, portrayed a cyclic dependent material softening.

Lateral stability of the fiber composites was quantified in terms of horizontal strain, horizontal stress, and stress ratio, Figure 66. The

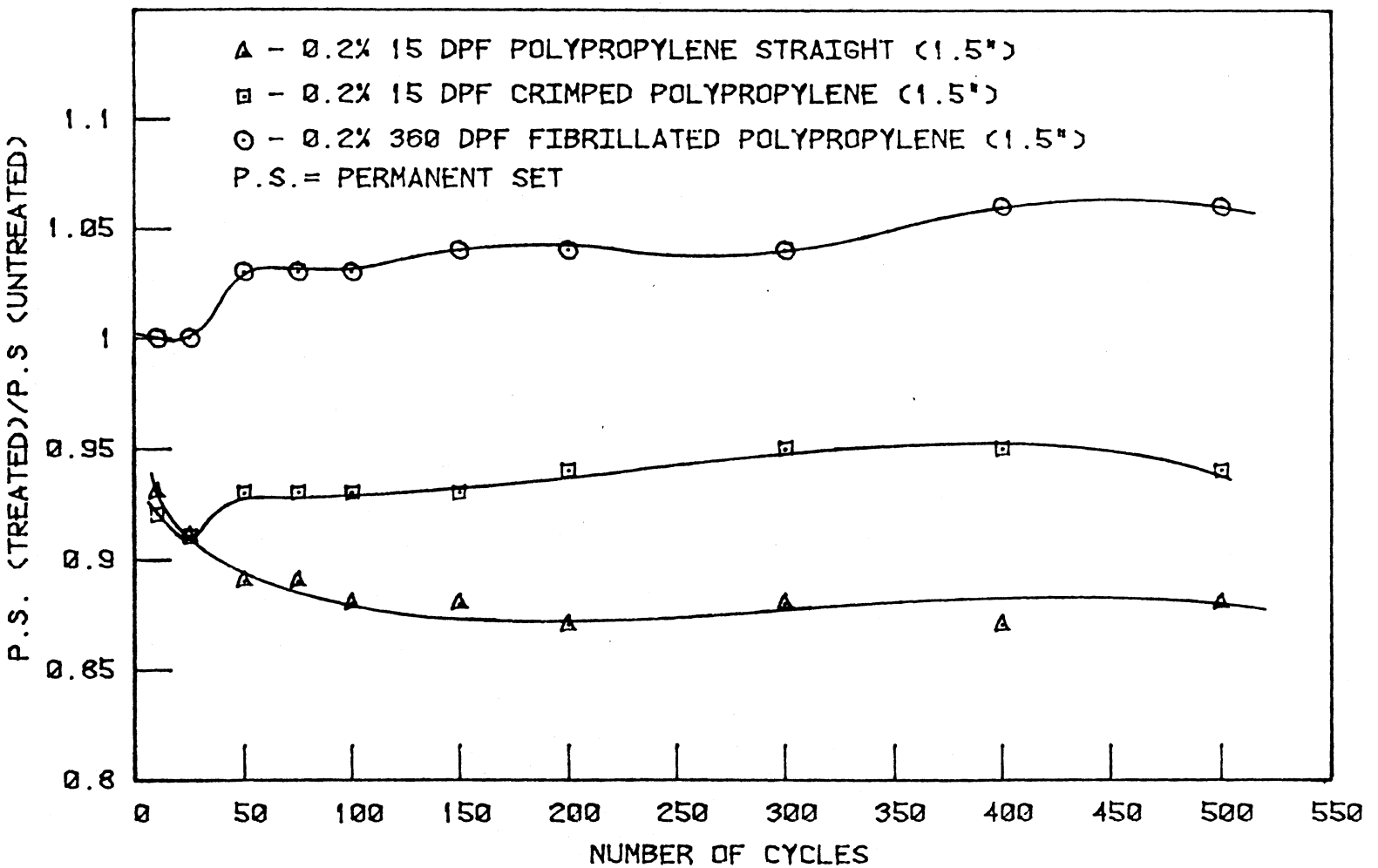

Figure 64. Permanent set versus cycles for varying fiber types

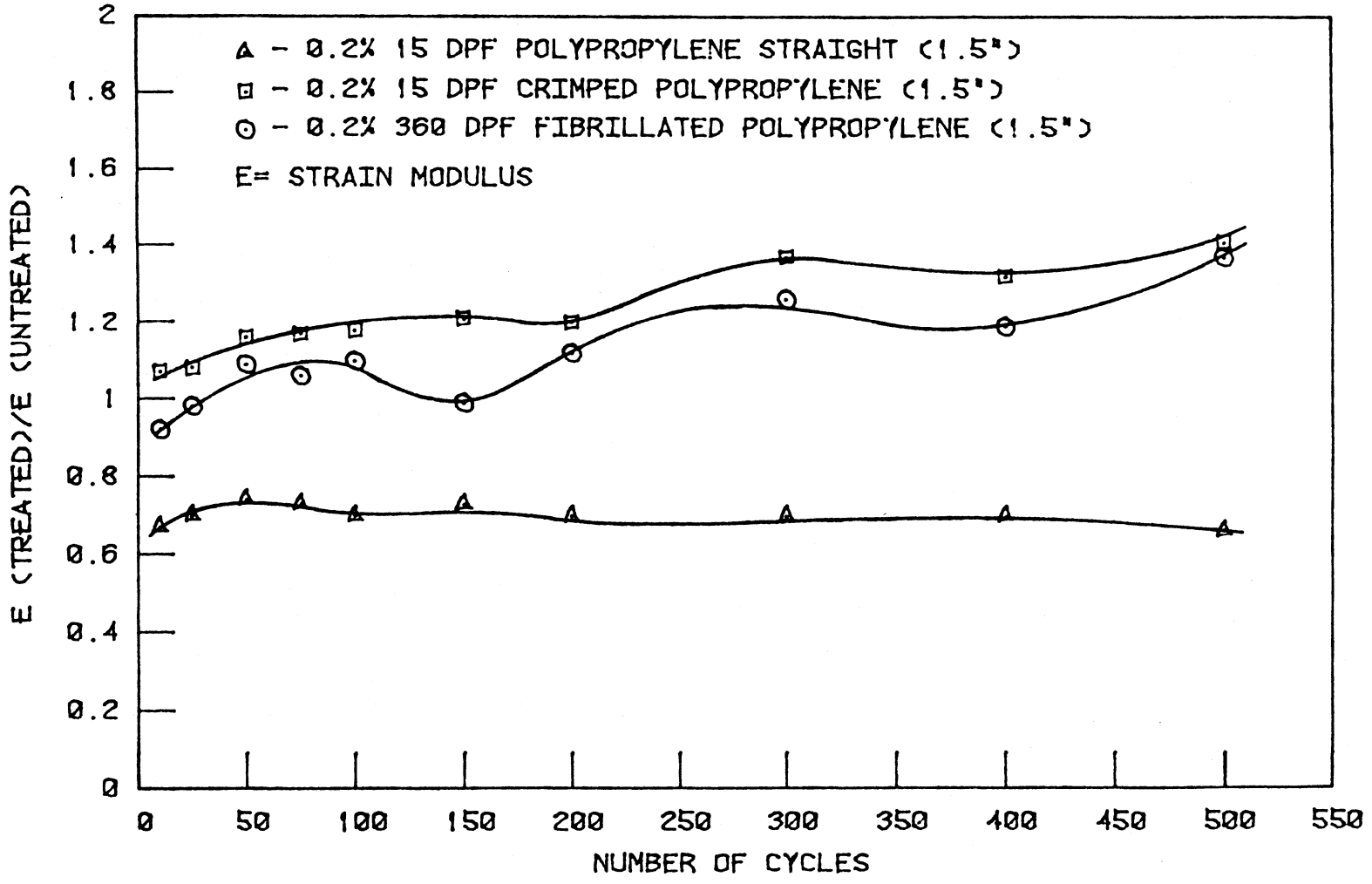

Figure 65. Vertical strain modulus versus number of cycles for varying fiber types

15 dpf crimped polypropylene fibers produced a reduction of about 16% in all three parameters, with the other fibers producing lesser values. This would imply that fiber reinforcement is effective in reducing the amount of lateral strain mobilized within a soil-fiber composite. Rutting in most pavements is caused by excessive lateral movements that occur when the road base or sub-base provides insufficient lateral restraint to deformations.

The 15 dpf crimped fibers provided a reduction in volumetric strain, while the other two fibers showed increases, Figure 67. This again illustrated the sensitivity of volumetric strain of a soil and/or soil-fiber composite to changes in vertical strain.

Unconfined compression testing showed that fiber reinforcement was more effective at higher levels of moisture. Therefore, a series of specimens were molded at 2% above optimum, utilizing the same three fibers of the previous section at a fiber weight fraction of 0.2%. In general, results obtained from this series of tests showed that all parameters exhibited definite changes when compared to similar properties at optimum moisture content.

The 15 dpf crimped polypropylene and 360 dpf fibrillated polypropylene fibers were effective in reducing the amount of vertical strain experienced by the soil specimens. The crimped fibers reduced vertical strain by about 10%, a greater reduction than the 7% obtained at optimum moisture content, Figure 63. The 360 dpf fibrillated polypropylene reduced vertical strain by about 7%; again better than the no change obtained at optimum moisture content. The 15 dpf polypropylene straight experienced

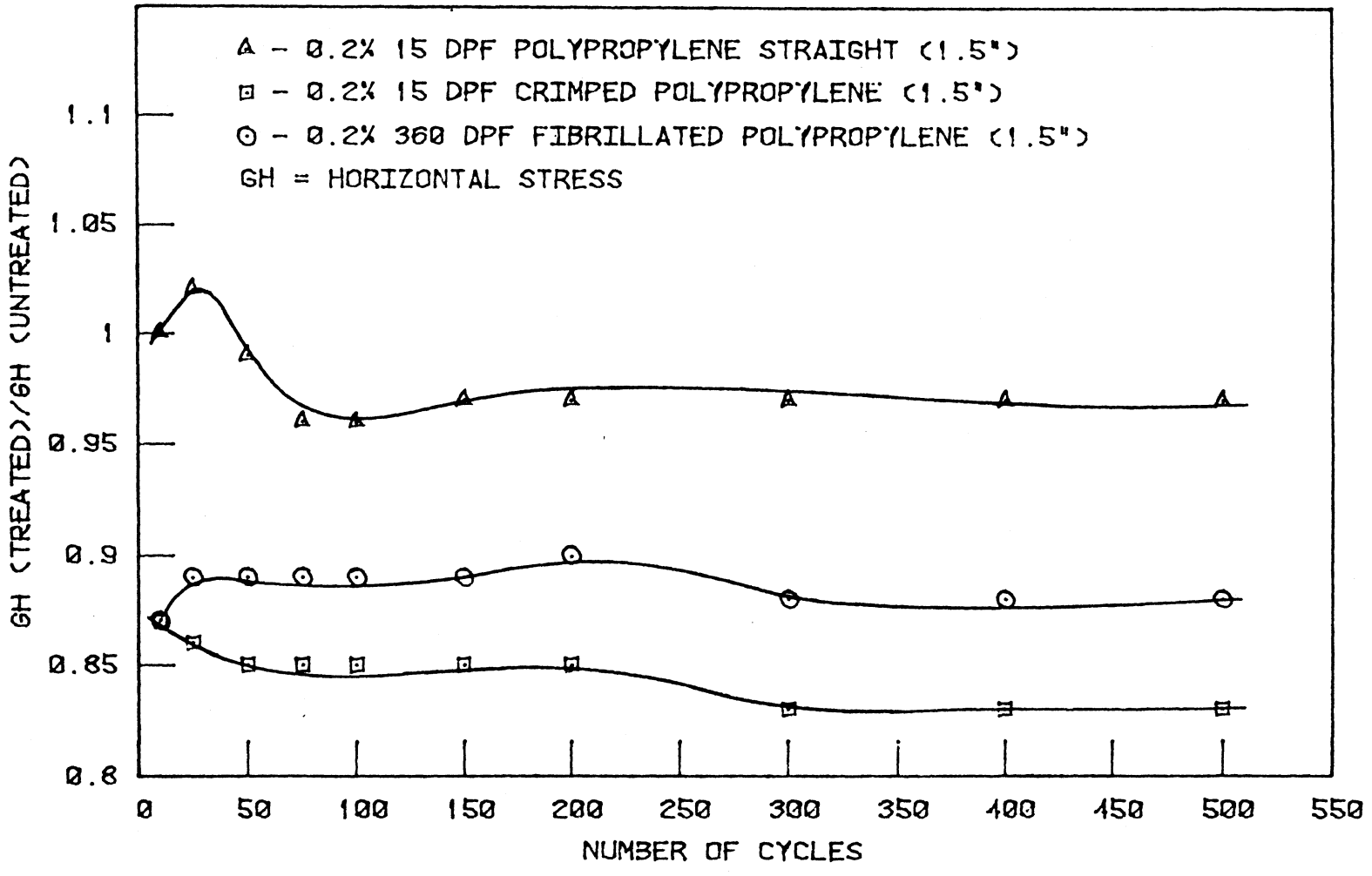

Figure 66. Horizontal stress versus number of cycles for varying fiber types

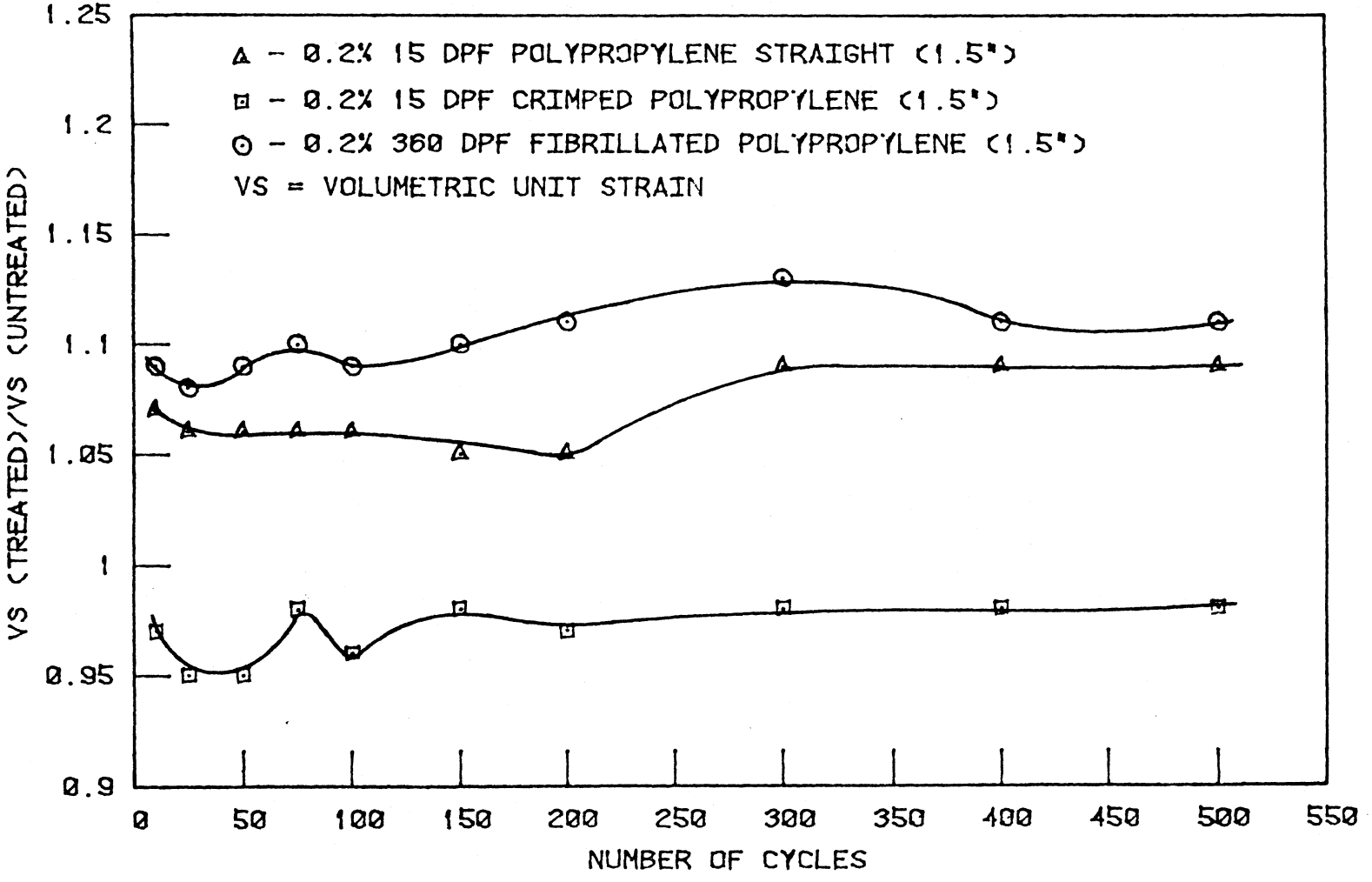

Figure 67. Volumetric strain versus number of cycles for varying fiber types

a 3% increase in vertical strain, still slightly better than the 5% increase at optimum moisture content. These results thus implied that fiber reinforcement was considerably more effective in resisting vertical deformation at the higher moisture.

The 15 dpf crimped polypropylene and 360 dpf fibrillated polypropylene fibers reduced permanent set by percentages similar to those achieved with vertical unit strain. Crimped polypropylene fibers reduced the permanent set by about 10%, almost the same amount as that observed for vertical strain. This same trend was observed for crimped fibers at optimum moisture content, tending to confirm that these fibers did not alter the amount of elastic rebound experienced by the soil. The 360 dpf fibrillated polypropylene reduced permanent set by about 7%, but it should be recalled that at optimum moisture content a 5% increase was observed for this fiber; i.e., a reversal in permanent set trends due to increased moisture content. The 15 dpf polypropylene straight increased permanent set by about 5%, contrary to what was observed at optimum moisture content where these fibers showed about a 13% reduction in permanent set. Positive improvements were thus obtained in permanent set by the crimped and fibrillated polypropylene fibers, indicating improved soil matrix-fiber contact. The increased permanent set obtained with the straight fiber indicated a reduction in matrix-fiber contact due to increased moisture content.

Above OMC, the 15 dpf crimped and 360 dpf fibrillated polypropylene fibers showed a general decrease in vertical strain modulus with number of cycles. The 15 dpf polypropylene straight showed a general increase in vertical strain modulus after an initial decrease in this parameter.

These results would imply that the crimped and fibrillated polypropylene soil-fiber composites experienced some cyclic dependent softening, while with the 15 dpf polypropylene straight, some cyclic dependent hardening occurred. This was contrary to what was observed for specimens tested at optimum moisture content, where for example, the vertical strain modulus, E increased with increasing number of cycles for 15 dpf crimped and 360 dpf fibrillated polypropylene, and decreased with increasing number of cycles for the 15 dpf polypropylene straight.

In general, above optimum moisture each of the fibers reduced the amount of horizontal strain but not in similar proportions. The 15 dpf polypropylene straight produced a 16% or greater reduction in horizontal strain. The 15 dpf crimped fibers produced an average of less than 9% reduction, while the 360 dpf fibrillated polypropylene initially provided about a 10% reduction but generally increased to a unity ratio at about 150 cycles. At optimum moisture content, the 15 dpf crimped and 360 dpf fibrillated polypropylene fibers produced about a 16% and 13% reduction in horizontal strain respectively, showing that at higher moisture contents, reinforcement with these fibers was not as effective as at optimum moisture content. This behavior is potentially attributable to the interfacial soil-fiber bond above OMC being at least partially destroyed initially, then remobilizing as additional cyclic loading occurred. In the case of the 15 dpf polypropylene straight there was only a 3% reduction in lateral strain at optimum moisture content, implying that at higher moisture contents, this fiber is more effective in resisting the mobilization of lateral strain, than at lower moisture contents.

Horizontal stresses and stress ratios of the three fibers above OMC, followed trends similar to those noted for horizontal strain.

Above optimum moisture, the 15 dpf crimped and 360 dpf fibrillated polypropylene fibers produced a reduction between 10 and 15% in volumetric strain when compared to the untreated. A 12% increase in volumetric strain was observed for the 15 dpf polypropylene straight. In comparison with volumetric strains obtained at optimum moisture content, there was a significantly greater reduction of volumetric strain at the higher, than at the lower moisture contents.

Based on the preceeding data obtained from cyclic load Iowa K-Tests of the fiber treated Mortenson Road material, the following general observations were obtained:

1. Increases in vertical stress appear to have the same effect as increasing the moisture content, in that the introduction of fibers showed improved performance at both higher vertical stresses and moisture contents above optimum. This observation appears to be due to the fact that at higher moisture contents and stresses, larger vertical deformations were obtained. Higher vertical deformations appear to produce higher lateral displacements necessary to mobilize tensile strength of the fibers. Also, there appears to be a critical stress and moisture content beyond which fiber reinforcement becomes ineffective. This phenomenon can be attributed to the fact that at a critical moisture content and vertical stress, the interfacial shear stress exceeds the interfacial shear strength, thus initiating fiber debonding. The efficiency of soil-fiber reinforcement depends largely on the integrity of the soil-fiber interfacial bond.

2. The greatest potential for fiber reinforcement appears related to parameters associated with horizontal or lateral stability. This was evidenced by the observations that all parameters related to the strength of the composites in a horizontal direction were enhanced by addition of fibers into the soil matrix. This could have far reaching implications for roadway soils, since the problem of rutting is attributable to lack of sufficient lateral restraint.

3. The 15 dpf crimped polypropylene fibers provided the best overall performance among the three fibers considered, and may be due to the improved frictional properties between these fibers and the soil as derived from the crimping. The 360 dpf fibrillated polypropylene produced the second best results, followed by the 15 dpf polypropylene straight fibers. Although the 15 dpf crimped polypropylene fibers showed good performance in the laboratory, they were difficult to mix into the plastic Mortenson Road soil. From a workability point of view, the 360 dpf fibrillated polypropylene fibers were the easiest to mix in the laboratory.

Sioux City Soil

Cyclic load K-Tests were performed on the A-4 Sioux City borrow soil in order to obtain further mechanistic evaluations due to soil material differences. Specimens were molded at varying fiber weight fractions using both the loess soil or a loess plus type I portland cement matrix. Fibers used in this series of tests were the same as used with the Mortenson Road material. The first series of cyclic load tests were performed on duplicate specimens of the untreated and fiber treated loess molded at optimum moisture content.

Figure 68 presents the actual vertical unit strain versus number of cycles for each weight fraction of the 15 dpf polypropylene straight fibers. Vertical strain data obtained with the 360 dpf fibrillated polypropylene and 15 dpf crimped polypropylene fibers were similar to that illustrated in Figure 68. In general, vertical unit strain increased up to about 200 cycles, and then tended to level thereafter. The 360 dpf fibrillated polypropylene indicated an optimum fiber content of about 0.2% producing in excess of a 10% reduction in vertical strain. All specimens incorporating the 15 dpf crimped polypropylene produced lower vertical unit strains than the untreated, with the optimum 0.1% fiber content showing about a 12% reduction from that of the untreated average. As noted in Figure 68, 0.3% fiber weight of the 15 dpf polypropylene straight was required to produce similar reductions in vertical unit strain. The reduction of fiber content due to the effect of crimping of the 15 dpf fiber is therefore obvious.

Figure 69 illustrates actual average permanent set as recorded for varying percentages of the 15 dpf crimped polypropylene. Magnitude of permanent set for the other two fibers were similar to that shown in Figure 69. The optimum fiber weight fraction for each of the three fibers was assumed as the maximum reduction of permanent set relative to the untreated and were thus noted as identical to that obtained with vertical unit strain; i.e., 360 dpf fibrillated polypropylene, 0.2%, 15 dpf polypropylene straight, 0.3%, and 15 dpf crimped polypropylene, 0.1%. Maximum reduction of permanent set at each optimum fiber weight fraction was about 0.01 in/in implying that fibers within the loess soil matrix did not

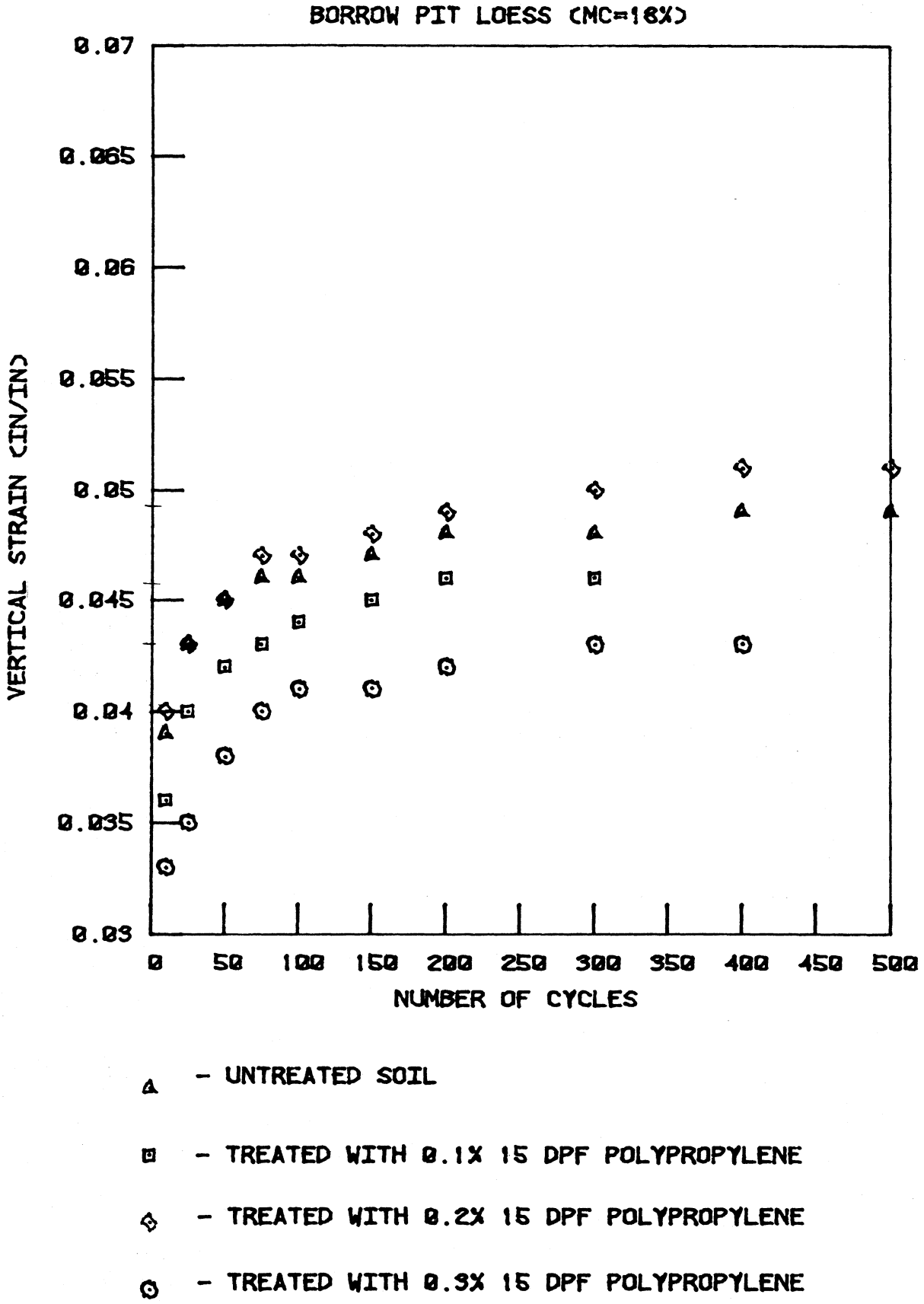

Figure 68. Vertical unit strain versus number of cycles for varying fiber contents

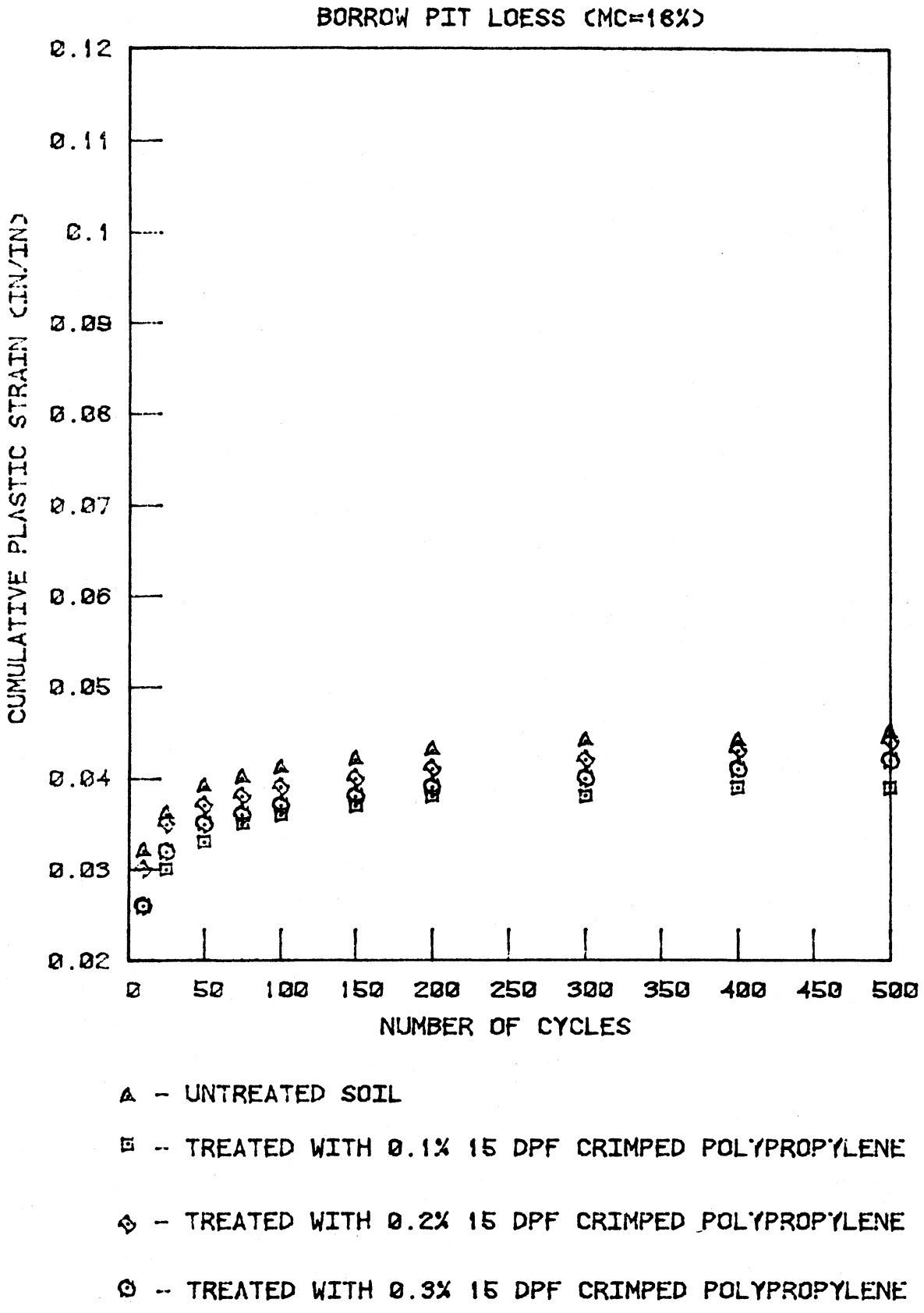

Figure 69. Permanent set versus number of cycles for varying fiber contents

appreciably influence the elastic-plastic behavior of the soil.

Figure 70 illustrates the behavior of actual vertical strain modulus versus number of cycles using varying fiber weight fractions of the 360 dpf fibrillated polypropylene. Once again, patterns of strain modulus versus fiber type were quite similar, tending to increase with increasing number of cycles, and implying that cyclic strain hardening was occurring. In general, each fiber type produced strain moduli lower than the untreated soil. However, after 500 cycles, the vertical strain modulus at 0.2% of each fiber was nearly identical to that of the untreated soil.

Figure 71 presents actual horizontal unit strain versus number of cycles for varying fiber contents of the 15 dpf crimped polypropylene. Magnitude of reduction of actual values of horizontal unit strain of the loess, due to incorporation of the three fiber types, was not as large as observed with the more plastic Mortenson Road material at its optimum moisture content since actual lateral strains of the Mortenson Road material was considerably greater than with the loess. Fiber tensile strength of the Mortenson Road composites were thus probably mobilized to a larger extent than within the loessial composites. The largest reductions in horizontal unit strain produced with the 15 dpf crimped fibers were obtained at about 0.3% fiber content, Figure 71. Figure 71 also indicates that 0.1% of the crimped fibers produced slightly larger horizontal strain than the untreated. Recalling that the crimped fibers indicated an optimum fiber treatment of 0.1% relative to vertical unit strain, it thus appears that the useable optimum fiber content would be dependent on the parameter of interest to the roadway designer. If 0.3% of the 15 dpf

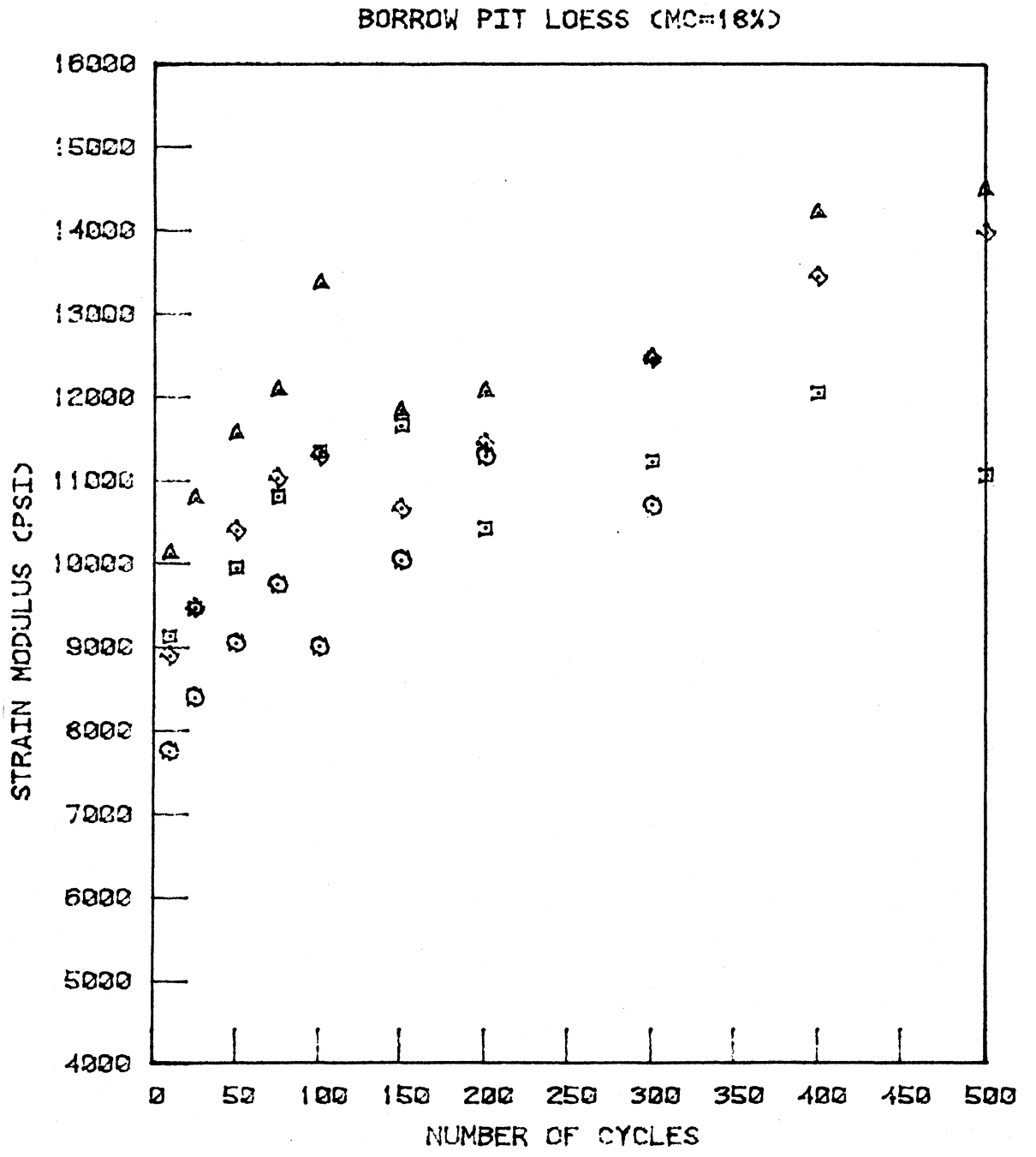

Figure 70. Vertical strain modulus versus number of cycles for varying fiber contents

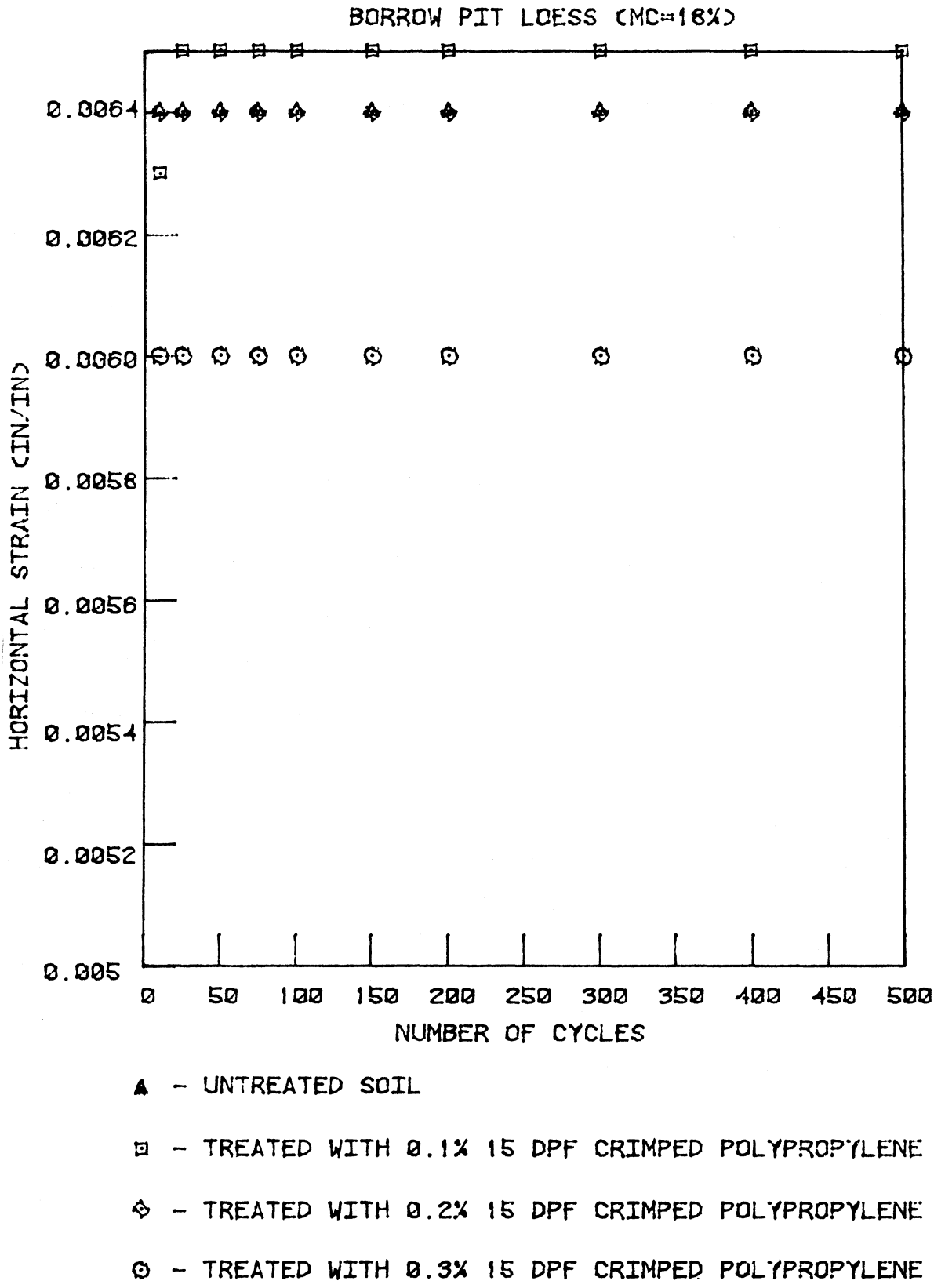

Figure 71. Horizontal unit strain versus number of cycles for varying fiber contents

crimped fibers were utilized within a loessial roadway test section, both vertical and horizontal strain parameters would potentially be improved from that of the untreated soil.

The 360 dpf fibrillated polypropylene produced optimum reduction in horizontal unit strain at a fiber weight fraction of 0.2 to 0.3%. The 15 dpf polypropylene straight fibers provided maximum reduction in horizontal unit strain at a fiber content of 0.3%; i.e., identical to that obtained from the vertical unit strain parameter.

Since the measurement of horizontal stress is directly related to horizontal unit strain, the trends of horizontal stress observed for the loess-fiber composites at optimum moisture content were very similar to those obtained for horizontal unit strain. Regardless of fiber type, the magnitude of measured horizontal stresses ranged from about 1.1 to about 1.25 psi.

Trends observed with the stress ratio parameter were quite similar to those obtained with both the horizontal stress and unit strain. Based on reduction of stress ratio from that of the untreated loess, the optimum fiber weight fraction for all three fiber types appeared to be about 0.3%.

Figure 72 illustrates actual volumetric strain versus number of cycles for varying fiber contents of the 360 dpf fibrillated polypropylene. Regardless of fiber type, volumetric unit strain of the loess-fiber composites were considerably reduced from that of the untreated soil. Maximum volumetric strains at optimum fiber contents were reduced by 15% or more from the untreated. Optimum fiber weight fractions based on volumetric strain were respectively 0.2, 0.1, and 0.3% for the 360 dpf fibrillated polypropylene.

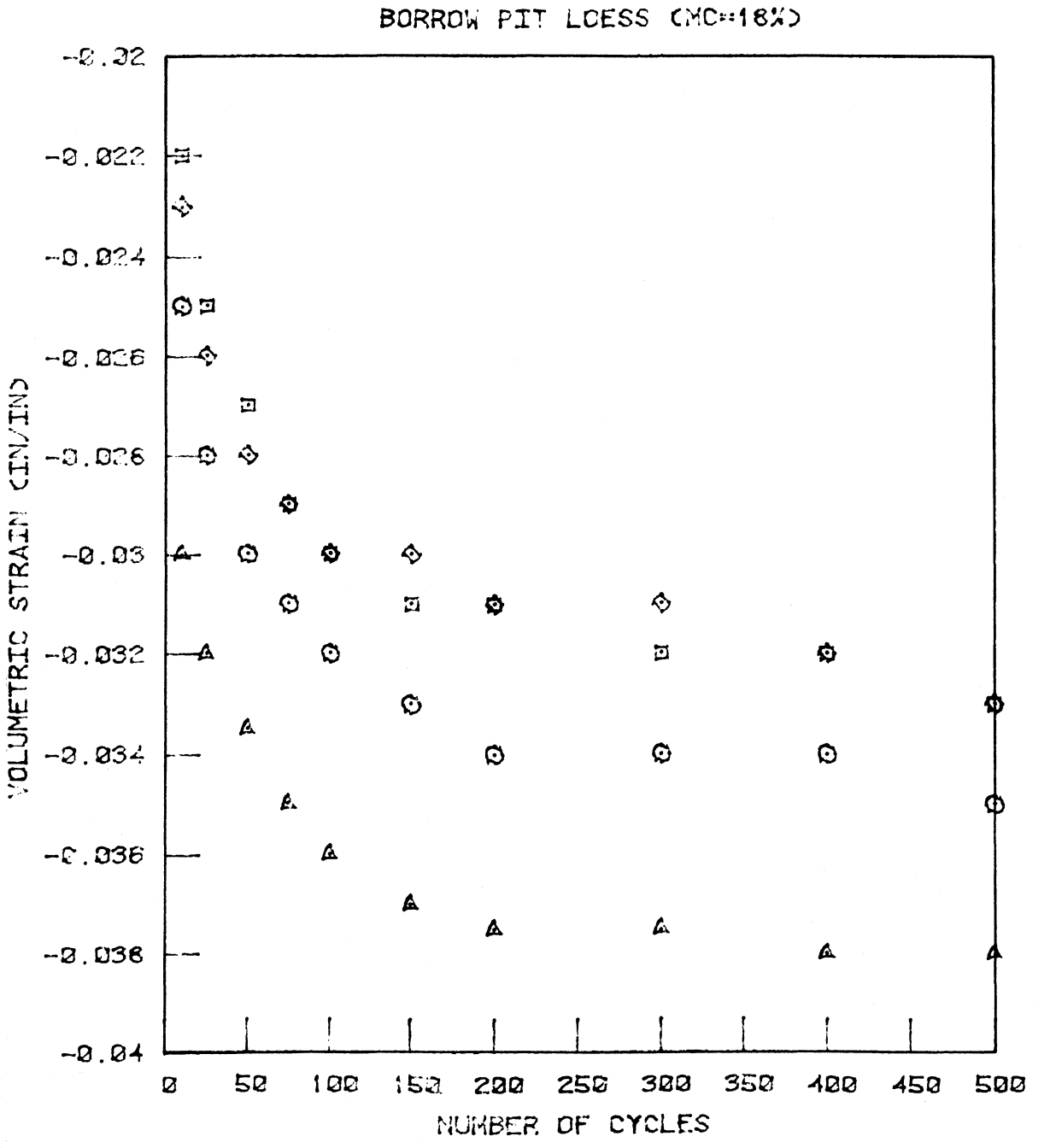

Figure 72. Volumetric strain versus number of cycles for varying fiber contents

15 dpf crimped polypropylene, and 15 dpf straight polypropylene.

The second series of cyclic load tests were performed on duplicate specimens of untreated and fiber treated borrow pit loess molded at a moisture content 3% above optimum. Fiber types and contents were identical to those performed on the optimum moisture specimens.

Figure 73 presents the variation of vertical unit strain versus number of cycles for the three fiber weight fractions of 15 dpf straight polypropylene. Comparison of Figures 68 and 73 typify the average increase in vertical unit strain observed for each fiber type and content. Optimum fiber weight fraction appeared to be about 0.2% for each fiber type, with the 15 dpf straight polypropylene producing the largest reduction in vertical unit strain, i.e., a reduction in excess of 20%.

Figure 74 illustrates the variation of permanent set (cumulative plastic strain) for each fiber weight fraction of the 360 dpf fibrillated polypropylene. At 0.1% fiber content both the 360 dpf and the 15 dpf crimped polypropylene fibers exhibited a considerable increase in permanent set. Permanent set with both the 360 dpf and 15 dpf crimped fibers at 0.2 and 0.3% weight fraction were similar to the untreated loess soil. In general, none of the fibers indicated an appreciable positive alteration of permanent set when compared to the untreated loess.

Increased moisture content lowered the vertical strain moduli of both the untreated and fiber treated loess soil regardless of fiber type, Figures 75 and 70. However, as illustrated in Figure 75, 0.2% of the 15 dpf straight fiber increased strain modulus from the untreated condition by about 50%. A similar increase of vertical strain modulus was obtained with

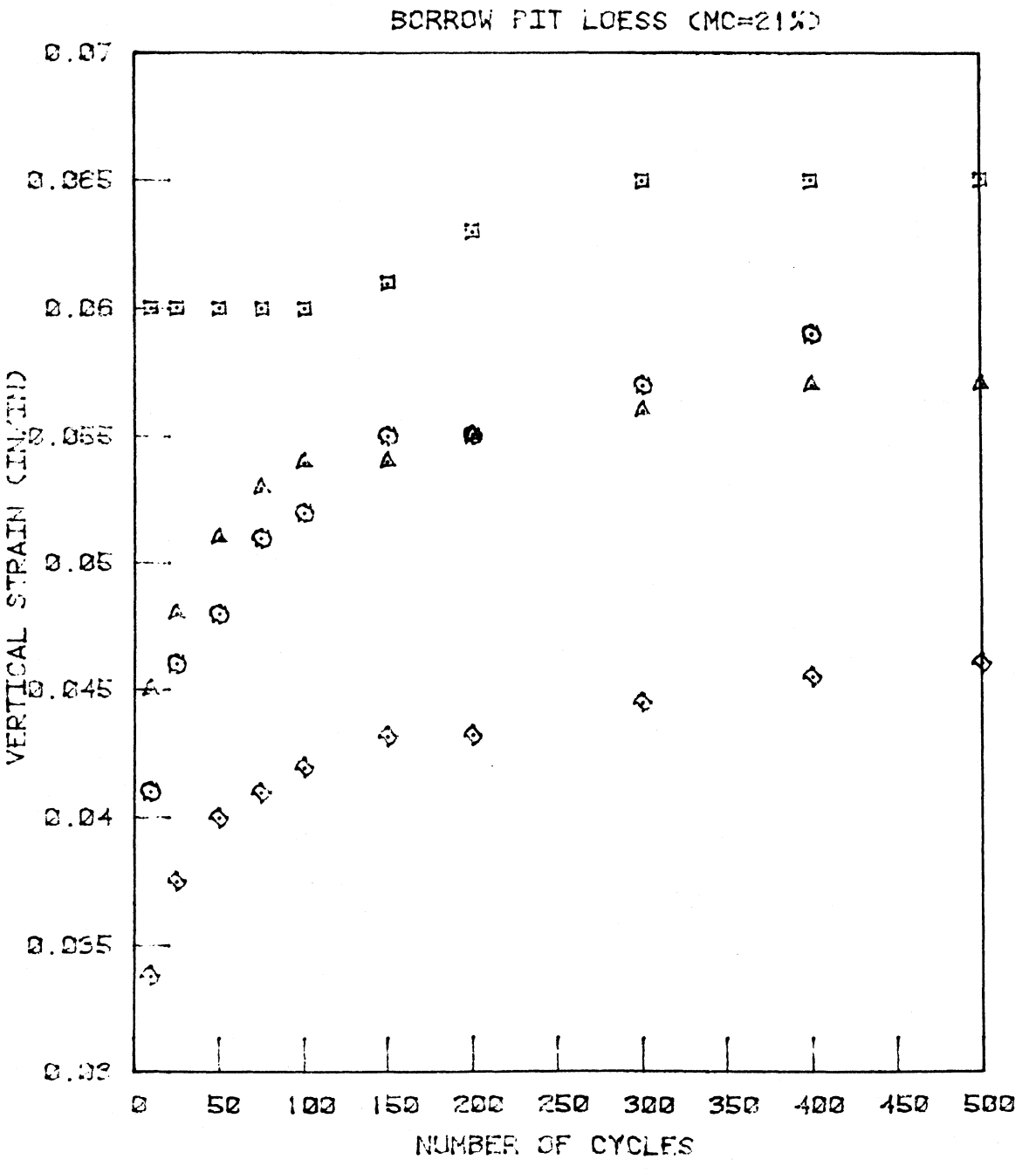

Figure 73. Vertical unit strain versus number of cycles for varying fiber contents

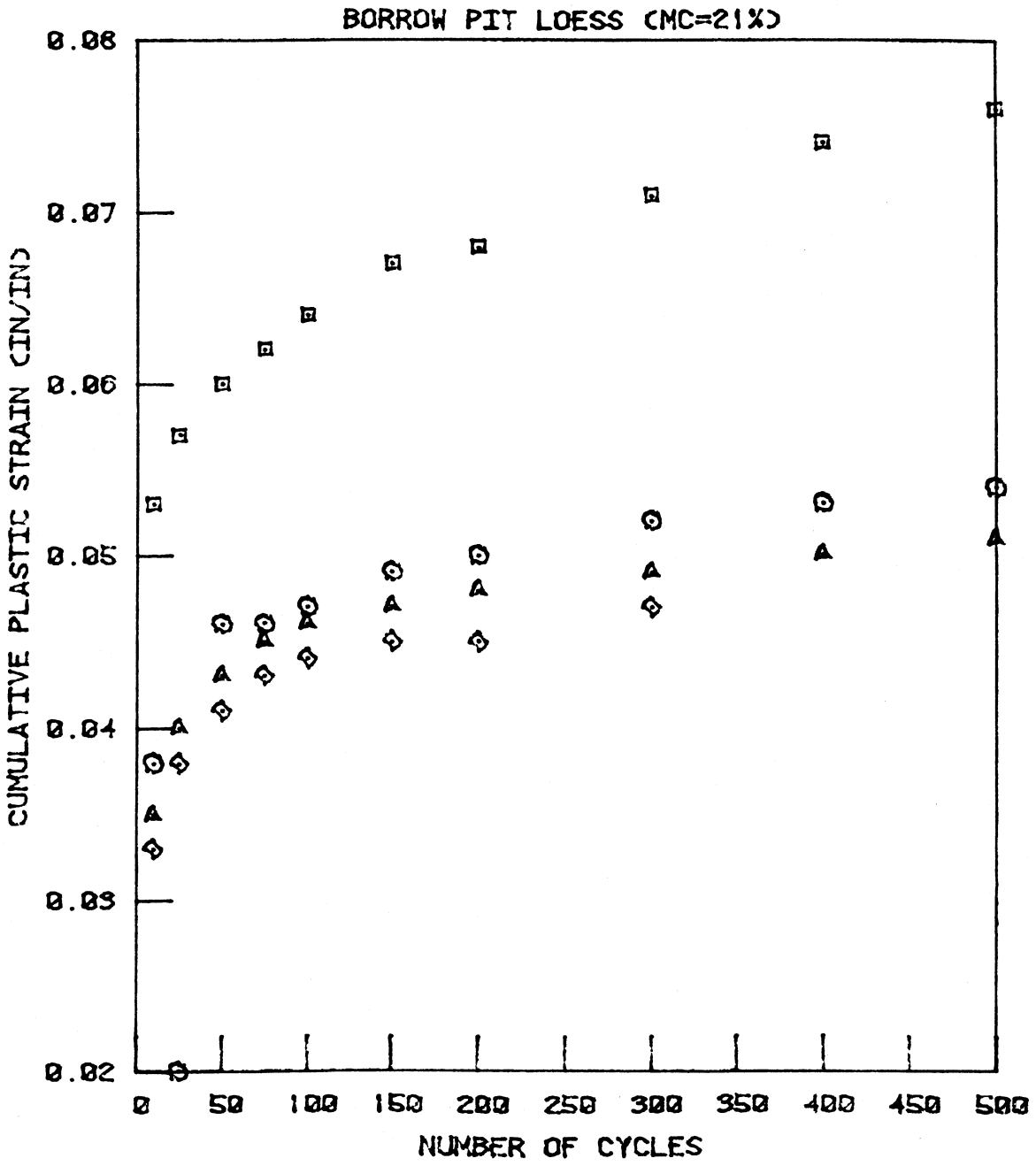

Figure 74. Permanent set versus number of cycles for varying fiber contents

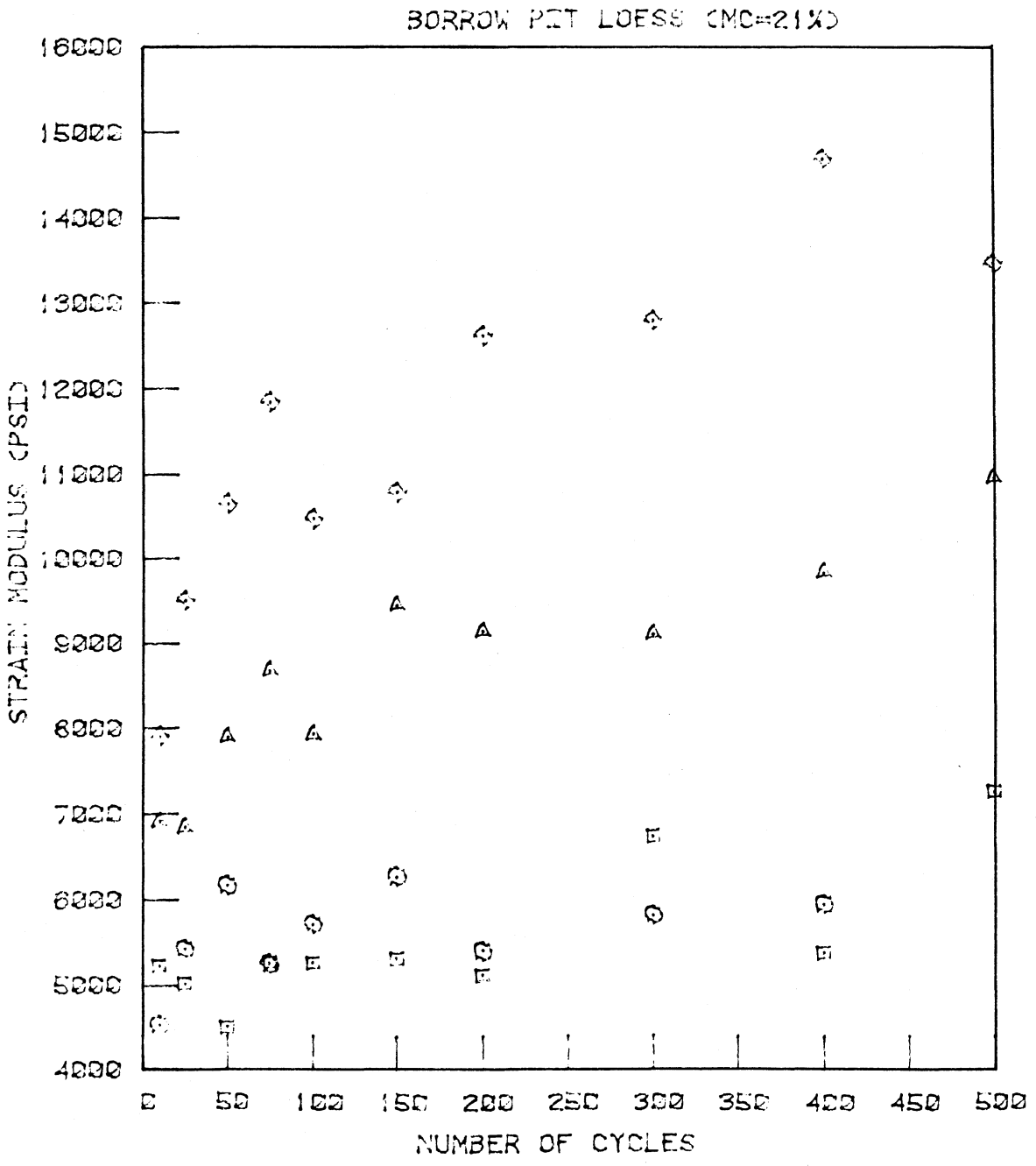

Figure 75. Vertical strain modulus versus number of cycles for varying fiber contents

the incorporation of 0.2% fiber weight fraction of the 360 dpf fibrillated polypropylene. Some improvement of vertical strain modulus occurred due to incorporation of the 15 dpf crimped fiber at both 0.1 and 0.2% weight fraction. Incorporation of 0.3% of each of the three fibers significantly reduced the vertical strain modulus from that of the untreated soil above optimum moisture.

As shown in Figure 76, the 15 dpf straight fiber produced in excess of 20% reduction of horizontal unit strain at 0.3% fiber weight fraction. For both the 360 dpf fibrillated and 15 dpf crimped fibers, a slight reduction in horizontal unit strain was also obtained at 0.3% content. All other fiber weight fractions produced little or no change of horizontal unit strain from that of the untreated soil above optimum moisture content.

As might be anticipated, measured horizontal stresses and stress ratios of both the untreated and fiber treated loess were slightly greater than those produced at optimum moisture content. Only the 15 dpf straight polypropylene, at 0.3% fiber weight fraction, produced an appreciable reduction in stress ratio from that of the untreated loess above optimum moisture.

At 21% moisture, volumetric strains were somewhat greater than at optimum as indicated by comparison of Figures 72 and 77. However, volumetric strains were significantly reduced due to incorporation of the fibers in the higher than optimum moisture content loess, Figure 77. Incorporation of the 360 dpf fibrillated or 15 dpf crimped fibers produced nearly identical volumetric strains at each of the three fiber contents, each being quantitatively similar to that shown in Figure 77 at 0.2 and 0.3% fiber

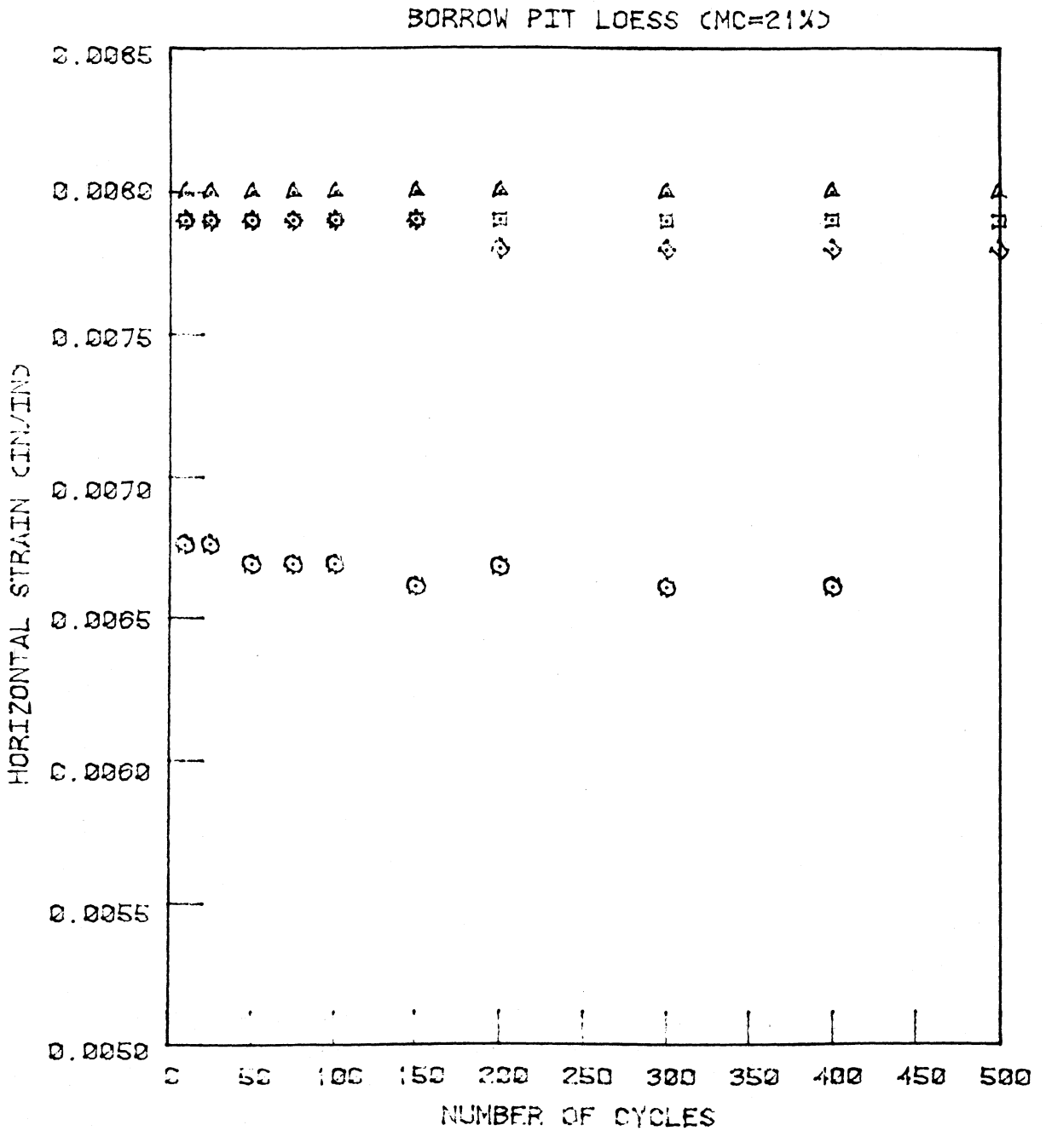

Figure 76. Horizontal unit strain versus number of cycles for varying fiber contents

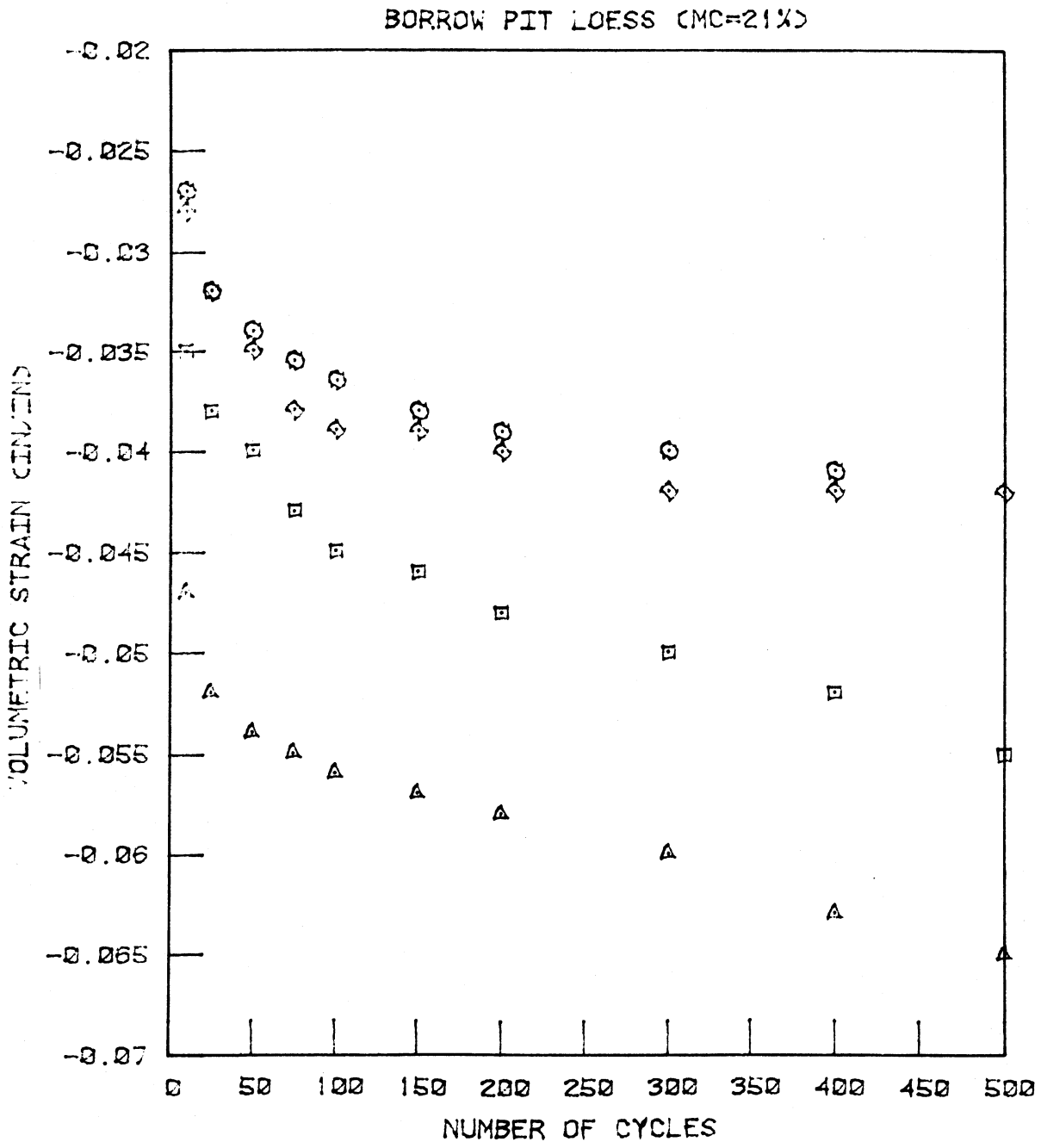

Figure 77. Volumetric strain versus number of cycles for varying fiber contents

weight fraction. In general, volumetric strains produced within the optimum fiber treated specimens was about 40% less than that of the untreated loess, a significant improvement for a material above optimum moisture.

As noted with the unconfined compression tests, the soil-fiber bond appeared critical to enhancement of composite loess-fiber strength. As a consequence, a third series of cyclic load K-Tests were conducted on the loess, using a cement modified matrix, through incorporation of 3% Type I portland cement.

Four fiber types were selected for this study; 15 dpf polypropylene straight (1.5 in), 360 dpf fibrillated polypropylene (1.5 in), 15 dpf crimped polypropylene (1.5 in), and No. 832BB Type E fiberglass (1.25 in). For purposes of this series of tests, all fiber weight fractions were 0.2% only. Duplicate cement modified specimens, with and without fibers, were molded under AASHTO T-99 compaction at the optimum moisture of the untreated soil, wrapped, sealed, and cured for 7 days in a constant temperature room at 100% relative humidity.

With the exception that the cyclic load K-Tests were run for 2000, rather than 500 cycles, the test procedure was identical to that used with all other cyclic testing of the loess and loess-fiber composites.

Figure 78 presents the vertical unit strain versus number of cycles for the cement modified loess, with and without 0.2% 360 dpf fibrillated polypropylene fiber. Regardless of fiber type, incorporation of fiber with the cement modified loess produced a slight increase in vertical unit strain

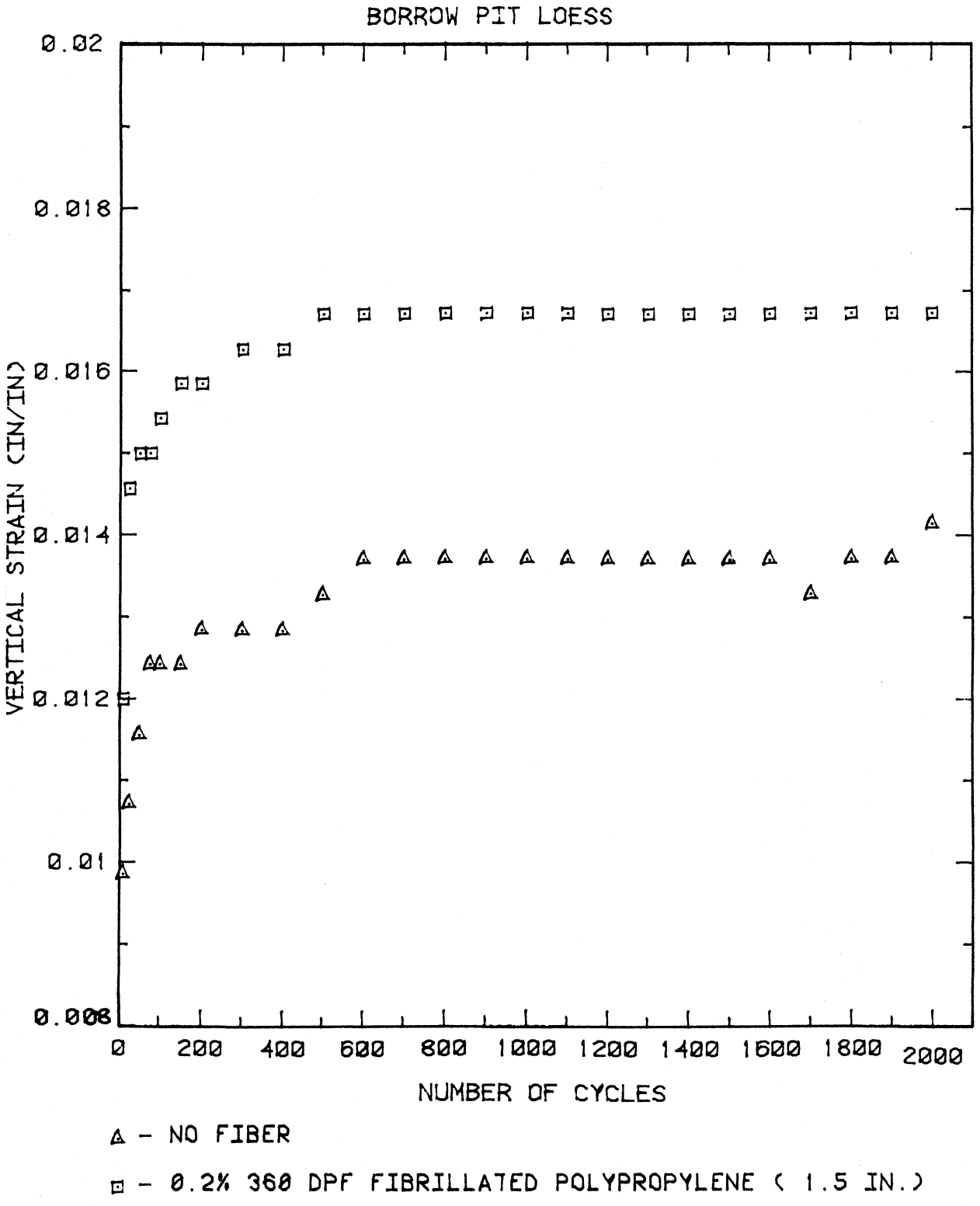

Figure 78. Vertical unit strain versus number of cycles for cement modified loess

when compared with the fiberless matrix material; all increases being of about the magnitude shown in Figure 78. Vertical strains increased during the first 600 cycles, remaining constant thereafter for the fiber treated material, whereas the cement modified only material began to show some fracturing after about 1500 cycles. Comparisons of Figures 68 and 78 illustrate that the magnitude of actual vertical strains however, were only about one-third of those accompanying the untreated and fiber treated loess.

Permanent set of the four fiber treatments of cement modified loess exhibited trends similar to those for vertical unit strain, Figure 79. Comparison of Figures 69 and 79 illustrate that the magnitude of actual permanent set however, was about one-fourth to one-third of that produced in the untreated and fiber treated loess without cement modification of the matrix. Particularly noticeable in Figure 79 are slight variations of permanent set in the fiberless specimens. Such variations may be indicative of slight fracturing, followed by a reconstitution of frictional resistance once fracturing occurs.

Figure 80 presents the variation in vertical strain modulus versus number of cycles for the cement modified loess with and without 0.2% 15 dpf straight polypropylene fibers. Strain moduli of the fiberless, as well as with each of the four fiber treatments was quite erratic. As with the non-modified loess, Figure 70, all fiber treated specimens produced lower values of strain modulus than the cement modified material, an indicator of loss of composite stiffness through fiber inclusion. In general, vertical strain moduli with each of the four fibers increased

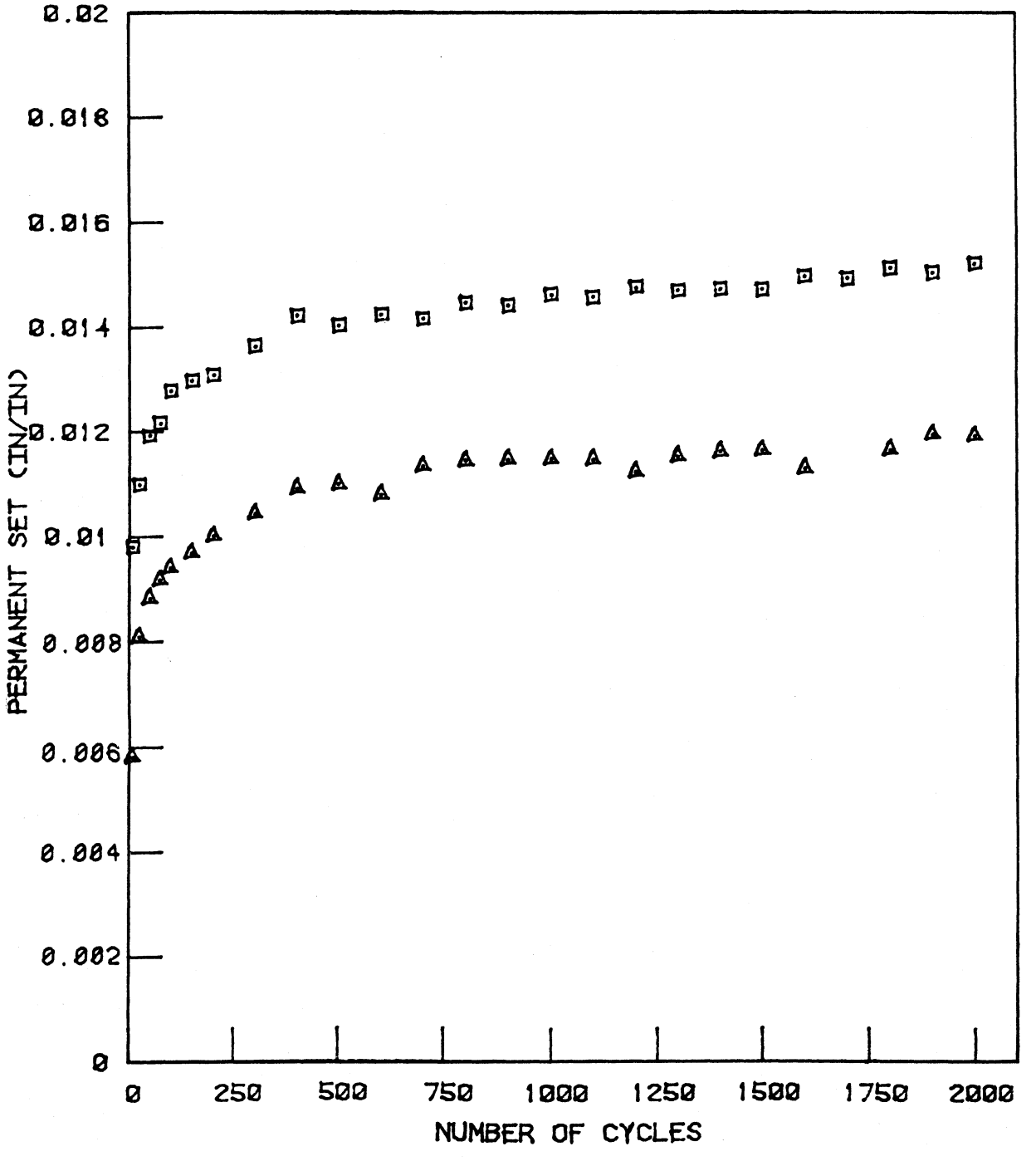

Figure 79. Permanent set versus number of cycles for cement modified loess

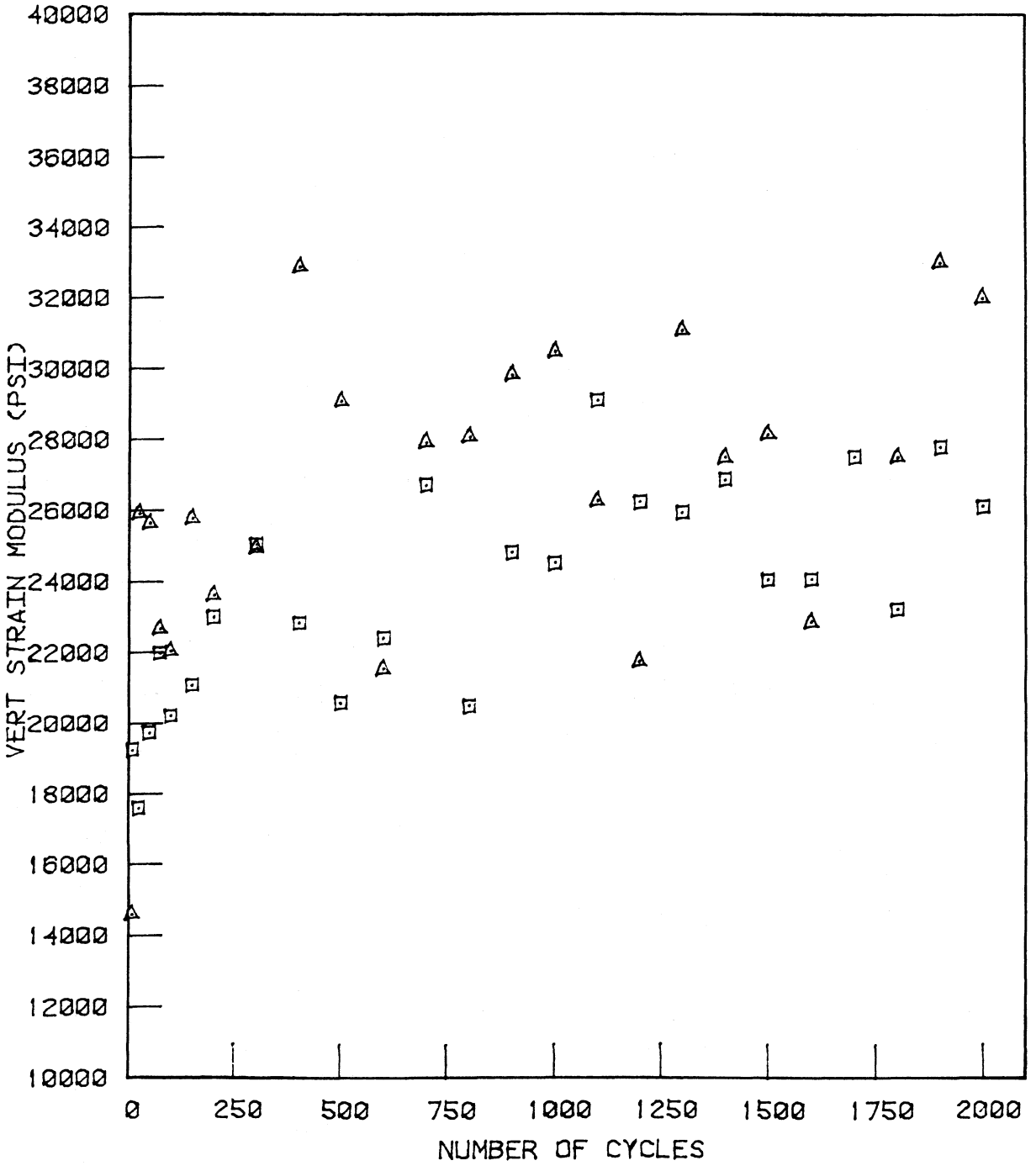

Figure 80. Vertical strain modulus versus number of cycles for cement modified loess

with increasing number of cycles, an indication of cyclic dependent strain hardening. As may be noted through comparison of Figures 70 and 80, the vertical strain moduli due to cement modification was generally doubled from that of the non-modified matrix loess.

Figure 81 presents actual horizontal strain versus number of cycles for the cement modified loess with and without 0.2% 15 dpf crimped polypropylene. Comparison with Figure 71 illustrates the significant modifications in actual values, as well as patterns of horizontal strain, due to the inclusion of 3% cement in the soil matrix. The Type E fiberglass was the only fiber that did not improve horizontal strain, actually showing greater strain from 0 to about 1000 cycles than the cement modified only specimens. The 360 dpf fibrillated polypropylene fibers reduced horizontal strain by nearly 100%, while the 15 dpf crimped fibers, Figure 81, approached a 200% reduction in horizontal unit strain.

Results of the horizontal strain measurements were consistent with the previously noted observation that the most beneficial effect of random fiber reinforcement of a soil may be related to laterally oriented parameters. Figure 81 also illustrates the occurrence of fiber tensile mobilization in the lateral dimension. Such mobilization occurred within the first 150 cycles of 75 psi vertical loading, producing only about 0.0004 in/in of lateral strain within the fiber treated specimens. Horizontal strain of the fiberless cement modified loess increased to near 0.002 in/in at about 500 cycles before tending to equilibrate. At about 600 to 800 cycles of loading, both the fiber treated and fiberless

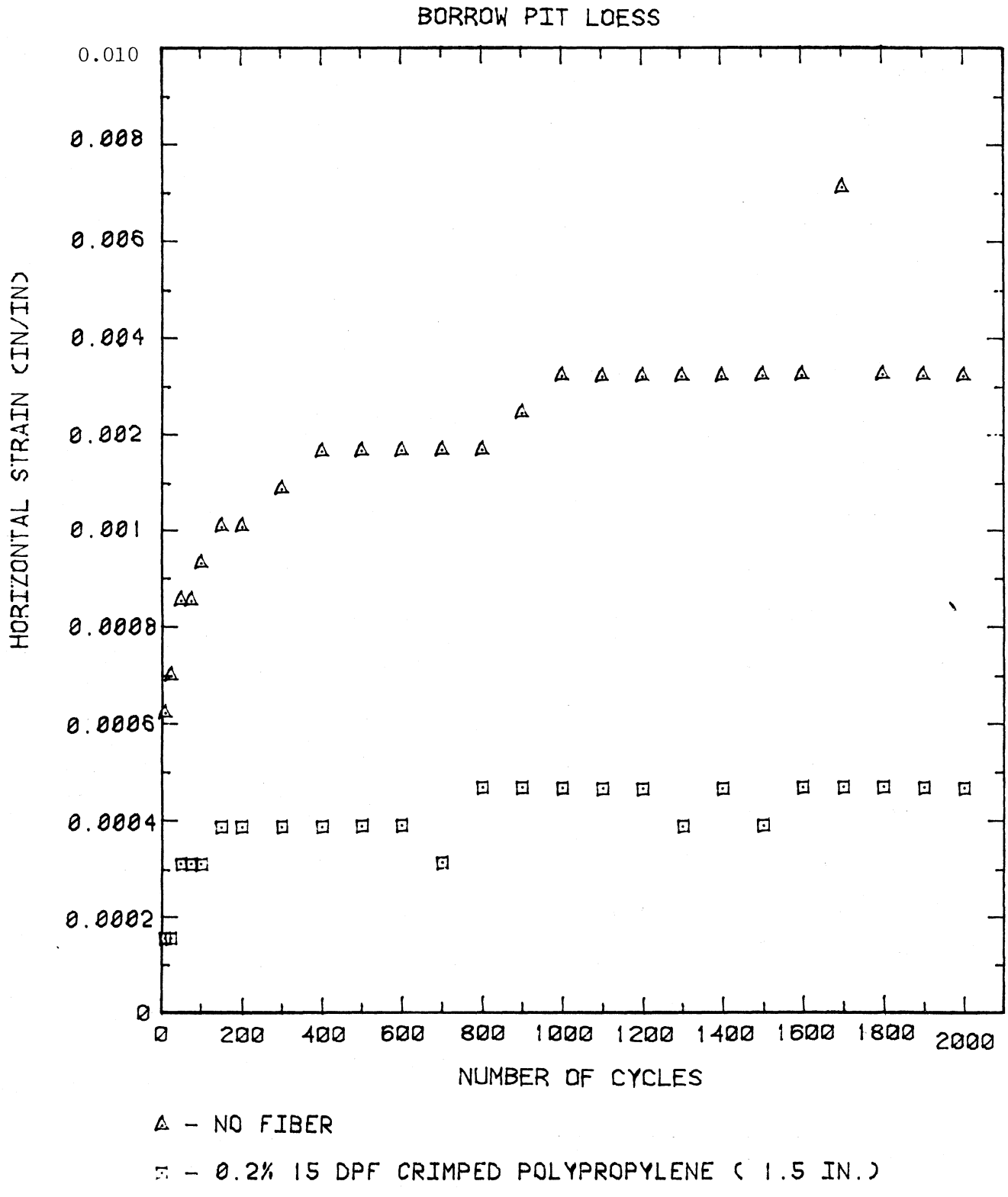

Figure 81. Horizontal unit strain versus number of cycles for cement modified loess

cement modified loess apparently produced additional fracturing, but recovery due to fiber tensile mobilization was quicker and of less magnitude. Tensile mobilization of the 360 dpf fibrillated fibers occurred within the first 25 cycles and remained equillibrated at 0.0007 in/in horizontal strain through 2000 cycles.

Due to their interrelationship, trends observed with horizontal stresses were nearly identical to those of horizontal strain. The 15 dpf crimped fiber produced the greatest lowering of horizontal stress; actual values were less than 0.1 psi during 2000 cycles of loading.

Actual stress ratio values followed the trends established within the horizontal stress and strain measurements due to their direct relationship, Figure 82. However, because of the magnitude of horizontal stresses produced within the cement modified specimens, the consequent values of stress ratio were extremely small when compared to the values obtained for the non-modified matrix untreated and fiber treated specimens. As noted in Figure 82, stress ratio for the 0.2% 15 dpf crimped polypropylene cement modified specimens was generally equilibrated at about 0.0012. At optimum moisture content, incorporation of 0.2% of the 15 dpf crimped fiber within the non-modified loess produced a stress ratio of 0.017 (14 times greater), while at greater than optimum moisture an actual stress ratio of 0.019 was observed (nearly 16 times greater).

Figure 83 presents actual values of volumetric strain of the 0.2% weight fraction 15 dpf polypropylene fiber treated cement modified specimens. The magnitude of actual volumetric strain was significantly

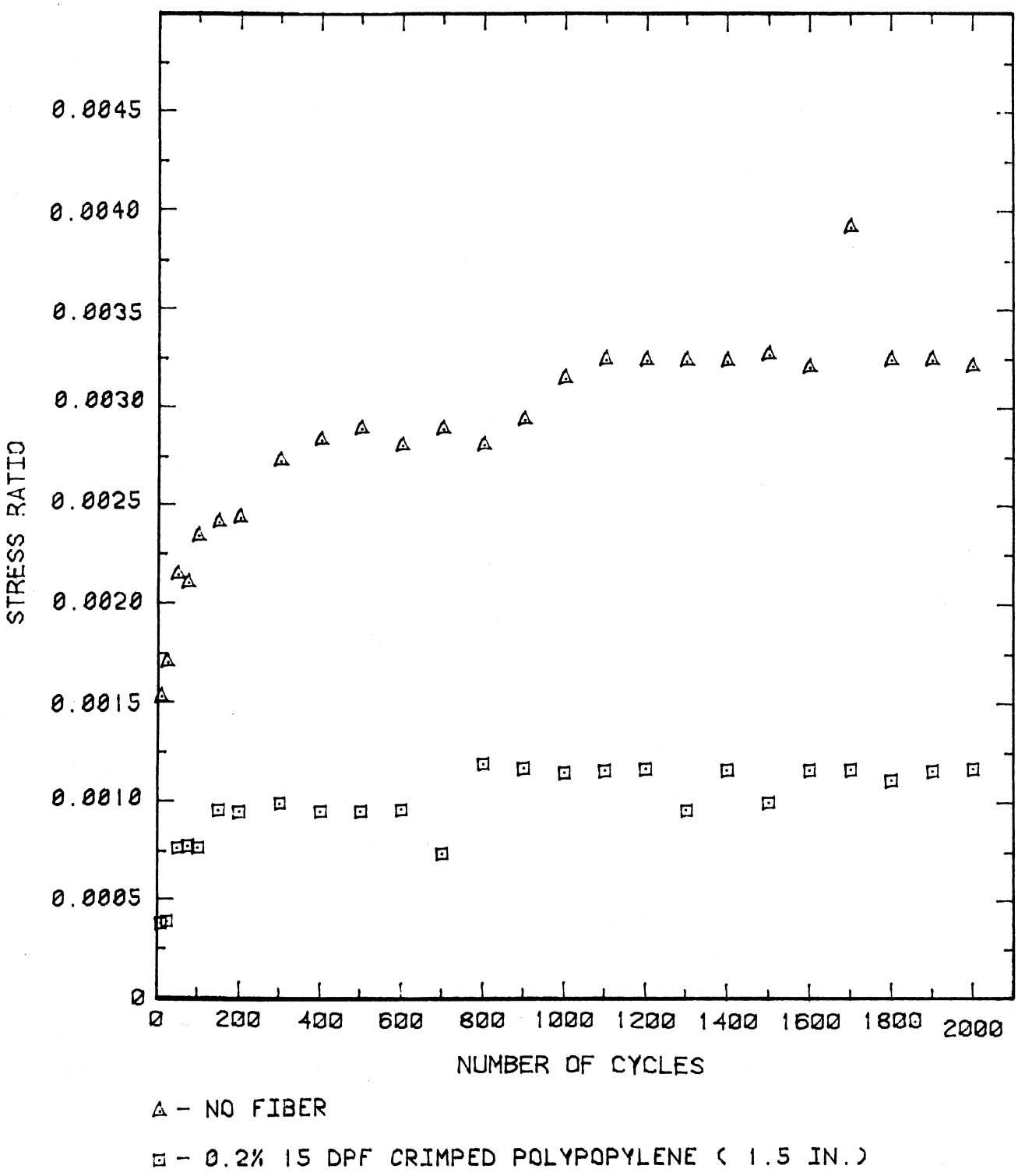

Figure 82. Stress ratio versus number of cycles for cement modified loess

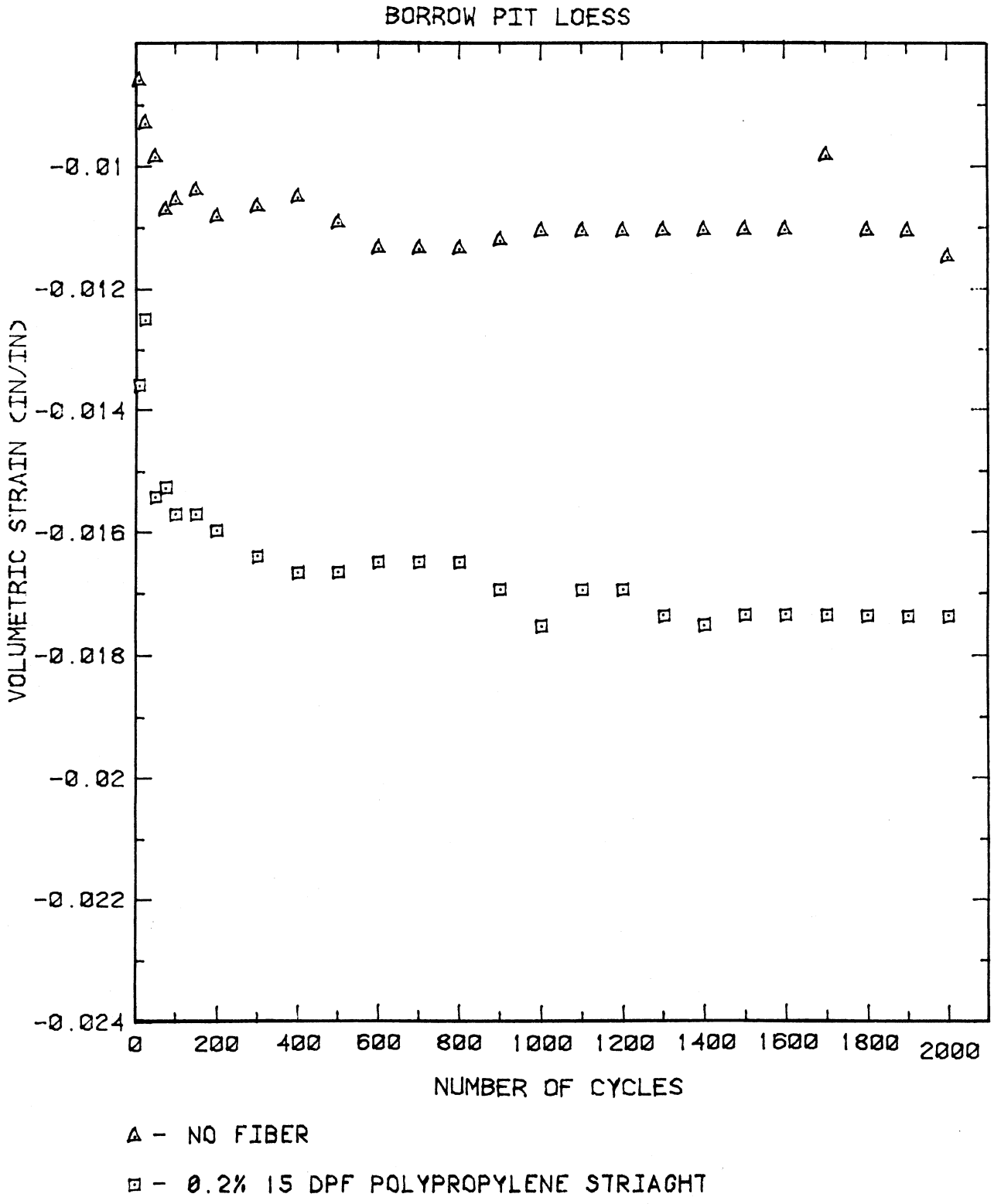

Figure 83. Volumetric strain versus number of cycles for cement modified loess

improved due to matrix modification with 3% cement, as may be seen by comparison of Figure 83, 72, and 77.

Based on the preceeding data obtained from the cyclic load Iowa K-Tests of the fiber treated Sioux City loess material, the following general observations were obtained:

1. Potential of fiber reinforcement predominantly appears related to horizontal or lateral stability, although vertical and volumetric strain characteristics of the fiber treated non-modified loess was appreciably enhanced, both at optimum as well as greater than optimum moisture contents. Modification of the loess soil matrix through the addition of 3% Type I portland cement further enhanced the lateral stability of the soil-fiber composites.

2. As with the Mortenson Road soil, the 15 dpf crimped and 360 dpf fibrillated polypropylene fibers provided the best overall performance among the fibers considered. From the point of view of workability, the 360 dpf fibrillated fibers were easiest to mix in the laboratory, though the 15 dpf crimped fibers were not as difficult to mix into the more friable loess as with the Mortenson Road soil.

Freeze-thaw, K-Tests, Sioux City loess

Two series of Sioux City borrow pit loess specimens were molded in order to conduct combined freeze-thaw, static K-Tests and cyclic load K-Tests of the untreated and fiber composites. One series combined the fiber and non-modified soil, while the second series consisted of the fibers and a modification of the soil matrix with 3% Type I portland

cement. Two-tenths percent fiber weight fraction of the 360 dpf fibrillated polypropylene (1.5 in) and 15 dpf crimped polypropylene (1.5 in) were used in each test series. All specimens for each series were molded at optimum moisture content under AASHTO T-99 compaction.

Freeze-thaw tests were performed using the Iowa Freeze-thaw apparatus. Each specimen is placed in a plexiglass container, in a Dewar flask, and allowed to freeze from the surface for a period of 16 hours, while in contact with liquid water at its base for capillary absorption. Thawing is then allowed for a period of 8 hours. During 10 cycles of freeze-thaw, average vertical elongation measurements of each specimen are made after each freeze and thaw period.

Following freeze-thaw, all specimens were tested through either the static Iowa K-Test or the cyclic loading K-Test. Selection of the K-Test performed was dependent on the condition of each specimen following freeze-thaw.

Figures 84 and 85 present average calculated volumetric change during freeze-thaw for duplicate specimens of the non-modified loess, untreated and treated with the respective fibers. During the first few cycles, all specimens expanded. During the freezing phase of the fourth cycle, the untreated specimens expanded severely indicating a breakdown of soil particle to particle bonding. From the fourth through tenth cycles, the untreated specimens continued a slight volumetric expansion. Following initial expansion, all fiber treated specimens stabilized if not slightly decreased in volume. It may be hypothesized that the fibers were mobilized during initial expansion and then resisted further volume change due to the

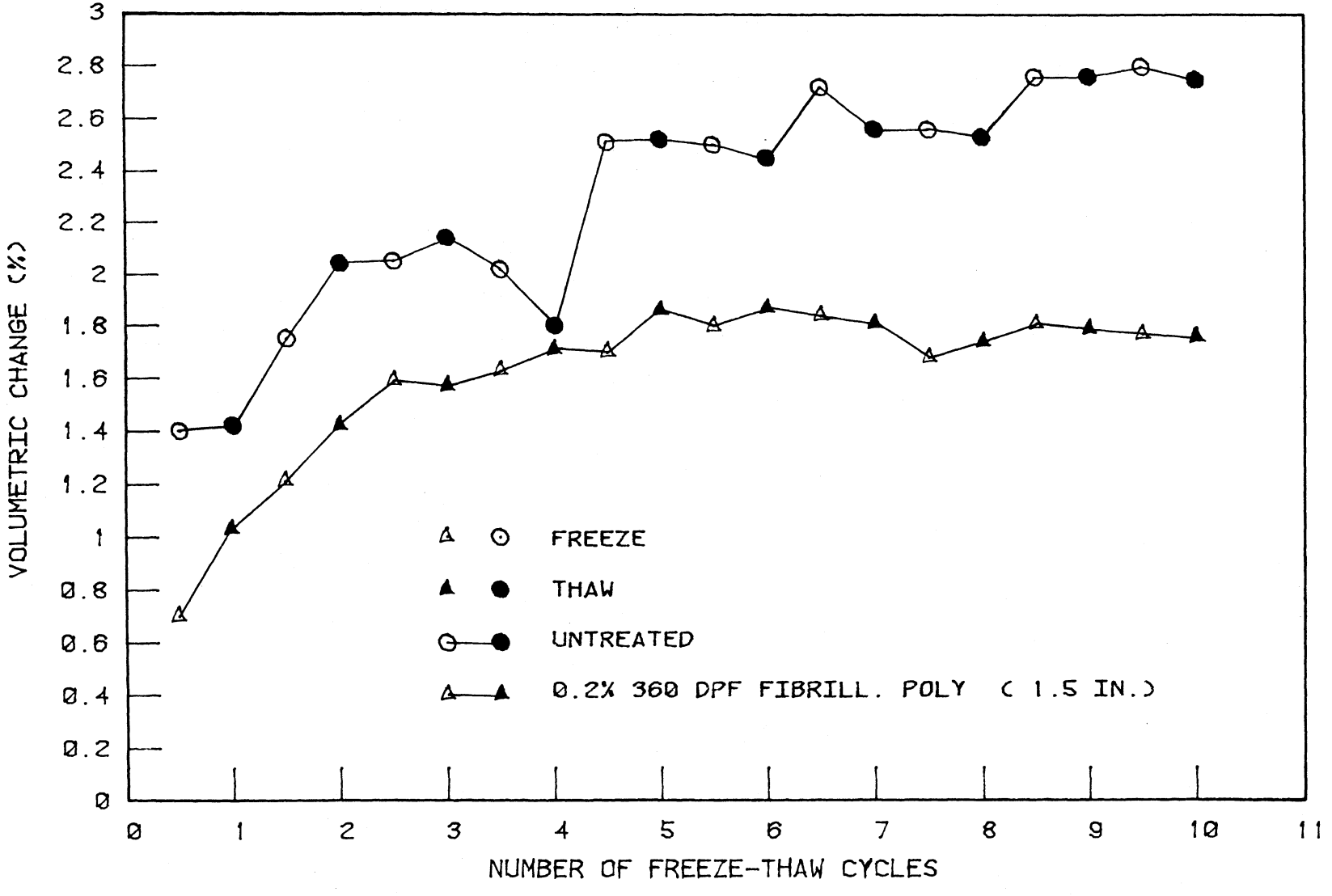

Figure 84. Volumetric change versus number of freeze-thaw cycles, non-modified loess soil

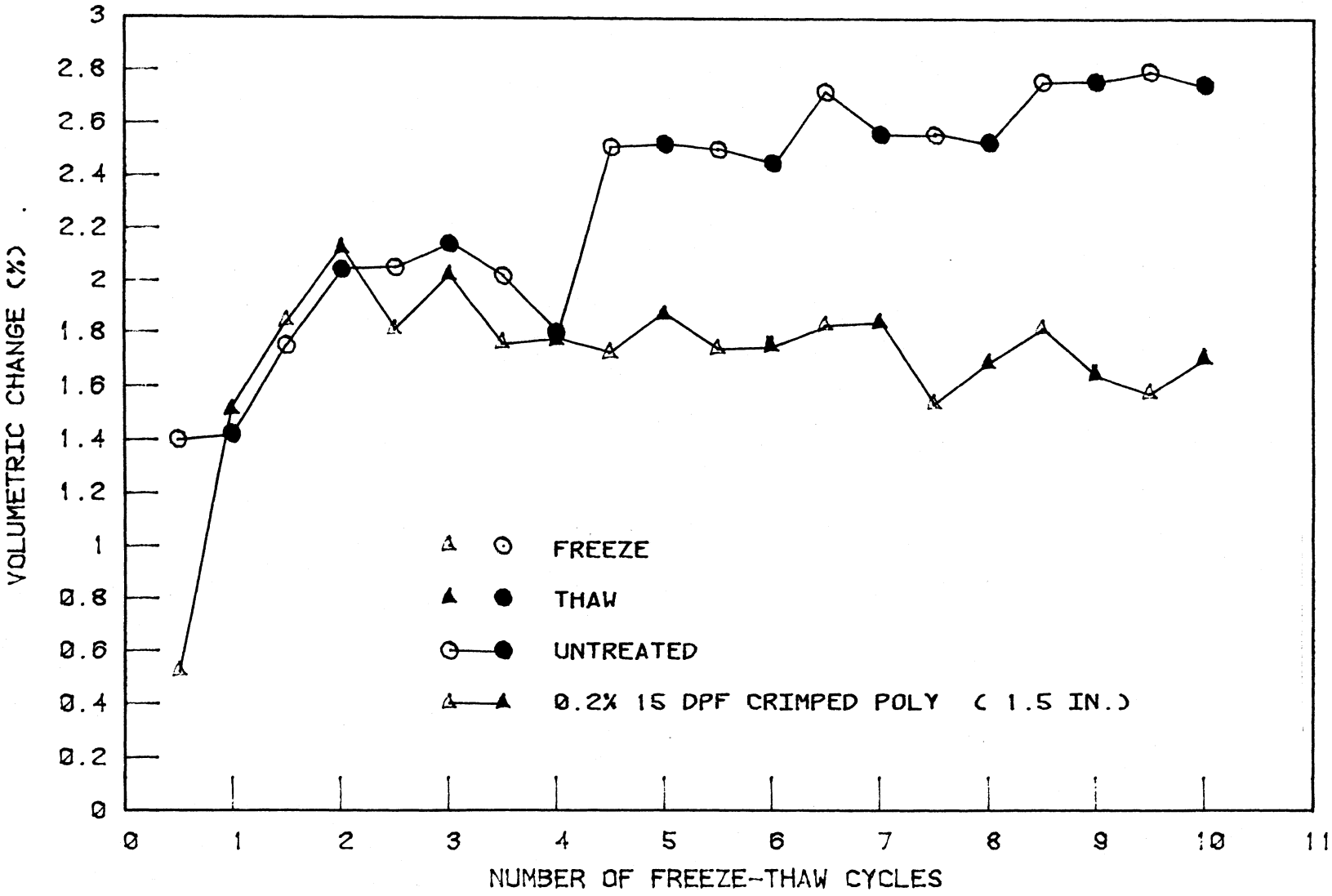

Figure 85. Volumetric change versus number of freeze-thaw cycles, non-modified loess soil

fiber tensile strength. Figures 84 and 85 indicate that use of the fibers decreased volumetric change on the order of 40% as compared with the untreated soil, an important factor in reinforcement and/or reduction of heave-boil characteristics of a frost susceptible roadway soil.

Following freeze-thaw, all specimens were static K-Tested, the average results of which are presented in Table 20. The untreated specimens appeared to produce a slightly higher value of friction angle than the fiber treated specimens, while the latter produced some improvement in the modulus E, but were coupled with slight increases in stress ratio K. Based on such values, it would appear that the fiber treated specimens would not produce gains in stability. This observation however, is contrary not only to the freeze-thaw data but also to visual as well as handling observations of both the untreated and fiber treated specimens following freeze-thaw. Prior to static K-testing the untreated specimens were extremely difficult to handle and easily spalled; the reverse was noted with the fiber treated specimens. The apparent discrepancy between observations and static K-test data again appeared due to the incapability of the static K-Test to measure the lateral stability properties of the soil-fiber composites.

Average volumetric changes produced during freeze-thaw of the cement modified loess, and cement modified plus fiber treatment, are presented in Figures 86 and 87. As noted, the cement modified loess experienced a gradual increase in expansion coupled with increasing expansion and contraction between freezing and thawing. The latter phenomena indicated

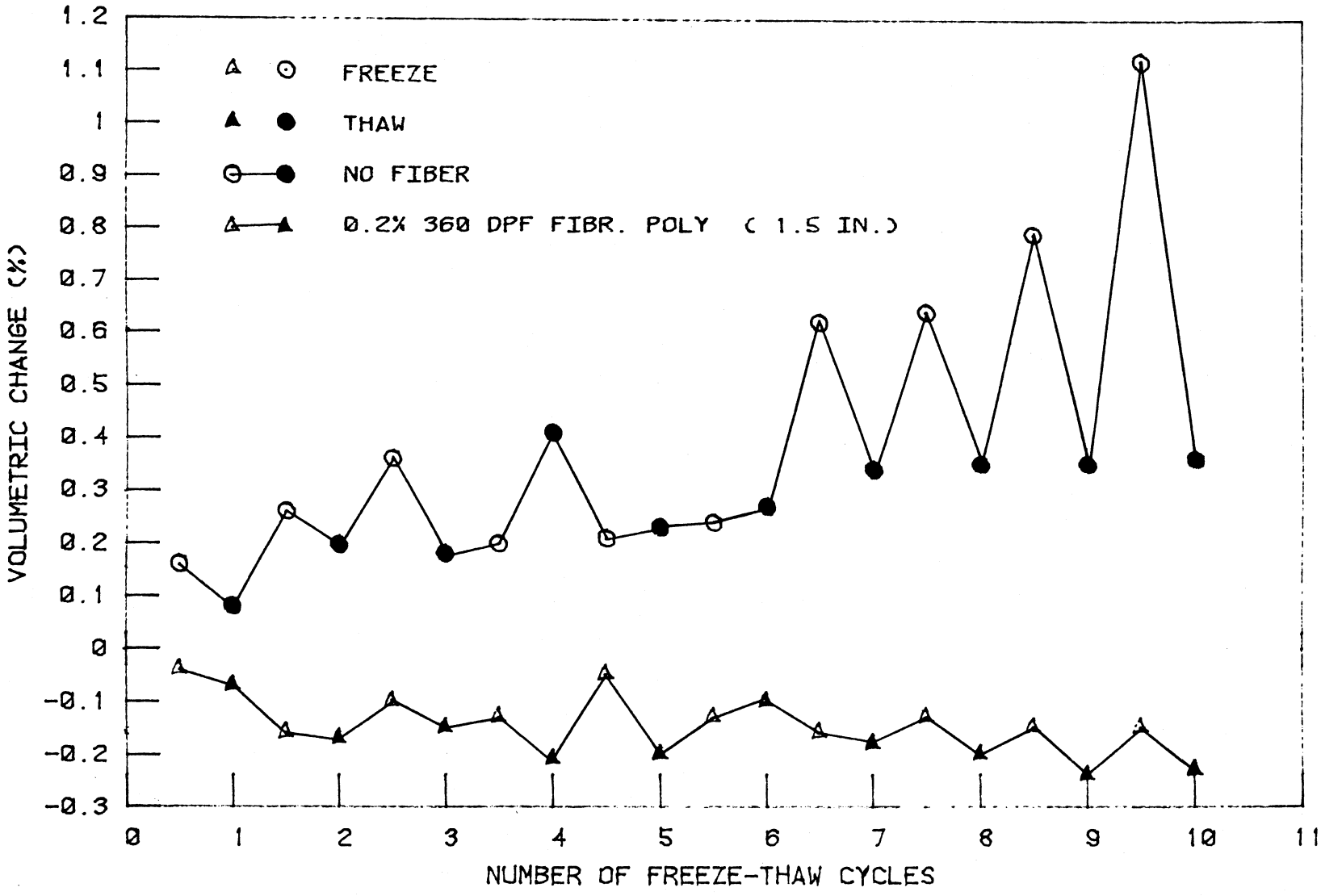

Figure 86. Volumetric change versus number of freeze-thaw cycles, cement modified loess soil

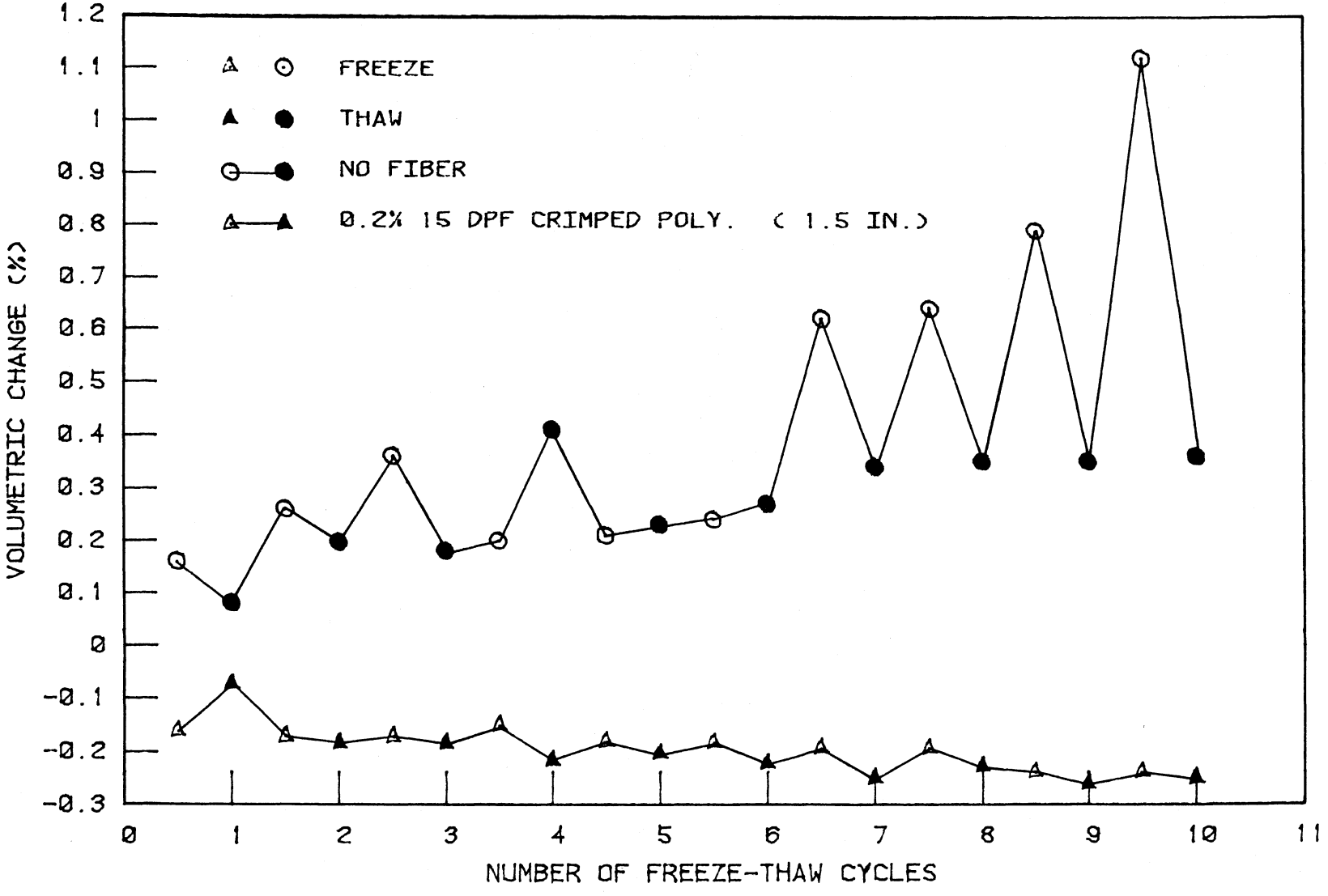

Figure 87. Volumetric change versus number of freeze-thaw cycles, cement modified loess soil

Table 20. Static K-Test results of loess soil-fiber composites

Treatment	Friction Angle, $\phi°$	Cohesion c, psi	Stress Ratio, K	Strain Modulus, E, psi
0% fiber	42.4	2.3	0.216	1710
0.2% 360 dpf fibrillated polypropylene	20.1	0.6	0.244	2402
0.2% 15 dpf crimped polypropylene	37.6	2.3	0.251	1849

a general debonding of cementing action between soil particles. The fiber treated specimens portrayed totally different trends, slightly contracting during initial freeze-thaw and remaining in relative equilibrium thereafter. In general, fiber inclusion in the cement modified loess soil matrix produced in excess of a three-fold residual volumetric change during the 10 cycles of freeze-thaw. When compared to the untreated soil, Figures 84 and 85, the fiber-cement modified composite specimens reduced volumetric characteristics by a factor of about 15, indicating that fiber incorporation into this type of modified soil matrix, may produce an extremely stable composite material, significantly minimizing frost susceptibility characteristics.

All cement modified specimens were subjected to the cyclic load K-Test following freeze-thaw. Figures 88 and 89 present average actual vertical unit strains for the cement modified and fiber treated cement modified loess specimens. Both fibers produced less vertical strain than

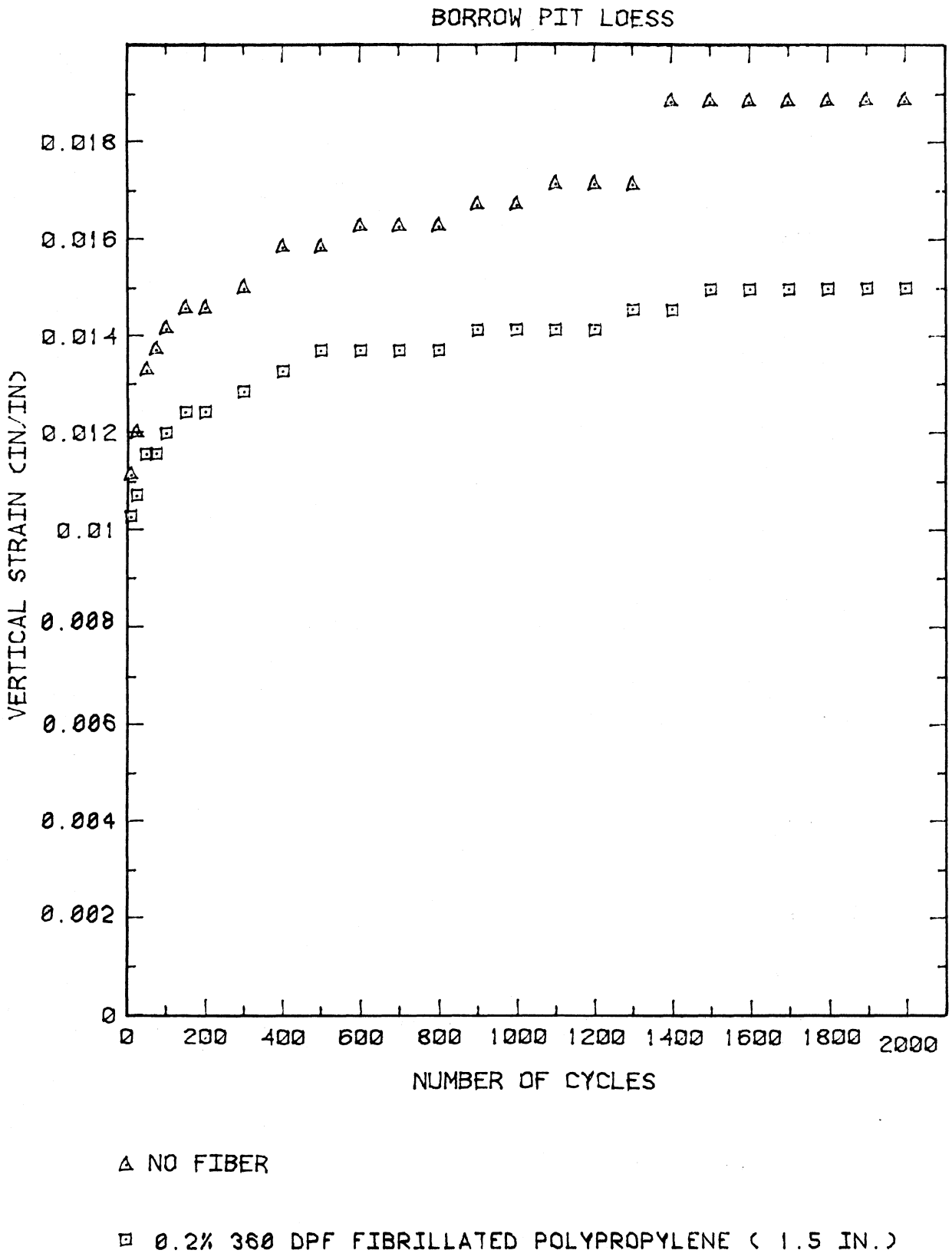

Figure 88. Vertical unit strain versus number of cycles for cement modified loess following freeze-thaw

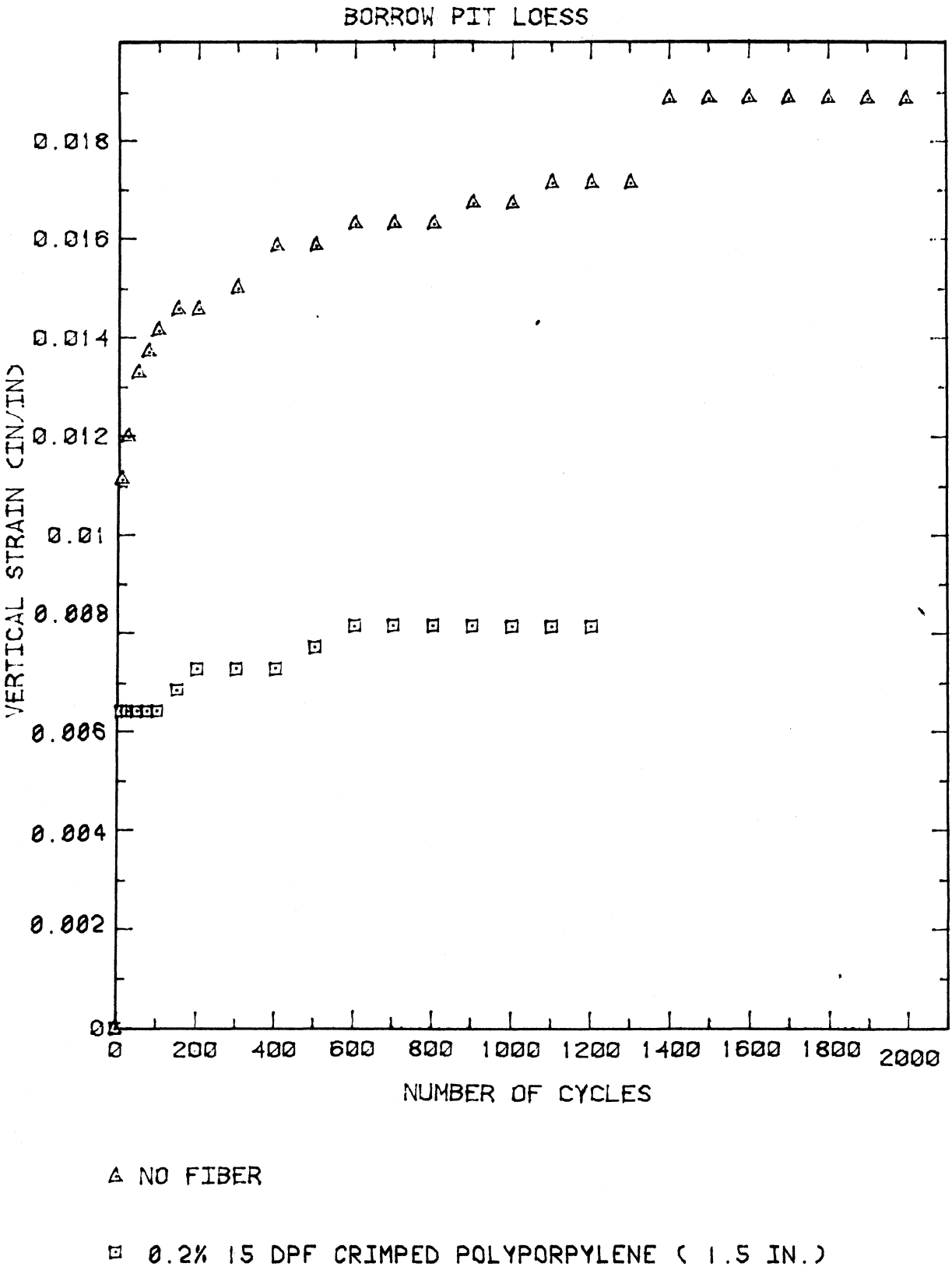

Figure 89. Vertical unit strain versus number of cycles for cement modified loess following freeze-thaw

the fiberless cement modified specimens; the 15 dpf crimped polypropylene showing a reduction in vertical strain in excess of one-half and the 360 dpf fibrillated producing about a 20% reduction. The latter reduction is quite different from the vertical strain noted for the non-freeze-thaw testing performed with the 360 dpf fibrillated fibers, Figure 78, and is partially related to the effect of additional curing of the specimens producing additional matrix bonding during the 10 days of freeze-thaw testing. Shapes of the vertical strain curves of Figures 88 and 89 reveal fracturing potential of the cement modified loess, whereas the fiber treatment illustrates slight fracturing coupled with fiber mobilization and recovery. Due to the foregoing, it will be noted that the two sets of curves become more widely separated with increasing number of cycles, indicating an increased breakdown of the fiberless cement modified material.

Measurements of permanent set followed patterns identical to those of vertical strain. As with the vertical strain moduli of Figure 80, moduli produced after freezing and thawing were also erratic. Median and one standard deviation of vertical strain moduli of the freeze-thaw cement modified specimens was 20,000 $\pm$ 1770 psi, of the 360 dpf fibrillated polypropylene treated specimens, 22,000 $\pm$ 2200 psi, and for the 15 dpf crimped polypropylene treated specimens, 28,600 $\pm$ 4000 psi. In general, the 15 dpf crimped fibers increased the composite stiffness about 40%.

Figures 90 and 91 show that fiber treatments significantly reduced average horizontal strains from those of the fiberless cement modified loess specimens, the values being nearly negligible. Comparison of Figures 81, 90 and 91, shows an increased separation of the fiberless cement

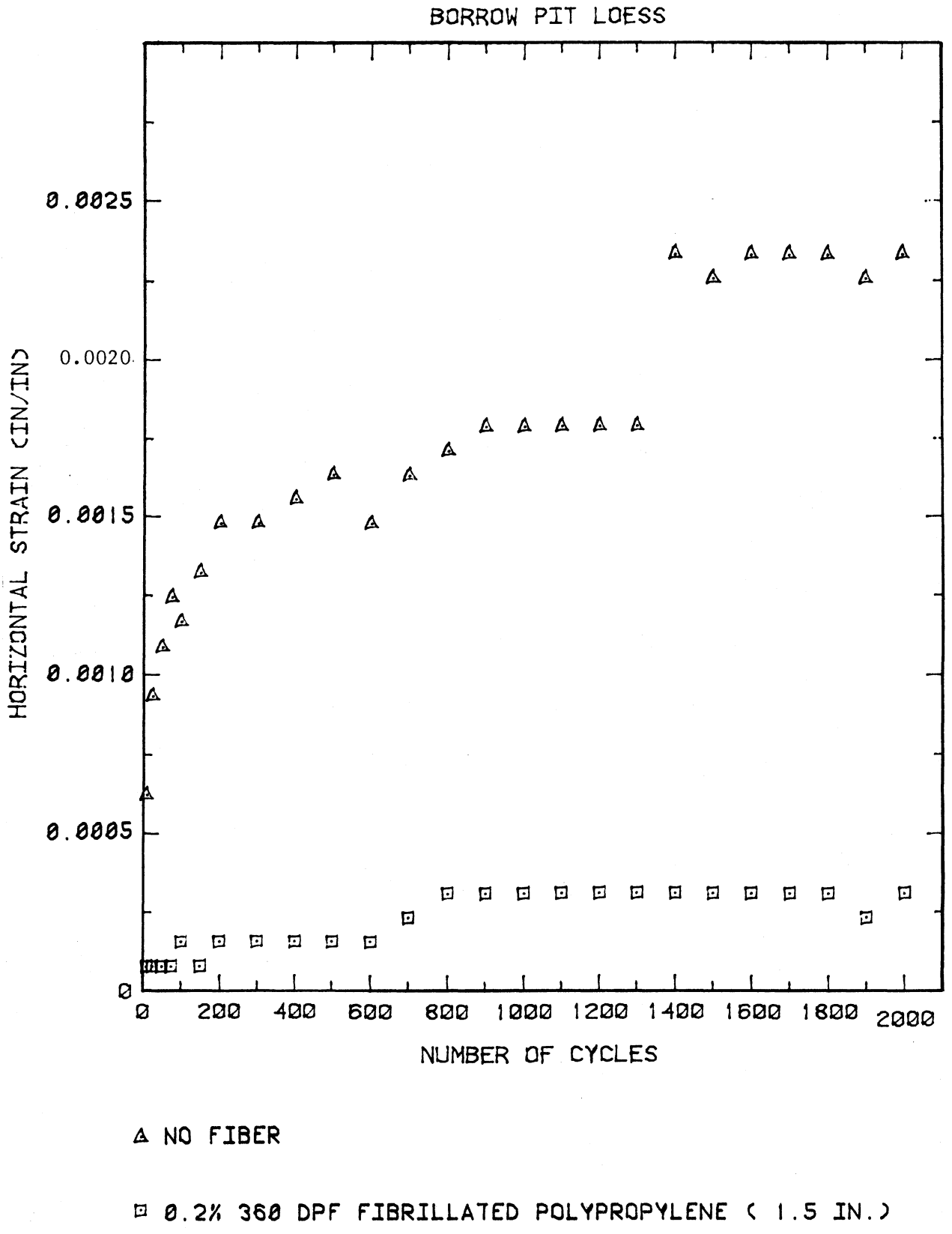

Figure 90. Horizontal strain versus number of cycles for cement modified loess following freeze-thaw

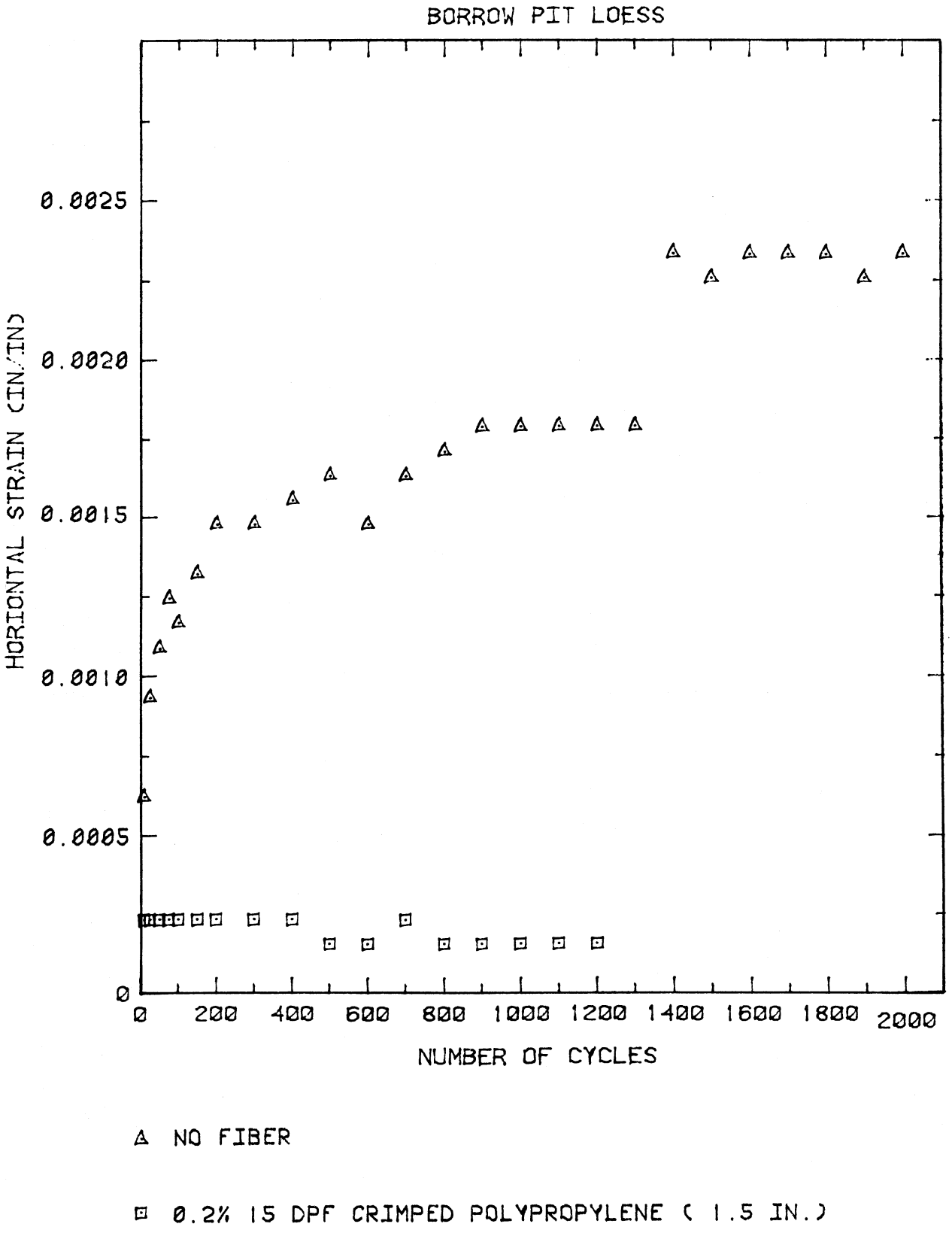

Figure 91. Horizontal strain versus number of cycles for cement modified loess following freeze-thaw

modified curve from that of the specimens containing fibers, indicating that freeze-thaw of the fiberless material affected the ability of the matrix to resist horizontal straining.

The effect of freeze-thaw on horizontal stress and stress ratio of the cement modified and fiber treated loess followed nearly identical patterns to those produced for horizontal strain.

Following freeze-thaw, the 360 dpf fibrillated fiber treatment of the cement modified loess did not alter volumetric strain of the fiberless material, whereas the 15 dpf crimped fiber reduced volumetric strain about 30%. On first observation, the lack of alteration of volumetric strain by the 360 dpf fiber appears somewhat incongruous since large reductions in both vertical and horizontal strain were observed. However, it should be kept in mind that there is a cancelling effect within the volumetric strain computations. With the fiberless specimens, large values of vertical and horizontal strains were measured, thus the net change was small. With the 360 dpf fibrillated fiber specimens low values of both vertical and horizontal strains occurred, with a resulting net change again being small, and in this case nearly equal to the fiberless material.

Within the confines of this combined freeze-thaw, cyclic load testing study of the cement modified loess, both the 360 dpf fibrillated and 15 dpf crimped polypropylene fibers performed quite well, the 15 dpf being somewhat superior. The study again illustrates (1) the critical importance of soil-fiber matrix bonding, and (2) that the primary mechanism of random fiber reinforcement of a roadway soil is predominantly through improved lateral stability.

Micro-Properties of Soil-Fiber Composites

The overall integrity of a soil-fiber composite depends on the interaction occurring between the fiber and soil matrix. In order to more fully define the mechanism(s) of soil-fiber reinforcement, several micro-investigations involving the soil-fiber interface were conducted. Through the following investigations, trends were exhibited which could be correlated with either previous studies of fiber concrete, or the macro-properties of soil-fiber composites presented in preceeding sections of this report.

An overall fiber efficiency factor, λ, was calculated using an approach taken in fiber reinforced concrete, as expressed through the following modification of equation 18:

$$E_C = E_f V_F \lambda + E_m (1 - V_f)$$

where E = Young's Modulus, V = volume, λ = overall efficiency factor, and subscripts c, f, and m refer to the composite, fiber and matrix moduli respectively (16). For analysis of soil-fiber composites, untreated Sioux City soils were considered as the matrix, the fiber reinforced soils as the composite. One difficulty in applying this equation was in determining the volume of fibers in a soil-fiber specimen. Since the fiber was added as a weight fraction, it was essential to know the number of fibers present in a given weight. To obtain this information, several small amounts of each fiber type were weighed to the nearest 0.0001 gram and the number of fibers was counted. Dividing the number of fibers by the weight, resulted in number of fibers per gram. Determining the median and standard deviation

of several trials for each fiber resulted in a reasonable estimate of number of fibers per gram for each fiber type, Table 21.

Table 21. Number of fibers per gram for each fiber type

Fiber Type	Number of Fibers Per gram
15 dpf polypropylene monofilament, 1 1/2 inch length	9720 ± 175
15 dpf crimped polypropylene monofilament 1 1/2 inch length	13470 ± 345
832 bb Type E fiberglass, 1 1/4 inch length	438 ± 7
360 dpf fibrillated polypropylene, 1 inch length	962 ± 8
360 dpf fibrillated polypropylene, 1 1/2 inch length	861 ± 8

Comparing the results of Table 21 with calculations involving the fibers specific gravity and manufacturers dimensions did not match the counting results. Reasons for this lack of correlation include; 1) individual fiber dimensions appear to slightly vary; 2) contamination of counted fibers with dust particlulates; and 3) absorption of moisture by the fibers.

Knowing the number of counted fibers per gram and using fiber dimensions provided by the manufacturers, the volume of fibers were calculated for various weight fractions. Volume of the composite was chosen as one cubic foot. For ease of calculation, soil dry density was assumed as a constant 100 pcf and 105 pcf for the borrow pit and West 3rd Street soil specimens, respectively. Only E values from specimens near optimum moisture content were utilized.

Table 22. Fiber efficiency factors for loess-fiber composites

Fiber	E_f, psi	Fiber Weight Fraction, %	E_c, psi	λ
Borrow Pit Loess Em = 750 psi				
15 dpf polypropylene monofilament, 1 1/2 inch	1.1×10^6	.1	825	.057
		.17	1090	.152
		.2	900	.057
		.3	850	.026
15 dpf crimped polypropylene, 1 1/2 inch	1.1×10^6	.05	1100	.383
		.1	1170	.230
		.2	960	.058
832 bb fiberglass type E, 1 1/4 inch	10×10^6	.1	885	.019
		.17	1100	.029
		.2	1005	.018
		.3	955	.010
360 dpf fibrillated polypropylene, 1 inch	1.1×10^6	.1	1000	.142
		.17	1050	.101
		.2	905	.045
		.3	945	.037
360 dpf fibrillated polypropylene, 1 1/2 inch	1.1×10^6	.1	840	.039
		.2	910	.034
		.3	935	.027
West 3rd Street Loess Em = 530 psi				
832 bb fiberglass type E, 1 1/4 inch	10×10^6	.02	955	.280
		.08	1100	.104
		.15	1070	.048
		.3	1030	.022
		.5	1085	.015
360 dpf fibrillated polypropylene, 1 inch	1.1×10^6	.02	750	.145
		.04	570	.013
		.06	535	.001
		.08	655	.021
		.15	690	.041
		.3	905	.017
		.5	860	.009

Table 22 presents the results of the overall efficiency factor of the loessial soil-fiber composites. These results must not be considered fully conclusive. Values of E varied widely, and at several fiber weight fractions only one specimen was near optimum moisture. Further, the random orientation of the fiber and testing procedure may have caused E to fluctuate. In spite of these reservations, the 15 dpf crimped polypropylene fiber composites had the highest efficiency factors which is consistent with highest improvement in unconfined compression and other parametric values. Without exception, the efficiency factor decreased as the fiber weight fraction increased, yet unconfined compressive strength generally increased. This phenomena may be due to the increased number of fibers randomly distributed in a specimen. Many fibers probably do not reinforce against unconfined failure, yet at the same time more are oriented to resist failure than at lower fiber weight fractions.

Efficiency factors for cement treatments were calculated in the same manner, though the matrix was considered as the cement-modified soil. Table 23 presents the results for 1 percent type I Portland cement treatment. Again the smaller 15 dpf polypropylene fibers were the better performers, with the crimped fiber attaining the highest efficiency factor. These results are consistent with improvements of q_u, strain at failure and E, noted earlier for 1 percent cement and fiber composites.

Calculation of overall efficiency factors for the 3 percent type I Portland cement were also accomplished with the cement modified soil providing the matrix values. After 7 days curing, only the 15 dpf crimped polypropylene fiber composite had a value of E greater than the matrix,

Table 23. Fiber efficiency factors for loess, 1 percent type I Portland cement and fiber composites.

E_m, psi Fiber added, 0.17% FWF	24 hour cure 820		7 day cure 910	
	E_c	λ	E_c	λ
15 dpf polypropylene monofilament, 1 1/2 inch	995	0.079	1200	0.130
15 dpf crimped polypropylene, 1 1/2 inch	1260	0.142	1480	0.184
832 bb fiberglass 1 1/4 inch	1225	0.033	1265	0.029
360 dpf fibrillated polypropylene, 1 inch	1005	0.062	1150	0.081
360 dpf fibrillated polypropylene, 1 1/2 inch	1020	0.050	1050	0.037

meaning that λ would become negative for the remaining fiber treatments, Table 24.

In an effort to better understand bonding characteristics between the loessial soils and fiber, two approaches were taken. First, incorporation of fibers into the soil system was analyzed in terms of surface area ratios of fiber to soil particles, coupled with examination by Scanning Electron Microscope of fiber surfaces before and after compaction in the soil. Second, the relative magnitude of soil-fiber bond strength was obtained by use of an improvised fiber-pull-out test.

Soil-fiber composites are systems that may have very high void ratios, especially when compared to plastic or resin fiber composites. Typical values of void ratios of the compacted Sioux City borrow pit loess-fiber

Table 24. Fiber efficiency factors for loess, 3 percent type I Portland cement and fiber composites

E_m, psi Fiber added, 0.17% FWF	24 hour cure 4525 E_c	λ	7 day cure 9435 E_c	λ
Borrow Pit Loess treated with 3% Portland cement Type I				
15 dpf polypropylene 1 1/2 inch	5005	0.218	7790	-
15 dpf crimped polypropylene 1 1/2 inch	7915	1.00	11175	0.567
832 bb fiberglass 1 1/4 inch	6680	0.175	8925	-
360 dpf fibrillated polypropylene 1 inch	6055	0.5134	8500	-
360 dpf fibrillated polypropylene 1 1/2 inch	5875	0.339	7210	-

composites were higher than untreated soil and ranged from 0.6 to 0.7. Such void ratios imply that fiber does not occur in the soil voids only, but may separate soil particles, thus increasing the void ratio. In addition, bonding between the soil and fiber may occur within relatively small areas of the fiber surface. The fairly uniform particle size gradation of the loess contributes to high void space in the matrix. It is hypothesized that to be more reinforcement effective, fibers should fill void spaces rather than create additional void space; a condition probably explaining why the smaller diameter 15 dpf polypropylene fibers displayed the better performance.

Surface area of the fibers was calculated using fiber dimensions provided by the manufacturers. When coupled with the number of fibers per unit weight, Table 21, the surface area exposed by fibers of a selected fiber weight fraction could be calculated. Surface area of the soil particles was much more complex. Handy (13) showed that the area of loess particles, similar to those of the Sioux City borrow pit, presented about 1.37 square centimeters of area per gram of dry soil. Assuming a dry density of 100 pcf, this information was transformed to a standard proctor size specimen, comparing the soil particle surface area to fiber surface area for a given fiber weight fraction as shown in Table 25. End areas of fibers were neglected.

Table 25 shows significant variation in surface area between fiber types at the same fiber weight fractions. The smaller diameter 15 dpf fibers exhibited better strength enhancement at lower fiber weight fractions than the larger diameter fibers. Perhaps this is related to the ratio of the soil particles' surface area to fibers' surface area being close to unity. Comparison of surface area ratios of the various fibers at the weight fraction achieving maximum unconfined compressive strengths, supported a previous observation of increasing fiber content producing increasing strengths. As area ratios decreased, fiber weight fraction increased and the composite attained a higher q_u. The highest increase was achieved with the crimped 15 dpf polypropylene at about 0.8 surface area ratio. In addition, the 0.2 and 0.3 percent fiber weight fractions of both 15 dpf polypropylene fibers were relatively difficult to adequately mix with the loess soil. These fibers produced surface area ratios between 0.8 and 1.2 indicating a possible limiting surface area ratio near unity

Table 25. Ratio of soil particle surface area to fiber surface area of standard proctor specimens, dry density = 100 pcf

Fiber Weight Fraction, %	0.05	0.1	0.17	0.2	0.3
Fiber					
15 dpf polypropylene monofilament 1 1/2 inch	-	2.3	1.4	1.2	0.8
15 dpf crimped polypropylene monofilament, 1 1/2 inch	3.3	1.7	1.0	0.8	-
832 bb type E fiberglass, 1 1/4 inch	-	15.4	9.1	7.7	5.1
360 dpf fibrillated polypropylene, 1 inch	-	7.8	4.6	3.9	2.6
360 dpf fibrillated polypropylene, 1 1/2 inch	-	5.8	3.4	2.9	1.9

must not be exceeded if workability (mixing) of a soil-fiber composite is to be accomplished.

Three randomly selected fresh, undamaged fiber specimens of 15 dpf polypropylene monofilament, 360 dpf fibrillated polypropylene and 832 bb type E fiberglass were examined in a JEOL JSM-U3 Scanning Electron Microscope (SEM). In addition, three specimens of the same fiber types were randomly selected from a number recovered following unconfined compression testing of soil-fiber composite standard Proctor size specimens and also examined by SEM.

Comparison of the three types of fiber before and after compacted incorporation in the loess soil revealed several conditions. Both the monofilament and fibrillated polypropylene fibers showed fairly smooth surfaces prior to incorporation in the soil. Type E fiberglass was observed to be

composed of a bundle of smooth, very small diameter strands. Manufacturer's information indicated that both fiberglass and polypropylene fibers were nearly chemically inert. Since the fibers exhibited no signs of chemical alteration after incorporation in the soil, it must be assumed that any bonding occurring between the fibers and soil was primarily frictional in mechanism.

The 15 dpf fiber exhibited severe surficial damage after compaction and testing in the soil, probably as a result of soil particles scratching and indenting the surface. The fibrillated polypropylene also incurred surface damage, though not as extensive as the smaller diameter polypropylene. The harder fiberglass fiber did not appear to be damaged after incorporation, compaction, and UCS testing in the loess soil. The more extensive surficial damage to the 15 dpf polypropylene fiber tends to support its reinforcing performance as evidenced through potentially greater frictional contact with the soil particles. Such mechanism might be enhanced even further by the crimped 15 dpf polypropylene fiber, whose geometric configuration would (1) allow for tight soil particle to fiber packing, as well as (2) filling the void spaces as indicated by its lower composite void ratios.

A fiber-pull-out test was devised to measure the average frictional strength of the soil-fiber bond under varying soil stress conditions. A direct shear mold was modified by cutting a small keyway between the top and bottom half of the mold. This allowed for a measured length of fiber to be horizontally embedded in the soil within the mold, yet adequately protrude so that a tensile force could be applied to pull the fiber from the soil. The known volume of the mold was filled with a measured amount

of soil near optimum moisture content, then compacted to attain 95 percent maximum standard T-99 density. The soil was vertically loaded to varying stress states, each state of stress being allowed to equalize for 5 minutes. The exposed length of fiber was passed over a pulley and attached to a plastic container, which was slowly siphon filled with water until the fiber pulled out or broke. At that instant, water flow was halted, and the container plus water was weighed to determine the force required to pull out or break the fiber for each state of vertical stress on the soil specimen.

The 15 dpf polypropylene monofilament and the 360 dpf fibrillated polypropylene fibers were used with borrow pit loess for this testing. Both fibers were obtained in tow (spool) form for use in this test in order to obtain adequate exposed length for attachment to the plastic container. The average frictional bond strength τ_{avg}, was calculated as the force required to pull out, or break the fiber, divided by the surface area of fiber exposed to the soil, neglecting end area.

The fibrillated tape posed unique problems in performing this test due to its rectangular like cross section. Some tests were conducted with the long side of the rectangle vertically oriented. These tests resulted in lower values of frictional bond strength than when the fiber was oriented with the long dimension horizontal. For ease of testing and comparison, all remaining tests were conducted with the crosssection oriented horizontally. Also, the fibrillated fiber occasionally split apart, slightly increasing the exposed surface area over that of the monofilament fiber that did not split. Regardless of these conditions, the manufacturers equivalent diameter was used to calculate embedded surface area of each fiber.

The 15 dpf polypropylene monofilament also posed a problem in that the exposed fiber tended to easily break. However, as the embedded part of the fiber resisted pull-out up to the break load, the bond strength was apparently equal to or greater than the break force. Therefore, for any tests where fibers broke, that force divided by the fiber surface area was considered the bond strength. Though the embedded length of the 15 dpf fiber was reduced from 2 to 0.75 inches, the exposed fiber continued to break when vertical soil pressures were equal to or greater than 30 psi.

Although the test procedure was subject to experimental errors, several repetitions yielded comparative results for various vertical stress levels on the soil, Table 26.

Table 26. Average soil-fiber frictional bond strength

Vertical Stress, psi	τ_{avg} 15 dpf polypropylene monofilament, psi	τ_{avg} 360 dpf fibrillated polypropylene, psi
0.11	10.1 ± 1.4	17.9 ± 2.6
0.95	10.0 ± 0.9	17.9 ± 0.9
5	11.9 ± 1.5	16.3 ± 0.9
10	14.6 ± 1.0	20.1 ± 2.4
20	19.9 ± 2.8	35.0 ± 3.5
30	20.4 ± 2.6[a]	- -
50	24.5 ± 2.1[a]	62.3 ± 1.1
63.4	- -	94.6 ± 3.2
75	30.3 ± 3.1[a]	84.5 ± 15.4[a]

[a]All fibers broke during tests at this level of soil stress and length of embedded fiber.

Results of Table 26 present a logical trend. After vertical loading was applied, 5 minutes elapsed for stresses in the soil to equilibrate, during which time the loading cap was observed to lower, indicating soil specimen consolidation. This confined consolidation means that the void ratio of the soil decreased, and in turn, potentially increased the number of points of contact between soil and fiber. This would result in higher normal forces at all points of contact, providing for stronger frictional bond between the soil and fiber. The amount of consolidation was not measured as the configuration of the test apparatus prohibited monitoring vertical strain.

The data of Table 26 was applied within equation 8 adapted from Agarwal and Broutmann (1) for determination of critical load transfer length of short fibers: $\ell_c = \frac{(\sigma_f)_{ult} d}{2\tau_{avg}}$ where ℓ_c = critical fiber length, $\sigma_{f_{ult}}$ = maximum fiber stress, d = fiber diameter, and τ_{avg} = average frictional bond strength. Results of the determination of ℓ_c are presented in Table 27.

Table 27. Critical fiber length for various soil stress conditions

	15 dpf		360 dpf	
Vertical Soil Stress, psi	$\tau_{avg.}$, psi	ℓc, inches	$\tau_{avg.}$, psi	ℓc, inches
0.11	10.1	6.3	17.9	16.1
0.95	10.0	6.4	17.9	16.1
5	11.9	5.4	16.3	17.7
10	14.6	4.4	20.1	14.4
20	19.9	3.2	35.0	8.2
30	20.4	3.1	-	-
50	24.5	2.6	62.3	4.6
63.3	-	-	94.6	3.0
75	30.3	2.1	84.5	3.4

The results of Table 27 demonstrate that as soil-fiber bond is increased, the length of fiber required to effectively transfer matrix stress to the fibers ultimate stress capacity tends to decrease. Since fiber lengths used in this study were less than the ℓc's calculated above, the soil-fiber composite should not fail by fiber fracture, but by sliding along the soil-fiber interface. Examination of soil-fiber composite specimens following maximum unconfined compressive loadings supported this mode of failure, and indicated that the frictional soil-fiber bond force was adequate to impart increases in composite strength properties discussed previously. In addition, this mode of failure may potentially explain the previously observed ductility (toughness) of the soil-fiber composites.

Trafficability Test

The trafficability test utilized replicate Marshall size specimens (4.00 in. diameter by 2.75 in. height), subjected to simulated conditions of repetitive traffic loading and adverse environment. The trafficability apparatus consists of a rigid steel frame with electric powered travelling carriage moving longitudinally along the frame. Within the carriage, an 8 inch diameter by 1 1/4 inch wide solid rubber tired wheel is positioned to roll along a wheel track containing six specimens still within their respective molds. Contact pressure of the wheel is adjusted through a vertical pneumatic cylinder to which the wheel is attached. The cylinder also serves to automatically lift the wheel at the end of each loading pass. A water spray device is attached to the carriage, providing the capability of rain simulation either during, or without traffic loading.

Quantitative data consisted of measuring wheel path rut depth to the nearest 0.001 inch, at intervals of wheel load repetitions. The difference between the average of triplicate wheel path readings prior to and following load repetitions provided the quantity of rut depth, failure being defined as equal to 0.5 inch. The following test procedure was used at 75 psi wheel contact pressure for all specimens:

1. 1000 passes without rain.
2. 1000 passes with a simulated rain of about 0.15 in/hr.
3. Two hour fogging period consisting of a fine water mist.
4. 1000 passes with a simulated rain of about 0.15 in/hr. Rut depth measurements at prescribed intervals or until achievement of 0.5 in. rut depth, whichever might first occur.

All specimens were molded at near their respective optimum moisture contents. All specimens were tested immediately following molding, with the exception of the Sioux City specimens containing 3 percent portland cement which were wrapped, sealed and moist cured for 7 days prior to testing.

Rut depth measurements presented in Figures 92 through 96 should be viewed from the mechanisms occurring during the testing process. Initially a densification and seating of each specimen within the holding ring occurred, but appeared to be dependent on both the matrix (soil or soil and cement) and fiber. For example, in Figure 92 a very small densification occurred within the Sioux City specimens containing cement during the first 50 cycles, and remained constant throughout the first 1000 cycles. The

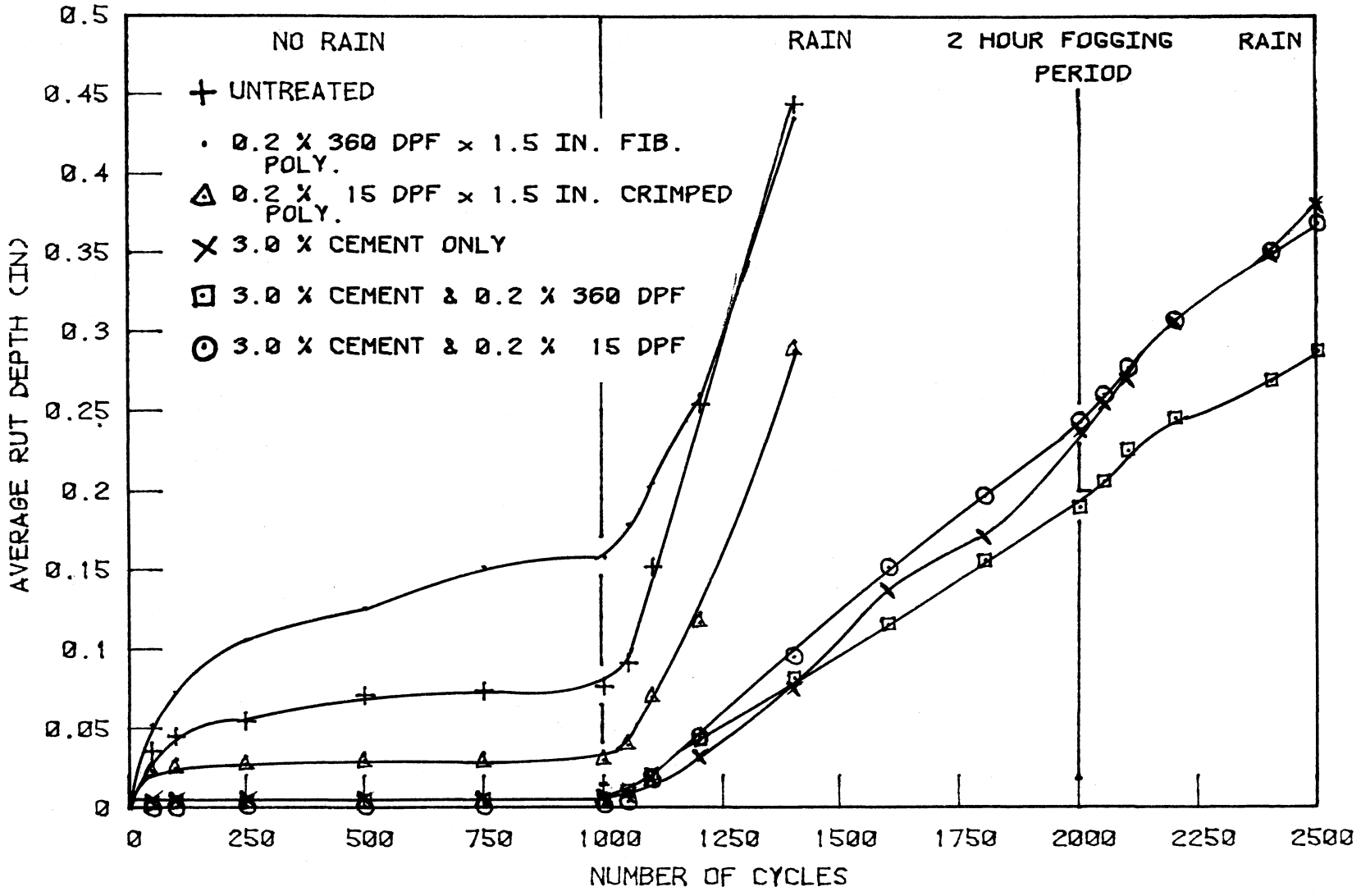

Figure 92. Traffic simulator results, Sioux City barrow soil.

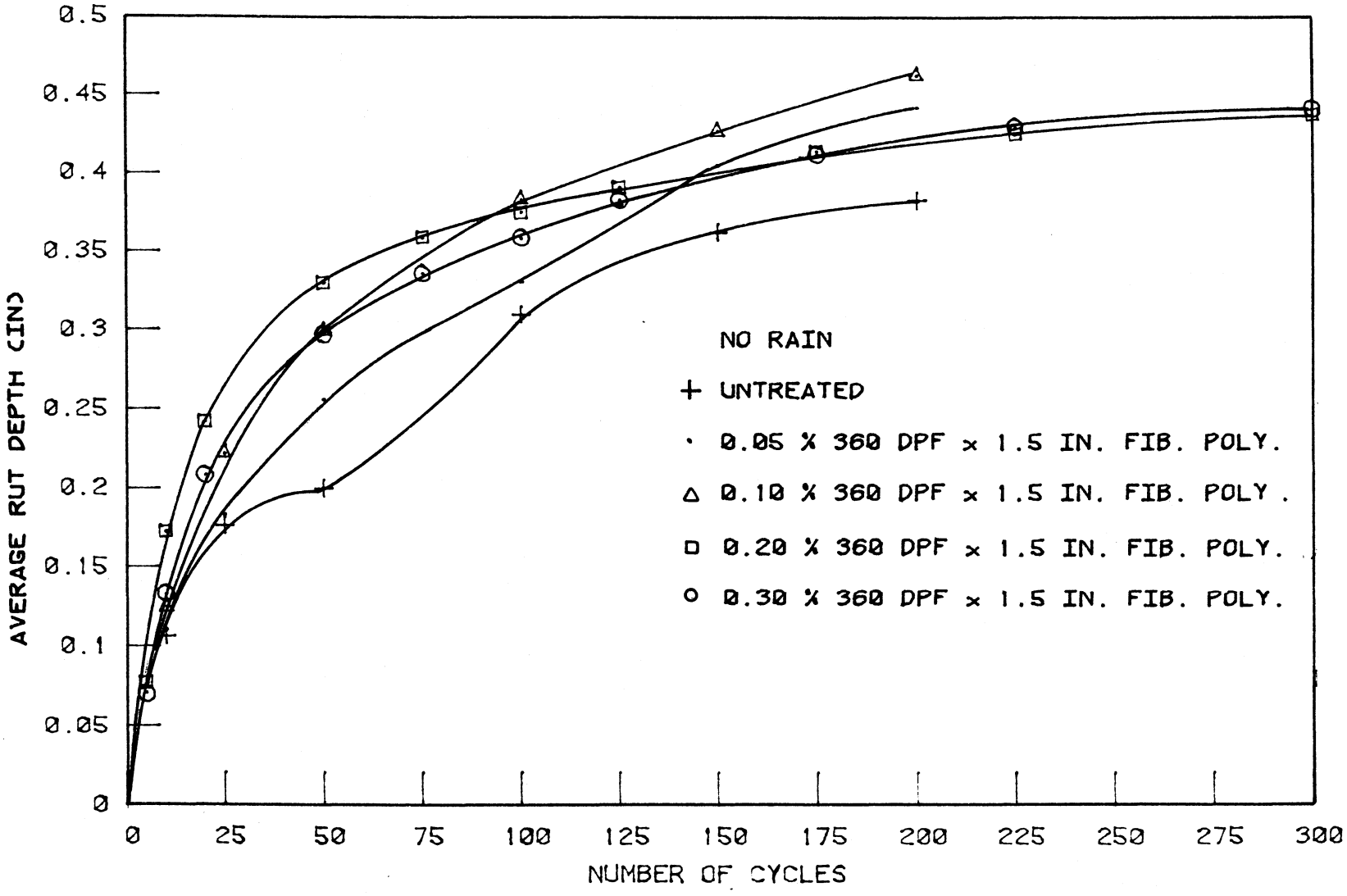

Figure 93. Traffic simulator results, Story County Mortenson Road soil.

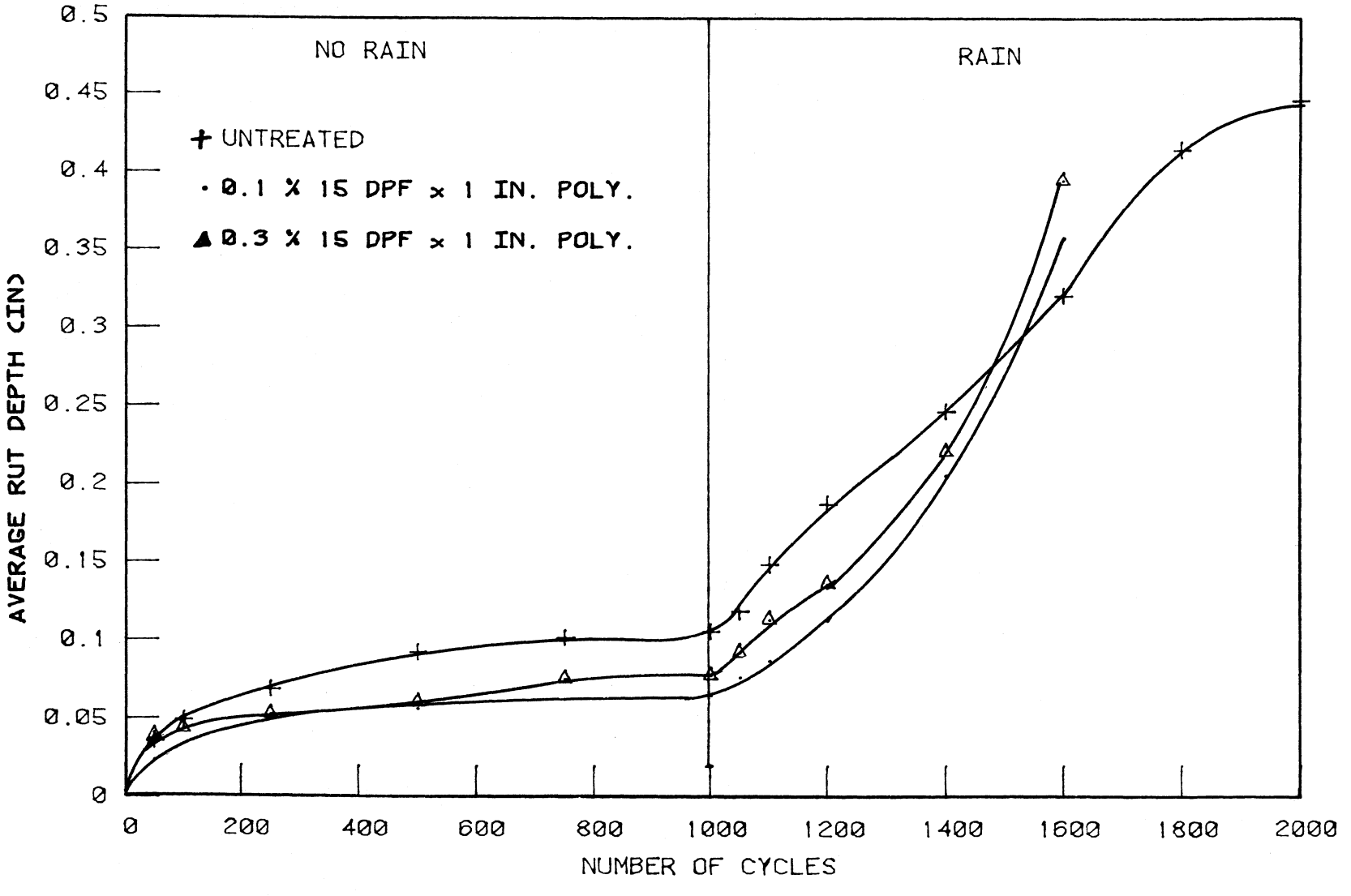

Figure 94. Traffic simulator results, Linn County Prairieburg soil.

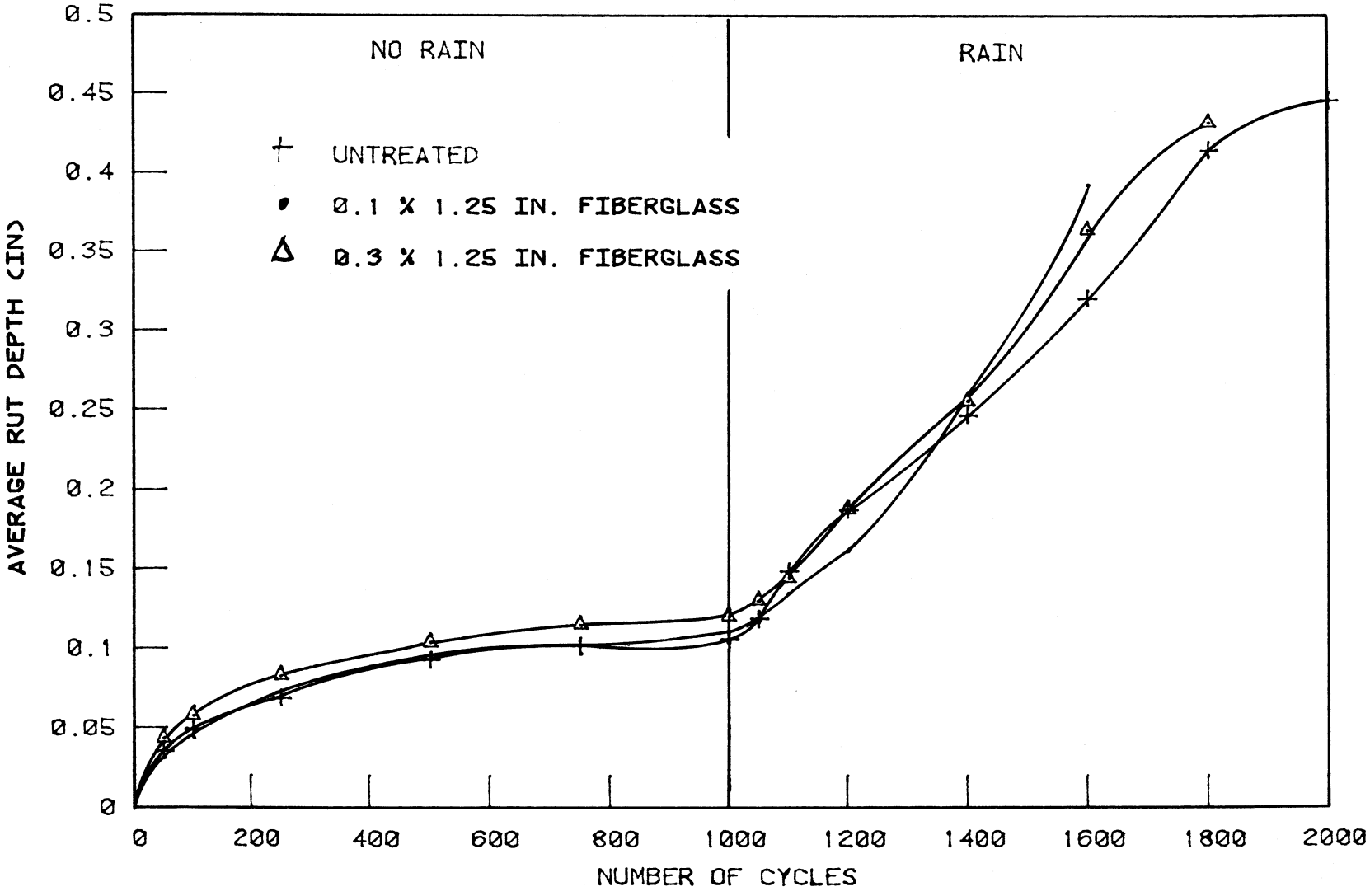

Figure 95. Traffic simulator results, Linn County Prairieburg soil.

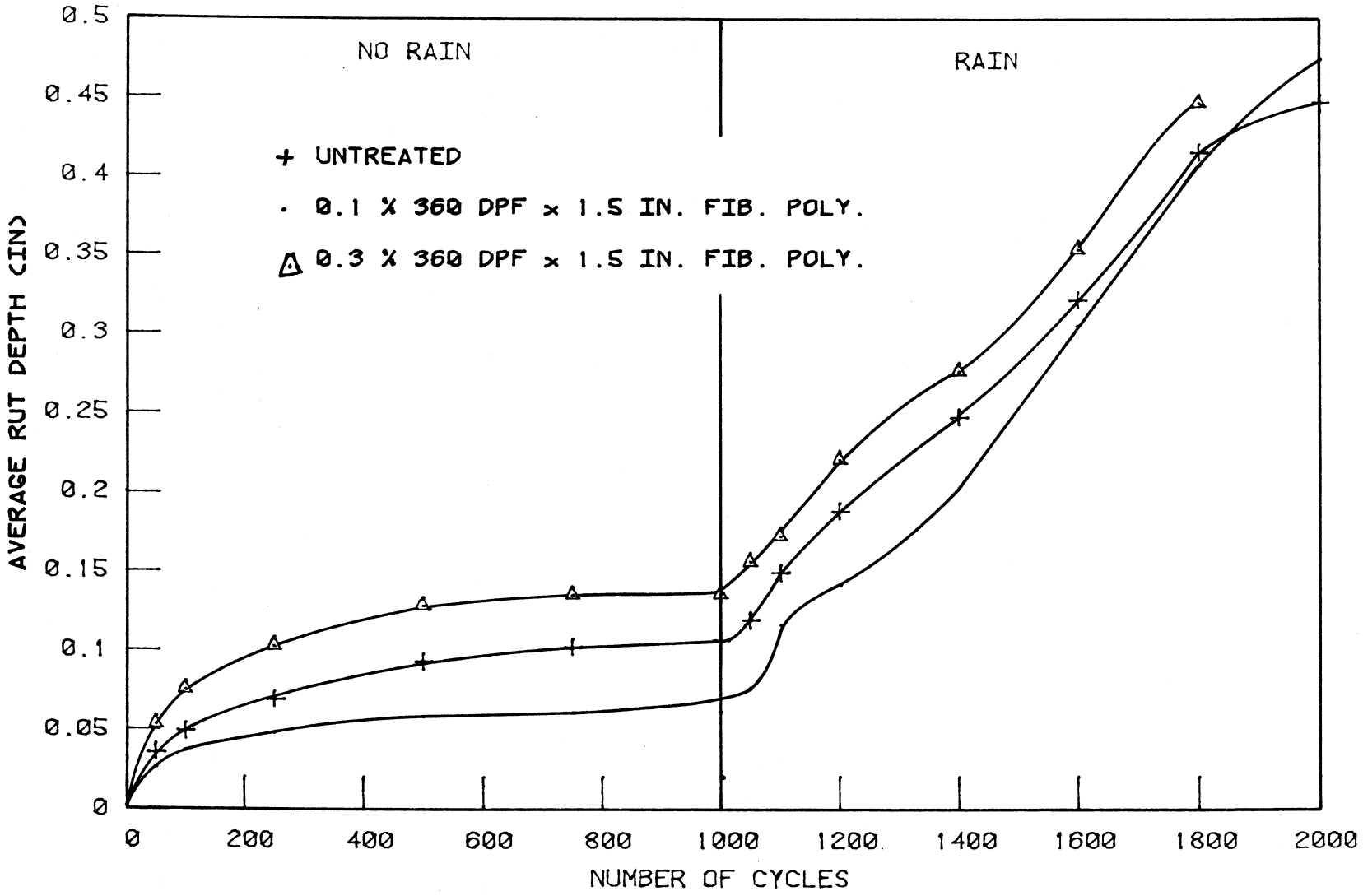

Figure 96. Traffic simulator results, Linn County Prairieburg soil.

crimped fiber produced somewhat larger rut depth at 50 cycles but again remained constant at about 0.025 inch for the remainder of 1000 cycles. The untreated soil rapidly densified during the first 100 cycles to about 0.05 in. depth, then slowly continued densification to about 0.06 in depth at 1000 cycles. The 360 dpf fibrillated specimens showed a greater densification than the untreated which continued to 0.15 in. rut depth at 1000 cycles.

Substantial densification during the first 300 cycles was observed through average rut depth with the Mortenson Road specimens, Figure 93. Fiber contents from 0.05 to 0.3% produced no basic change in rutting and were slightly higher in average rut depth than the untreated soil.

During the first 1000 cycles, the 0.1 and 0.3% 15 dpf x 1 inch straight and 0.1% 360 dpf x 1.5 inch fibrillated polypropylene fibers produced some reduction in rutting densification with the Linn County Prairieburg soil, Figures 94 and 96. Regardless of content, the 1.25 inch Type E fiberglass produced no basic variation in rut depth, Figure 95.

During the initial period of rain, 1000 to 2000 cycles, there is a near immediate "tracking out" of any unbound fines. As a distinct rut is formed, water puddles in the wheel path, resulting in further flushing and tracking-out of fines, a process which occurs to lesser degrees with effectively stabilized soil matrixes as compared to untreated. This process may continue at varying rates until the wheel path surface appears composed of coarse particles with fines removed (most evident in untreated or unstable specimens), or where fibers are exposed among coarse particles though portions may still be embedded within the yet stable finer matrix. During the period of rain, unstable materials may also produce one or more

forms of shear failure. Initially, a general bulging and upheaval along the wheel path edges, indicative of plastic flow or local shearing; a process which may continue to progress to development of full shear away from the wheel path at or into the wall of the holding mold. This latter development may produce failure surfaces similar to those of the classic Prandtl-Terzaghi bearing capacity failure geometry due to reduction of c-ϕ characteristics by intruding water.

Each of the untreated Sioux City and Prairieburg soils produced all actions noted in the preceeding paragraph during the period of rain, including bulging, upheaval and shear failure. Sioux City specimens containing cement and cement plus fiber produced an increased quantity of rut depth, Figure 92, through 2500 cycles, but showed only limited signs of bulging and no signs of shear failure. The 360 dpf fibrillated polypropylene and Sioux City soil composite without cement treatment, showed definite signs of bulging, upheaval and shear failure up to less than 1500 cycles while the 0.2% crimped fiber composite remained much more stable.

Between 1000 and 2000 cycles, rut depths of the Prairieburg fiber treated specimens tended to react similarly to the untreated soil, Figures 94, 95, and 96. In general bulging was not as great with fiber treatment as with the untreated. However, during this period of rain, little variation of tracking-out of fines was visible between the untreated and fiber treated specimens, though the latter showed loose unbonded fiber ends in the wheel path. Between 1000 and 1400 cycles the 15 dpf x 1 inch straight polypropylene exhibited somewhat less average rut depth than the untreated, Figure 94. At about 1500 cycles, a definite debonding appeared to develop,

and was accompanied with some shear failure to the point at which testing was halted at 1600 cycles.

As illustrated in the preceeding discussion, the trafficability test provided some quantitative measurements of the effect of fibers in the three soil matrices, as well as qualitative indications of the composite materials stability under a heavy moving load and the imposed environmental conditions. Both the measurements and observations indicate that the untreated soils are incapable of sustained traffic support at the level of loading and environmental conditions imposed when utilized as surface course. Under identical test conditions however, the 15 dpf x 1.5 in. crimped polypropylene fiber provided improved vertical load stability for the Sioux City soil, and the 15 dpf x 1 in. straight polypropylene provided some sustained stability for a greater number of cycles with the Linn County Prairieburg soil. Inclusion of each of the above fibers prevented lateral shear and/or displacement for a greater number of cycles than their untreated counterparts, not unlike the lateral actions described under the cyclic load tests. Further improvement of stability under the traffic simulation test was provided by modification of the soil matrix through addition of cement, once again noting the interrelatonship of soil matrix and fiber interfacial bonding.

Tensile Test

Methods for evaluating the tensile strength of materials may be conducted by applying direct tensile force to a specimen, or through indirect

techniques such as flexure of a beam or splitting a cylindrical specimen by applying opposing strip loads along the sides of a test cylinder. The direct test is difficult to perform because of undesirable stress concentrations which occur at the point of applied loading. The flexural test was deemed undesirable because of difficulties associated with molding beam specimens, particularly inconsistencies in reproducing proper densification. Thus it was decided that a trial study of tensile properties of fibrous reinforced soil be measured using the splitting technique on Proctor sized specimens, compacted under AASHTO T-99 energy, and evaluated through the following relation for tensile stress.

$$S_t = \frac{2\ P_{max}}{\pi\ L\ d}$$

where S_t = tensile stress, P_{max} = the load at failure, L = specimen length, and d = specimen diameter. Results of a series of tests on the Prairieburg A-4(0) and Mortenson Road A-6(3) soils are presented in Figures 97 through 99. At a constant 0.4 percent fiber content, tensile strength increased independent of fiber type or moisture content with the Prairieburg soil, Figure 97. The Mortenson Road soil showed slight improvement with the 360 dpf polypropylene only at higher moisture contents, Figure 99.

When fiber content was varied in the Prairieburg soil at a constant moisture content near optimum, Figure 98, a difference in fiber type and diameter was particularly noticeable at fiber weight fractions below the 0.3 percent level; the small diameter, 15 dpf polypropylene caused the most improvement at about 0.2 percent concentration. Similar results were obtained for the Mortenson Road soil with varying amounts of 360 dpf polypropylene. However, tensile strength increase was only slight, but did occur at fiber contents as low as 0.05%.

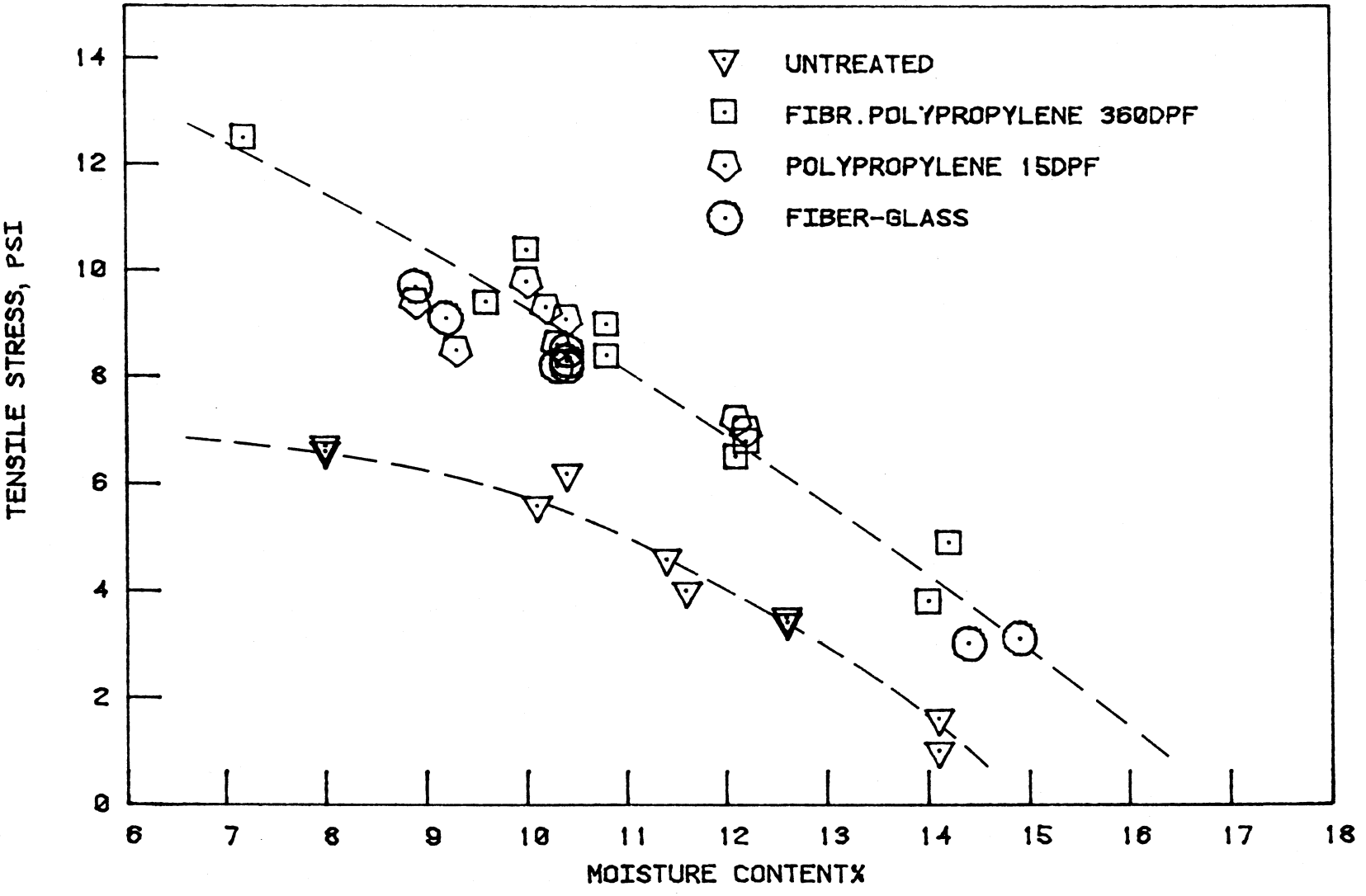

Figure 97. Tensile stress versus moisture content at a constant 0.4% fiber weight fraction, Linn County Prairieburg soil.

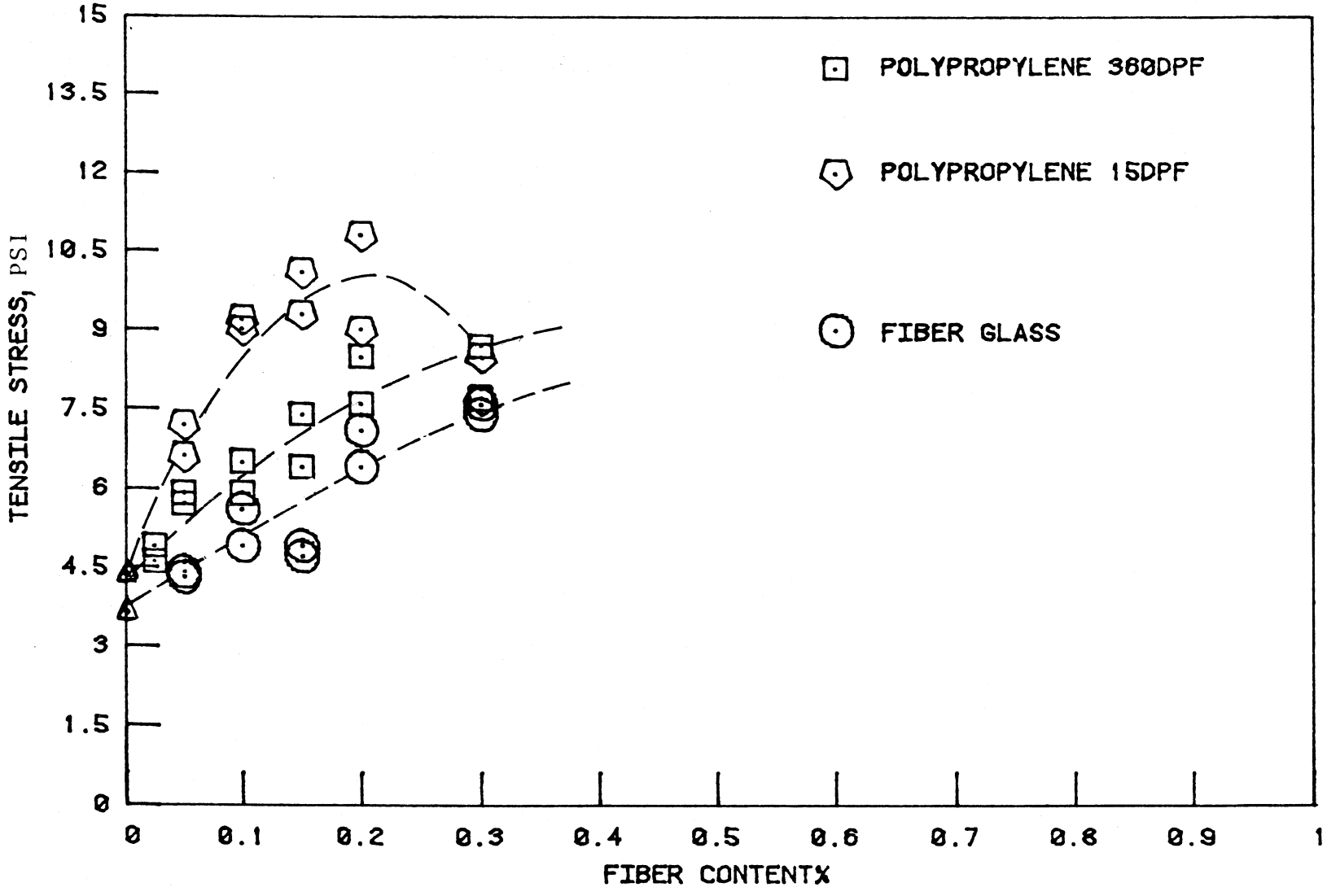

Figure 98. Tensile stress versus fiber content, Linn County Prairieburg soil.

Results of this study illustrate that improved tensile properties may be attained with a soil due to the introduction of randomly oriented fibers but appear dependent on soil and fiber types, and the accompanying interfacial bond. In addition, tensile properties of a soil-fiber composite may be improved at moisture contents above the untreated optimum.

FIELD INVESTIGATIONS

Field Test Sections

During the fall of 1980, seven test sections were constructed in Linn and Story Counties using three types of fibers showing some potential from the laboratory compression testing evaluation. Test section description is contained in Table 28.

Linn County (Prairieburg) construction

This first attempt of field application illustrated that the main difficulty associated with practical application of fibers was dispersal at the site. Mixing did not appear to be a problem. The initial plan for the six Linn County Sections was to air inject the fiber into the shroud of a rotary mixer, but finding a suitable air delivery system proved to be a problem. Both a 2 inch diameter commercial insulation blower, and a fabricated 4 inch diameter blower proved useless because of clogging in the ports and tubing. However, a commercial mulch spreader owned by Linn County provided adequate capacity, and the simple addition of an eight inch diameter flexible tube to the discharge spout offered a unit which could amply deliver as well as separate the boxed and compressed fibers. This technique was used during the initial phase of construction, but breakdown of the rotary mixer and the nonavailability of parts, or a

Table 28. Test section descriptions.

Test Section	Fiber Type	Section Length (ft.)	AASHTO Classification	Applied Fiber Content[a]	Distribution Method
Linn County (Prairieburg)					
1	15 dpf x 1 in. Polypropylene	200	A-4(0)	0.06	Pneumatic
2	15 dpf x 1 in. Polypropylene	200	A-4(0)	0.13	Pneumatic
3	Type E Fiberglass 1.25 in.	200	A-4(0)	0.1	Pneumatic
4	Type E Fiberglass 1.25 in.	200	A-4(0)	0.29	Pneumatic
5	360 dpf x 1.5 in. Fibrillated Polypropylene	200	A-4(0)	0.29	Hand Distribution
6	360 dpf x 1.5 in. Fibrillated Polypropylene	200	A-4(0)	0.10	Hand Distribution
Story County Mortenson Road	360 dpf x 1.5 in. Fibrillated Polypropylene	630[b]	A-6(3)[b]	0.05	Hand Distribution

[a]Percent by dry weight of soil, computed as weight of number of boxes of fiber within 6 inch depth and 28 ft width.

[b]Soil was found to vary over the length of test section. This classification was determined from a composite sample.

replacement mixer, resulted in blowing the fiber on the 6 inch depth scarified roadway, mixing with a blade grader, and compaction with a rubber tired roller. A crushed rock surface was applied to all sections.

Story County (Mortenson Road) construction

Available equipment included a rotary mixer, rubber tired and sheepsfoot rollers, and a motor grader. Since a machine suitable for pneumatic distribution was not available, this phase of the operation was performed by hand spreading of the fiber following preparation of the 6 inch depth of roadway soil. The clayey nature of the bulk of the roadway soil made it necessary to devote considerable effort to preparation or break-up of clods in major portions of the test section; the construction operation revealing that two and possibly three changes of soils may have been represented on the site, depending upon topography. For performance evaluation, the 630 ft. section was sampled and tested at six locations, all test data generally being averaged. A single seal coat wearing surface was applied to this section and its comparison controls.

Field Tests and Observations

In-Situ Moisture-Density

Measurements taken, and sampling performed at time of construction, included moisture content prior to mixing, moisture content and density after compaction, depth of fiber distribution, and samples of the fiber/soil composite prior to compaction. The objective was to achieve a six-inch lift of treated material compacted to 95 percent of standard AASHTO density, and near optimum moisture content. Field density measurements were made

with a nuclear gage. To avoid error in the nuclear moisture measurements, potentially caused by hydrocarbons in some of the fibers, a speedy moisture tester was also used to minotor moisture content.

In situ compaction achieved during construction was compared to samples of the soil-fiber composite collected at the site then later subjected to the standard AASHTO laboratory compaction test. For example, the following means and standard deviations were measured for the Mortenson Road section:

Field moisture content - 12.2 $\pm$ 1.5 percent

Field density - 105.8 $\pm$ 5.7 pcf

Laboratory density - 104.6 $\pm$ 7.1 pcf

An 11.5 percent laboratory optimum moisture content for the treated Mortenson Road soil-fiber composite indicated that construction moisture conditions were slightly wet, while the similarity in field and laboratory densities suggested that a reasonable degree of compaction of the soil fiber composites could readily be achieved with conventional equipment. Similar comparative achievements in density were attained in the Linn County Prairieburg sections at time of construction.

Table 29 illustrates the mean and one standard deviation of in-situ moisture-density tests of the Mortenson Road sections as obtained during 1981. As noted above, at time of construction, field densities were above 100% of laboratory standard AASHTO T-99 compaction of 104.6 pcf. Densities of the succeeding series of tests indicated increases of 10 pcf or greater as compared to either the initial field compaction and/or standard laboratory density of the fiber treated soil. Moisture contents of the fiber base were reduced about 2.0% from time of construction to the spring 1981 tests,

Table 29. Mean of in situ moisture density tests, Story County, Mortenson Road

Section	Date	Dry Density, γ_d, pcf	Moisture Content w, %
Control:			
Base equivalent	May, 1981	116.7 ± 6.7	12.5 ± 2.0
Subgrade	May, 1981	119.3 ± 3.2	12.1 ± 1.5
Treated:			
Fiber base	May, 1981	116.2 ± 2.5	10.3 ± 2.0
Subgrade	May, 1981	115.6 ± 4.5	10.4 ± 2.2
Control:			
Base	July, 1981	114.5 ± 4.9	9.4 ± 1.6
Subgrade	July, 1981	119.5 ± 1.9	8.6 ± 1.5
Treated:			
Fiber base	July, 1981	119.5 ± 9.4	9.6 ± 2.4
Subgrade	July, 1981	123.7 ± 7.3	9.3 ± 2.0
Control:			
Base	October, 1981	117.7 ± 5.8	9.8 ± 1.3
Subgrade	October, 1981	118.3 ± 7.5	9.8 ± 1.3
Treated:			
Fiber base	October, 1981	117.8 ± 6.3	8.8 ± 2.6
Subgrade	October, 1981	118.1 ± 6.8	8.7 ± 2.4

[a]Values of γ_d and w represent the mean and one standard deviation. Number of data points for each value range from 7 to 27.

with less than two percent further reduction to late fall. Normally it would be anticipated that spring moisture contents would increase from the preceeding late fall conditions, followed by reductions of moisture during the late spring and early summer. Such conditions are not apparent in the data, and may be attributable to the below normal moisture conditions which prevailed in this region during 1980-81.

Table 30 presents the mean and one standard deviation of in-situ moisture-density tests of the Linn County Prairieburg sections from time of construction through late fall 1981. Tests were conducted in such a manner as to provide data within the granular surfacing, each fiber treated base, and the top of the subgrade. Part of the reasoning for such a format of M-D testing was due to (1) the fact that the test sections were incorporated as a portion of a new grade, the latter having been completed only a few weeks prior to construction of the fiber treated sections, and (2) most new construction will tend to consolidate and densify over a period of time. The data of Table 30 indicates the occurrence of such physical actions. Subgrade densities at time of construction averaged about 126 pcf, increasing to about 134 during the late spring and summer but decreasing slightly to about 133, Fall 1981. Average fiber treated base densities were about 123 pcf immediately following construction, increasing to about 134 pcf in early June, then decreasing about 2 pcf to 132 pcf in July through October. Granular surface densities averaged about 122 pcf at time of construction, then jumped to about 136 pcf in early June, decreasing to about 129 pcf in July and increasing to about 131 pcf in October. Average moisture contents of the subgrades, fiber incorporated bases, and

Table 30. In-situ moisture-density tests,* Linn County, Prairieburg.

Section	October 1980		June 1981		July 1981		October 1981	
	Dry Density γ_d, pcf	Moisture Content,w %	Dry Density, γ_d, pcf	Moisture Content,w %	Dry Density, γ_d, pcf	Moisture Content,w %	Dry Density, γ_d, pcf	Moisture Content,w %
Control: Granular surface	123.8±4.8	6.8±1.0	136.0±3.8	7.1±1.9	130.2±2.4	5.4±0.6	135.4±5.6	4.7±0.8
Base equivalent	128.3±5.0	6.5±0.8	133.9±4.5	7.4±1.8	136.3±1.3	5.0±0.5	136.3±5.0	4.4±0.6
Subgrade	131.3±4.4	6.3±0.6	133.0±4.3	7.4±1.9	137.1±2.3	4.9±0.7	135.9±3.6	4.5±0.7
Section 1: Granular surface	122.4±2.8	6.9±1.0	136.2±0.2	8.9±0.7	131.8±2.0	6.0±0.9	131.0±6.1	4.4±0.4
Base, 0.06% 15 dpf x 1.0 in. Poly.	123.9±2.7	6.6±0.8	135.8±1.7	8.8±0.8	135.3±2.3	5.7±0.7	134.5±2.0	4.1±0.2
Subgrade	125.5±4.1	6.5±0.8	135.2±2.6	9.0±0.7	136.4±0.8	5.4±0.7	136.4±0.7	4.1±0.3
Section 2: Granular surface	118.0±1.6	6.5±0.5	133.1±5.2	6.0±0.5	127.0±4.5	6.1±0.6	124.6±1.1	5.8±0.4
Base, 0.13% 15 dpf x 1.0 in. Poly.	120.4±2.8	6.4±0.5	128.0±2.7	6.3±0.2	127.8±4.7	5.8±0.7	125.9±1.7	5.3±0.2
Subgrade	125.6±2.9	6.0±0.4	129.6±4.9	6.2±0.2	127.7±1.4	5.8±0.4	127.8±1.8	5.4±0.2
Section 3: Granular surface	122.3±2.2	5.8±1.2	140.4±1.3	5.4±0.8	128.1±1.7	5.4±0.6	130.2±2.3	5.2±1.1
Base, 0.10% 1.25 in Type E Fiberglass	124.0±2.5	5.7±0.9	136.8±1.1	5.8±0.4	133.1±2.9	4.9±0.7	132.9±2.1	5.0±1.0
Subgrade	124.8±4.7	5.9±0.7	136.3±1.3	5.6±0.2	137.0±3.1	4.8±0.7	131.2±0.6	5.0±1.1
Section 4: Granular surface	125.9±0.6	6.3±2.8	138.0±0.7	6.2±0.2	125.3±0.7	6.2±1.0	131.2±0.6	4.6±0.4
Base, 0.29% 1.25 in Type E Fiberglass	125.3±2.6	6.1±2.2	137.6±1.0	5.8±0.2	130.7±1.6	5.8±0.8	133.3±3.4	4.6±0.5

Subgrade	126.0±3.0	6.2±2.5	139.2±1.8	5.6±0.6	131.9±1.6	5.4±0.6	133.2±3.5	4.7±0.5
Section 5: Granular surface	117.3±4.7	7.4±2.3	133.3±6.5	6.8±0.1	128.2±0.6	6.2±0.8	131.4±3.1	4.8±0.8
Base, 0.29% 360 dpf x 1.5 in Fib. Poly.	121.3±1.9	6.9±1.9	133.3±2.5	6.8±0.2	130.9±0.8	6.2±0.4	132.1±0.4	4.6±0.6
Subgrade	124.4±3.7	6.6±1.7	132.4±0.8	6.8±0.3	132.0±1.6	5.9±0.3	131.4±1.7	4.6±0.8
Section 6: Granular surface	124.2±3.6	6.6±1.0	135.1±2.8	6.8±0.2	130.5±0.1	6.4±0.1	132.0±5.4	4.9±0.1
Base, 0.10% 360 dpf x 1.5 in Fib. Poly.	123.7±3.2	6.7±0.8	135.7±1.5	6.5±0.6	134.0±0.9	5.9±0.1	136.2±0.7	4.6±0.2
Subgrade	127.9±1.4	6.2±0.9	135.8±1.1	6.7±0.4	133.9±0.7	5.9±0.7	136.5±0.4	4.6±0.2

*Values of γ_d and w represent the mean and standard deviation. Number of data points for each value range from 2 to 12.

granular surface remained relatively constant over the measurement periods though slight reductions are apparent for the October tests. The slight decline of average density of the fiber bases, coupled with a rather significant decrease in average granular surfacing density may be indicative of (1) granular surface degradation, (2) intrusion and/or intermixing of surfacing and base materials, or (3) a combination thereof.

Table 30 also illustrates the variability of densities between fibers, fiber contents, and the untreated control. Average density of the untreated base equivalent for the three series of tests is about 134 pcf. Similar averaging for the 15 dpf x 1.0 inch polypropylene (sections 1 and 2) illustrate about 132 pcf at 0.06% fiber, and 128 pcf at 0.13% fiber content. The 1.25 inch length Type E fiberglass produced average densities of about 131 pcf regardless of the fiber weight fractions of 0.10 and 0.29%, respectively sections 3 and 4. The 360 dpf x 1.5 inch length fibrillated polypropylene (sections 5 and 6) produced average densities of about 128 (0.29%) and 131 pcf (0.10%) respectively, i.e., very similar to those averages obtained with the 15 dpf x 1.0 inch polypropylene.

At least a portion of the above variability of densities appears associated with fiber diameter and weight. Diameter of the 15 dpf and 360 dpf polypropylene fibers are respectively about 0.002 and 0.009 inch, while the Type E fiberglass is about 0.008 inch diameter. As illustrated previously, the weight of each fiber type varies considerably. Thus the size and weight of each fiber produces a significant variation in numbers of fibers associated with each fiber weight fraction, or content, within the soil. As based on numbers of fibers, per gram weight of fiber type, the 360 dpf fibrillated polypropylene contains about twice as many fibers

per gram of fiber weight as does the fiberglass. The 15 dpf polypropylene produces about fifteen times the number of fibers per gram of fiber weight when compared to the fiberglass. Thus, as the number of individual fibers are increased within the soil-fiber matrix, the greater is the potential for reduced densities of the mixture with increasing fiber contents.

In-Situ Samples

During construction, samples of all field mixed materials were randomly obtained over the full depth of each fiber section following in-place mixing and immediately prior to compaction. These samples were returned to the laboratory where specimens were molded under AASHTO T-99 compaction at field moisture content, wrapped, sealed, and stored in the controlled temperature humid room. These specimens were utilized for unconfined compression testing and for cyclic load K-Test; the latter at 75 psi vertical pressure and 0.3 sec. dwell time as noted in the cyclic load test section of this report.

Table 31 presents the average unconfined compressive strength data from the field mixed Mortenson Road specimens, while Table 32 presents the mean and standard deviation of all unconfined compressive strength tests performed on the field mixed Prairieburg specimens. The maximum initial Young's modulus of Tables 31 and 32 represent E as observed within the initial straight line portion of the unconfined stress-strain curve. Unit strain at maximum unit stress represents the unit strain occurring at maximum q_u, and is indicative of the toughness of each mix as described in the laboratory section of this report. Since toughness is expressed

Table 31. Average unconfined compressive strength data of field mixed specimens, Story County Mortenson Road

Section	Dry Density γ_d, pcf	Moisture Content, w, %	Unconfined Compressive Strength, q_u, psi	Maximum Initial Young's Modulus, E, psi	Unit Strain at Max. Unit Stress, in/in
Untreated-Control	117.5	10.7	32.0	1260	0.028
0.05% Fib. Poly. Fiber	108.7	10.2	37.4	1428	0.046

Table 32. Median unconfined compressive strength data of field mixed specimens, Linn County, Prairieburg.

Section	Dry Density γ_d, pcf	Moisture Content, w, %	Unconfined Compressive Strength, q_u, psi	Maximum Initial Young's Modulus, E, psi	Unit Strain at max. Unit Stress, in/in
Untreated-near laboratory optimum moisture content	118.6 ± 0.6	11.8 ± 0.3	24.7 ± 2.1	532 ± 87	0.071 ± 0.008
Untreated - at field moisture content	117.4 ± 0.9	7.4 ± 0.4	49.6 ± 1.2	5949 ± 2936	0.014 ± 0.004
Section 1, 0.06% 15 dpf x 1.0 in. polypropylene	114.4 ± 0.8	6.3 ± 0.2	47.7 ± 8.2	1658 ± 104	0.034 ± 0.004
Section 2, 0.13% 15 dpf x 1.0 in. polypropylene	113.2 ± 1.1	7.2 ± 1.3	48.0 ± 7.8	1571 ± 287	0.037 ± 0.009
Section 3, 0.10%, 1.25 in. Type E Fiberglass	113.3 ± 0.4	5.6 ± 0.3	43.2 ± 3.5	3083 ± 1579	0.022 ± 0.009
Section 4, 0.29%, 1.25 in. Type E Fiberglass	113.3 ± 1.7	7.1 ± 0.9	42.8 ± 8.4	1927 ± 651	0.031 ± 0.008
Section 5, 0.29%, 360 dpf x 1.5 in. Fib. Poly.	117.2 ± 3.1	6.3 ± 2.0	56.9 ± 13.0	1050 ± 386	0.080 ± 0.025
Section 6, 0.10%, 360 dpf x 1.5 in. Fib. Poly.	117.1 ± 0.1	7.3 ± 1.0	49.9 ± 21.4	1150 ± 292	0.058 ± 0.011

in energy units $(\frac{\text{in-lb}}{\text{cu-in}})$, the modulus may crudely represent a capacity for resisting impact loading when determined from a gradually applied static loading, as in an unconfined compression test. Thus a fiber-soil mixture producing both higher q_u and unit strain at q_u than its untreated soil counterpart, would indicate a definite degree of improved toughness coupled with reduced brittleness.

Though field-mixed Mortenson Road fiber specimens were less dense than the untreated control, average q_u, unit strain at maximum unit stress, and E values were higher. Each would be indicative of somewhat improved stability through increased stress and elasto-plastic characteristics.

From Table 32 it may be seen that each of the Prairieburg fiber field mixes showed significantly improved q_u and E characteristics as compared to their laboratory untreated counterpart at optimum moisture content. However, it may also be ascertained from Table 32 that each of the fiber field mixes were several percentage points of moisture less than the lab untreated specimens. Comparison of the fiber field mixes with the untreated field mixed control, each at similar moisture contents, shows that the untreated produced a significantly higher initial E and lower unit strain at q_u than any of the fiber mixes; i.e., indicative of somewhat greater brittleness and rigidity. However, at field moisture content, the untreated showed little or no improvement of q_u from that of five of the six fiber sections, and was considerably less than the q_u obtained with 0.29% fiber weight fraction of 360 dpf fibrillated polypropylene. Unit strain at maximum unit stress of each fiber field mix was greater than the untreated. Thus each field mix appeared to show a greater degree of plastic toughness coupled with reduced brittleness than the untreated control.

Based on the properties noted in Table 32, it appeared that the fiberglass and 360 dpf fibrillated polypropylene may have produced the better stress-strain characteristics of the three fiber types used in the Prairieburg site; a condition not unlike that which will be noted within the in-situ tests reported in succeeding sections of this report.

Figure 100 illustrates actual average vertical unit strains for each fiber weight fraction and fiber type of the Prairieburg sections containing 15 dpf polypropylene fibers as obtained from cyclic load tests. Vertical unit strains were improved from those of the untreated at the higher content of 15 dpf fiber. A slight improvement was obtained with the lower content Type E fiberglass.

Incorporation of the 360 dpf fibrillated polypropylene fibers increased vertical strains regardless of fiber content. Average deformations at 75 psi under in-situ plate bearing test data, indicated a few similarities to the reduction of vertical unit strain in the cyclic load tests.

As anticipated, permanent set of the Prairieburg composites followed the same trends as illustrated with vertical unit strain, Figure 101. Fiber types and optimum fiber weight fractions showing maximum reduction of permanent set were identical to those noted under vertical strain. Comparison of average permanent deformations during in-situ plate tests showed some similarities to the reduction of permanent set from the cyclic load tests.

Figure 102, illustrates the calculated values of strain modulus for the field mixed, laboratory molded, fiberglass specimens. Though strain modulus data appeared rather erratic, in broad generalities, a slight

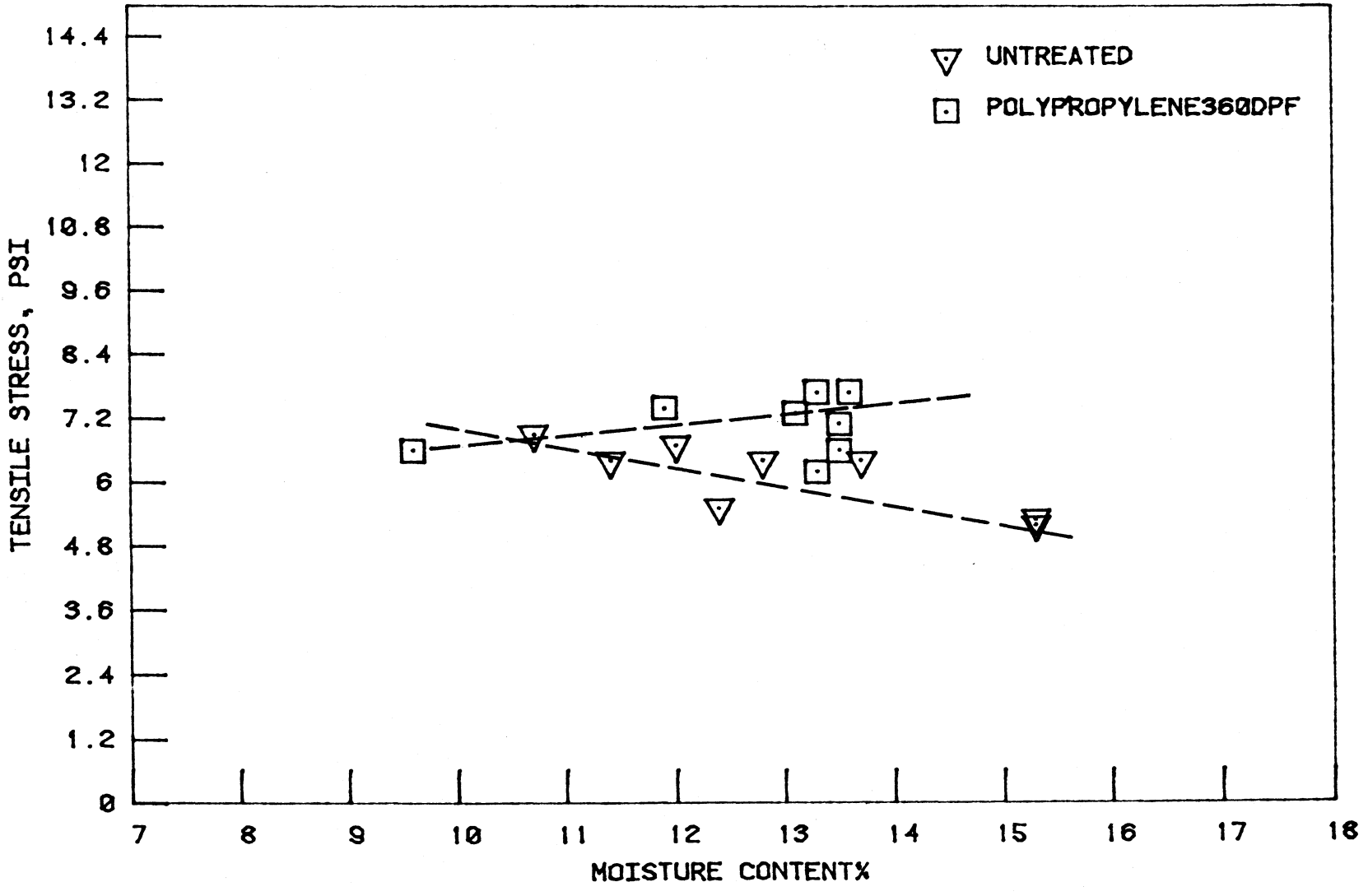

Figure 99. Tensile stress versus moisture content at a constant 0.2% fiber weight fraction, Story County Mortenson Road soil.

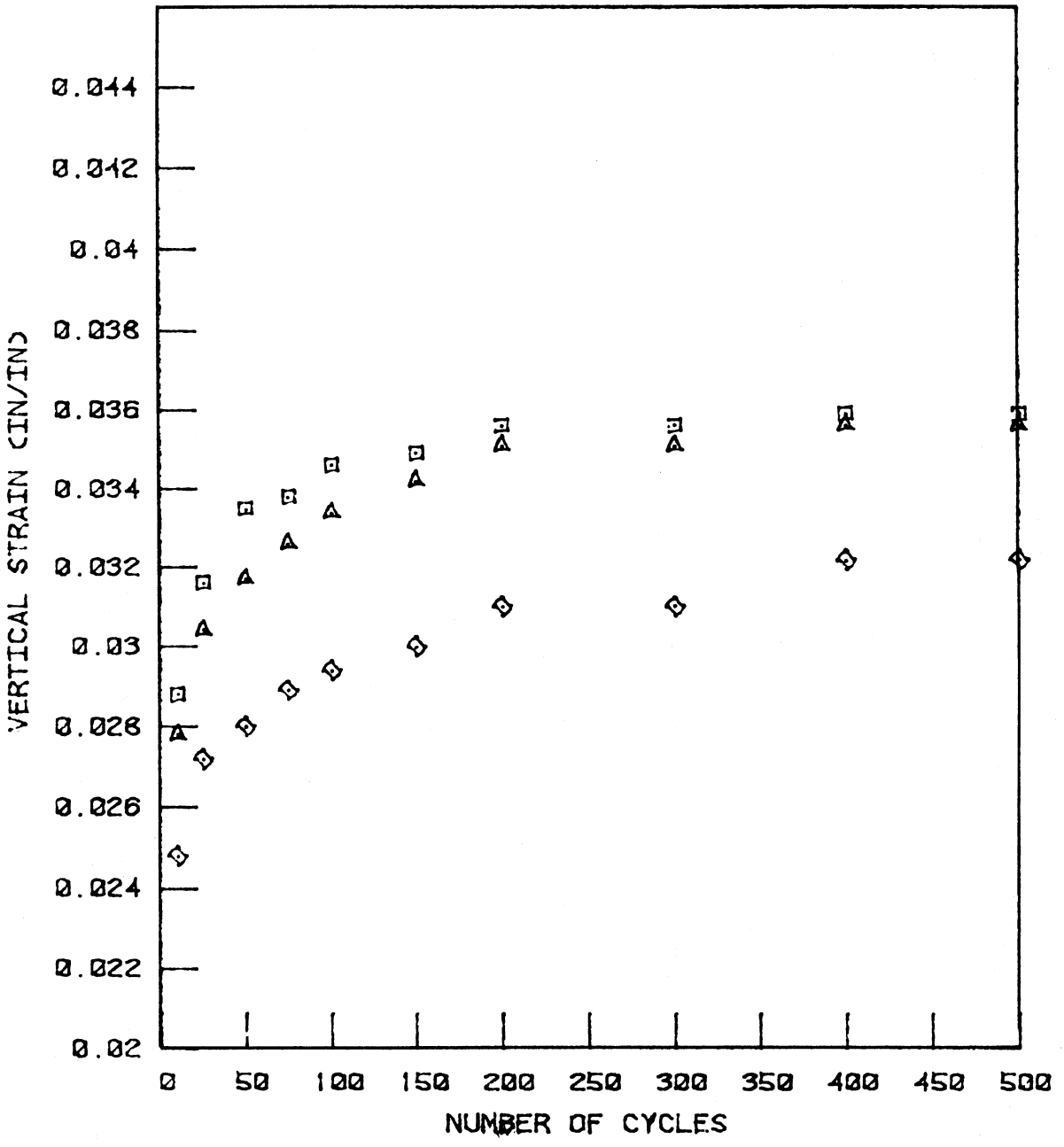

Figure 100. Vertical unit strain versus number of cycles for varying field mixed fiber contents, Linn County Prairieburg.

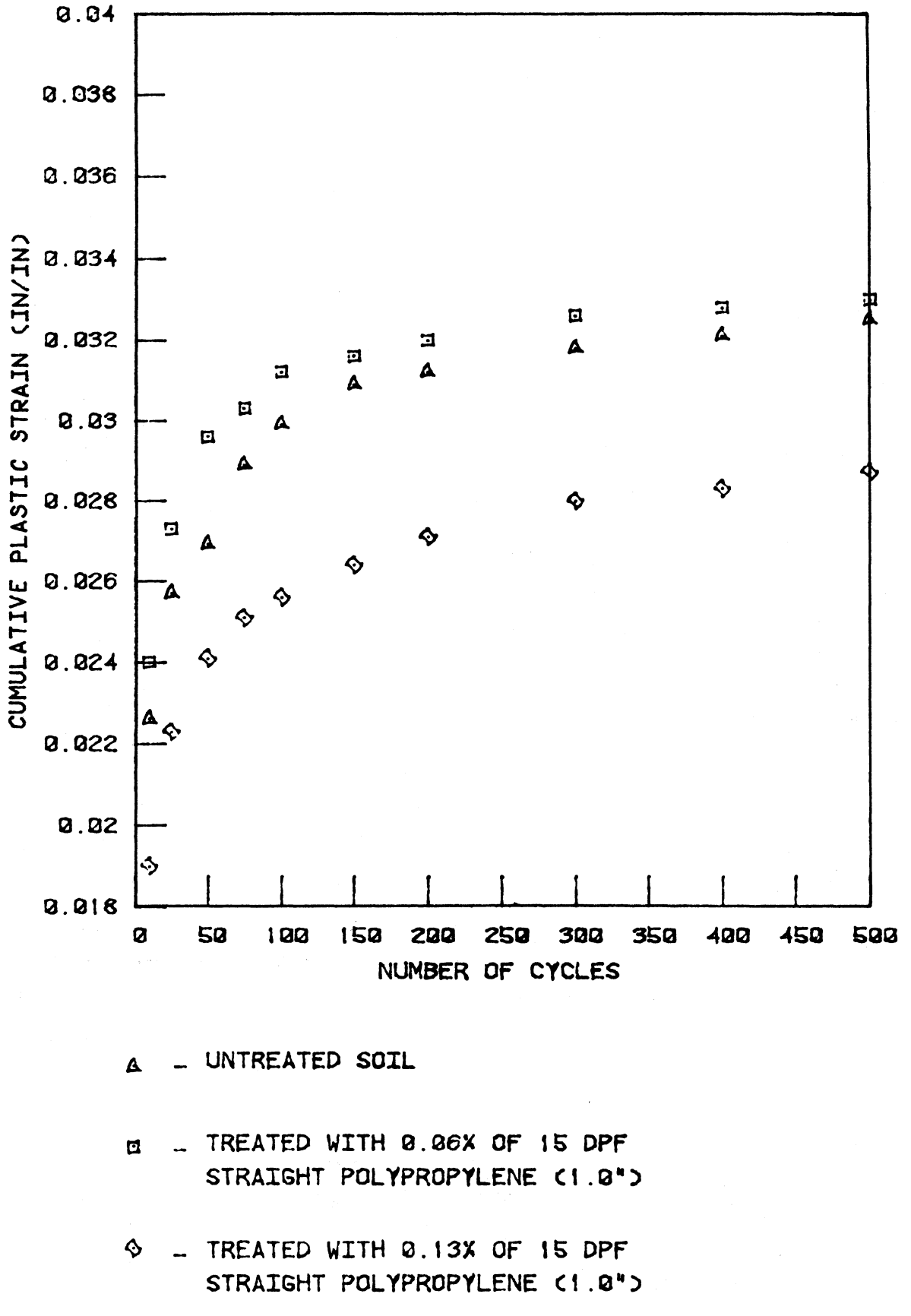

Figure 101. Permanent set versus number of cycles for varying field mixed fiber contents, Linn County Prairieburg.

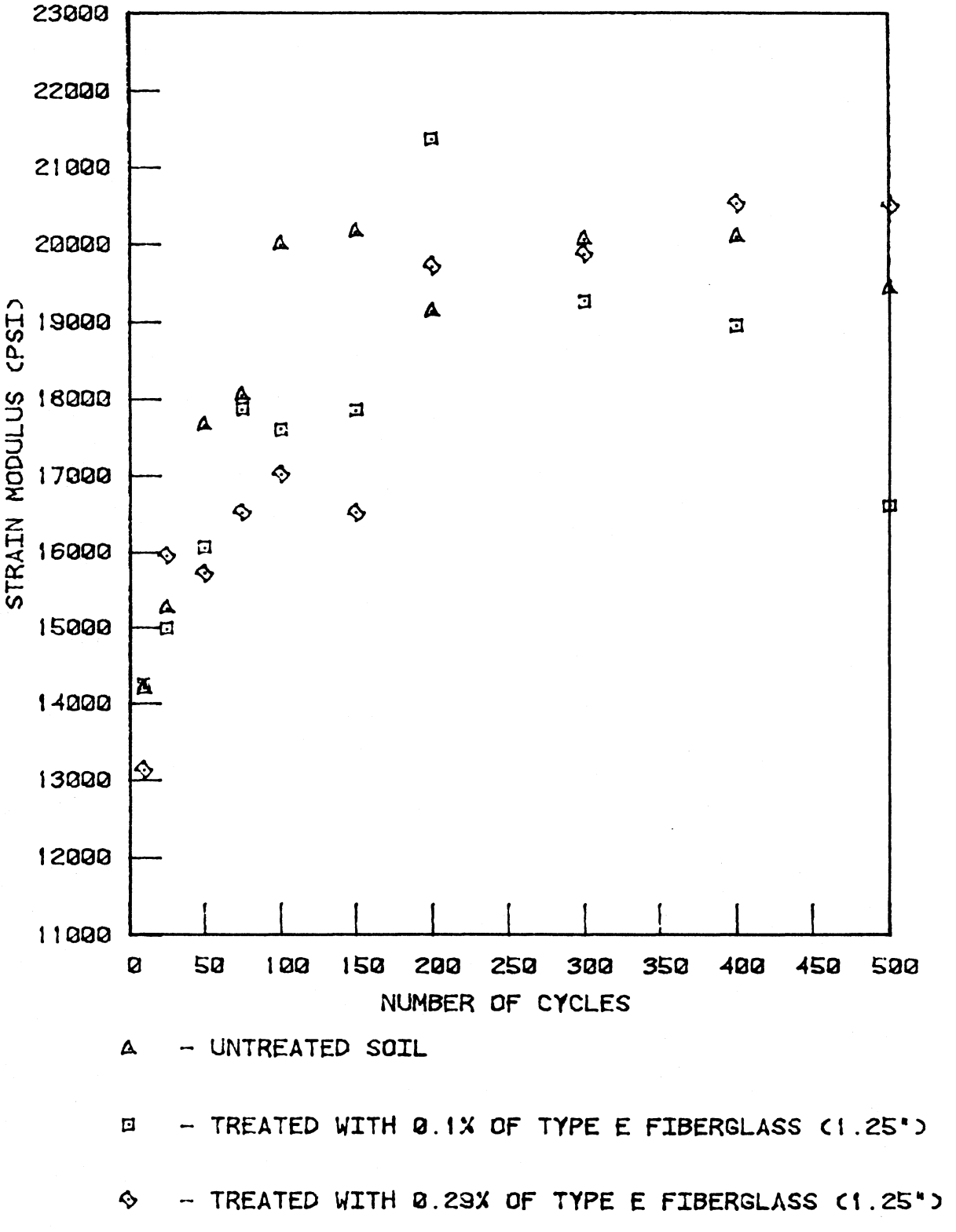

Figure 102. Permanent set versus number of cycles for varying field mixed fiber contents, Linn County Prairieburg.

improvement in strain moduli occurred through incorporation of the 0.06% 15 dpf straight and 0.1% 360 dpf fibrillated polypropylene fibers. All other fiber contents showed either no improvement or a possible reduction of strain modulus. After about 250 cycles of loading, the 0.1% Type E fiberglass exhibited some characteristics of strain softening.

Horizontal strains and stresses, as well as stress ratios of the field mixed Prairieburg soil-fiber composites, were significantly improved from those measurements obtained in the untreated soil due to incorporation of the 15 dpf straight and 360 dpf fibrillated polypropylene fibers, as illustrated in Figure 103. Horizontal stress-strain and stress ratio of the soil-Type E fiberglass composites were neither basically increased or reduced from those values obtained with the untreated soil. Optimum benefit of the 15 dpf straight and 360 dpf fibrillated fibers was respectively achieved at 0.06 and 0.29% fiber contents for each of these lateral stability measurements. As previously noted, the fiberglass did not particularly enhance any lateral stability of the cement modified loess, thus raising some question as to its suitability for use as a randomly oriented reinforcement material.

Figure 104 illustrates actual average values of volumetric strain versus number of cycles for the 360 dpf fibrillated polypropylene field mixed fibers. In general, none of the fibers provided substantially improved volumetric strain characteristics from that of the untreated soil. The 0.06% 15 dpf straight polypropylene and 0.1% Type E fiberglass produced some slight reductions in volumetric strain which may be associated with their respective reductions of vertical strain.

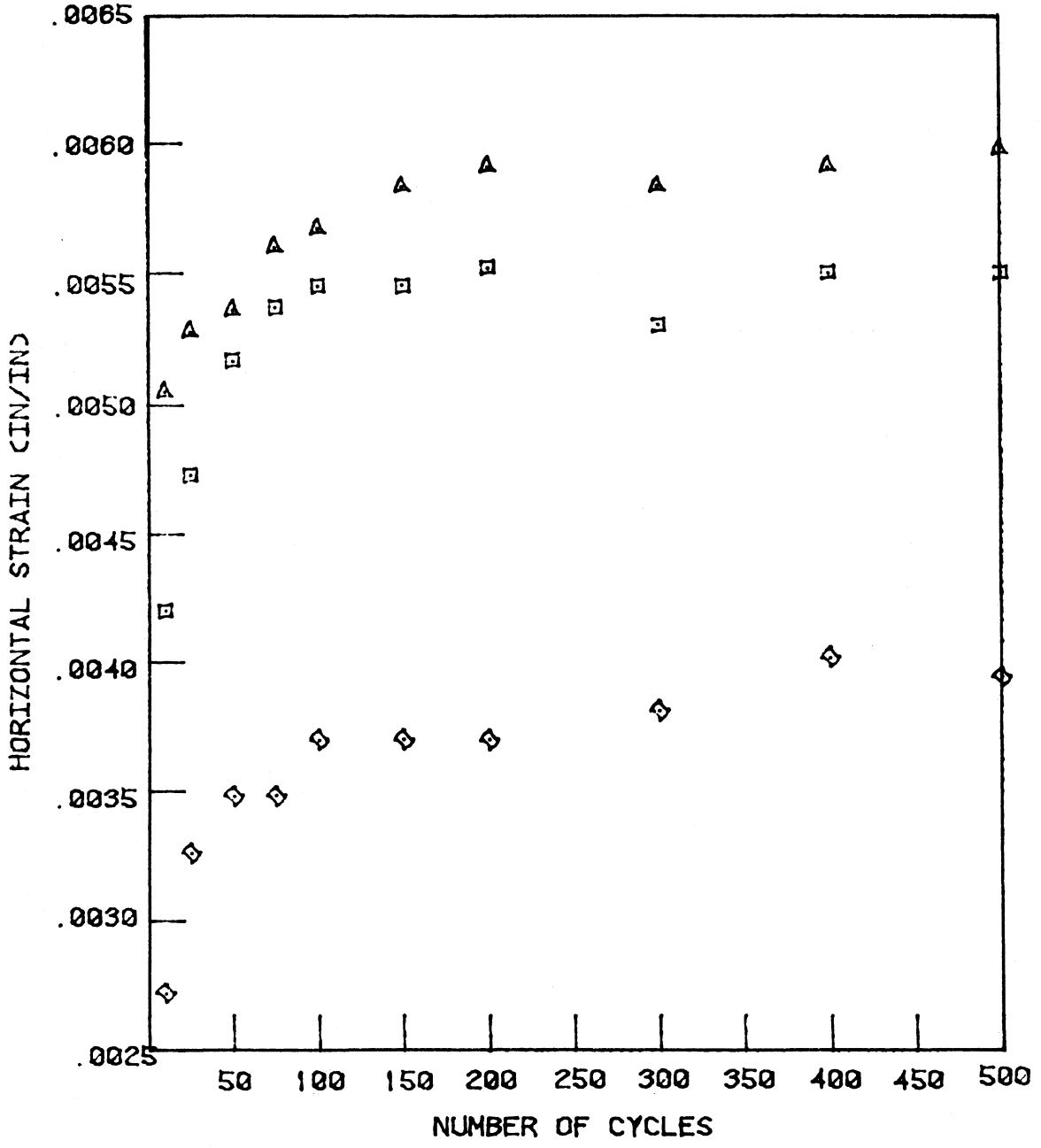

Figure 103. Horizontal strain versus number of cycles for varying field mixed fiber contents, Linn County Prairieburg.

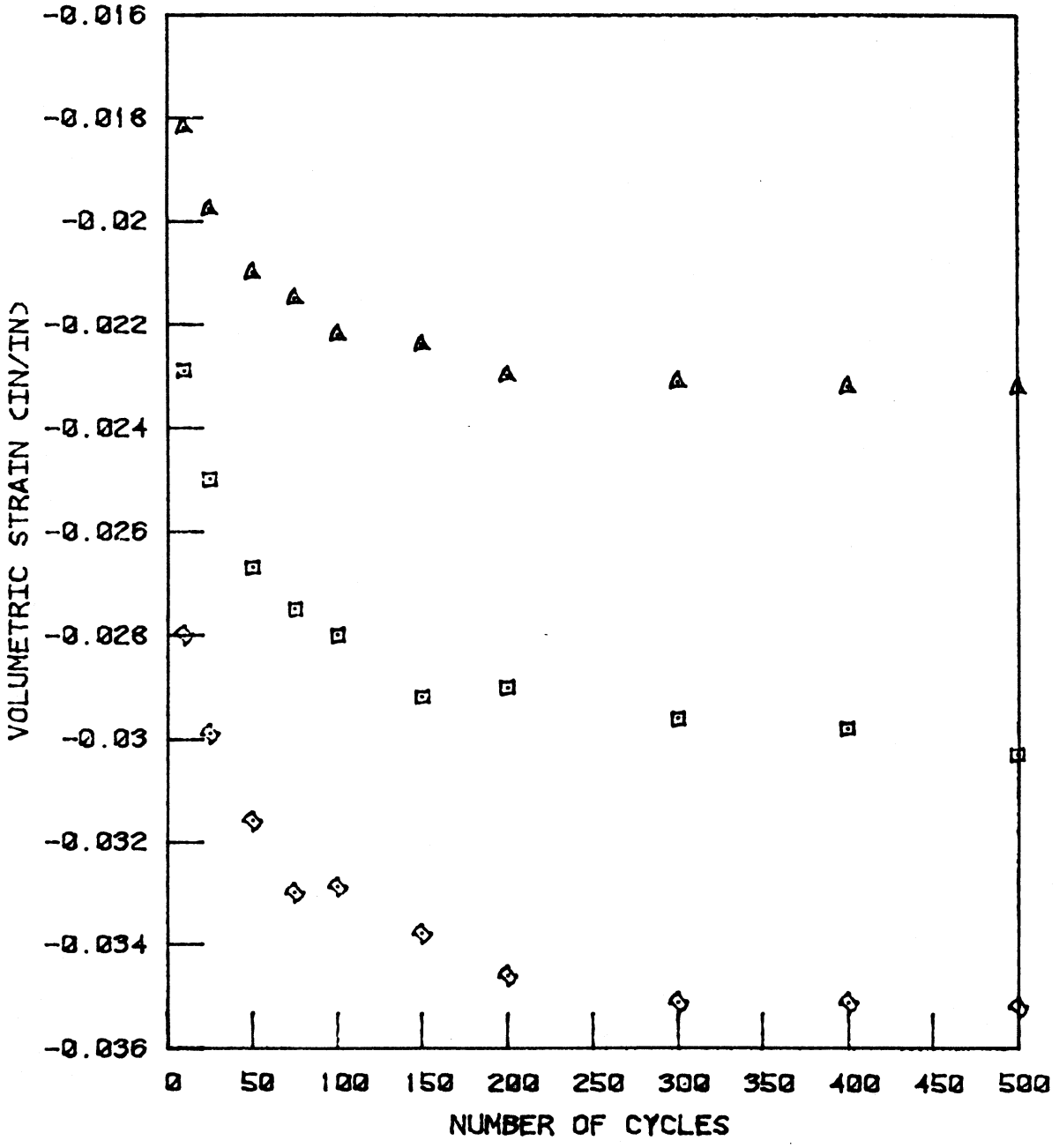

Figure 104. Volumetric strain versus number of cycles for varying field mixed fiber contents, Linn County Prairieburg.

In summary, cyclic load testing of the field mixed Linn County Prairieburg soil provided substantially the same conclusion as that previously observed with the Mortenson Road and Sioux City soils; i.e., random fiber reinforcement is predominantly oriented to improvement in lateral stability characteristics of a soil. In general, the finer of the three fibers, i.e., the 15 dpf polypropylene straight, appeared to provide maximum lateral reinforcement benefits coupled with some improvements in vertical stability.

Benkelman Beam Deflection Test

Table 33 presents average in situ Benkelman beam data of both the Story and Linn County sections. The data for each section includes average maximum deformation under a tire contact pressure of 75 psi, average residual deformation remaining in the section after passage of the 75 psi pressure, and a computed deformation modulus, E. The deformation modulus was calculated from a modification of the Burmister relation for E from a plate bearing test; $E = \frac{\pi pD\ (1 - \nu^2)}{4W}$, where E = deformation modulus, p = plate stress, D = plate diameter, ν = Poisson's ratio, and W = plate settlement. Poisson's ratio was assumed as 0.33, a value commonly used for unsaturated soils. The tire contact pressure of 75 psi was assumed as the plate stress, an equivalent tire diameter of 12 inches was assumed for D, and W was taken as the maximum deformation.

Variability of each of the values obtained from the Benkelman beam test versus time, test section location, and fiber type are noted in Table 33, the magnitudes of variation ranging from slight to significant. Immediately following construction, the 0.05% fibrillated polypropylene incorporated in the Mortenson Road section, showed an average decrease

Table 33. Average Benkelman Beam test results.*

Section	Date	Maximum Deformation at 75 psi, in.	Deformation Modulus, E, psi	Residual Deformation in.
Story County, Mortenson Road				
Control	Oct. 1980	0.125	5048	0.024
0.05% Fib. Poly. Fiber	Oct. 1980	0.099	7423	0.015
Control	May, 1981	0.082	7682	0.009
0.05% Fib. Poly. Fiber	May, 1981	0.106	6206	0.007
Control	July 1981	0.113	5645	0.008
0.05% Fib. Poly. Fiber	July 1981	0.142	4652	0.016
Control	Oct. 1981	0.102	6234	-
0.05% Fib. Poly. Fiber	Oct. 1981	0.094	7202	-
Linn County, Prairieburg				
Control	Oct. 1980	0.038	21,360	0.012
Sect. 1, 0.06% 15 dpf x 1.0 in. Poly.	Oct. 1980	0.083	7585	0.013
Sect. 2, 0.13% 15 dpf x 1.0 in. Poly.	Oct. 1980	0.053	11,879	0.018
Sect. 3, 0.10% 1.25 in. Type E Fiberglass	Oct. 1980	0.077	8176	0.015
Sect. 4, 0.29% 1.25 in. Type E Fiberglass	Oct. 1980	0.077	8176	0.021
Sect. 5, 0.29% 360 dpf x 1.5 in. Fib. Poly.	Oct. 1980	0.047	13,395	0.013
Sect. 6, 0.10% 360 dpf x 1.5 in. Fib. Poly.	Oct. 1980	0.063	9993	0.010
Control	June 1981	0.074	8598	0.033
Sect. 1, 0.06% 15 dpf x 1.0 in. Poly.	June 1981	0.050	12,591	0.017
Sect. 2, 0.13% 15 dpf x 1.0 in. Poly.	June 1981	0.036	17,488	0.023
Sect. 3, 0.10% 1.25 in. Type E Fiberglass	June 1981	0.078	8071	0.040
Sect. 4, 0.29% 1.25 in. Type E Fiberglass	June 1981	0.089	7074	0.052
Sect. 5, 0.29% 360 dpf x 1.5 in. Fib. Poly.	June 1981	0.080	7870	0.042
Sect. 6, 0.10% 360 dpf x 1.5 in. Fib. Poly	June 1981	0.040	15,739	0.016
Control	July 1981	0.072	8717	0.041
Sect. 1, 0.06% 15 dpf x 1.0 in. Poly.	July 1981	0.051	12,344	0.017
Sect. 2, 0.13% 15 dpf x 1.0 in. Poly.	July 1981	0.074	8508	0.021

Table 33. continued

Section	Date	Maximum Deformation at 75 psi, in.	Deformation Modulus, E, psi	Residual Deformation in.
Sect. 3, 0.10% 1.25 in. Type E Fiberglass	July 1981	0.062	10,154	0.022
Sect. 4, 0.29% 1.25 in. Type E Fiberglass	July 1981	0.051	12,344	0.023
Sect. 5, 0.29% 360 dpf x 1.5 in. Fib. Poly.	July 1981	0.087	7236	0.066
Sect. 6, 0.10% 360 dpf x 1.5 in. Fib. Poly.	July 1981	0.079	7969	0.042
Control	Oct. 1981	0.033	19,090	-
Sect. 1, 0.06% 15 dpf x 1.0 in. Poly.	Oct. 1981	0.029	21,720	-
Sect. 2, 0.13% 15 dpf x 1.0 in. Poly.	Oct. 1981	0.044	14,316	-
Sect. 3, 0.10% 1.25 in. Type E Fiberglass	Oct. 1981	0.028	22,496	-
Sect. 4, 0.29% 1.25 in. Type E Fiberglass	Oct. 1981	0.027	23,330	-
Sect. 5, 0.29% 360 dpf x 1.5 in. Fib. Poly.	Oct. 1981	0.022	28,632	-
Sect. 6, 0.10% 360 dpf x 1.5 in. Fib. Poly.	Oct. 1981	0.027	23,330	-

*Mortenson Road data is average of 7 to 10 tests per section. Prairieburg data is average of 3 to 8 tests per section.

in maximum and residual deformations, coupled with a near 50% increase in deformation modulus as compared to the untreated control. Succeeding tests through July showed a slight reversing of the data, though visual inspection of the fiber section indicated superior performance as compared with the control. A further reversal appeared in the October 1981 data indicating that treated average deformations were slightly reduced from those of the control, thus creating a slight increase in deformation Modulus E. As noted previously, the 360 dpf fibrillated polypropylene fiber treatment of the Mortenson Road soil produced a slight improvement in vertical unit strain, horizontal stress and strain, and stress ratio, from that of the untreated during cyclic load testing.

Immediately following construction, average Benkelman beam data from the Linn County fiber sections indicated lower support capacities than the untreated control, Table 33. However, maximum deformation, deformation modulus, and residual deformation indicated distinct differences between type of fiber and fiber content. The 0.13% 15 dpf and 0.29% 360 dpf polypropylene sections indicated considerably greater stability than any of the other fiber sections. Regardless of fiber content the two fiberglass sections produced nearly equal results.

Successive Prairieburg Benkelman beam tests produced variations from that noted following construction, particularly in that several of the sections indicated rather significant performance improvement as compared with the untreated control. The 0.06% 15 dpf polypropylene provided improved parameters during succeeding series of tests. Definite improvement was observed in the early summer tests with 0.29% Type E fiberglass.

While the 360 dpf fibrillated polypropylene exhibited improved performance immediately following construction, beam data on these two sections suggested a lessening of performance during the summer. Such increases or decreases in performance data versus time may often be attributed to variations in moisture content with other types of incorporated materials or products. However, examination of the moisture data of Table 30 does not provide such a correlation since moisture contents between sections were relatively similar.

From time of construction through the July 1981 Benkelman beam tests, deformations were obtained through a so called maximum deflection technique in which the beam was inserted between the dual tires, the probe being 5 ft. ahead of the centerline of axle, and deflection calculated as the difference between an initial reading and the maximum dial reading taken as the tires moved adjacent to the probe. The October 1981 data, Table 33, was obtained through a so called rebound technique, in which the probe is placed immediately between the tires at axle centerline, an initial dial reading obtained, the truck moved forward, and a maximum rebound dial reading recorded. Deflection was obtained as the difference in dial readings, and is often assumed as being more indicative of the elastic properties of the roadway material. Use of the rebound technique indicated the greatest decrease in deformation and accompanying increase in modulus occurred with the 0.29% 360 dpf fibrillated polypropylene. This decrease in maximum deformation was in conflict with each of the vertically oriented measurements of the 360 dpf fiber observed from cyclic load tests. Vertically oriented measurements within the Prairieburg cyclic load tests

indicated that correlations might occur with the 0.13% 15 dpf straight polypropylene (Section 2) and the 0.10% Type E fiberglass (Section 3). Of these two sections a vertically oriented correlation occurred only with Section 3, the fiberglass treatment. However, horizontally oriented correlations were apparent from cyclic load test measurements of horizontal strain for each of the three fiber types in that the 0.06% 15 dpf polypropylene, 0.1% Type E fiberglass, and both percentages of the 360 dpf fibrillated polypropylene produced both decreased rebound deformation and reduced horizontal strain when compared to the untreated.

This correlation suggests the benefication mechanism of fiber reinforced soil, in that lowering of in situ rebound deformation and horizontal strain relates to the tensile properties of the soil-fiber composite. Thus the prime measurement systems for evaluation and performance of a soil-fiber composite roadway material should be associated with a tensile rather than a compression mode.

Plate Bearing Test

Table 34 illustrates the average results of in-situ plate-bearing tests performed on both the Story and Linn County sections. Modulus of Subgrade Reaction is defined as $K = \frac{P}{\Delta}$, where P = plate stress and Δ = the corresponding stable deformation value. K is normally obtained at a plate stress of 10 psi. Table 34 however, presents K as calculated at plate pressures of both 10 and 75 psi, the latter as a means of correlation with Benkelman beam deflections and moduli obtained at 75 psi tire contact pressure. The plate-bearing deformation modulus E was calculated in

Table 34. Average plate-bearing test results.*

	Date	Modulus of Subgrade Reaction K_{10}, pci	Modulus of Subgrade Reaction K_{75}, pci	Deformation at 75 psi, in.	Deformation Modulus, E, psi.	Permanent Deformation in.
Story County, Mortenson Road						
Control	Oct. 1980	592	444	0.178	3824	0.054
0.05% Fib. Poly. Fiber	Oct. 1980	534	415	0.192	3481	0.092
Control	May, 1981	759	585	0.122	4677	0.037
0.05% Fib. Poly. Fiber	May, 1981	725	524	0.144	4402	0.053
Control	July 1981	859	609	0.126	5112	0.043
0.05% Fib. Poly. Fiber	July 1981	677	537	0.157	4509	0.059
Linn County, Prairieburg						
Control	June 1981	1430	1361	0.056	11,422	0.027
Sect. 1, 0.06% 15 dpf x 1.0 in. Poly.	June 1981	1476	1420	0.049	11,917	0.021
Sect. 2, 0.13% 15 dpf x 1.0 in. Poly.	June 1981	1381	1163	0.060	9766	0.018
Sect. 3, 0.10% 1.25 in. Type E Fiberglass	June 1981	1181	1203	0.058	10,095	0.025
Sect. 4, 0.29% 1.25 in. Type E Fiberglass	June 1981	1476	1583	0.047	13,286	0.022
Sect. 5, 0.29% 360 dpf x 1.5 in. Fib. Poly.	June 1981	2250	1628	0.043	13,665	0.017
Sect. 6, 0.10% 360 dpf x 1.5 in. Fib. Poly.	June 1981	2143	1443	0.049	12,115	0.016
Linn County, Prairieburg						
Control	July 1981	1586	1408	0.059	11,820	0.032
Sect. 1, 0.06% 15 dpf x 1.0 in. Poly.	July 1981	1027	887	0.098	7444	0.060
Sect. 2, 0.13% 15 dpf x 1.0 in. Poly.	July 1981	1875	1457	0.053	12,231	0.022
Sect. 3, 0.10% 1.25 in. Type E Fiberglass	July 1981	2083	1565	0.048	13,138	0.023

Sect. 4, 0.29% 1.25 in. Type E Fiberglass	July 1981	1500	1358	0.057	11,396	0.028
Sect. 5, 0.29% 360 dpf x 1.5 in. Fib. Poly.	July 1981	1288	1365	0.055	11,462	0.023
Sect. 6, 0.10% 360 dpf x 1.5 in. Fib. Poly.	July 1981	1833	1602	0.047	13,450	0.021

*Mortenson Road data is the average of 4 to 6 tests per section. Prairieburg data is the average of 2 to 4 tests per section.

accordance with the previously noted Burmister relation at a plate stress of P = 75 psi. The permanent deformation value represents the intersection of the unloading curve with the abscissa of the plate stress versus deformation plot and suggests the permanent or plastic deformation that the materials experienced versus time.

As noted in Table 34, the parameters obtained from plate bearing tests on Mortenson Road indicate little variation between comparable control and 0.05% 360 dpf fibrillated polypropylene sections. The various parameters however, tend to reflect the previously noted reduction in moisture content from time of construction to spring/summer tests, in that each parameter produced similar gains in performance with the reduction in moisture.

When compared with the untreated control, the Prairieburg fiberglass and 360 dpf fibrillated polypropylene sections show some improvement of plate bearing test parameters, Table 34. As with the Benkelman beam data, plate bearing parameters reflect variations between succeeding test times. The early June tests showed improved performance of the 0.29% fiberglass and both percentages of 360 dpf fibrillated polypropylene. A month later only the 0.10% fiberglass and 360 dpf polypropylene showed improved performance. In addition, slight improvements were observed in parameters associated with the 0.13% 15 dpf polypropylene section.

No correlative relationships were noted between deformation moduli obtained from the plate bearing and Benkelman beam tests. However, some anomalies within the plate bearing data suggest characteristics concerning the tensile mechanism of soil-fiber reinforcement. The moduli of subgrade

reactions at 75 psi (K_{75}) were often less than that obtained at 10 psi (K_{10}). Where such lessening of K values occurred, the fiber sections often produced a lowering of deformation at 75 psi, coupled with improved deformation modulus E and lowering of permanent deformation, as compared to the untreated control. This action was particularly evident with the noted improvements within the Prairieburg fiberglass and 360 dpf fibrillated polypropylene sections. Such variations of data between the control and fiber sections suggest that larger applied stresses must be associated with the in situ soil-fiber composite before the fiber will begin to activate any tensile forces; the latter thus increasing E and reducing deformation at the larger vertical stress, coupled with a greater proportion of rebound as evidenced in reduced permanent deformation.

California Bearing Ratio Test

From time of construction through Fall 1981, visual inspections of all fiber test sections indicated improved performance as compared with their untreated controls. However, in-situ Benkelman beam and plate bearing tests appeared to only partially correlate with visual performance, in that data generally provided signs of variable performance. As an example of this lack of visual versus quantitative correlation, an examination was made of the Story County Mortenson Road section the morning following a two inch rain. Control sections adjacent to both the east and west ends of the fiber treated section were deeply rutted, the ruts ponded with water, severe shoving had occurred, little or no surface aggregate was visible, and in general each control area was difficult to drive a vehicle through. No similar characteristics were observed in the fiber section; in fact, a very distinct transition was noted from the control to the stable fiber

section. Since it was impossible to get load test equipment into the control sections at that point of time, in situ testing was postponed for a period of 24 hours in order to allow at least some surface drying of the untreated materials. The following morning a replication of six in-place California Bearing Ratio and moisture-density tests were conducted in each of the east control and fiber treated sections, all tests being performed within a length of fifty feet either side of the previously noted fiber/control demarcation. The CBR test was used as a means of providing a punching shear action, rather than a deformed bowl as normally associated with either Benkelman beam or plate bearing tests.

Table 35 presents the CBR test results as obtained about 36 hours following the two inch rain. Density of the untreated control was considerably less than that of the fiber section. Moisture content of the control was about one percent greater than the fiber section. However, CBR values of the fiber section were less than one percentage greater than the control, regardless of penetration, but showed considerably less scatter as indicated by the standard deviation.

The lack of considerably improved CBR values for the soil-fiber base may be associated with the CBR test as well as the mechanism of activation of the tensile component of the fiber within the composite. The CBR test produces a cone shaped punching shear, dependent on the compression developed immediately beneath the penetrometer, as well as shearing action immediately adjacent to the penetrometer and developing cone. Confinement of fibers within the upper 0.5 inch of the base matrix coupled with potential shear and/or pull out of individual fibers did not appear

Table 35. In situ California Bearing Ratio tests, Story County, Mortenson Road, approximately 36 hours following a two inch rain

Section	Dry Density γ_d, pcf	Moisture Content, w, %	CBR @ 0.1" pen.	CBR @ 0.2" pen.	CBR @ 0.3" pen.	CBR @ 0.5" pen.
Control						
Base equivalent	120.2 ± 4.6	9.7 ± 0.5	28.2 ± 4.2	27.8 ± 4.8	24.8 ± 5.1	20.6 ± 4.7
Subgrade	120.3 ± 0.8	9.3 ± 0.5	-	-	-	-
Fiber Base						
0.05% Fib. Poly.	127.7 ± 4.5	8.2 ± 1.0	29.4 ± 4.4	28.4 ± 2.6	25.5 ± 2.0	21.1 ± 2.7
Subgrade	124.2 ± 6.3	8.5 ± 1.5	-	-	-	-

to produce data which would be indicative of actual performance as related to CBR values.

Spherical Bearing Value Tests

Due to lack of significant correlation between laboratory and field test data, it was decided to try a testing procedure which might mobilize stresses in a lateral direction. The Spherical Bearing Value Test (SBV) appeared appropriate since stresses have been shown to mobilize in a radial direction from point of vertical compressive loading. This test procedure was developed under Iowa Highway Research Board project HR-117 (6). During penetration of a sphere into the roadway surface, contact area of the sphere is determined as πDh, where D = diameter of the sphere, and h = depth of penetration. A plot of load versus contact area is made, and a linear regression analysis is performed on the data points; SBV being defined as the slope of the regression line. In a number of the initial plots of load versus contact area however, two regression lines were observed, particularly with the fiber treated materials. At low values of load-contact area the regression line was steep, providing a high SBV value. At higher load-contact area a reversal was noted. Since the point at which the curves fell into two regression lines could denote a potential failure stress, SBV data was thus analyzed for the three conditions of (1) SBV before failure, (2) SBV after failure, and (3) breakpoint stress. Results are presented in Table 36.

Average conventional SBV results for the steeper portion of the regression of the Mortenson Road sections were 342 and 341 psi respectively, for the fiber treated and control. No basic difference was thus noted

Table 36. Average Spherical Bearing Value (SBV) test results

Section	SBV Before Failure, psi	SBV After Failure, psi	Breakpoint Stress, psi
Story County, Mortenson Road			
Control	341	340	377
0.05% Fib. Poly. Fiber	342	234	417
Linn County, Prairieburg			
Control	1100	712	1178
Sect. 1, 0.06% 15 dpf x 1.0 in. Poly.	1252	653	1249
Sect. 2, 0.13% 15 dpf x 1.0 in. Poly.	597	443	662
Sect. 3, 0.10% 1.25 in. Type E Fiberglass	740	529	803
Sect. 4, 0.29% 1.25 in. Type E Fiberglass	810	501	836
Sect. 5, 0.29% 360 dpf x 1.5 in. Fib. Poly.	960	578	1012
Sect. 6, 0.10% 360 dpf x 1.5 in. Fib. Poly.	1312	718	1417

between the control and fiber sections, implying that inclusion of randomly oriented fibers in the soil did not affect the strength of the roadway soils either adversely or beneficially. For the section of the curve where incipient failure was occuring, average SBV values were 340 and 234 psi for the control and fiber sections respectively. This difference was caused by an extreme variation between the west and east control sections, a variation that was not seen in any of the other in-situ testing. In this case, west control SBV plots were significantly steeper than those of the east control section. Therefore, the SBV values obtained were very high, thus producing very high average control values. If SBV values for the west control were omitted, average SBV's were then 239 and 234 for the

control and fiber sections respectively, again indicating no basic difference between control and fiber sections.

Average breakpoint stresses of the Mortenson Road fiber section were greater than that of the untreated control by about 10%, Table 36, indicating that higher stresses were required to initiate failure in the fiber section than in the untreated roadway soil. Beyond the breakpoint stress, however, the fiber treated soil appeared incapable of sustaining higher stresses, a situation potentially indicating occurrence of fiber pullout and/or debonding.

Similar analyses may be observed from the average SBV data obtained within the Prairieburg sections, Table 36. Sections 1 and 6 however, appeared to provide some positive improvements in conventional SBV's as well as breakpoint stresses when compared to the untreated control.

As a consequence of the conventional SBV tests, it appeared that two or more mechanisms of stress-deformation characteristics were occurring and should be further investigated as to the test sections performance. Therefore a modified SBV test was instituted which coupled SBV vertical loading and deformations with an accompanying measurement of lateral deformation. Lateral deformations were measured with a device essentially consisting of a bar mount having (1) a fixed end point inserted into the roadway outside the influence of all loading, and (2) a moveable pivot arm attached to a horizontally mounted 0.001 in. dial gage. The latter moved forward or backward depending on whether horizontal deformations were compressive or tensile respectively, and such deformations were monitored at 2, 3 and 4 inches from the centerline of vertical load application.

Horizontal deformation measurements were magnified by a factor of 2.6 due to the lever-arm ratio of the moveable pivot arm and were thus adjusted for actual values. Due to the configuration of the device, lateral compression deformations were expressed as negative values while tensile deformations were expressed positively.

Table 37 is a summary of average lateral deformations obtained within the six arbitrarily selected locations of the Mortenson Road test section, plus two adjacent control sections. In general, the amount of lateral deformation decreased with increasing distance from point of load application, and in most cases tensile deformations were observed.

Ratios of horizontal to vertical deformation were plotted versus energy, as illustrated in Figures 105 and 106. Energy was defined as the amount of work required to cause a vertical deflection. Work is defined as force times distance. In this case, force was the applied load in pounds, and distance was the corresponding amount of vertical deformation measured in inches. Therefore, the units of energy were lb-in.

As illustrated in Figure 106, six of the eight plots appeared to define at least three types of material behavior. At low energy values, the horizontal to vertical deformation ratios generally decreased with increasing energy. This was followed by an energy region in which the ratio remained relatively constant. At higher energy levels, the ratio increased with increasing amounts of energy. In two of the plots, as illustrated in Figure 105, the ratio increased with increasing energy during the entire test.

The primary behavior noted above, illustrates that only minor lateral deflections occur initially, even though accompanied by considerable

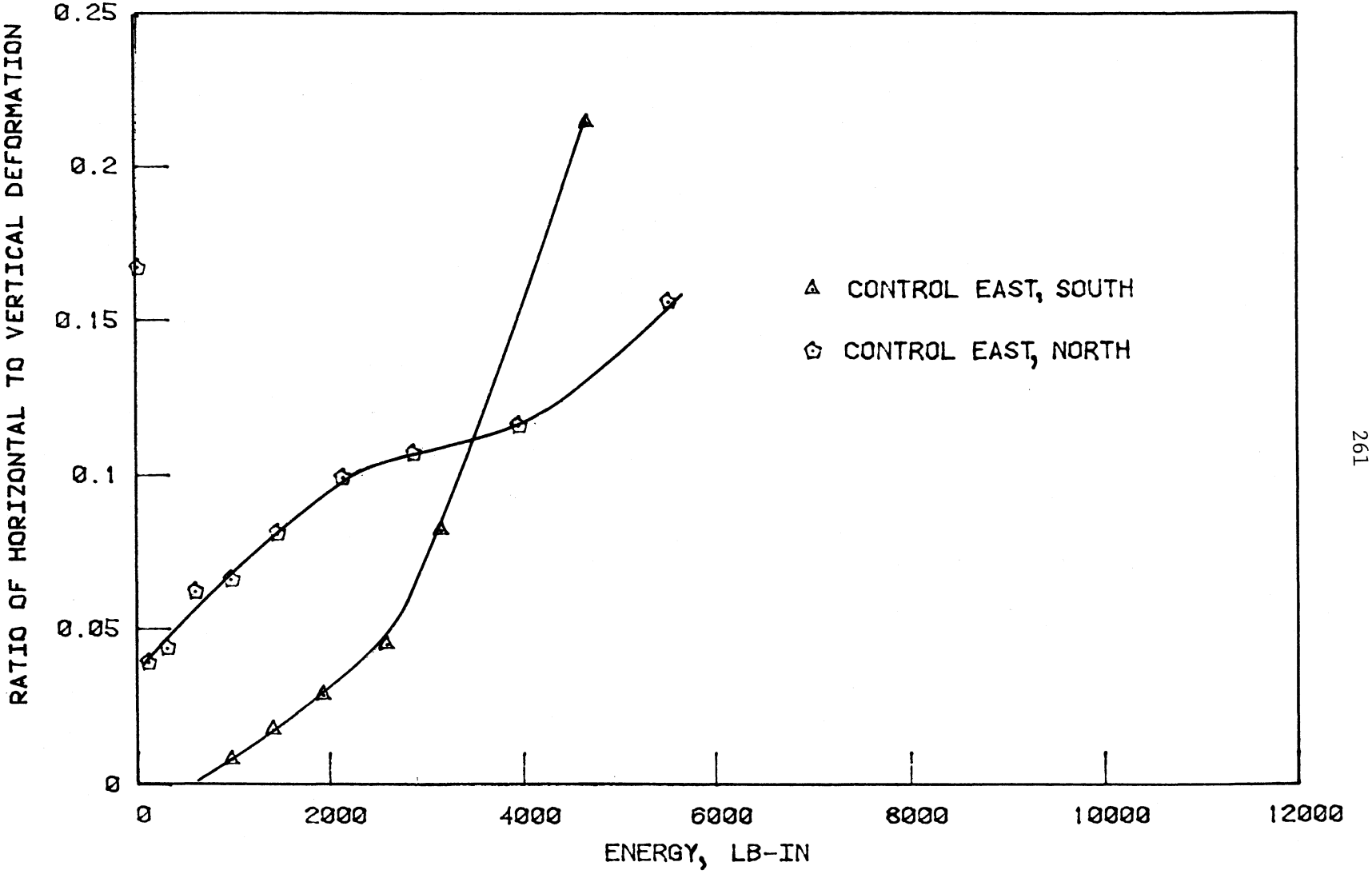

Figure 105. Insitic Deformation ratios versus energy, Story County Mortenson Road.

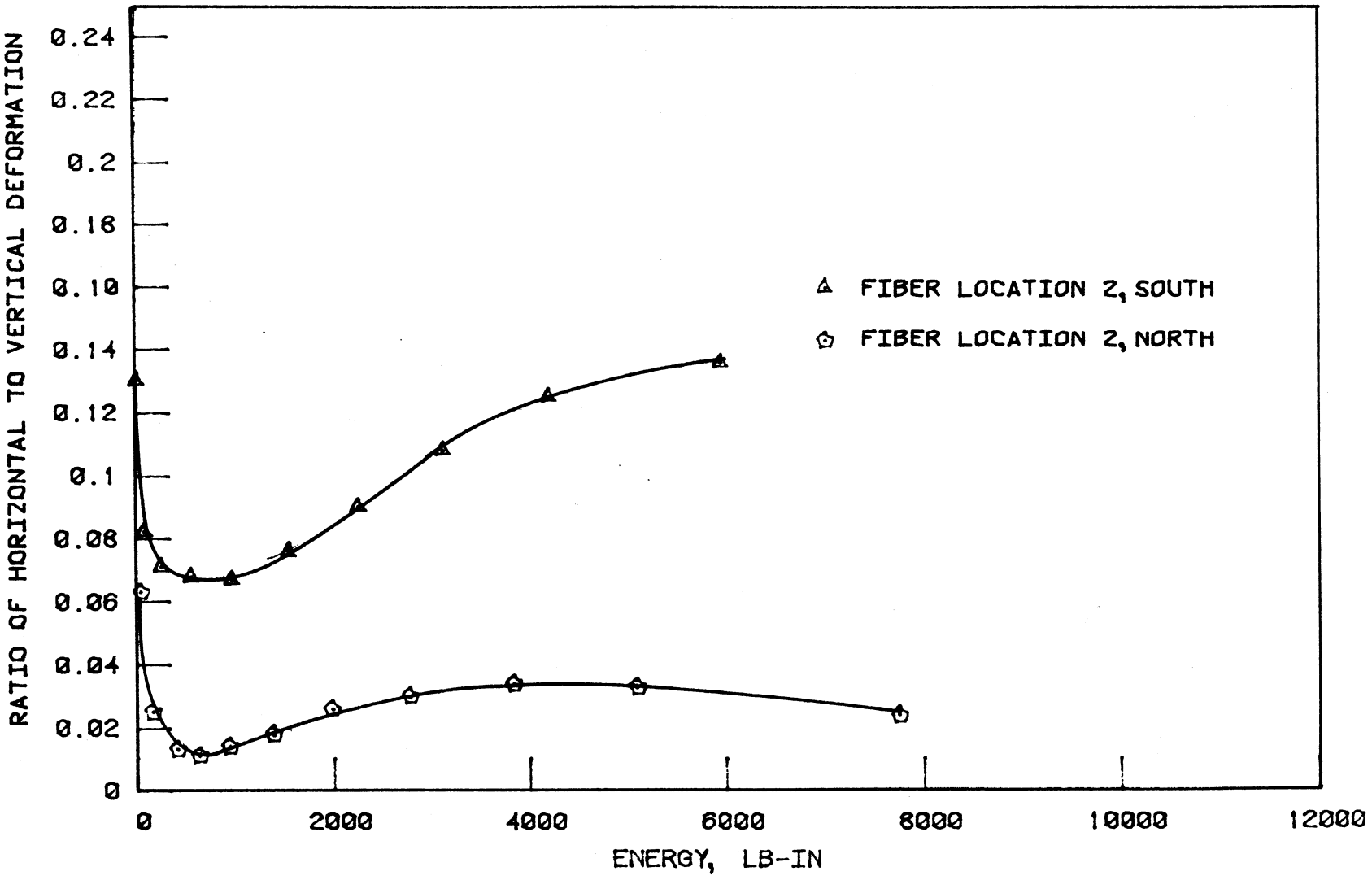

Figure 106. Insitic Deformation Ratios versus Energy, Story County Mortenson Road.

Table 37. Summary of average spherical bearing value data obtained June, 1982.

	East Control				Location 1				Location 2				Location 3			
Load (lb)	Contact Area (in^2)	Lateral Def. at 2" (in)	Lateral Def. at 3" (in)	Lateral Def. at 4" (in)	Contact area (in^2)	Lateral Def. at 2" (in)	Lateral Def. at 3" (in)	Lateral Def. at 4" (in)	Contact area (in^2)	Lateral Def. at 2" (in)	Lateral Def. at 3"	Lateral Def. at 4"	Contact area (in^2)	Lateral Def. at 2" (in)	Lateral Def. at 3" (in)	Lateral Def. at 4" (in)
447	0.37	0.003	0	0	0.31	0	0	0	0.26	0.003	0	0	0.35	0	0	0
894	1.83	0.003	0.002	0	0.95	0	0.002	0	1.37	0.006	0.002	0	0.81	0	0	0.003
1340	3.37	0.005	0.002	0	2.09	0.002	0.003	0.002	2.88	0.008	0.005	0.004	1.48	0.002	0.002	0.003
1787	5.07	0.011	0.001	-0.003	3.42	0.003	0.004	0.002	5.10	0.012	0.009	0.007	2.42	0.003	0.002	0.004
2234	6.77	0.015	0.002	-0.004	4.94	0.0041	0.006	0.002	6.75	0.016	0.013	0.008	3.90	0.003	0.004	0.004
2681	8.59	0.024	0.003	-0.007	6.75	0.007	0.008	0.004	8.73	0.025	0.018	0.011	5.89	0.005	0.007	0.003
3128	10.71	0.038	0.003	-0.007	8.52	0.011	0.010	0.005	10.96	0.037	0.023	0.015	8.15	0.007	0.008	0.004
3574	12.64	0.051	0.005	-0.009	11.49	0.023	0.015	0.009	13.44	0.054	0.028	0.017	10.17	0.010	0.009	0.005
4021	15.31	0.072	0.005	-0.007	14.57	0.043	0.018	0.012	16.34	0.075	0.029	0.022	12.44	0.013	0.012	0.005
4468	18.25	0.125	0.010	-0.004	18.22	0.091	0.022	0.013	20.63	0.107	0.036	0.025	14.43	0.021	0.013	0.007
4915													17.07	0.033	0.017	0.007
5362													20.98	0.152	0.018	0.008
5808																
6255																
6702																
7149																

Table 37. continued

Location 4				Location 5				Location 6				West Control			
Contact area (in^2)	Lateral Def. at 2" (in)	Lateral Def. at 3" (in)	Lateral Def. at 4" (in)	Contact area (in^2)	Lateral Def. at 2" (in)	Lateral Def. at 3" (in)	Lateral Def. at 4" (in)	Contact area (in^2)	Lateral Def. at 2" (in)	Lateral Def. at 3" (in)	Lateral Def. at 4" (in)	Contact area (in^2)	Lateral Def. at 2" (in)	Lateral Def. at 3" (in)	Lateral Def. at 4" (in)
0.40	0	0.002	0	0.10	0	0	0	0.58	0	0	0	0.09	0	0	0.002
1.22	0.002	0.002	0.002	0.60	0	0	0	1.17	0.002	0	0	0.45	0	0.003	0.003
2.22	0.003	0.003	0.002	1.08	0	0	0	2.35	0.003	0.002	0.002	0.89	0.002	0.004	0.003
3.45	0.004	0.003	0.003	1.63	0	0	0	3.77	0.007	0.002	0.002	1.51	0.003	0.006	0.004
4.69	0.004	0.004	0.004	2.30	0	-0.002	0	5.43	0.014	0.002	0.003	2.37	0.004	0.007	0.006
6.55	0.005	0.006	0.004	3.02	0	-0.002	0	7.16	0.021	0.002	0.003	3.55	0.007	0.007	0.006
8.18	0.007	0.008	0.005	3.92	0	-0.002	0	9.09	0.032	0.003	0.004	5.01	0.007	0.008	0.007
10.33	0.012	0.009	0.007	4.96	0	-0.002	0	11.36	0.047	0.004	0.006	6.83	0.009	0.008	0.007
12.35	0.016	0.013	0.008	5.84	0	0.000	0	14.10	0.073	0.008	0.008	9.03	0.009	0.013	0.007
14.38	0.027	0.016	0.010	6.79	0	0.000	0	16.88	0.108	0.015	0.012	11.78	0.012	0.013	0.008
16.11	0.044	0.017	0.010	7.94	0.003	0.000	0	19.97	0.158	0.018	0.017	15.70	0.020	0.013	0.008
19.06	0.072	0.018	0.011	9.26	0.004	0.000	0	24.90	0.223	0.022	0.020	19.28	0.057	0.012	0.007
22.56	0.099	0.018	0.012	10.60	0.007	0.000	0					23.27	0.090	0.012	-0.002
				12.22	0.011	0.000	0								
				14.04	0.017	0.000	0.002								
				16.33	0.030	0.003	0.002								

vertical deflection of the SBV sphere at the point of loading. Such phenomena takes place due to an initial compaction of the road materials, with subsequent deflections mainly in the vertical direction due to greater particle to particle contact and densification. As the vertical load continues to increase during the second stage of behavior, Figure 106, compaction ceases and lateral deflections are initiated. Deformation ratios remained approximately constant because the material was predominantly in the elastic state.

At this point, it should be noted that Poisson's ratio is defined as the ratio of horizontal to vertical strain; i.e., $\varepsilon_H/\varepsilon_v$. If $\varepsilon_H = \frac{\Delta H}{H}$, $\varepsilon_v = \frac{\Delta L}{L}$, ΔH = deflection in the lateral direction, H = original width, ΔL = change in length (height), and L = original length (height), then

$$\mu = \frac{\Delta H}{H}/\Delta L/L \text{ or } \frac{\Delta H}{\Delta L} \times \frac{L}{H}.$$

In a vertically loaded field test situation, L and H are unknown, and Poisson's ratio is thus difficult to define due to the influence of the unknown area and depth of influence of the test equipment. However, L/H remains relatively constant, regardless of the applied load, and Poisson's ratio might therefore be defined as $\Delta H/\Delta L$, or the ratio of horizontal to vertical deformations. Since Poisson's ratio is only valid in the elastic range, it does not remain constant when a material begins to experience plastic deformation. Therefore the range in which the horizontal to vertical deformation ratio remained constant, most likely represented the elastic range of the in-situ field materials.

It is also likely that in-situ elastic properties occur prior to rupturing of the surface crust of layered road materials. After the

surface is fractured, larger lateral deformations are mobilized relative to vertical deflections, and hence the deformation ratio increases with increasing amounts of applied energy; the third stage of behavior, Figure 106.

Data obtained from the conventional SBV test is generally presented in the form of a load vs. contact area plot as previously noted. In a uniform single layered material, a linear relationship is generally obtained between load and contact area and the spherical bearing value is defined as the slope of this line.

In a multilayered system, a different behavior should be expected. The load capacity of a multilayered system depends on the summation of stiffnesses of the various layers, and the number of layers that have not experienced some form of failure. For example, consider a system consisting of three different layers (a, b, and c) in which layer stiffnesses decrease from the top downward. If the SBV test is conducted on such a system, all three layers should resist applied stresses during early stages of loading and prior to any layer failure or fracturing. When layer "a" fractures, it no longer continues to resist the applied stress; only layers b and c would then resist any stress applications. Following the same argument, when layer b experiences failure, only layer c would be capable of resisting applied stresses. Therefore, slopes of load vs. contact areas (SBV) obtained during increased stages of loading should vary depending on the number of layers that have, or have not, experienced any form of failure. Ideally, SBV's should be higher initially, and should

decrease as successive layers experience failure.

The above hypothesis thus suggested possible stages of stress deformation characteristics, particularly for the in-situ soil-fiber composites.

Further Mortenson Road spherical bearing value tests were conducted on May 10th and June 24th, 1982. Since the results of each were similar, and utilizing the preceeding concepts, all data were averaged and plotted as shown in Figure 107. It can be observed that all load vs. contact area plots could be broken into at least three distinct lines of differing SBV slopes. The only exception was the west control, where four slopes were obtained. This anomaly could be attributed to the variation of surfacing material, and degree of compaction within the upper crust of the stone surfacing, and occurring within a vehicular stopping zone.

SBV's of the various slopes in each plot were computed and are summarized in Table 38, being denoted as 1, 2 and 3, representing the surfacing material, fiber base, and subgrade, respectively. Thus SBV (1) should represent the stiffness of the three layered system, SBV(2) should represent stiffness of the fiber base plus subgrade material, and SBV(3) should represent stiffness of the subgrade material only. As expected, SBV(1) > SBV(2) > SBV(3), in all cases. Examination of the data in Table 38, indicates that the western half of the Mortenson Road fiber test section was stronger than the eastern half, primarily due to the fact that the road materials were more granular towards the western half.

On close examination of SBV(3), it was observed that subgrade support varied considerably within the fiber test section. Subgrade support of the two control sections was approximately the same. Test locations 1, 2

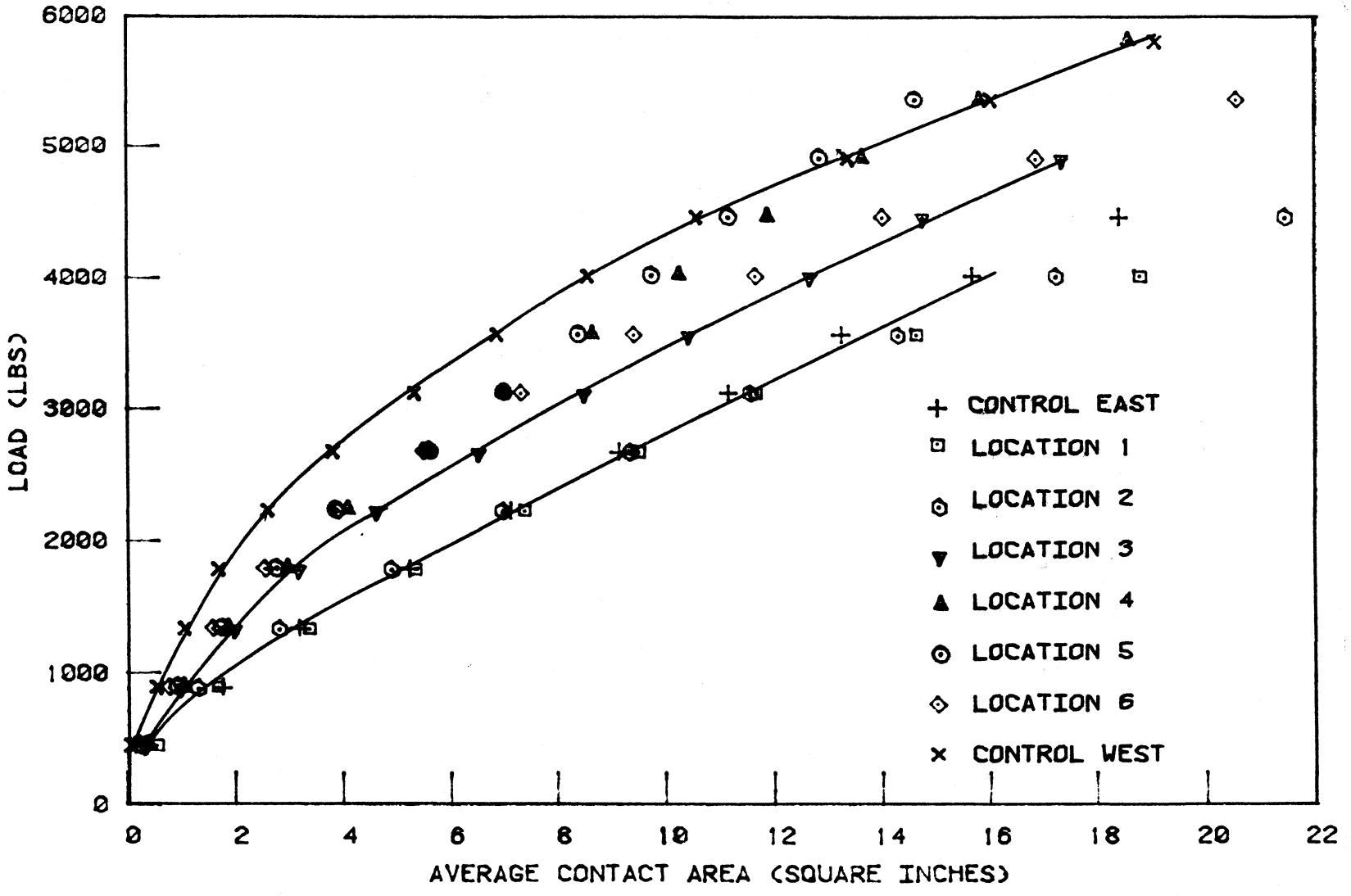

Figure 107. Average spherical Bearing Value plot, Story County Mortenson Road.

Table 38. Mean SBV results for Mortenson Road Test Section

Testing Locations	Fiber Content, %	SBV(1) Surfacing Material, psi	SBV(2) Fiber Base, psi	SBV(3) Subgrade psi
East Control	0.00	314	223	163
Location 1	0.076	315	216	126
Location 2	0.003	349	205	125
Location 3	0.029	472	253	194
Location 4	0.010	606	269	180
Location 5	0.035	525	321	257
Location 6	0.034	606	304	137
West Control	0.00	370	255	156
Ratio of Mean Value of Locations 1, 2, 6 vs. Mean Value for Controls		$\frac{423.3}{342.0}$ = 1.24	$\frac{241.7}{239.0}$ = 1.011	$\frac{129.3}{159.5}$ = 0.811
Ratio of Mean Value of Locations 3 & 4 vs. Mean Value for Controls		$\frac{539.0}{342.0}$ = 1.58	$\frac{261}{239}$ = 1.09	$\frac{187}{159.5}$ = 1.17
Ratio of Mean Value of Location 5 vs. Control		$\frac{525}{342}$ = 1.54	$\frac{321}{239.0}$ = 1.34	$\frac{257}{159.5}$ = 1.61
Ratio of Mean Value for all Fiber Locations Except Location 5 vs. Control		$\frac{469.6}{342.0}$ = 1.37	$\frac{249.4}{239.0}$ = 1.04	$\frac{152.4}{159.5}$ = 0.956
Ratio of Mean Value for all Fiber Treated Locations vs. Control		$\frac{478.8}{342.0}$ = 1.40	$\frac{261.3}{239.0}$ = 1.09	$\frac{109.8}{159.5}$ = 1.06

and 6 indicated a subgrade support which was about 80% that of the two controls. Subgrade support of locations 3 and 4 was about 17% higher than that of the controls, while location 5 was about 61% greater than the controls. When subgrade values for each fiber location were averaged, then compared to the average control, it was observed that the fiber section subgrade was only about 6% higher than that of the control.

Further analysis of results of Table 38 showed that overall SBV(1) for the fiber section was 40% greater than the control, while SBV(2) was 9% greater than the control. Initially, the three layers were completely intact, but when the surfacing material began to fracture, base fiber debonding started to occur. By the time the fiber base experienced failure, most of the fibers had debonded, and were thus rendered ineffective as reinforcement, insignificantly contributing to the enhancement of the remaining base-subgrade layered support. This explains why only a 9% increase, due to fiber inclusion, was observed for SBV(2). It should be noted that the 40% increase in overall composite layered strength was comparable to the increases obtained for unconfined compressive strength and vertical strain modulus during the laboratory investigation.

Laboratory data have also indicated greater increases in fiber composite strengths where more granular materials were utilized. An equivalent condition is noted in the average field data of Table 38. Only about a 24% increase in support was obtained for the finer grained material locations 1, 2 and 6, while a 58% increase in support was observed for the more granular locations 3 and 4.

Spherical bearing values have been correlated with other tests commonly used for evaluating in-situ characteristics of highway materials, Figure

108. Two more commonly used parameters for estimating required pavement thickness are CBR and Modulus of Subgrade reaction, K. Applying the average SBV(1) data from Table 38 (342 for the untreated and 479 for the fiber treated Mortenson Road materials) to Figure 108, produced an estimated unsoaked CBR value for the untreated of 39, while that of the treated material was 60; a 54% increase in CBR. Again applying the average SBV(1) data from Table 2 produced an estimated modulus of subgrade reaction for the untreated Mortenson Road material of 1020 psi, while that of the treated material was about 1440 psi, a 40% increase in K. Such suggested increases in both CBR and K are within the range observed for various parameters obtained during the laboratory investigations.

SBV contact area is a direct function of vertical deformation. A load vs. SBV contact area plot is essentially a plot of load vs. vertical deflection, since π and d remain constant during the test. The SBV results discussed above, thus represent the stiffness of the material in the vertical direction. As was noted in the laboratory investigation however, primary benefits may be achieved in the lateral direction. As a consequence, vertical loads versus corresponding lateral deformations were plotted and analyzed. Figure 109 presents the plot of average vertical load versus average lateral deformation obtained two inches from the center of load application for the various Mortenson Road SBV locations.

It can be observed in Figure 109, that each plot may again be broken into three states of mechanical behavior. The first is characterized by mobilization of little or no horizontal deformation. The second shows increasing horizontal deformation with increasing load. The third is

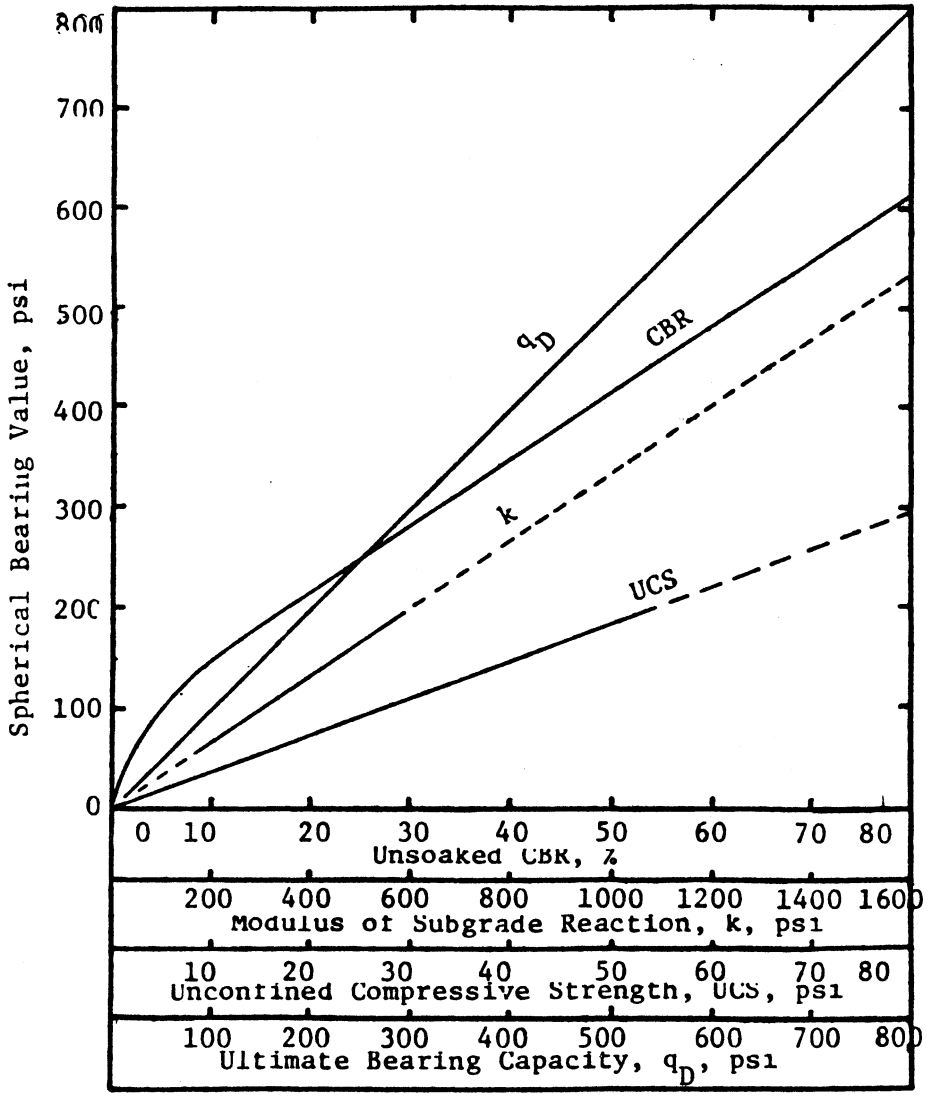

Figure 108. Spherical bearing value versus CBR, modulus of subgrade reaction, unconfined compressive strength, and ultimate bearing capacity (circular loaded area) of a silty clay subgrade (from Butt et al., 6).

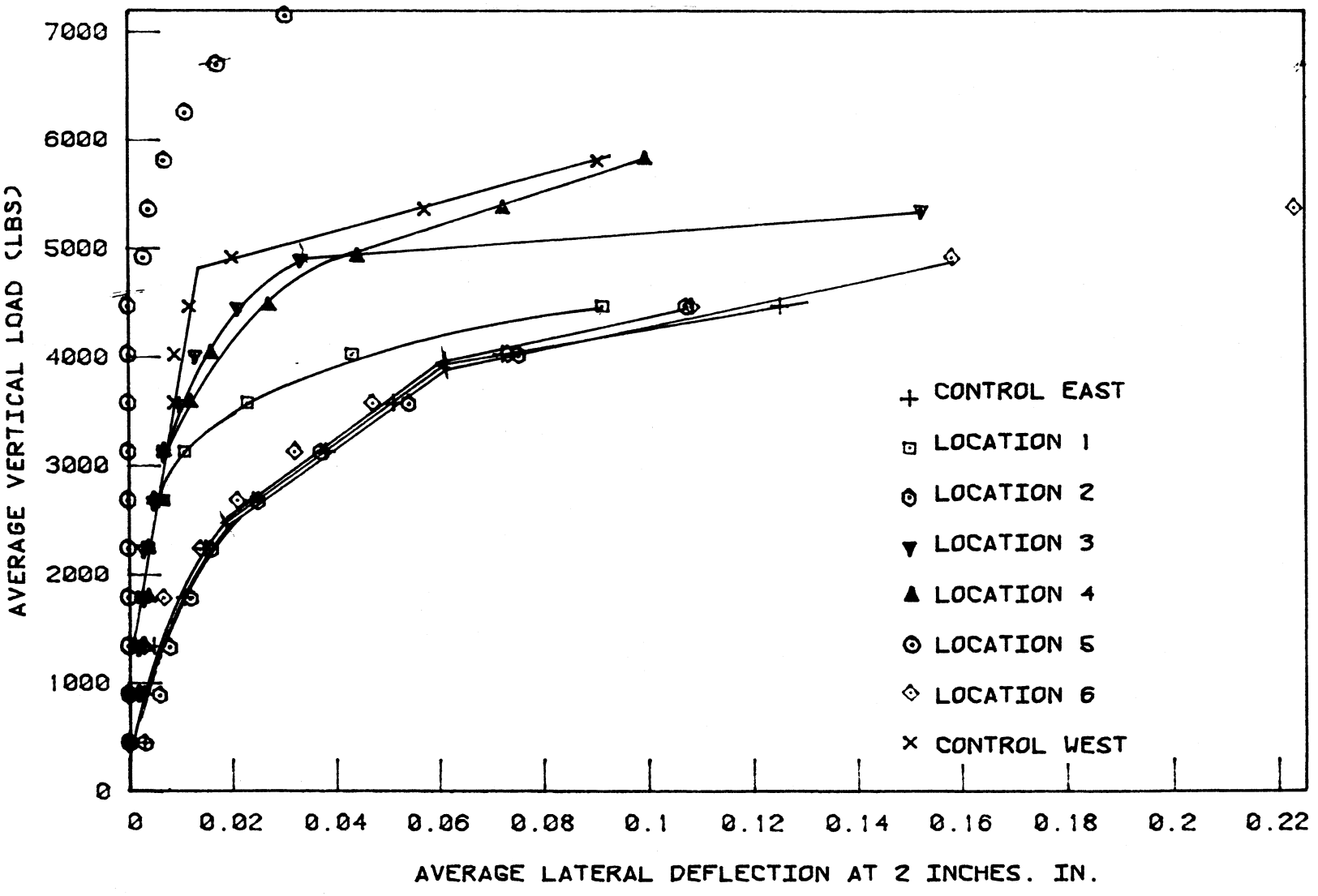

Figure 109. Average SBV Vertical Load versus Lateral Deformation, Story County Mortenson Road.

characterized by large increases in lateral deformation at relatively constant loads; i.e., a state of near plastic flow. Within the second state however, there appears a region of load versus lateral deformation where the rate of deformation begins to exceed the rate of loading; a stage not unlike the proportional limit from the stress-strain plot of a purely elastic material, indicating incipient failure. In-situ failure of the soil-fiber composite was thus defined from Figure 109 as the point at which the rates of lateral deformation and loading were about equal and thus failure would be starting. This condition would also be analogous to a roadway where a rate of increase of lateral deformation greater than the rate of increase of loading would be indicative of a considerable amount of rutting.

Table 39 presents data obtained from Figure 109 for the above noted failure condition. At the assumed point of failure, each load, vertical deformation, and horizontal deformation were obtained, and the ratio of horizontal to vertical deformation, contact area and failure stress were computed.

Vertical deformation is a function of the initial degree of compaction as well as the deformation characteristics of a material. Therefore the variation of vertical deformation may not be totally indicative of a soil-fiber composite material's properties, since the degree of compaction as well as the soil-fiber in-situ properties have already been noted to vary within the Mortenson Road test section. On the other hand, horizontal

Table 39. Average in-situ SBV deformations and stresses at defined failure, Mortenson Road

Testing Locations	Fiber Weight Fraction,* %	Vertical Deformation, in.	Horizontal Deformation, in.	Ratio of Horizontal to Vertical Deformation	Failure Stress, psi	Moisture Content, %
Control East	0.0	0.456	0.024	0.053	312	8.9
Location 1	0.076	0.452	0.011	0.024	367	8.7
Location 2	0.003	0.410	0.020	0.049	319	9.0
Location 3	0.029	0.906	0.032	0.035	288	7.6
Location 4	0.010	0.655	0.016	0.024	326	5.6
Location 5	0.035	0.745	0.017	0.023	477	6.9
Location 6	0.034	0.200	0.008	0.040	474	6.1
Control West	0.0	0.833	0.020	0.024	313	5.2
Average Fiber Section		0.561	0.017	0.033	375	7.33
Average Control		0.645	0.022	0.039	312.5	7.04
Ratio of Fiber to Control		0.87	0.77	0.85	1.20	1.04

*As determined by random screening tests of in-situ samples.

deformations begin to take place when the compaction process is virtually complete. Consequently, lateral deformation may be a more reliable parameter for predicting the integrity of soil-fiber composite materials. Ratio of horizontal to vertical deformation at the defined point of failure may be indicative of the overall stability of the entire roadway structure, since if a material is strong in the lateral direction it should resist a considerable amount of vertical deformation prior to failure; for a stronger material, this ratio should be lower than that of a weaker material. Failure stress defines the vertical stress at point of failure and was computed by dividing load at the point of failure with the corresponding contact area.

Examining Table 39, it is observed that the average vertical deformation at the defined point of failure for the fiber treated materials was 87% that of the control. Locations having higher moisture contents tended to fail at lower vertical deformations than locations with lower moisture contents; a normally anticipated condition, since a moisture softened soil would be more susceptible to large vertical deformations.

Horizontal deformations appeared to be influenced by quantity of the fiber. For example control east, and locations 1 and 2, Table 39, each experienced approximately the same average vertical deformation, but horizontal deformation in location 1 was 0.011 inch while that in location 2 and control east were 0.020 and 0.024 inch respectively. Noting that location 2 and control east apparently had lower percentages of fiber, the significant improvement in horizontal deformation in location 1 should be attributed to the 0.076%, 360 dpf fibrillated polypropylene that was present.

Moisture contents in each of these three locations was equivalent.

As may be seen in Table 39, the inclusion of fibers reduced the amount of horizontal deformation by about 23%. Results from the laboratory repetitive load Iowa K-Test showed that 0.2%, 360 dpf fibrillated polypropylene, reduced horizontal strain at optimum moisture content by about 13%, suggesting that such a laboratory test procedure may be valid in predicting field or in-situ lateral stability response.

Ratio of horizontal to vertical deformation at the defined failure appeared to be a reasonable parameter for expressing an overall stability related to strain characteristics of the Mortenson Road soil-fiber composite. Table 39 suggests that this parameter was influenced by both soil type and fiber content. Variation of moisture content did not suggest any marked effect on deformation ratios. Overall, inclusion of the fiber appeared to reduce this ratio by about 15%.

The defined failure stress expressed a contact stress at which plastic flow starts to occur. Again, this parameter appeared to be influenced more by fiber weight fraction and type of soil material than by moisture content, Table 39. The ratio of fiber treated failure stress to untreated control failure stress, indicated a general 20% improvement due to fiber inclusion. This parameter also tends to express the overall stability of a roadway soil fiber composite material. For example, if a weak material is encountered, contact area will increase considerably, while the corresponding increase in load would be negligible, therefore producing a low contact or failure stress.

Table 40 is a summary of the Linn County Prairieburg SBV data for average lateral deformations obtained within the various fiber and control sections. Sections 1, 3, 4 and control west experienced both compressive and tensile deformations. Compressive deformations resulted from initial compaction of roadway materials that occur at the beginning of load application. Section 3 experienced the lowest amount of lateral deformation while control west experienced the highest amount of lateral deformation. Section 2 appeared to be an exception, since failure apparently occurred within very early stages of the testing and prior to full mobilization of lateral deformations. Upon comparison with the average lateral deformations, the fiber treated sections produced lesser amounts of lateral deformation than either control, with the exception of sections 2 and 4.

Ratios of horizontal to vertical deformation were plotted versus energy, as illustrated in Figures 110 and 111. The plots appeared to define at least two, and in most cases, three types of material behavior. However, the trends of the plots were not similar to the trends observed with the finer grained Mortenson Road, Figures 105 and 106. In the case of the more sandy Prairieburg sections, ratios tended to increase with increasing energy implying the possibility of utilizing the concept of Poisson's ratio. In the Mortenson Road data, the deformation ratios initially decreased with increasing energy and then levelled. With the more sandy Prairieburg material, the initial densification deformation was not generally observed during the early stage of loading. There was generally good agreement between the two roadway materials during the latter stages of loading. It was thus apparent that the two materials professed different in-situ load-

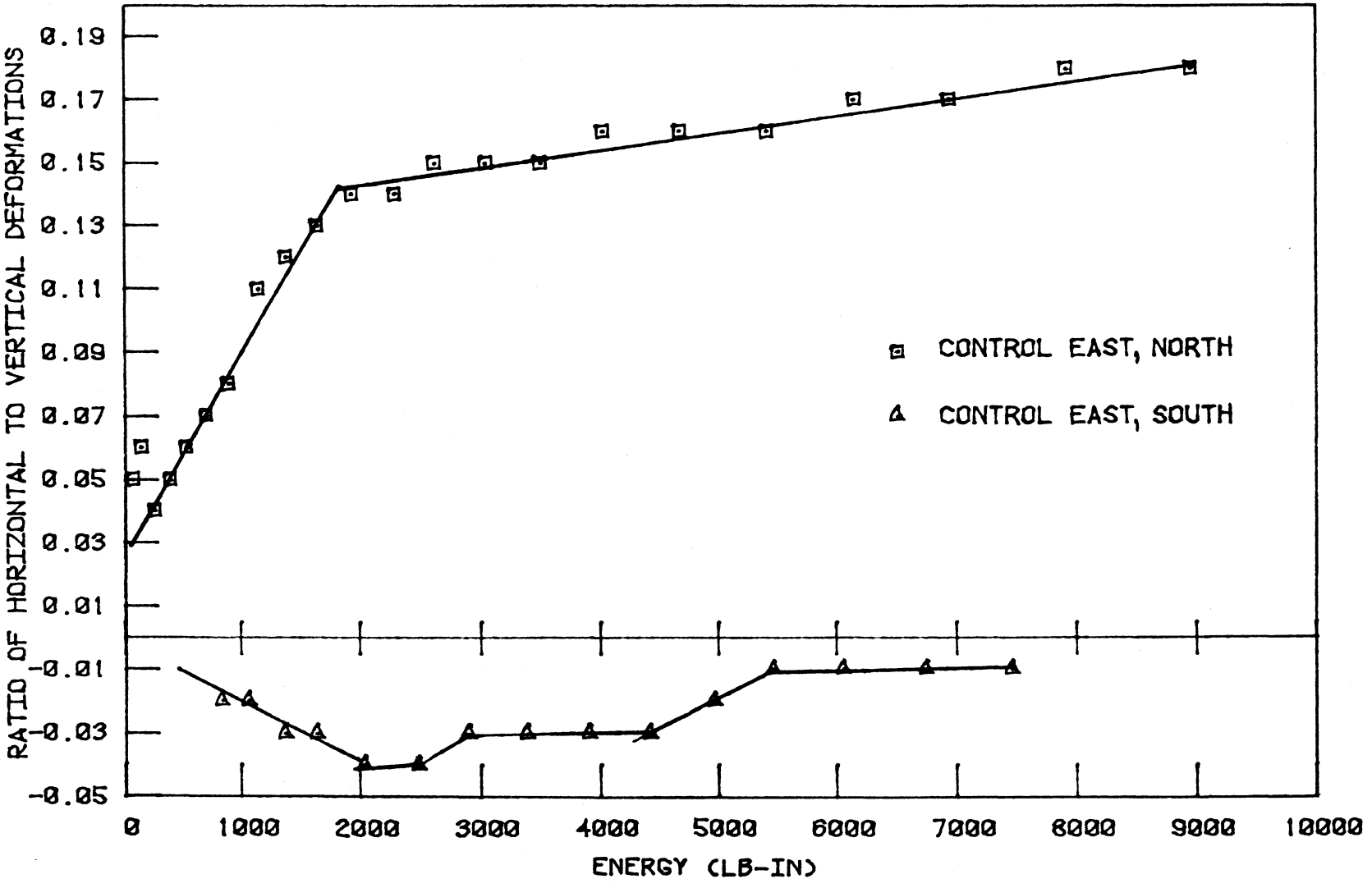

Figure 110. Insitic Deformation Ratios Versus Energy, Linn County Prairieburg.

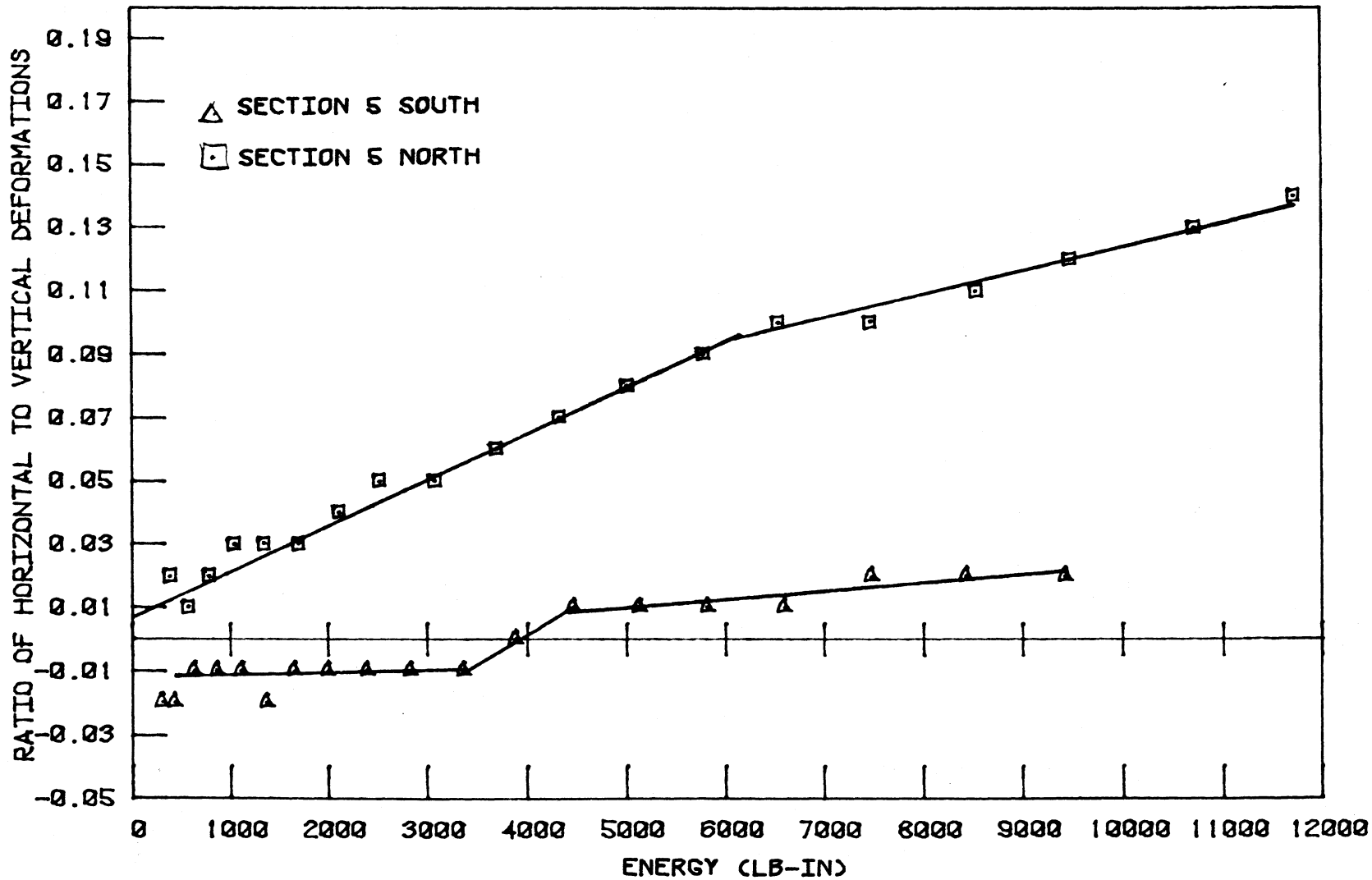

Figure 111. Insitic Deformation Ratios Versus Energy, Linn County Prairieburg.

Table 40. SBV load vs. lateral deformation at 2" from load centerline, Linn County, Prairieburg

Load, lbs.	Average Lateral Deformation, in.								
	Control East	Section 1	Section 2	Section 3	Section 4	Section 5	Section 6	Control West	Control Average
447	0	0	0	-0.001	0	0.000	0	0	0
894	0	-0.001	0.002	-0.001	0	0.000	0	0	0
1340	0.002	-0.003	0.002	-0.001	-0.501	0.000	0	0	0
1787	0.003	-0.004	0.001	-0.001	-0.001	0.001	0.001	-0.001	0.001
2234	0.003	-0.006	0.001	0.000	-0.001	0.001	0.001	-0.001	0.001
2681	0.004	-0.007	0.003	0.000	-0.001	0.001	0.001	-0.001	0.002
3128	0.005	-0.008	0.004	0.000	0.000	0.002	0.002	0.000	0.003
3574	0.007	-0.005	0.006	0.001	0.002	0.003	0.003	-0.001	0.003
4021	0.009	-0.008	0.010	0.001	0.006	0.004	0.004	0.001	0.005
4468	0.014	-0.008	0.013	0.001	0.010	0.005	0.005	0.003	0.009
4915	0.014	-0.005	0.017	0.002	0.014	0.007	0.009	0.006	0.010
5362	0.016	-0.002	0.021	0.004	0.020	0.009	0.010	0.010	0.013
5808	0.019	0.004		0.005	0.025	0.011	0.011	0.014	0.017
6255	0.020	0.010		0.007	0.028	0.014	0.012	0.020	0.020
6702	0.022	0.021		0.009	0.033	0.021	0.015	0.027	0.025
7149	0.025	0.032		0.010	0.038	0.029	0.020	0.035	0.030
7598	0.029	0.046		0.014	0.049	0.037	0.025	0.044	0.037
8042	0.033	0.058		0.019	0.061	0.047	0.035	0.056	0.045
8489	0.038	0.082		0.025	0.068	0.059	0.042	0.073	0.056
8936	0.045	0.110		0.033	0.072	0.073	0.047	0.106	0.076
9383	0.051			0.046	0.084	0.085		0.140	0.096
9830	0.057			0.067	0.097				
10276	0.065								
10723	0.074								

deformation characteristics.

Although trends exhibited by the Prairieburg results were somewhat different from those of Mortenson Road, breakpoints in the plots still tended to provide corresponding techniques of analysis. Table 41 summarizes the average load and contact areas obtained for the various Prairieburg fiber and control sections, and Figure 112 presents the average load versus contact area plots.

The plots of Figure 112 were broken into three sections, and SBV(1), SBV(2) and SBV(3) were again computed, Table 42. SBV(1) values exhibited a considerable amount of variation. SBV(1) for the fiberglass Section 3 was 1396.0 psi while that of the 15 dpf polypropylene Section 2 was 472.0 psi. This widespread variation between adjacent Sections 2 and 3 was attributed to the extremely weak subgrade within portions of Section 2, which was reflected in both the SBV(2) and SBV(3) data. In addition, it was visually observed that portions of Section 2 showed more rutting than any other section. All fiber sections except Section 3 produced lower SBV(1) values than either control, implying that fiber reinforcement might not be effective. SBV(2) values portrayed the same general trends as SBV(1). However, comparative use of the SBV values only, may be misleading for analytical purposes.

As noted previously, SBV(3) represented the potential stability of the subgrade material. Therefore, ratios of SBV(2)/SBV(3) and SBV(1)/SBV(3) were computed for each section and are summarized in Table 42.

The ratio of SBV(2) to SBV(3) represents the improvement in stability produced by incorporation of the fibers into the roadway materials. The average ratio for the controls was 1.53. Comparing 1.53 with the ratios

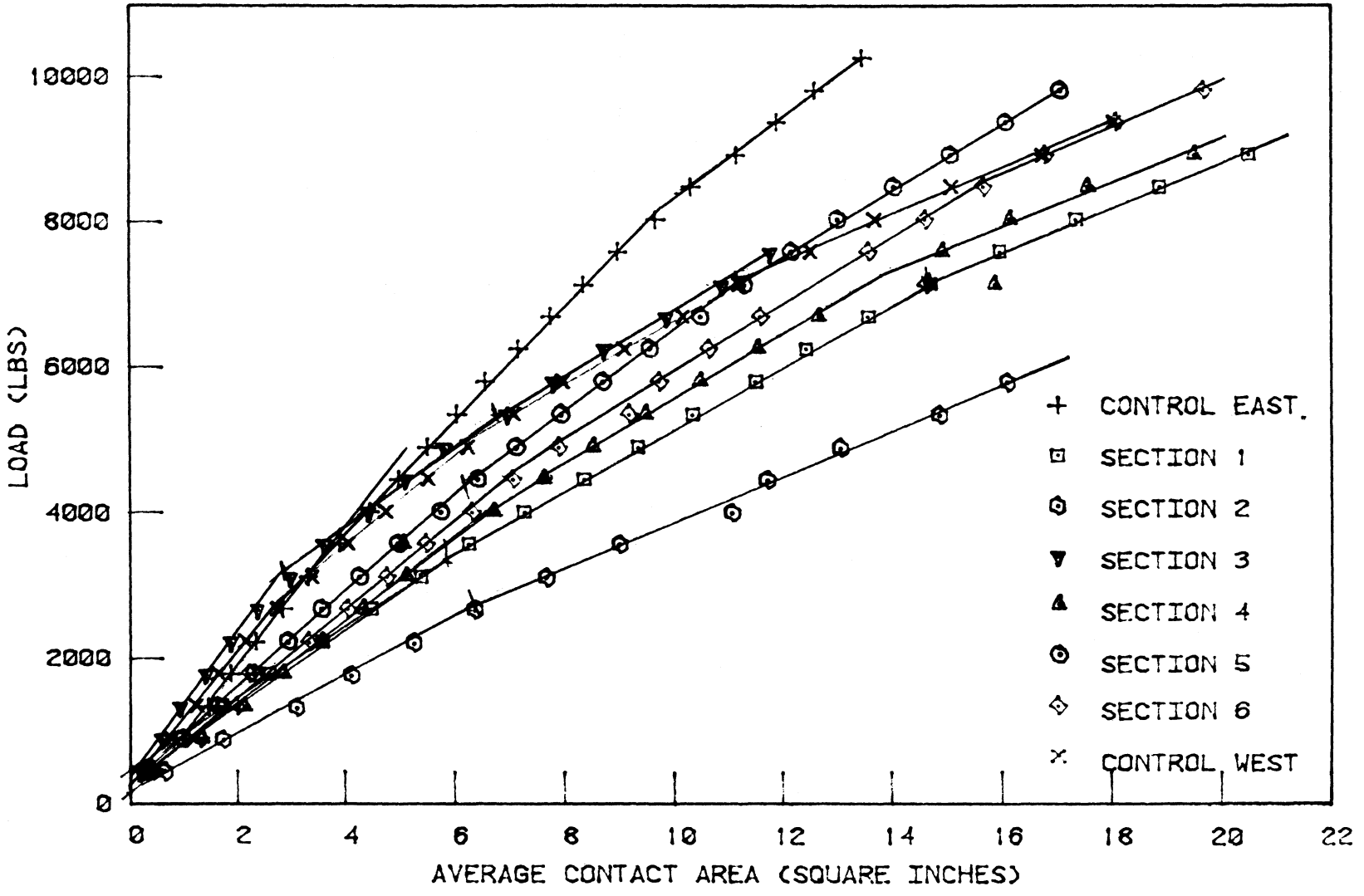

Figure 112. SBV average load versus contact area, Linn County Prairieburg sections.

Table 41. Average SBV load vs. contact area, Linn County, Prairieburg for tests conducted May 12, June 2, and June 16, 1982

	Average SBV Contact Area, sq. in.							
Load, lbs.	Control East	Section 1	Section 2	Section 3	Section 4	Section 5	Section 6	Control West
447	0.29	0.34	0.65	0.18	0.36	0.22	0.43	0.27
894	1.00	0.93	1.74	0.58	1.29	0.94	1.30	0.76
1340	1.45	1.71	3.11	0.93	2.09	1.59	1.99	1.23
1787	1.88	2.60	4.14	1.41	2.82	2.26	2.22	1.64
2234	2.35	3.59	5.28	1.88	3.55	2.91	3.35	2.15
2681	2.87	4.49	6.38	2.39	4.30	3.54	4.06	2.76
3128	3.33	5.40	7.67	3.00	5.09	4.23	4.77	3.41
3574	3.91	6.27	9.02	3.62	5.03	4.93	5.49	4.07
4021	4.46	7.28	11.08	4.43	6.68	5.71	6.32	4.75
4468	4.99	8.36	11.73	5.12	7.59	6.38	7.07	5.53
4915	5.51	9.35	13.09	5.82	8.48	7.08	7.89	6.25
5362	6.05	10.35	14.89	6.96	9.45	7.89	9.19	7.08
5808	6.56	11.51	16.13	7.79	10.44	8.65	9.74	7.96
6255	7.17	12.44		8.72	11.51	9.51	10.64	9.09
6702	7.74	13.59		9.85	12.64	10.43	11.60	10.16
7149	8.84	14.72		10.87	15.84	11.24	14.63	11.20
7596	8.96	15.98		11.77	14.89	12.11	13.58	12.52
8042	9.66	17.37			16.13	12.97	14.61	13.70
8489	10.31	18.88			17.54	13.99	15.67	15.09
8936	11.13	20.49			19.47	15.02	16.80	16.76
9383	11.89					16.03	18.08	18.05
9830	12.58					17.03	19.67	
10276	13.47							
10723								

Table 42. Mean of SBV results for Prairieburg Test Sections*

Section	Fiber Content %	SBV(1) psi	SBV(2) psi	SBV(3) psi	SBV Ratios SBV(1)/SBV(3)	SBV(2)/SBV(3)	SBV(1)/SBV(2)	Average Moisture Content, %
Control East	0	1063.5 ± 441.2	711.6 ± 176	517.5 ± 149.2	2.06	1.38	1.46	6.10
Section 1	0.06	547.7 ± 235	466.0 ± 171.2	266.2 ± 119.7	2.06	1.75	1.18	6.50
Section 2	0.13	472.0 ± 196	343.7 ± 134.8	252.2 ± 123.8	1.87	1.36	1.37	6.42
Section 3	0.10	1396.0 ± 874.8	705.8 ± 375.8	392.5 ± 167.3	3.56	1.80	1.98	5.47
Section 4	0.29	589.5 ± 76.0	429 ± 86.3	293.8 ± 68.3	2.01	1.46	1.37	5.83
Section 5	0.29	643.8 ± 116.5	495.2 ± 57.5	400.8 ± 66.3	1.61	1.24	1.30	6.16
Section 6	0.10	643.7 ± 77.4	446.2 ± 85.7	250.3 ± 87.4	2.57	1.78	1.44	5.92
Control West	0	736.0 ± 189	508.2 ± 125.9	304.3 ± 102.7	2.42	1.67	1.45	5.37

*All values are the mean from combining tests taken May 12, June 2, and June 16, 1982.

obtained for each fiber section, shows that Sections 1, 3, and 6 performed better than the controls. The stability increase appeared to be independent of type of fiber, but was dependent on the fiber weight fraction. Only those sections treated with low fiber weight fractions produced any stability increase.

Ratios of mean SBV(1) to SBV(3) represent the increase in stability due to addition of fiber and the surfacing material. The average SBV ratio for the controls was 2.24, Table 42. Comparing this with the ratios obtained for the fiber sections, it was observed that only sections 3 (fiberglass) and 6 (fibrillated polypropylene) produced improved stability. Noting that the SBV(1) to SBV(3) ratio for Section 3 was very high, it might be concluded that this large increase in ratio was potentially due to a larger quantity of surfacing material than in the other sections.

Ratios of mean SBV(1) to SBV(2) shown in Table 42, serve as an indicator of the effect of surfacing material support in relation to support provided by each individual base. With the exception of Section 3, support provided by the surfacing material was not as pronounced as support provided by the fiber bases, as obtained through the SBV(2) to SBV(3) ratios.

As previously discussed, conventional load vs. SBV contact area plots are essentially plots of load vs. vertical deformation, since π and d remain constant during the test. Such SBV results represent only the stiffness of an in-situ material in the vertical direction. Consequently, vertical loads versus corresponding lateral deformations were plotted and analyzed for the Prairieburg sections, Figure 113.

As may be observed in Figure 113, each plot could again be broken into

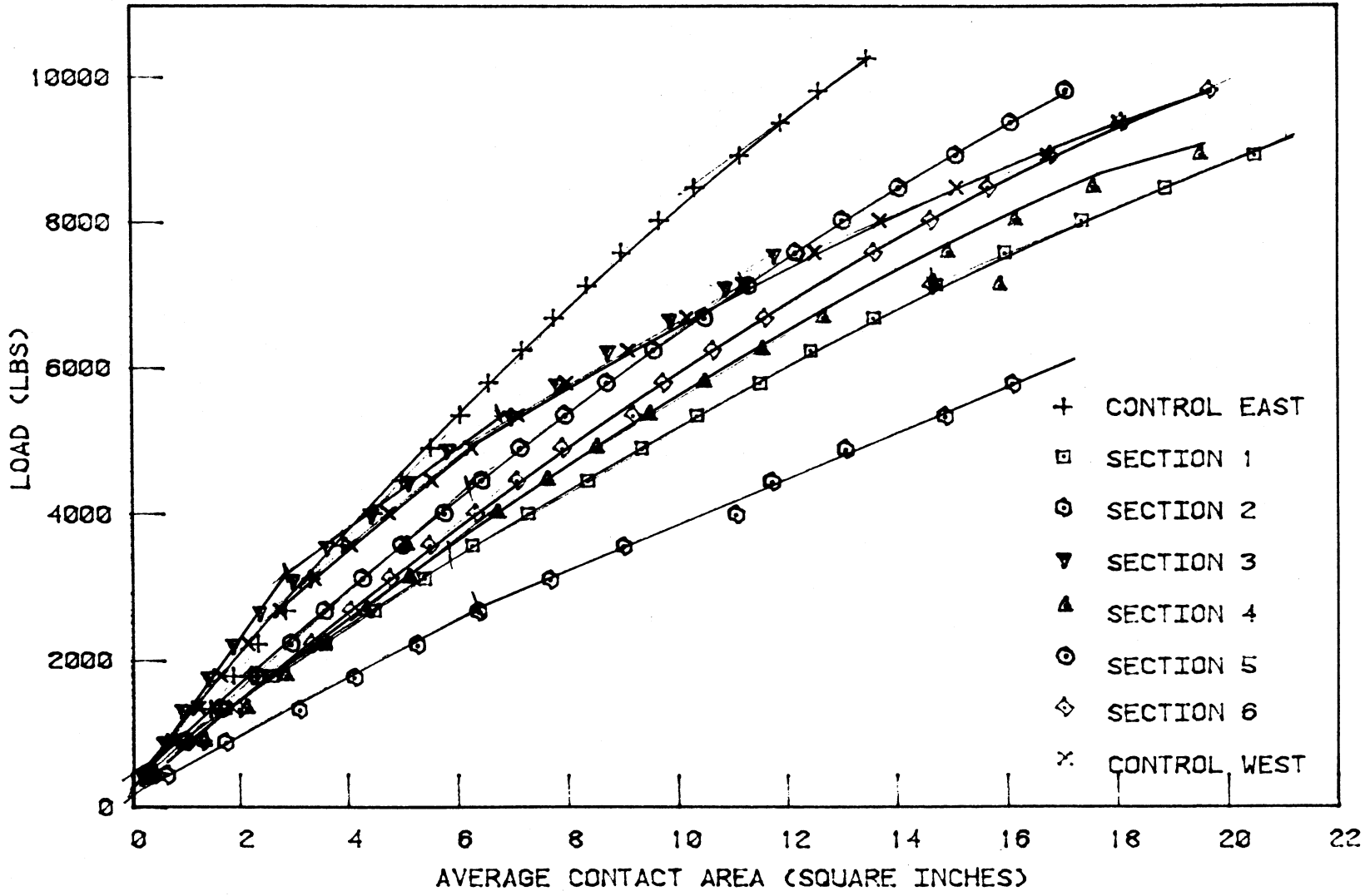

Figure 113. Average SBV Vertical Load versus Lateral Deformation, Linn County, Prairieburg.

three states of mechanical behavior; the first characterized by mobilization of little or no horizontal deformation, the second showing increasing horizontal deformation with increasing load, and the third characterized by large increases in lateral deformation at relatively constant loads; i.e., a state of near plastic flow. Such trends were very similar to those noted with the Mortenson Road in-situ modified SBV tests, thus confirming that vertical load versus lateral deformation analyses might better describe actual material behavior.

Table 43 presents data obtained from Figure 113 for the state of in-situ failure previously discussed with the Mortenson Road section. At the assumed point of failure, each load, vertical deformation and horizontal deformation were obtained, and the ratio of horizontal to vertical deformation contact area and failure stress were computed. In general the fiber treated sections appeared to experience higher vertical deformation than the controls, a condition consistent with observations made in the laboratory investigations. However, with the exception of Section 4, all fiber treated sections experienced smaller amounts of lateral deformations than the controls, again consistent with observations from the laboratory investigation.

Ratio of horizontal to vertical deformation at the defined failure point was assumed to be a reasonable parameter for expressing the overall stability related to strain characteristics of the roadway soil-fiber composite. All fiber treated sections produced lower ratios than the controls, implying an improvement in stability of the roadway materials. Sections 1, 3, and 6 produced the lowest ratios, confirming that fiber

Table 43. Average in-situ SBV deformations and stresses at defined failure, Prairieburg

Testing Location	Fiber Type and Weight Fraction	Vertical Deformation, in.	Horizontal Deformation, in.	Ratio of Horizontal to Vertical Deformation	Failure Stress, psi
Control East	None	0.51	0.03	0.059	828
Section 1	0.06% 15 dpf polypropylene	0.78	0.02	0.026	476
Section 2	0.13% 15 dpf polypropylene	-	-	-	-
Section 3	0.1% Type E Fiberglass	0.62	0.02	0.033	680
Section 4	0.29% Type E Fiberglass	0.74	0.035	0.047	520
Section 5	0.29% 360 dpf fib. polypropylene	0.50	0.02	0.040	652
Section 6	0.1% 360 dpf fib. polypropylene	0.56	0.015	0.027	582
Control West	None	0.54	0.025	0.046	639

reinforcement was most effective at the lower fiber weight fractions. The ratios for sections 1, 3, and 6 were 0.026, 0.033 and 0.027, respectively, indicating that the 360 dpf fibrillated and 15 dpf monofilament polypropylene fibers produced almost equal amounts of lateral to vertical deformation ratios, and again confirming that in-situ fiber reinforcement potential may be more sensitive to fiber weight fraction than to types of fiber.

Since the Linn County Prairieburg soil-fiber composite sections were covered with six inches of portland cement concrete pavement in late June, 1982, no further modified SBV tests could be conducted therein during the fall season. However, a series of tests were conducted on the Story County Mortenson Road section in September. In order to render further credibility to the testing and analytical procedure adapted with the modified SBV test, 8 tests were conducted on the east and west controls, while 14 tests were performed on the fibrillated polypropylene fiber section. In addition, lateral deformations were measured in duplicate at 2 inches from center of load application only.

Plots of this data could again be broken into the three mechanical states of load-deformation previously noted as SBV(1), SBV(2), and SBV(3), used to indicate respective stabilities and stiffnesses of the full depth structure, fiber base plus subgrade, and subgrade only, Table 44. Incorporation of the 360 dpf fibrillated polypropylene fibers increased the overall SBV(1) by 32%. Earlier SBV(1) results noted that the fibers improved stability by about 37%, indicating that the modified SBV test is reproducible. The September 1982 results however should be more

Table 44. Mean of SBV results for Mortenson Road section, September 1982

	Untreated Control*	Fiber Treated**	$\frac{\bar{x} \text{ Treated}}{\bar{x} \text{ Untreated}}$
SBV(1)	403.4 ± 133.3	530.8 ± 162.7	1.32
SBV(2)	232.1 ± 53.7	259.2 ± 62.7	1.12
SBV(3)	135.9 ± 37.3	133.7 ± 27.2	0.98
Ratio $\frac{SBV(1)}{SBV(3)}$	3.03 ± 0.79	4.18 ± 1.75	1.38
Ratio $\frac{SBV(2)}{SBV(3)}$	1.78 ± 0.43	1.97 ± 0.46	1.11
Stress at (1), psi	474.1 ± 128.5	612.0 ± 188.5	1.29
Stress at (2), psi	326.3 ± 90.4	346.9 ± 75.6	1.06
Stress at (3), psi	278.4 ± 79.9	286.2 ± 55.5	1.03

*Mean and standard deviation of 8 values.

**Mean and standard deviation of 14 values.

representative of performance improvement since a larger number of tests were involved, each being conducted at the same point of time. The increase in SBV(1) due to fiber treatment was also similar to data observed from several of the laboratory tests.

Improvement of SBV(2), base plus subgrade, was only about 12%. The earlier observation of SBV(2) was about 9%, further confirming reproducibility of the test data. Representing the stability and stiffness of the subgrade, SBV(3) for the untreated and fiber treated sections were basically identical, confirming the potential for use of SBV(3) as a common denominator for any performance ratio analysis.

Ratios of SBV(1) to SBV(3), and SBV(2) to SBV(3), are also presented in Table 44. Percentages of improvement were quite similar to those noted above.

Stresses for each break point at which the slopes of the individual load versus contact curves changed are presented in Table 44. The stress at break point (1) represented the stress condition at which the surfacing material lost most of its load capacity. Similarly the stress conditions were defined for the fiber base (stress at (2)) and the subgrade (stress at (3)). The latter may represent the stress at which the subgrade, as well as the roadway structure tends to fail, or at least experiences considerable plastic flow. As may be noted from the table, the potential percentages of improvement of breakpoint stresses due to fiber incorporation into the Mortenson Road material were not unlike those noted above.

SUMMARY AND CONCLUSIONS

The purpose of the study reported herein was to conduct a laboratory and field investigation into the potential of improving (a) soil-aggregate surfaced and subgrade materials, and (b) localized base course materials, through fibrous reinforcement. The study was also directed to determining (a) what type or types of fibers were effective as reinforcement agents, (b) were workable fibers commercially available, and (c) whether such fibers would be effectively incorporated with conventional construction equipment and employed in practical field applications.

A review of literature demonstrated that fiber composites are comprised of a matrix material, plus fibrous materials. Matrix materials could be classified into organic and inorganic, while fibers could be classified into synthetic and natural depending on their origin. Parameters influencing the integrity of fiber composites were fiber volume fraction, fiber diameter, fiber length, fiber orientation, and strength of the fiber-matrix interfacial bond. The two most important parameters appeared to be fiber volume fraction and fiber-matrix interfacial bond. Short fiber composite efficiency factors appeared to account for the effects of length and orientation. What sparse studies of soil fiber composites that could be found showed behavior similar to fiber reinforced concrete. Therefore techniques applied in fiber concrete might be appropriate in regard to a study of soil-fiber composites.

Types of fibers that were initially screened for possible investigation included nylons, polypropylenes, dacron, kevlar, lycra, polyesters and fiberglass. Configurations of these fibers ranged from 1.5 to 360

denier, 0.25 to 6 inch lengths, monofilaments, crimped and uncrimped, pentalobal cross section, tape, yarn, and fibrillated tape. Costs, survivability in a soil, availability, geometry, mechanical properties, and ability for incorporation by conventional mixing techniques into a soil reduced the final fiber selections to Type E fiberglass, polypropylene monofilament (both uncrimped and crimped), and fibrillated polypropylene tape. Diameters and lengths of these fibers were 0.002 - 0.009 inch and 0.25 to 1.5 inch respectively. Laboratory mixing of such selected fibers could easily be accomplished by either hand or mechanical mixing techniques. Fibers longer than 2-3 inches were extremely difficult to laboratory mix with any soil. Crimped fibers were somewhat more difficult to mix than the uncrimped fibers.

Guidelines for selection of soils for this investigation involved the potential for field test sections of selected fibers. Roadway sites, and their respective soils, were sampled from Sioux City, Story County, and Linn County. AASHTO classifications of the sampled soils ranged from A-2-4(0) to A-6(3). Ultimately, test sections were constructed in Linn County near Prairieburg, Iowa, and in Story County, on Mortenson Road near the southwest corner of Ames.

In the laboratory investigation, Iowa K-Test data was analyzed through the computer aided Statistical Analysis System (SAS). While some relationships were attained between the untreated and fiber treated soils, no basic improvements were noted. Any reinforcing mechanism of fiber which tended to show improvement in c, ϕ, E, K or Q_o required large vertical strains in order to become apparent. The stiff constant elasticity

K-Test mold prohibited the amount of radial strain necessary to mobilize fiber reinforcement, causing the more conventional K-Test to act like a consolidation test, with the soil matrix failing in shear prior to fiber reinforcement mobilization.

Results from unconfined compression testing of the untreated soils and soil-fiber composites provided considerable input into selection of fibers for use in the field test sections.

Incorporation of fibers within each soil tended to decrease maximum dry density and increase optimum moisture content of the composites, due to increased voids caused by fiber seperation of the soil particles.

Unconfined compressive strengths generally increased with increasing fiber weight fraction up to a maximum, with no further increase due to increased fiber contents. In most cases, optimum fiber weight fraction was between 0.05% and 0.4% by dry soil weight. Greater percentage increases in unconfined compressive strengths were generally obtained at higher rather than at lower moisture contents.

Unit strain at failure of unconfined compressive strength specimens, generally increased with increasing fiber weight fraction, indicating improved ductile properties. In some instances, failure did not occur with the higher fiber weight fractions and UCS testing was stopped to avoid causing damage to equipment.

No consistent trends were obtained regarding vertical strain moduli within the UCS testing. E varied from positive improvement to reduction. This parameter exhibited such large variability that statistical modelling was not possible.

Fibers significantly increased the modulus of toughness as determined from the UCS testing, serving as an indicator of how fibers influenced the ductility of the soil-fiber composites.

Compressive strength improvements due to fiber incorporation appeared dependent on gradation characteristics of the soils. While the A-2(4), A-4(0), and A-6(2) soils were all fairly well graded, they did not provide equal amounts of strength increase with equal, or variable, fiber weight fractions. The A-2(4) produced the best results, followed by A-4(0) and A-6(2) soils in that order, and tended to correlate with plasticity of the soils.

Smaller diameter fibers tended to provide the best increases in compressive strength parameters. Overall, the 15 dpf crimped polypropylene fibers appeared to produce the most beneficiation in compressive strength characteristics. Larger aspect ratios, coupled with crimped configurations, thus appeared to most influence integrity of the soil fiber composites.

Modification of the soil matrix through the introduction of low percentages of hydrated lime or type 1 portland cement provided improved matrix-fiber interfacial bonding, resulting in improvements in compressive characteristics, ductility, and control of cracking through brittle failure.

Increased compactive effort, from standard to modified AASHTO, resulted in increased soil matrix strength and somewhat improved interfacial fiber-matrix bond.

Laboratory California Bearing Ratio values indicated improved ratios with the soil-fiber composites, being the most effective in the sandy A-2-4(0) soil and less effective in the finer grained soils.

Cyclic load tests were conducted using a thin-walled variable expansion Iowa K-Test mold in order to study portions of the mechanistic behavior of the soil-fiber composites. In general, the composites showed improved performance at both high vertical stresses and moisture contents above optimum, but appeared due to increased vertical deformations producing higher lateral displacements needed to mobilize tensile properties of the fibers. The efficiency of soil-fiber reinforcement appeared largely dependent on the integrity of the soil-fiber interfacial bond. Maximum beneficiations of fiber reinforcement appeared associated with parameters of horizontal or lateral stability which were sizeably enhanced by addition of fibers into the soil matrix. The 15 dpf crimped polypropylene fibers provided the most improvement in cyclic load test stability parameters, followed by the 360 dpf fibrillated polypropylene and the 15 dpf monofilament fibers. Modification of the Sioux City loessial soil matrix through the addition of 3% Type I portland cement further enhanced the lateral stability characteristics of the soil-fiber composites.

Combined freeze-thaw and cyclic load K-Tests were conducted on Sioux City loessial soil and soil-fiber composites. Use of the fibers decreased freeze-thaw volumetric change on the order of 40% as compared with the untreated soil. When the soil-fiber matrix was modified with a low percentage of cement, freeze-thaw volumetric expansion was eliminated, indicating an extremely stable composite material. Compared to the modified soil matrix, the modified soil-fiber matrix provided up to 40% improvement in composite stiffness as evaluated through the cyclic load test following 10 cycles of freeze-thaw.

Utilizing data from unconfined compression tests, and a concept from fiber reinforced concrete, an overall efficiency factor for several fibers was calculated. The 15 dpf crimped polypropylene fiber composites had the highest efficiency factors, a condition consistent with most of the laboratory investigations.

Ratios of soil particle surface area to fiber surface area were calculated for various fiber weight fractions within the Sioux City loessial soil. These ratios ranged from as high as 15.4 for the fiberglass to less than 1.0 for the 15 dpf polypropylene monofilament fibers. In general, the study suggested a surface area ratio of near 1.0 as probably producing the most beneficial compressive strength and workability (mixing) characteristics.

Through Scanning Electron Microscopy, three types of fibers were compared before and after compacted incorporation and UCS testing within the Sioux City loessial soil. The 15 dpf straight polypropylene exhibited severe surficial damage after compaction and testing, the 360 dpf fibrillated polypropylene incurred less surficial damage, and the fiberglass appeared undamaged. This examination coupled with the UCS testing, suggested that surface damage may relate to greater frictional contact with the soil particles with an accompanying improved reinforcement capability.

A fiber pull-out test was designed to assist in understanding some of the micro-properties of a soil-fiber composite. Utilizing a concept from fiber composite technology and the determined frictional bond strengths from the pull-out test, critical fiber lengths were calculated for the 15 dpf monofilament and 360 dpf fibrillated polypropylene under vertical stresses up to 75 psi. The study demonstrated that as soil-fiber bond was

increased, the length of fiber required to effectively transfer matrix stress to the fibers ultimate stress capacity decreased. Since fiber lengths used in most of the laboratory investigations were less than the calculated critical lengths, the soil-fiber composites should not fail by fiber fracture, but by sliding along the soil-fiber interface. This mode of failure may explain the observed ductility (toughness) of the soil-fiber composites.

Trafficability testing of untreated Sioux City, Mortenson Road and Prairieburg soils indicated that each were incapable of sustained 75 psi wheel loadings when utilized as surface course. Incorporation of fibers in each soil indicated varying degrees of improved stability through rut depth measurements. Further improvement in stability was observed when cement modification of a soil matrix provided increased soil-fiber interfacial bonding.

Results of a study of tensile properties of fiber reinforced soil illustrated that improved tensile properties may be attained when compared to the untreated soil. The magnitude of improvement however appeared dependent on soil and fiber types, though tensile properties may be improved at moisture contents above the untreated optimum.

Construction of the Linn County Prairieburg, and Story County Mortenson Road test sections, demonstrated that fibers could readily be incorporated into a scarified soil material using conventional construction equipment. The most satisfactory mixing technique was provided by blowing fiber into a rotary mixer chamber with a mulch spreader equipped with a flexible hose. Blade mixing provided a reasonably satisfactory random distribution of fibers.

Immediately prior to field compaction, random samples of each Prairieburg and Mortenson Road section were obtained over their full depth and returned to the laboratory, where Proctor size specimens of each were prepared under standard AASHTO T-99 conditions. Average q_u, and E values of the Mortenson fiber section showed distinct improvement over the untreated control during UCS testing, indicative of somewhat improved stability. Each Prairieburg field mix appeared to produce a greater degree of toughness, coupled with reduced brittleness than the untreated control, but only the 360 dpf fibrillated polypropylene specimens showed a definite gain in compressive strength.

Specimens of the Prairieburg field mixed, laboratory compacted materials, were subjected to the cyclic load test. In general, the finer of the three fibers (15 dpf monofilament polypropylene) provided lateral reinforcement benefits coupled with some improvements in vertical stability.

Benkelman beam, plate bearing, and CBR tests were initially used to measure in situ influence and performance of the fiber incorporated test sections versus their adjacent control sections. Results obtained with these tests were considerably varied, and were relatively limited in correlation with the laboratory studies. The reason for this anomaly appeared due to the laboratory tests primarily indicating improved lateral stability characteristics, while each field test was more associated with vertically oriented parameters.

Due to results obtained with the three aforementioned in situ tests, the Spherical Bearing Value (SBV) test was then employed since it has previously been shown to mobilize stresses in a radial direction. While

the conventional SBV test utilizes vertical deformations only, the procedure was modified to also provide measurement of horizontal deformations.

Results obtained from the modified SBV field test were analyzed by several processes. Ratios of measured horizontal to vertical deformations were plotted versus energy, the latter defined as applied vertical loading times the corresponding vertical deflection. Such plots showed three states of material mechanical behavior. Each plot could be associated with properties of the three layered roadway structure of aggregate surface, fiber base and subgrade. SBV(1) represented stability of the composite three layers, SBV(2) the fiber base plus subgrade, and SBV(3) the subgrade only. Results of SBV(1) from several series of such tests of the fiber treated sections showed roughly 30% improvement from that of the untreated controls. SBV(2) data illustrated about a 10% gain, while SBV(3) was essentially equal for subgrade stability values. SBV(1) stability improvements due to fiber incorporation in the Prairieburg sections appeared somewhat independent of fiber type, but dependent on fiber weight fraction. Improvements were noted at fiber weight fractions of 0.1% or less, while poorer performance was obtained at the higher contents of each of the three fibers. Results of SBV(2) did not appear significant and may be attributed to initiation of fiber debonding following rupture of the surfacing. Thus fiber reinforcement of roadway soils should be associated with base or subbase courses having adequate surfacing.

RECOMMENDATIONS

1. In order to validate laboratory investigations with the loessial soils, test sections should be instituted for long duration evaluation in the Sioux City area, and should consist of an untreated base, soil-fiber base, cement modified base, and cement modified soil-fiber base.

2. Laboratory studies should be expanded to include soil moisture contents well into the plastic range and/or approaching their respective liquid limits. Such testing should at least include freeze-thaw durability and cyclic loading, the latter, both with and without subjection of freeze-thaw. In addition, this study should also examine the effects of soil matrix modification with low contents of cement, lime, or fly ash.

3. Though implied in both items above, methods to improve soil-fiber bond should be further investigated, including lengths of fibers that approach or exceed the critical length required for soil stress conditions present in roadway bases and subbases.

4. Utilizing data and techniques developed in HR-211, coupled with information obtained from items 1-3 above, analytical models should be developed for roadway thickness design procedures incorporating fiber reinforced base and/or subbase courses.

ACKNOWLEDGMENTS

This investigation was conducted by personnel of the Geotechnical Research Laboratory, Engineering Research Institute, Iowa State University. The project was sponsored by the Iowa Highway Research Board, Iowa Department of Transportation. Special appreciation and sincere thanks are

extended to the following for their interest and assistance during the conduct of this investigation:

Members of the Iowa Highway Research Board, Iowa Department of Transportation.

Mr. Vernon J. Marks, Research Engineer, Highway Division, Iowa Department of Transportation.

Mr. Del Jesperson, Story County Engineer, his staff, and Board of Supervisors.

Mr. Jerry D. Nelson, Linn County Engineer, his staff and Board of Supervisors.

Mr. Bill Amundson, Director of Public Works, Sioux City, Iowa.

The many suppliers of fiber samples.

The many student laboratory technicians of the Geotechnical Research Laboratory.

Kathryn E. Handy, Secretary, Geotechnical Research Laboratory.

SELECTED REFERENCES

1. Agarwal, Blagwan D. and Lawrence J. Broutman. Analysis and Performance of Fiber Composites. New York: John Wiley and Sons, Inc., 1980.

2. Allen, H. G. "The Purpose and Methods of Fiber Reinforcements." Proceedings of an International Building Exhibition Conference on Prospects for Fiber Reinforced Construction Materials. London: Building Research Establishment, November, 1971.

3. American Concrete Institute Committee 544. "State-of-the-Art Report on Fiber Reinforced Concrete." Proceedings of the American Concrete Institute Journal 70, No. 11 (1973), 729-744.

4. American Society for Testing Materials. 1974 Annual Book of ASTM Standards, Part 19. Philadelphia, Pa.: American Society of Testing Materials, 1974.

5. Burmister, Donald M. "The Theory of Stresses and Displacements in Layered Systems and Applications to the Design of Airport Runways." Highway Research Board Proc., 23 (1943), 126-143.

6. Butt, G. S., Turgut Demirel, R. L. Handy. Soil Bearing Tests using a Spherical Penetration Device. Highway Research Record 243, pp. 62-74, 1968.

7. Catheral, J. R. Fiber Reinforcement. London: Mills and Boon Limited, 1973.

8. Cooper, G. A. and A. Kelly. "Role of the Interface in the Fracture of Fiber Composite Materials." Proc. ASTM Symp. on Interfaces in Composites. ASTM STP-452 (1968), 90-107.

9. Fang, H. Y. and H. C. Meleta. "Utilization of Sulfur-Treated Bamboo for low Volume Road Construction." Unpublished paper, presented at the 2nd International Conference on Low Volume Roads. TRB, Iowa State University, Ames, Iowa, 1979.

10. Gray, D. H. and H. Ohashi. "Mechanics of Fiber Reinforcement in Sand." Unpublished paper. Dept. of Civil Engineering, University of Michigan, Ann Arbor, Michigan.

11. Halpin, J. C. and S. W. Tsai. "Effects of Environmental Factors on Composite Materials." Airforce Materials Laboratory, Wright-Patterson AFB, Ohio, TR 67-432, June, 1969.

12. Hoover, J. M., Pitt, J. M., Handfelt, L. D., and Stanley, R. L. Performance of soil-aggregate fabric systems in frost susceptible roads, Linn County, Iowa. Transportation Research Board 827, Transportation Research Board, National Academy of Sciences, 1981, pp. 6-14.

13. Handy, Richard L. "Petrography of Selected South Western Iowa Loess Sample." Unpublished M.S. Thesis, Iowa State University, Ames, Iowa, 1953.

14. Handy, Richard L. "Stabilization of Iowa Loess with Portland Cement." Unpublished Ph.D. Dissertation, Iowa State University, Ames, Iowa, 1956.

15. Hannant, D. J. Fiber cements and fiber concretes. Chichester, England: John Wiley and Sons, Inc., 1978.

16. Hoff, G. C. Chemical, Polymer and Fiber Additives for Low Maintenance Highways. Pork Ridge, N.J.: Noyes Data Corporation, 1979.

17. Krenchel, Herbert. "Fiber Reinforced Brittle Matrix Materials." An International Symposium on Fiber Reinforced Concrete, Ottawa, Detroit: American Concrete Institute, 1973.

18. Krenchel, Herbert. Fiber Reinforcement. Copenhagen, Denmark: Akademisk Forlag, 1964.

19. Majundar, A. J. "Prospects of Fiber Reinforcements in Civil Engineering Materials." Conference at Shirley Institute on Fibers in Civil Engineering. Manchester, England: Shivley Institute, 1975.

20. Mangat, P. S. "Tensile Strength of Steel Fiber Reinforced Concrete." Cement and Concrete Research, 6, No. 2 (March 1976), 245-252.

21. McGown, A., K. Z. Andrewes, and M. M. Al-Hasani. Effect of Inclusion Properties on the Behavior of Sands." Geotechnique, 28, No. 3, (March 1978), 327-346.

22. Moncrieff, R. W. Man Made Fibers. London: Butterworths Publishing Co., Ltd., 1975.

23. Parrat, N. J. Fiber Reinforced Materials Technology. London: Van Nostrand Reinhold Company, 1972.

24. Swany, R. N., P. S. Mangat and C. V. S. K. Rao. "The Mechanics of Fiber Reinforcement of Cement Matrices." Fiber reinforced concrete, Publication SP-44. Detroit: American Concrete Institute, 1974.

25. Swamy, R. N. and P. S. Mangat. "Influence of Fiber Geometry on the Properties of Steel Fiber-Reinforced Concrete." Cement and Concrete Research, 4, No. 3 (1974), 451-465.

26. Vidal, Henri. "The development and future of reinforced earth." Proc. ASCE Symp. on Earth Reinforcement (1978), 1-62.

27. International Conference on the Use of Fabrics in Geotechnics, Volumes I, II, and III. Ecole Nationale des Ponte et Chaussees and the Laboratoire Central des Ponts et Chaussees, Paris. April, 1977.

28. Daw, N. F. Study of Stresses Near a Discontinuity in a Filament-Reinforced Composite Material. General Electric Company Report No. T1S R63 SD61, 1963.

29. Holister, G. S. and Thomas, C. Fiber Reinforced Materials. London: Elsevier Publishing Co., Ltd., 1966.

30. Handy, R. L., Lutenegger, A. J., and Hoover, J. M. The Iowa K-Test. Transportation Research Record 678, Transportation Research Board, National Academy of Sciences, 1978, pp. 42-49.

31. Shah, S. P. and Rangan, B. V. "Fiber Reinforced Concrete Properties." Proceedings of American Concrete Institute Journal, 68, No. 2, Febr. 1971, pp. 126-135.